

Alma Mater Studiorum – Università di Bologna

DOTTORATO DI RICERCA IN

ONCOLOGIA, EMATOLOGIA E PATOLOGIA

Ciclo XXXIII

Settore Concorsuale: 06/D3 - Malattie del sangue, oncologia e reumatologia

Settore Scientifico Disciplinare: MED/06-Oncologia Medica

**THERAPEUTIC STRATEGIES TO OVERCOME
TUMOR HETEROGENEITY IN HER2
POSITIVE MAMMARY CARCINOMA**

Presentata da: Dott.ssa Arianna Palladini

Coordinatore Dottorato

Supervisore

Prof.ssa Manuela Ferracin

Prof. Pier-Luigi Lollini

Esame finale anno 2021

Abstract

Target therapy has significantly improved the management and the outcome of different types of tumors, including HER2-positive breast cancers. Nevertheless, overall, target therapy has also shown several limitations over the years, as demonstrated by the significant rate of patients who developed resistance to therapy. This is also true for the monoclonal antibody trastuzumab, the gold standard therapy against HER2-positive breast cancer.

Tumor heterogeneity is a key factor in resistance to target therapy. This heterogeneity can be intended as spatial, both within a single tumor and among multiple metastases, and temporal.

The goal of this thesis was to find alternative strategies and potential druggable targets to overcome tumor heterogeneity in HER2-positive mammary carcinoma through models able to reproduce multiple traits of HER2-positive breast cancer.

The research was addressed towards the study of the HER2-VLP, an anti-HER2 cancer vaccine, and approaches aimed at reinforcing vaccine activity. The ability of immune checkpoint inhibitors to modulate immune response and, directly or indirectly, tumor progression was also investigated.

To identify new therapeutic targets against progressed breast cancers, mammary carcinoma cell lines derived from HER2 transgenic mice and patient-derived xenograft (PDX) mice were studied. In these models, tumor progression showed epithelial to mesenchymal transition (EMT) traits and increased stemness. Molecules involved in these processes might become new targets for therapeutic approaches. In addition, tumor progression may be also counteracted by turning off alternative survival circuits to HER2 (*e.g.*, IL6/STAT3/SORBS3 and PHLDA1). Finally, the progression of HER2-positive mammary carcinomas can lead to the loss of HER2 expression and acquisition of a claudin-low phenotype and PDGFR-B expression. Sunitinib was effective in slowing the growth of these HER2-negative tumor cells.

Table of Contents

List of Acronyms and Abbreviations	10
Introduction.....	15
1. BREAST CANCER.....	17
1.1 Intrinsic subtypes and molecular signatures.....	17
1.1.1 Luminal subtype.....	20
1.1.2 HER2-enriched subtype	21
1.1.3 Basal-like subtype.....	22
1.1.4 Claudin-low subtype	22
1.2 HER2.....	23
1.2.1 HER2 and cancer	24
1.2.2 HER2 isoforms	25
1.3 Anti-HER2 approved therapies and mechanisms of resistance.....	28
1.3.1 Trastuzumab	28
1.3.2 Pertuzumab	33
1.3.3 Trastuzumab-emtansine.....	34
1.3.4 TKI: lapatinib and neratinib.....	34
1.4 Drivers of HER2-positive breast cancer progression	36
1.4.1 Receptor conversion.....	36
1.4.2 Epithelial to mesenchymal transition and stemness	38
1.4.3 Angiogenesis	39
2. CANCER VACCINES AND IMMUNE CHECKPOINT INHIBITORS.....	40
2.1 Antigens for cancer vaccines.....	42
2.2 Vaccine types	43
2.3 Immune checkpoint inhibitors.....	45
2.3.1 PD-1 and PD-L1	47
2.3.2 Resistance to ICI	51
2.3.2.1 Hyperprogressive disease	52
Aim of the work.....	57
Results	61

1. IMMUNOLOGICAL STRATEGIES	63
1.1 Anti-HER2 cancer vaccines: HER2-VLP and pHuRT	63
1.1.1 Anti-HER2 cancer vaccines in the prevention of mammary carcinoma ..	63
1.1.2 Anti-HER2 antibodies induced by cancer vaccines in the preventive set-up ..	65
1.1.3 HER2-VLP vaccine activity in the therapeutic set-up.....	66
1.1.4 Isotypes, affinity and avidity of anti-HER2 antibodies	68
1.1.5 <i>In vitro</i> activity of anti-HER2 antibodies.....	71
1.1.6 Cytokine production.....	72
1.2 Triggering the immune response	74
1.2.1 The break of tolerance against IGF2	75
1.2.2 The break of tolerance against IGF1R.....	78
1.2.3 Modulation of the immune checkpoint OX40.....	81
1.2.4 Modulation of the immune checkpoint PD-L1	87
1.2.4.1 Therapy of B16 and B16-F10 with polyclonal anti-PD-L1 antibodies	88
1.2.4.2 Therapy of B16 and B16-F10 with monoclonal anti-PD-L1 antibodies	89
1.2.4.3 Mechanisms underlying resistance to PD-L1 treatment.....	93
2. DISCOVERY OF NEW THERAPEUTIC TARGETS	96
2.1 Dynamic model of HER2 expression	96
2.1.1 Dynamic model of HER2 expression panel.....	96
2.1.2 Molecular portrait of HER2 dynamic expression	104
2.1.3 p95HER2 and PHLDA1	109
2.1.4 PDGFR-B as a therapeutic target for HER2 loss cells.....	110
2.2 Dynamic model of HER2-positive breast cancer progression	112
2.2.1 Progression of HER2-positive PDX-BRB4 line	113
2.2.2 Molecular profile associated to HER2-positive PDX subline progression	115
Discussion	119
1. IMMUNOLOGICAL STRATEGIES	123
1.1 Cancer vaccines	123

1.2 Triggering the immune response	125
2. DISCOVERY OF NEW THERAPEUTIC TARGETS	129
2.1 Dynamic model of HER2 expression	130
2.2 Dynamic model of HER2-positive breast cancer progression	133
3. CONCLUSIONS	135
Materials and Methods	137
1. IMMUNOLOGICAL STRATEGIES	139
1.1 Anti-HER2 cancer vaccines	139
1.1.1 Mice	139
1.1.2 Cell lines.....	139
1.1.3 HER2-VLP and pHuRT vaccines	140
1.1.4 HER2-VLP and pHuRT immunization	141
1.1.5 Growth inhibition by HER2-VLP-induced antibodies.....	142
1.2 The break of tolerance against IGF1R and IGF-2	143
1.2.1 Mice	143
1.2.2 Cell lines.....	143
1.2.3 Anti-IGF1R and anti-IGF2 vaccines	144
1.2.4 Anti-IGF1R and anti-IGF2 <i>in vivo</i> treatments.....	144
1.2.4.1 Anti-IGF1R and IGF-2 DNA vaccines	144
1.2.4.2 Anti-IGF1R cell vaccines	145
1.2.4.3 Anti-IGF2 antibodies.....	145
1.2.5 3D-growth inhibition of IGF circuit.....	146
1.3 Modulation of the immune checkpoint OX-40	147
1.3.1 Mice	147
1.3.2 Cell lines.....	147
1.3.3 Triplex vaccine combined to aOX40 treatment.....	147
1.4 Modulation of the immune checkpoint PD-L1	148
1.4.1 Mice	148
1.4.2 Cell lines.....	148
1.4.3 Anti-PD-L1 treatments	148

1.4.4 IFN- γ sensitivity	149
1.4.5 Real-Time PCR.....	150
1.5 Quantification and characterization of anti-vaccine antibodies.....	150
1.5.1 Anti-HER2 antibodies induced by HER2-VLP or pHuRT	150
1.5.2 Anti-IGF1R antibody detection	151
1.5.3 Anti-IGF2 antibody detection.....	152
1.5.4. Anti-HER2/neu antibody detection	153
1.5.5 Anti-PDL1 antibodies	153
1.6 Cytokine production	154
1.7 <i>In vitro</i> restimulation assay and cytokine release	154
1.8 Detection of lymphocyte subpopulations.....	154
2. DISCOVERY OF NEW TARGETS.....	154
2.1 Mice	155
2.2 Cells	155
2.3 <i>In vivo</i> studies.....	156
2.3.1 MamBo cell lines <i>in vivo</i> growth and inhibition by sunitinib	156
2.3.2 PDX establishment, propagation and metastatization	157
2.4 <i>In vitro</i> assay	157
2.4.1 3D-growth inhibition by sunitinib	157
2.4.2 Cell migration	158
2.4.3 Mammosphere formation assay	158
2.4.4 Induction of HER2 loss <i>in vitro</i>	159
2.4.5 IL-6 quantification	159
2.5 Tumor and cell phenotyping	159
2.5.1 Flow Cytometry	159
2.5.2 Molecular analysis.....	160
2.5.2.1 RNA-Sequencing	160
2.5.2.2 Real-Time PCR.....	161
2.5.2.3 HER2 copy number	162
2.5.2.4 Molecular metastasis detection	162
2.5.2.5 <i>In situ</i> HER2 detection	163

2.5.3 Western Blotting	163
2.5.4 Immunohistochemistry and immunofluorescence	164
3. ETHICAL STATEMENTS	165
4. STATISTICAL ANALYSIS	165
References	166

List of Acronyms and Abbreviations

10F.9G2, rat anti-mouse PD-L1 antibody
ADCC, antibody-dependent cell cytotoxicity
AIOM, Italian association of medical Oncology (Associazione italiana di oncologia medica)
AKT1, AKT serine/threonine kinase 1
aOX40, rat IgG1 monoclonal antibody OX86 with agonistic activity
AP-1, Activator protein 1
AURKA, Aurora kinase A
BCL-2, B-cell lymphoma 2
BCSC, Breast cancer stem cells
BMP, Bone morphogenetic protein
BRCA1/2, Breast cancer type 1/2 susceptibility protein
CAV, Caveolin
CDC, complement dependent cytotoxicity
CDH1, E-cadherin
CDKN1A, cyclin dependent kinase inhibitor 1A
CECAM1, Carcinoembryonic antigen-related cell adhesion molecule 1
CHCHD10, coiled-coil-helix-coiled-coil-helix domain containing 10
CK, cytokeratin
c-KIT, KIT proto-oncogene, receptor tyrosine kinase
c-MYB, MYB proto-oncogene, transcription factor
CNP, 2',3'-cyclic nucleotide 3' phosphodiesterase
COL1A2, collagen type I alpha 2 chain
COL3A1, collagen type III alpha 1 chain
CRUK, Cancer Research United Kingdom
CTGF, cellular communication network factor 2
CTLA4, cytotoxic T-lymphocyte associated protein 4
DCN, decorin
DHCR7, 7-dehydrocholesterol reductase
DHX58, DEXH-box helicase 58
DNAJC15, DnaJ heat shock protein family (Hsp40) member C15
DPYSL3, dihydropyrimidinase like 3
DSP, desmoplakin
EFEMP2, EGF containing fibulin extracellular matrix protein 2
EFNB1, ephrin B1
EGFR, epidermal growth factor receptor
EGR1, early growth response 1
EMP3, epithelial membrane protein 3
EMT, epithelial to mesenchymal transition
ER, estrogen receptor
FAP, fibroblast activation protein alpha

Fc, fragment crystallizable region
FGFBP1, fibroblast growth factor-binding protein 1
FN1, fibronectin 1
FOS, Fos proto-oncogene, AP-1 transcription factor subunit
FOXA1, forkhead box A1
FOXC1, forkhead box C1
FSCN1, fascin actin-bundling protein 1
GADD45A, growth arrest and DNA damage inducible alpha
GATA3, GATA binding protein 3
GHITM, growth hormone inducible transmembrane protein
GLIPR1, GLI pathogenesis related 1
GPX8, glutathione peroxidase 8 (putative)
GSTM1, glutathione S-transferase mu 1
HER2 (ErbB2), erb-b2 receptor tyrosine kinase 2, human epidermal growth factor receptor 2
HER2 mice, FVBhuHER2 transgenic mice
HER2/Delta16 F1 or F1 mice, mice transgenic for full-length HER2 and Delta16 splicing isoform
HER2-CTFs, HER2 Carboxy-Terminal Fragments
HER2-ECD, HER2 extracellular domain
HIF1- α , Hypoxia-inducible factor 1-alpha
HPD, hyperprogressive disease
HTRA1, HtrA serine peptidase 1
i.m., intramuscular
i.p., intraperitoneal
i.v., intravenous
ICI, Immune checkpoint inhibitor
IFF2, Eukaryotic translation initiation factor 5A-2
IFN- γ , gamma interferon
IGF1R, insulin like growth factor 1 receptor
IGF2, insulin-like growth factor 2
IGFBP2/4/6, insulin like growth factor binding protein 2/4/6
IL, interleukin
IL1RN, Interleukin 1 Receptor Antagonist
INPP4B, inositol polyphosphate-4-phosphatase type II B
IPO4, importin 4
Isotype control, rat anti-keyhole limpet hemocyanin IgG2b
ITGB3, integrin subunit beta 3
JUN, Jun proto-oncogene, AP-1 transcription factor subunit
JUP, junction plakoglobin
KIT, KIT proto-oncogene, receptor tyrosine kinase
LGALS1, galectin 1
LMO7, LIM domain 7
LOX, lysyl oxidase

LPCAT3, lysophosphatidylcholine acyltransferase 3
LRP1, LDL receptor related protein 1
m.f.p., mammary fat pad
mAbs, monoclonal antibodies
MAP2K4, mitogen-activated protein kinase kinase 4
MAP3K1, Mitogen-activated protein kinase kinase kinase 1
MDSC, myeloid-derived suppressor cells
MKI67, marker of proliferation Ki-67
MMP, Matrix metalloproteinase 1
MYC, MYC proto-oncogene
NCOA7, nuclear receptor coactivator 7
NES, nestin
NF1, neurofibromin 1
NF-KB, nuclear factor kappa-light-chain-enhancer of activated B cells
NGS, Next Generation Sequencing
NK, natural killer
NOTCH1, notch receptor 1
NSCLC, Non-small cell lung cancer
OCL, occludin
PAK1, p21 (RAC1) activated kinase 1
PCA, principal component analysis
PCOLCE, procollagen C-endopeptidase enhancer
PD-1, programmed cell death protein 1
PDGFRB, platelet derived growth factor receptor beta
PD-L1, programmed death ligand 1
PDX, patient-derived xenograft
PHLDA1, pleckstrin homology like domain family A member 1
PIK3CA, phosphatidylinositol-4,5-bisphosphate 3-kinase, catalytic subunit alpha
PIM3, Pim-3 proto-oncogene, serine/threonine kinase
PLSCR1, phospholipid scramblase 1
PR, progesterone receptor
PRRX1, paired related homeobox 1
PSMB8, proteasome 20S subunit beta 8
PTEN, phosphatase and tensin homolog
PTGS2, prostaglandin-endoperoxide synthase 2
PTPN1, protein tyrosine phosphatase non-receptor type 1
QSOX1, quiescin sulfhydryl oxidase 1
RAB31, RAB31, member RAS oncogene family
RB, RB transcriptional corepressor 1
RNA-Seq, RNA Sequencing
RTKs, receptor tyrosine kinases
RTN3, reticulon 3

RUNX1, RUNX family transcription factor 1
s.c., subcutaneous
SERMs, Selective Estrogen Receptor Modulators
SFRP1, secreted frizzled related protein 1
SGCD, sarcoglycan delta
SLUG, snail family transcriptional repressor 2
SNAIL, snail family transcriptional repressor 1
SNGT1, Syntrophin Gamma 1
SNTB1, syntrophin beta 1
SORBS3, Sorbin And SH3 Domain Containing 3
SP1, Sp1 transcription factor
SPARC, Secreted Protein Acidic And Cysteine Rich
STAT, sterol O-acyltransferase 1
SUCLA2, succinate-CoA ligase ADP-forming subunit beta
SYNM, Synemin
TAA, tumor associated antigens
T-DM1, trastuzumab-emtansine
Tem, T effector memory cells
TGFB1, transforming growth factor beta 1
TIMP2, TIMP metalloproteinase inhibitor 2
TKI, Tyrosine Kinase Inhibitor
TNF, tumor necrosis factor
TNFAIP2, TNF alpha induced protein 2
TP53, tumor protein p53
TPM2, tropomyosin 2
Treg, regulatory T cells
TWIST, twist family bHLH transcription factor 1
VCAN, versican
VEGFA, vascular endothelial growth factor A
VIM, vimentin
VLPs, virus-like particles
WHO, World Health Organization
WT1, Wilms' tumor protein 1
XBP1, X-box binding protein 1 ZEB1
ZEB1, zinc finger E-box binding homeobox 1
ZEB2, zinc finger E-box binding homeobox 2

Introduction

1. BREAST CANCER

Breast cancer is currently the most common cancer in women: according to the World Health Organization (WHO) it affects about 2.1 million women each year and it represents 11.6% of all types of cancer. The worldwide breast cancer incidence rate is 23.7% and the mortality rate 6.8% (WHO, 2019).

Breast cancer is the leading cause of cancer death in women, accounting for 28% of cancer deaths before the age of 50, 21% between 50 and 69 and 14% after 70. Nevertheless, in Italy, five-year survival rate is 87%, and 10-year survival rate is 80%. This is due to the increased dissemination of early detection programmes used for screening tests and to the numerous therapeutic advances (Italian Association of Medical Oncology, Associazione Italiana di Oncologia Medica, AIOM, 2019).

Breast cancer incidence increases exponentially from 30 to 50 years reaching a plateau immediately after menopause, and then rising sharply between 60 and 75 years. This trend is related to both the endocrinological history of women and the presence of the currently available mammographic screening programs, in which women are included after the age of 50 (Cancer Research United Kingdom, CRUK, 2019). Other breast cancer risk factors are related to fertility, hormonal, dietary and metabolic factors, previous radiotherapy and previous dysplasia or breast cancer onset. Finally, about 5-7% of breast cancers is related to hereditary factors, in particular mutations of *BRCA1* (Breast Cancer Type 1 susceptibility protein 1) and/or *BRCA2* genes (Breast Cancer Type 1 susceptibility protein 2).

1.1 Intrinsic subtypes and molecular signatures

Breast cancer is a heterogeneous disease which includes numerous distinct entities that not only have different biological features but also different clinical behaviours (Vargo-Gogola and Rosen 2007; Reis-Filho and Lakhani 2008; Simpson et al. 2008; Weigelt and Reis-Filho 2009; Weigelt et al. 2010).

Histopathological examination is fundamental for the prognostic stratification of breast cancer, providing the classification of the histological grade and type and

contributing to the definition of the Union for International Cancer Control (UICC)/ American Joint Committee on Cancer (AJCC) Tumour, Node, Metastasis (TNM) stage of the cancer itself. Currently, the grading of breast cancer is based on the Nottingham Histologic Score, derived from the score developed by Bloom and Richardson and modified by Elston and Ellis in 1991 (Bloom and Richardson 1957; Elston and Ellis 2002; Rakha et al. 2008). The histological type is defined according to the WHO/ International Agency for Research on Cancer (IARC) classification, the internationally adopted histopathological classification of breast cancer which identifies 20 histotypes and more than 50 variants of invasive breast cancer (Lakhani et al. 2012). Moreover, estrogen receptor (ER), progesterone receptor (PR) and human epidermal growth factor receptor 2 (HER2) are assessed by immune-histochemical or molecular analysis, as they are recognized as predictive and prognostic markers in breast cancer. Nevertheless, the previously reported classifications cannot fully appreciate the high biological heterogeneity of breast cancer in order to meet all the requirements of prognostic stratification and therapeutic differentiation (Viale 2012). To overcome the limits of these multiple classifications, great efforts have been made to both increase the molecular and genetic knowledge of breast cancer and integrate the classification schemes (Figure I) in order to make them more adherent to the biology of the tumor and more useful in the clinical practise (Viale et al. 2009).

In 2000, Perou, Sorlie and colleagues published a study of gene expression by microarray analysing the cDNA of about 9000 gene loci of 65 breast cancer samples from 42 individuals. They identified five clusters of gene expression, called intrinsic subtypes, defined as Luminal (which can be subdivided into Luminal-A and Luminal-B), HER2-enriched, Basal-like and Normal-like (Perou et al. 2000). Subsequent studies found the same molecular subtypes in many other cohorts of breast cancer (Sorlie et al. 2003; Hu et al. 2006; Yersal and Barutca 2014). Further, a new subtype, classified as Claudin low, has also been identified (Prat et al. 2010). Intrinsic subtypes differed from each other by their associated prognosis, biological behaviour and response to neoadjuvant and adjuvant therapies (Sørliie et al. 2001; Hennigs et al. 2016). The

contribution of the Next Generation Sequencing (NGS) techniques enabled to combine gene expression data with copy number alterations (Natrajan et al. 2009; Russnes et al. 2011; Morganella et al. 2016) and point mutation data (The Cancer Genome Atlas Network 2012; Stephens et al. 2012; Pereira et al. 2016). The analysis of thousands of breast cancer samples allowed the creation of large databases hosting information on the molecular and genetic characteristics of these samples, with particular reference to "The Cancer Genome Atlas project" (TCGA), "International Cancer Genome Consortium" (ICGC) and "Molecular Taxonomy of Breast Cancer International Consortium" (METABRIC) (Arias-Romero et al. 2010; The Cancer Genome Atlas Network 2012; Ellis and Perou 2013; Hennigs et al. 2016). The high heterogeneity of the different intrinsic subtypes was proved by Caldas, Dawson and colleagues, who, in an effort to harmonise the different molecular breast cancer classification approaches, carried out a clustering analysis based on both gene expression and copy number alterations, identifying 10 molecular subgroups called integrative clusters which show differences not only at the molecular but also at the clinical and prognostic level (Dawson et al. 2010).

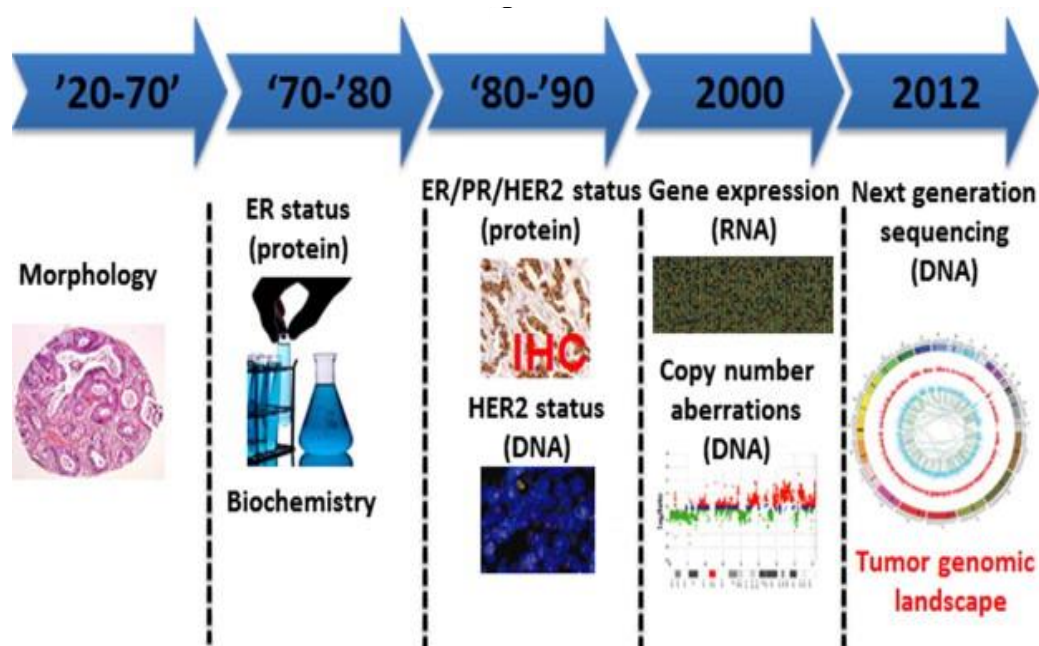


Figure I. Timeline of the multi-step process of breast cancer subtype classification (Sonnenblick et al. 2014).

1.1.1 Luminal subtype

The tumors included in the luminal subtype are characterized by a high expression of *ESR1* (coding for ER) and *GATA3*, *FOXA1*, *XBP1* and *c-MYB* (Prat et al. 2015). The expression level of genes related to proliferation, cell cycle, luminal differentiation and hormone regulation allow us to distinguish two subtypes of Luminal tumors: Luminal-A and Luminal-B. The Luminal-A subtype represents about 50-60% of all breast carcinomas and it is characterized by a high expression of luminal differentiation markers and estrogen-related molecules (CK8, CK18, PR, ER, FOXA1) and low expression of proliferation-related genes (Yersal and Barutca 2014). The Luminal-B subtype, which includes 15-20% of all breast cancers, is characterized, unlike Luminal-A, by a higher expression of genes related to proliferation and cell cycle, such as *MKI67* and *AURKA*, and by a relatively lower expression of luminal differentiation genes (although the ER is expressed similarly in the two luminal subtypes) (Loi et al. 2013; Sonnenblick et al. 2014). A rate of Luminal-B tumors results HER2-positive by immunohistochemistry.

The most frequently observed somatic mutations concern genes involved in cell cycle differentiation and regulation processes, in particular *PIK3CA* (49%), *MAP3K1* (14%), *GATA3* (14%) and *TP53* (12%), while *CDH1*, *MAP2K4*, *FOXA1*, *RUNX1* and *NF1* are less common mutations (The Cancer Genome Atlas Network 2012).

Luminal-A tumors are characterized by a low histological grade (low nuclear pleomorphism, limited mitotic activity, marked morphological differentiation) and are frequently ascribed to special histotypes associated with a good prognosis (Yersal and Barutca 2014). Luminal-B subtype is characterized, unlike Luminal-A, by a more aggressive biological behaviour, a higher histological grade and proliferative index, and a worse prognosis, regardless of the used adjuvant therapy (Ellis et al. 2008; Yersal and Barutca 2014; Hennigs et al. 2016).

Hormone therapy, which is indicated in all patients with a detectable expression of ER (defined as a positivity of more than 1% of cancer cells), includes three main approaches: modulation of the estrogen receptor through Selective Estrogen Receptor

Modulators (SERMs), including tamoxifen; inhibition of the aromatase enzyme; and hypothalamic-hypophyseal axis blockade, which results in ovarian suppression, through the use of the LH-RH analogous (Yersal and Barutca 2014). Therapy for HER2-positive tumors includes also anti-HER2 drugs (Goldhirsch et al. 2011).

1.1.2 HER2-enriched subtype

The HER2-enriched subtype represents 15-20% of all breast cancers. At the transcriptional level, these tumors present a high expression of HER2 and molecules involved in HER2-signaling pathway. The expression of ER and PR is variable, although generally negative. Further genes related to luminal differentiation are expressed at an intermediate level compared to Luminal and Basal-like subtypes, while the expression of genes related to basal differentiation, such as *CK5* and *FOXC1*, is reduced (Prat et al. 2015).

The majority of HER2-enriched tumors show HER2 amplification (80%) (The Cancer Genome Atlas Network 2012). Moreover, HER2-enriched tumors are characterised by the highest mutational rate among the five breast cancer subtypes. The highest frequency of mutations was observed in *TP53* (75%) and *PIK3CA* (42%) (Prat et al. 2015).

HER2-enriched breast carcinomas have a poor prognosis due to the ability to metastasize, through lymphatic and hematogenous dissemination, to different visceral organs and brain (Gonzalez-Angulo et al. 2009). Nevertheless, the introduction of anti-HER2 therapy in clinical practice has improved the outcome of these tumors (Dawood et al. 2010; Ferretti et al. 2010; Kast 2017). The anti-HER2 therapeutic agents approved for clinical use include the monoclonal antibodies (mAbs) trastuzumab and pertuzumab, the small tyrosin-kinase inhibitors (TKIs) lapatinib and neratinib, and the conjugated complex trastuzumab-emtansine (T-DM1).

1.1.3 Basal-like subtype

The Basal-like subtype accounts for 8% to 27% of all breast cancers. These tumors express high levels of myoepithelial basal markers such as CK5, CK14, CK17 and laminin. Conversely, these tumors do not express ER, PR and HER2, and thus they are known as triple-negative breast cancers. The Basal-like subtype presents high expression of *P-CDH*, *FSCN1*, *CAV1* and 2, *NES*, and *EGFR*. On the other hand, these tumors express low levels of genes codifying for markers of the luminal epithelium such as CK8/18 and c-KIT (Eroles et al. 2012). An altered regulation of integrin expression was also observed. This alteration could contribute to the high biological aggressiveness of the Basal-like phenotype (Yersal and Barutca 2014; Prat et al. 2015).

TP53 mutations, the loss/mutation of *RB* and mutations of genes involved in the mismatch repair system, such as *BRCA1*, are frequent among these tumors. Indeed a further trait of these tumors is the genomic instability, which promote neo-antigen occurrence (The Cancer Genome Atlas Network 2012).

Conventional chemotherapy is currently the only treatment option for Basal-like carcinomas.

1.1.4 Claudin-low subtype

Claudin-low tumors account for 7-14% of all invasive breast cancers. These tumors are triple-negative breast cancers with low gene expression of tight junction proteins such as Claudin 3, 4 and 7 and E-Cadherin (Prat et al. 2010). These tumors are significantly enriched in epithelial to mesenchymal transition (EMT) and stemness components, showing a low expression of luminal and proliferation-associated genes (Prat and Perou 2011). Furthermore, Claudin-low tumors are enriched of genes associated with immune cell infiltration, IFN- γ activation and typically variable levels of genomic instability (Dias et al. 2017).

Claudin-low tumors have a response rate to standard neoadjuvant chemotherapy that is between that of Basal-like and Luminal tumors.

1.2 HER2

HER2 (ErbB2) is a transmembrane receptor with tyrosine-kinase activity and it belongs to the ErbB family (Arteaga and Engelman 2014). ErbB receptors activate different intracellular signaling pathways in response to extracellular signals (Moasser 2007). So far, 12 ligands, that can interact with ErbB receptors, have been identified (Barnes and Kumar 2004; Citri and Yarden 2006).

After the binding with the ligand, the ErbB receptor acquires an open conformation which allows the dimerization with another ErbB receptor partner (Garrett et al. 2002; Ogiso et al. 2002; Burgess et al. 2003). HER2 ligands have never been identified, thus this receptor probably does not swing between the closed inactive and the open active conformation, but it remains instead constitutively open and, therefore, active (Garrett et al. 2003; Cho et al. 2003). Dimer formation does not happen by chance, but it follows a hierarchy of preferential dimerization: first of all, heterodimers are favoured over homodimers; secondly, HER2 is the preferential partner in the heterodimers and, finally, HER2 is the preferential partner of HER3 (Yarden and Sliwkowski 2001; Yarden and Pines 2012). The signal transduction activity is related to the different dimers: homodimers are less active than heterodimers. The most active heterodimers are those containing HER2, and the most active HER2 heterodimer is the one formed by HER2 and HER3 (Tzahar et al. 1996; Pinkas-Kramarski et al. 1996; Graus-Porta et al. 1997; Yarden and Sliwkowski 2001), although HER2 and HER3 have distinctive features which make them functionally incomplete if taken individually.

ErbB receptors promote the activation of several signal transduction pathways, including RAS/RAF/MEK/ERK, PI3K/AKT/mTOR, Src pathway, JAK/STAT and phospholipase C γ (PLC γ) pathway. The activation of these signaling cascades induces, at a nuclear level, the transcription of proto-oncogenes such as those coding for FOS, JUN, MYC, SP1, and EGR1 transcription factors (Yarden and Pines 2012; Arteaga and Engelman 2014). The activation of such transcriptional programs influences important biological functions, many of which are needed for the process

of tumorigenesis, including cell proliferation, cell migration, cell adhesion, cell motility, angiogenesis, differentiation and apoptosis (Yarden and Sliwkowski 2001).

1.2.1 HER2 and cancer

Data supporting the proto-oncogenic nature of rat HER2/neu and human HER2 have been accumulated for more than 30 years and are now incontrovertible (Schechter et al. 1984; Bargmann et al. 1986; Di Fiore et al. 1987; Hudziak et al. 1987; Muller et al. 1988; Bouchard et al. 1989; Weiner et al. 1989; Benz et al. 1992; Chazin et al. 1992; Andrechek et al. 2000; Finkle et al. 2004).

In human HER2-positive mammary carcinomas, the overexpression of the wild-type form of human HER2 is enough to observe the effects of the oncogenic nature of the receptor and, in addition, activating HER2 mutations are sporadically found (Segatto et al. 1988; Moasser 2007). On the other hand, the presence of HER2 somatic mutations was found in mice transgenic for the rat HER2/neu protooncogene that developed spontaneous mammary carcinogenesis. These mutations occurred in the juxtamembrane region of the receptor and promoted the receptor dimerization (Guy et al. 1992; Siegel and Muller 1996; Siegel et al. 1999). Somatic mutations were also found in 80% of the cell lines derived from spontaneous tumors developed in FVB mice transgenic for the human HER2: these mutations occurred in the juxtamembrane region of the HER2 extracellular domain (Finkle et al. 2004). In rat HER2/neu or human HER2 transgenic mouse models, HER2 mutation is therefore a frequent event, unlike human HER2-positive breast cancer, in which the presence of HER2 overexpression is enough to promote tumorigenesis.

In 1987 Slamon and colleagues reported an amplification of the HER2 gene in human breast cancer samples that was associated with a worse prognosis (Slamon et al. 1987). Subsequently, HER2 overexpression was also found in other human cancers, including ovarian cancer, gastric carcinoma, esophageal carcinoma, and endometrial carcinoma. Regardless of the tissue of origin, the overexpression of HER2 always correlated with a worse prognosis (Slamon et al. 1989; Mimura et al. 2005; Morrison et

al. 2006; Yano et al. 2006). HER2 amplification is an early event in breast cancer, since it was detected in half of *in situ* ductal carcinomas (Liu et al. 1992; Park et al. 2006). In addition, invasive mammary carcinomas maintained HER2 amplification after tumor progression and dissemination (Latta et al. 2002; Carlsson et al. 2004; Park et al. 2006). The implementation of anti-HER2 targeted therapies has improved the prognosis of both early and advanced HER2-positive breast cancers, proving that HER2-positive tumors are, at least partially, dependent on HER2 signaling (Moasser 2007).

1.2.2 HER2 isoforms

Transcriptional, translational, and post-translational modifications of HER2 full-length result in alternative HER2 isoforms (Figure II). The alternative splicing of HER2 leads to three identified isoforms: Delta16 ($\Delta 16$), Herstatin and p100. Delta16 splicing isoform is related to increased tumorigenesis while p100 and Herstatin are associated to HER2 signaling inhibition (Jackson et al. 2013).

Delta 16 isoform was detected by Kwong and Hung in 1998 in mammary carcinoma cell lines and breast cancer samples (Kwong and Hung 1998) and it was subsequently confirmed by Siegel and colleagues (Siegel et al. 1999). The splicing isoform Delta16 lacks the exon 16, consisting of 48 base pairs, that encodes a sequence of 16 amino acids placed within the juxtamembrane region of the HER2 extracellular domain (Kwong and Hung 1998). The lack of exon 16 causes the loss of two cysteine residues at the level of the juxtamembrane region. The imbalance in intramolecular cysteines foster the formation of Delta16 ligand-independent homodimers that are particularly stable and constitutively active (Mitra et al. 2009; Castagnoli et al. 2014).

The expression of Delta16 isoform was found able to transform cell lines *in vitro* (Siegel et al. 1999; Castiglioni et al. 2006) by inducing a higher activation of PI3K-AKT, MAPK and Src pathways (Mitra et al. 2009). The overexpression of Delta16 in breast cancer cell lines has been associated to increased expression of mesenchymal markers, EMT-involved and stemness-related molecules (Alajati et al. 2013; Castagnoli et al. 2014; Castagnoli et al. 2017).

Analysing 46 samples of human HER2-positive breast cancer through Real-Time PCR, Castiglioni and colleagues highlighted how the mRNA codifying the isoform Delta16 constituted on average 9% compared to the HER2 full-length transcript (Castiglioni et al. 2006). In other studies the expression of the isoform Delta16 has been reported in about half of all the human HER2-positive breast cancers analysed, and in 90% of locally advanced ones, in which the level of this transcript represented 8-10% compared to the HER2 full-length mRNA (Mitra et al. 2009; Castagnoli et al. 2014). *In vitro*, Delta16 isoform expression was related to a reduction of binding affinity to trastuzumab (Castiglioni et al. 2006) and in addition, the isoform induced resistance to trastuzumab (Mitra et al. 2009). Nevertheless, subsequent *in vitro* and *in vivo* studies have shown significant responses to trastuzumab, both in the murine model transgenic for Delta16 isoform and in cell lines derived from spontaneous mammary carcinomas developed in Delta16 transgenic mice, as well as in patients with HER2-positive breast carcinomas expressing the Delta16 isoform at high levels (Alajati et al. 2013; Castagnoli et al. 2014).

A subpopulation of HER2-positive mammary carcinomas expresses C-terminal HER2 fragments, collectively known as HER2 Carboxy-Terminal Fragments (HER2-CTFs) or p95HER2 fragments. The percentage of HER2-positive human breast cancers expressing these fragments is 20-40% (Molina et al. 2002; Scaltriti et al. 2010; Arribas et al. 2010).

p95HER2 fragments increased cell proliferation of p95HER2-transduced tumor cells and induced a rapid growth of spontaneous mammary tumors in p95HER2 transgenic mouse models (Anido et al. 2006; Pedersen et al. 2009). C-terminal fragments can originate through two different mechanisms, which give rise to different p95HER2 isoforms. Post-translational proteolytic cleavage of HER2 full-length produces two HER2 fragments: a soluble fragment called p105, which includes a large portion of the extracellular domain of HER2, and a fragment that remains anchored to the plasma membrane called 648-CTF (Christianson et al. 1998; Codony-Servat et al. 1999). The use of alternative translation start sites, located at the level of the two residues of

methionine 611 and 687, leads instead to the formation of two products called 611-CTF and 687-CTF. 687-CTF fragment can translocate to the nucleus (Anido et al. 2006), while the 611-CTF is constitutively active and able to form homodimers due to particularly resistant intermolecular disulphide bridges (Pedersen et al. 2009).

In patients, the expression of p95HER2 fragments correlated with an increased metastatic involvement at the lymph node level (Molina et al. 2002; Sáez et al. 2006). Some data showed a higher prevalence of trastuzumab resistance in p95HER2 expressing tumors (Scaltriti et al. 2007; Sperinde et al. 2010), but this evidence is not yet solid, since following studies have shown a good response to trastuzumab in HER2-positive mammary carcinoma expressing 611-CTF, when treated with a combination therapy based on doxorubicin and trastuzumab (Parra-Palau et al. 2014; Scaltriti et al. 2015). p95HER2 is an independent negative prognostic factor in human breast cancer (Scaltriti et al. 2007; Arribas et al. 2011). Since the C-terminal fragments of HER2 maintain their own kinase activity, p95HER2 expressing tumors may be sensitive to small tyrosine-kinase inhibitors, as the response rate to capecitabine and lapatinib association therapy seemed to suggest (Scaltriti et al. 2010).

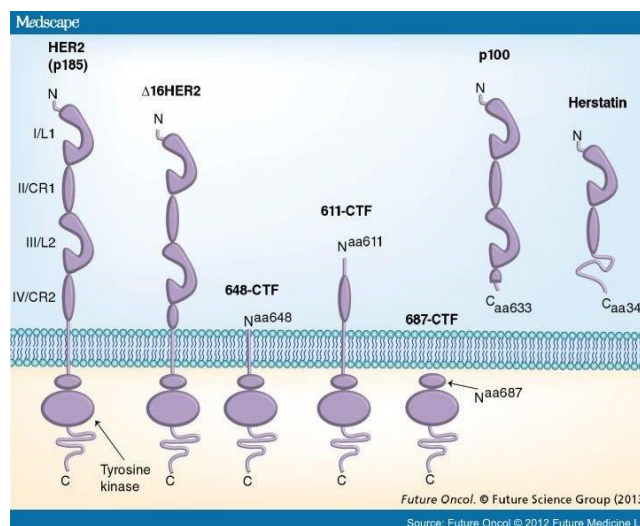


Figure II. HER2 isoforms (Wang et al. 2013).

1.3 Anti-HER2 approved therapies and mechanisms of resistance

Anti-HER2 drugs have significantly improved the prognosis of HER2-positive breast cancer patients (Figure III) (Moasser 2007; Swain et al. 2013a; Iqbal and Iqbal 2014; Singh et al. 2014).

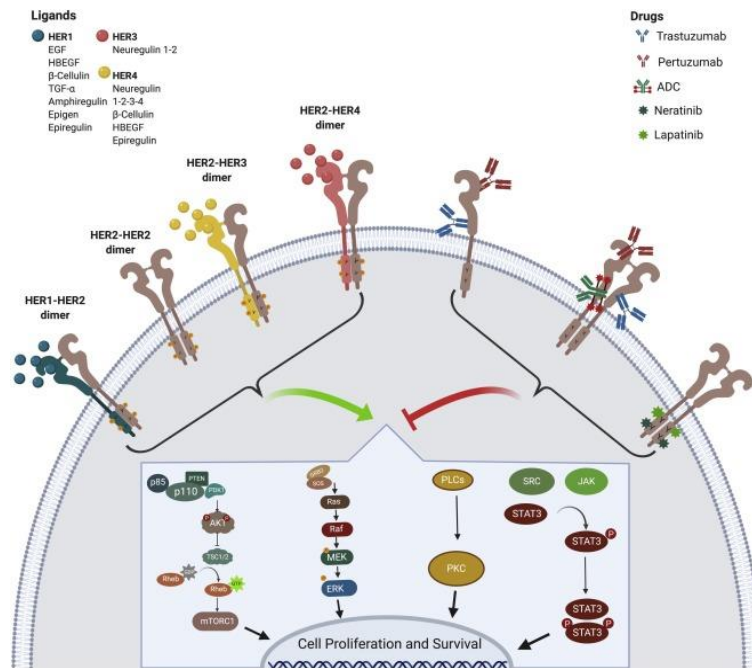


Figure III. HER2 downstream pathway activation, anti-HER2 targeted agents. Therapeutic approaches, based on the modulation of HER2 activation, include different targets of the protein. Monoclonal antibodies bind the extracellular domain of HER2 leading to a reduction of the signaling cascade. Antibody-drug conjugates are designed to release the drug after internalization by the tumor cell, with the decrease of systemic side effects. The small molecules tyrosine kinase inhibitors (TKIs), such as lapatinib and neratinib, inhibit the catalytic activity of the HER2 receptor in a reversible or irreversible way, respectively, through the specificity for the ATP binding site of the kinase domain. ADC: Antibody-Drug Conjugate (Marchiò et al. 2020).

1.3.1 Trastuzumab

Trastuzumab is a humanized IgG1 antibody that binds the domain IV of the HER2 extracellular region (Arteaga and Engelman 2014). Trastuzumab was approved in 1998 for the treatment of metastatic HER2-positive breast cancer as monotherapy, in patients already undergoing at least two conventional chemotherapeutic regimens, and in the first-line setting in combination with taxan, in patients not yet undergoing conventional chemotherapy (Figure IV) (Slamon 2001). The combination of chemotherapy and trastuzumab represents the standard of care in HER2-positive

breast cancer, both in the metastatic setting and in the adjuvant and neoadjuvant ones (Emde et al. 2012; Senkus et al. 2015).

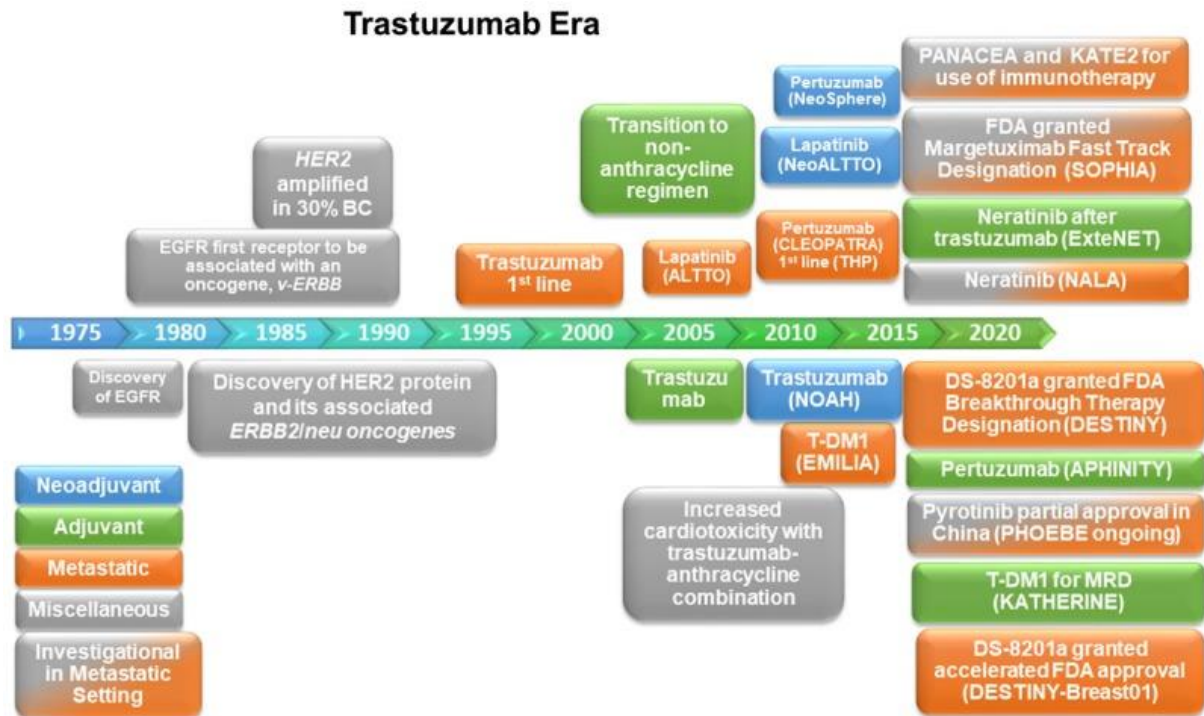


Figure IV. Timeline of key events, Food and Drug Administration (FDA)-Approved Therapies, Therapies on the Horizon, and their Clinical Settings for HER2-positive breast cancer (BC). The specific clinical trials were reported in the brackets. Trastuzumab emtansine (T-DM1) (Kreutzfeldt et al. 2020).

The mechanisms of action activated by the binding of trastuzumab to its HER2 epitope are many and, although not yet fully defined, they can be grouped into two categories: inhibition of receptor signaling and stimulation of the antitumor immune response. Specifically, the binding of trastuzumab to its epitope causes internalization and degradation of the HER2 receptor (Sliwkowski et al. 1999; Baselga 2001). Moreover, trastuzumab inhibits the proteolytic cleavage of the extracellular HER2 region, preventing the formation of 648-CTF fragments (Molina et al. 2002). Eventually, trastuzumab inhibits HER2 homodimerization, partially inhibiting HER2 signaling (Tsuruo et al. 1983; Junttila et al. 2009; Ghosh et al. 2011). Although historically the antitumor action of trastuzumab has been attributed to the inhibition of HER2 intracellular signaling pathways, increasing amount of both preclinical and clinical

pieces of evidence showed that the immune system actively contributes to the therapeutic effect of trastuzumab (Bianchini and Gianni 2014). One of the most important immune mechanisms activated by trastuzumab is the antibody-dependent cellular cytotoxicity (ADCC) (Cooley et al. 1999; Clynes et al. 2000; Stockmeyer et al. 2003; Gennari et al. 2004; Fan et al. 2012). Other immunological mechanisms involved in trastuzumab therapeutic effects are complement-dependent cytotoxicity (CDC), phagocytosis of cancer cells and improvement of antigen presentation to T helper cells (Park et al. 2010; Mortenson et al. 2013; Bianchini and Gianni 2014; Gall et al. 2017). In line with these observations, the antitumor activity of trastuzumab can be enhanced by immunomodulatory molecules (Stagg et al. 2011).

Primary resistance to trastuzumab affects both the neoadjuvant setting, with 15% of not responsive patients, and the metastatic setting, with 70% of patients that develop resistance (Cobleigh et al. 1999; Vogel et al. 2002; Harris et al. 2007; Narayan et al. 2009; Petrelli and Barni 2011). In the adjuvant setting, 20-70% of patients show local or distant relapse (Gajria and Chandarlapaty 2011). Trastuzumab resistance mechanisms are multiple and multiform (Rexer and Arteaga 2012). First, the alteration of the extracellular domain of HER2 can prevent the binding of trastuzumab to HER2, although controversial results were reported for both Delta16 and p95HER2, as previously described. A further strategy that has been associated with trastuzumab resistance is the masking of the trastuzumab binding epitope by other molecules. *In vitro*, the overexpression of mucin 1 or mucin 4 glycoproteins made the cells resistant to trastuzumab, probably through the masking of the trastuzumab epitope (Rexer and Arteaga 2012).

Somatic mutations on the tyrosine-kinase domain of HER2 were found in lung, gastric, colorectal, mammary and head-neck carcinomas (Stephens et al. 2004; Lee et al. 2006; Ross et al. 2014). The great majority of somatic mutations were observed in the absence of HER2 gene amplification (Chmielecki et al. 2015). Preclinical and clinical data proved that some of these mutations were responsible for trastuzumab and TKI resistance (Figure V) (Wang et al. 2006; Kancha et al. 2011; Petrelli and Barni 2011; Bose et al. 2013).

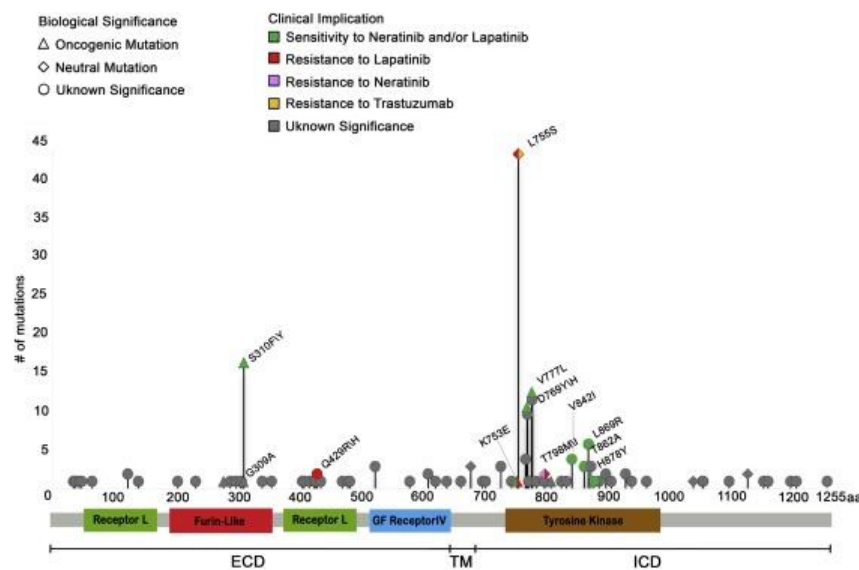


Figure V. Domain distribution, prevalence, and significance of HER2 somatic mutations. Lollipop plot representing the absolute frequency and the aminoacidic residues involved in the most common mutations reported for the HER2 gene. The lollipop plot underlines the presence of rare hot-spot variants, belonging to exons 19-20 and encompassing the tyrosine kinase domain. The biological significance for each mutation is represented by different shapes: mutations with oncogenic boost effect are pictured with triangles, whereas squares and circles represent variants of neutral or unknown significance. Some of the reported mutations showed differential behaviours with respect to anti-HER2 treatments: in particular, green alterations describe mutations conferring sensitivity to the tyrosine kinase inhibitor neratinib and lapatinib. The red, pink, and orange filled shapes summarize the different mutations associated with resistance to lapatinib, neratinib and trastuzumab, respectively. Most of the mutations are with unknown significance (grey). ECD: extracellular domain, TM transmembrane domain, ICD: intracellular domain. (Marchiò et al. 2020).

The gain-of-function mutation of PIK3CA was associated to a reduction in the rate of complete pathological response achieved by conventional chemotherapy combined to trastuzumab in neoadjuvant setting, while no differences were found related to trastuzumab response in the metastatic and adjuvant setting (Campbell et al. 2004;

Bachman et al. 2004; Ibrahim et al. 2015). Trastuzumab resistance was also related to AKT1 mutations, loss of INPP4B onco-suppressor and loss of inactivation of the onco-suppressor PTEN (Garrett and Arteaga 2011).

The inhibition of HER2 signaling pathways by anti-HER2 therapies causes the compensatory recruitment of other receptors that allow the maintenance of HER2 downstream signaling (Niederst and Engelman 2013). Increased receptor activity may depend on receptor overexpression and/or increased ligand concentration (Rexer and Arteaga 2012). Increased expression of HER1 and HER3 was found in patients with HER2-positive breast cancer characterized by the appearance of acquired resistance to trastuzumab. The activation of the enzyme TACE/ADAM17 may lead to an increased concentration of ErbB receptor ligands, such as amphiregulin and neuregulin (Wang et al. 2008). MET has also been implicated in mechanisms of resistance to trastuzumab: hyper-activation of MET due to gene amplification and/or increased stimulation by ligands can bypass trastuzumab-mediated HER2 inhibition (Shattuck et al. 2008). An increased expression and/or activity of IGF1R can also be associated with resistance to trastuzumab: IGF1R indeed dimerizes with trans-activating HER2, thus nullifying the pharmacological action of trastuzumab (Nahta et al. 2005). These mechanisms of bypass-track resistance involve not only trastuzumab, but almost all anti-ErbB drugs. These resistance mechanisms are revertible by means of a combined therapy, which includes the simultaneous use of several anti-ErbB agents with different mechanisms of action (Rexer and Arteaga 2012).

The deficiency of immune mechanisms reduces trastuzumab efficacy. Polymorphisms of Fc γ RIII receptor, which is involved in NK (Natural Killer)-mediated ADCC, altered the efficacy of trastuzumab (Rexer and Arteaga 2012). In patients with estrogen receptor-negative and HER2-positive locally advanced breast cancer, the synergistic advantage of trastuzumab in terms of a complete pathological response, when combined with conventional chemotherapy, was found to be associated with high expression of the immunoglobulin metagene (Bianchini and Gianni 2014). Also, the abundance of lymphocytic tumor infiltrate was associated with

a lower risk of recurrence in patients treated with conventional chemotherapy and trastuzumab. Besides, high IFN- γ expression was significantly related to a higher rate of complete pathological response following combination therapy with conventional chemotherapy and trastuzumab (Loi et al. 2011). Gianni and colleagues also proved how a high expression of PD-L1 was associated to resistance to trastuzumab-based neoadjuvant therapy (Gianni et al. 2011; Loi et al. 2013).

Lastly, deficit in apoptotic mechanisms (Fink and Chipuk 2013) and polymorphism of clathrin-dependent mechanisms (Freudenberg et al. 2009) were also found to be associated with trastuzumab resistance.

1.3.2 Pertuzumab

Pertuzumab is a monoclonal antibody that binds the extracellular domain of HER2, recognizing an epitope placed on the domain II, which is primarily implicated in HER2-HER3 heterodimerization. As a consequence, pertuzumab treatment causes a limited activation of the PI3K/AKT signaling pathway (Adams et al. 2006).

The efficacy of pertuzumab monotherapy in metastatic HER2-positive carcinomas was low. On the other hand, the clinical trial of phase III CLEOPATRA evidenced the advantage of pertuzumab when combined with trastuzumab and docetaxel in HER2-positive mammary carcinoma (Swain et al. 2013b; Swain et al. 2015). Currently, conventional chemotherapy combined with trastuzumab and pertuzumab represents the first line of therapy in metastatic HER2-positive breast cancer (Senkus et al. 2015; Labidi et al. 2016).

In the context of neoadjuvant treatment of locally advanced carcinomas, the two randomized controlled clinical trials NEOSPHERE and TRYPHAENA showed an improvement in the rate of complete pathological response with the therapy based on trastuzumab and pertuzumab, compared to anti-HER2 monotherapies (Gianni et al. 2011; Schneeweiss et al. 2013). Thus, pertuzumab, in combination with trastuzumab and chemotherapy, has been approved as a neoadjuvant therapy to treat patients at high risk of metastases or death with HER2-positive, locally advanced, inflammatory,

or early-stage breast cancer. The APHINITY trial, NCT01358877, evaluated the use of pertuzumab in association with trastuzumab in the adjuvant setting (Minckwitz et al. 2017). The addition of pertuzumab to therapy improved disease-free survival, but no overall survival benefit has yet been demonstrated for patients with early-stage disease. Furthermore, the 0.9% improvement in 3-year disease-free survival in the APHINITY trial should be balanced against the additional adverse effects and financial costs of 1 year of pertuzumab therapy.

1.3.3 Trastuzumab-emtansine

Trastuzumab-emtansine is a monoclonal antibody conjugated to emtansine molecule (DM1), a maytansinoid that inhibits the microtubules polymerization. The binding of the trastuzumab to its epitope causes the internalization of the complex T-DM1/HER2, which is degraded at the lysosomal level, resulting in release of DM1, which induces cell lysis (Lewis Phillips et al. 2008). Since T-DM1 maintains, in addition to this cytotoxic effect, a binding affinity for HER2 that is similar to that of trastuzumab alone, consequently the ADCC activity and the HER2-signaling inhibition observed with trastuzumab are consequently also maintained (Junttila et al. 2009).

In the second line of treatment, after taxane and trastuzumab, or in the first-line therapy, in patients with a rapid progression (≤ 6 months) after adjuvant therapy with trastuzumab, TDM-1 has shown greater efficacy than lapatinib and capecitabine in the phase III EMILIA trial (Verma et al. 2012). Consequently, TDM-1 has become the standard second-line treatment in HER2-positive advanced breast cancer patients. However, patients enrolled in the randomized trials with T-DM1 had not previously received pertuzumab. Therefore, we lack solid evidence on T-DM1 efficacy following trastuzumab/pertuzumab-containing regimens (Bon et al. 2020).

1.3.4 TKI: lapatinib and neratinib

Lapatinib is a small reversible tyrosine-kinase inhibitor which inhibits, by competition with ATP, the tyrosine-kinase activity of HER2 and EGFR, reducing the activation of

PI3K/AKT and MAPK cascades (Konecny et al. 2006). Lapatinib is indicated in combination with capecitabine for the treatment of patients with advanced or metastatic HER2-overexpressing breast cancers who have received prior therapy, including anthracycline, taxane, and trastuzumab. Nevertheless, clinical trials have proved that other HER2-targeting agents, such as T-DM1 and pertuzumab, have also shown a higher efficacy in patients pre-treated with trastuzumab. However, these regimens remain unavailable in some countries such as China. Therefore, lapatinib plus capecitabine regimen is a common option for patients who have developed resistance to trastuzumab (Wood et al. 2004). In the neoadjuvant setting, trastuzumab and lapatinib combined therapy proved superior to the anti-HER2 monotherapy by trastuzumab alone in terms of pathological complete response rate. However, since this advantage has not resulted in increased overall long-term survival, current guidelines do not recommend such association therapy (Guarneri et al. 2012; Baselga et al. 2012; Piccart-Gebhart et al. 2016).

Neratinib is a small tyrosine-kinase inhibitor that binds covalently, and therefore irreversibly, to a cysteine residue placed inside the binding pocket for ATP of HER2. In the United States, neratinib is approved for the extended adjuvant treatment of adult patients with early stage HER2-positive breast cancer, following adjuvant trastuzumab-based therapy. In Europe, neratinib is approved for the extended adjuvant treatment of adult patients with early-stage hormone receptor-positive HER2-overexpressed/amplified breast cancer and who are less than one year from completion of prior adjuvant trastuzumab-based therapy. Recently, on February 25, 2020, the FDA approved neratinib in combination with capecitabine for adult patients with advanced or metastatic HER2-positive breast cancer who have received two or more prior anti-HER2 based regimens in the metastatic setting. Of note, the American Society of Clinical Oncology (ASCO) post by Dr. Vogl in 2017 evidenced some limits of neratinib use both from a therapeutic and cost-effectiveness points of view (<https://ascopost.com/issues/december-25-2017/neratinib-is-approved-should-we-reject-it-anyway/>).

1.4 Drivers of HER2-positive breast cancer progression

Several factors might influence breast cancer progression and resistance to anti-HER2 therapies, including receptor conversion, EMT, stemness and angiogenesis.

1.4.1 Receptor conversion

The status of hormonal and HER2 receptors might change over time during the mammary carcinoma progression (Figure VI). This phenomenon is defined as receptor discordance. A recent systematic review and meta-analysis has collected the evidence from multiple studies assessing the receptor conversion during disease progression (Schrijver et al. 2018). For the estrogen receptor, the conversion rate was 22.5% from positive to negative and 21.5% from negative to positive. For the progesterone receptor, the conversion rate was 49.4% from positive to negative and 15.9% from negative to positive. HER2 loss occurred in 21.3% of cases with a HER2-positive primary tumor, while HER2 acquisition was a less frequent event, occurring in 9.5% of cases with a HER2-negative primary tumor. Receptor loss leading to a triple-negative phenotype on metastasis has been associated with a worse survival rate (Dieci et al. 2013). Moreover, molecular intrinsic subtype can shift from primary tumor to metastasis. According to an analysis of 123 patients, the distribution of molecular intrinsic subtype in primary tumor vs metastasis was 39% vs 26% for Luminal-A ($p=0.029$), 26% vs 35.8% for Luminal-B ($p=0.097$), 11.4% vs 22% for HER2-enriched ($p=0.026$) and 9.8% vs 12.2% for Basal-like ($p=0.540$) (Cejalvo et al. 2017). Of note, 2 primary tumors with HER2-enriched subtype converted to Basal-like subtype (15.38%). Data from a prospective cohort of patients showed that clonal remodelling was associated with phenotype conversion from primary tumor to metastasis. The cancer cell fraction (CCF) of different mutations in primary and metastatic pairs was estimated as a surrogate of tumor clonal architecture, with the aim of obtaining a measure of tumor clonal heterogeneity. Changes in CCF composition between matched primary and metastatic tumors were analysed in the presence or absence of

subtype conversion. Metastases showed a higher frequency of distinct mutations compared to primary tumors. These changes were more prominent in metastases with clinical subtype conversion suggesting that changes in breast cancer subtypes are linked to clonal remodelling during breast cancer evolution (Lluch et al. 2019). Schrijver and colleagues evidenced in their metanalysis how the responsibility of chemotherapy and trastuzumab on receptor conversion was debateable, since controversial data have been reported (Schrijver et al. 2018). A recent analysis of the SePHER study showed that the addition of pertuzumab to trastuzumab reduces the amount of available HER2 receptor on plasma membrane, limiting the binding of T-DM1 in cancer cells. This may justify the less favourable outcomes of second-line T-DM1 in trastuzumab/pertuzumab pre-treated patients compared to their pertuzumab-naïve counterpart (Bon et al. 2020).

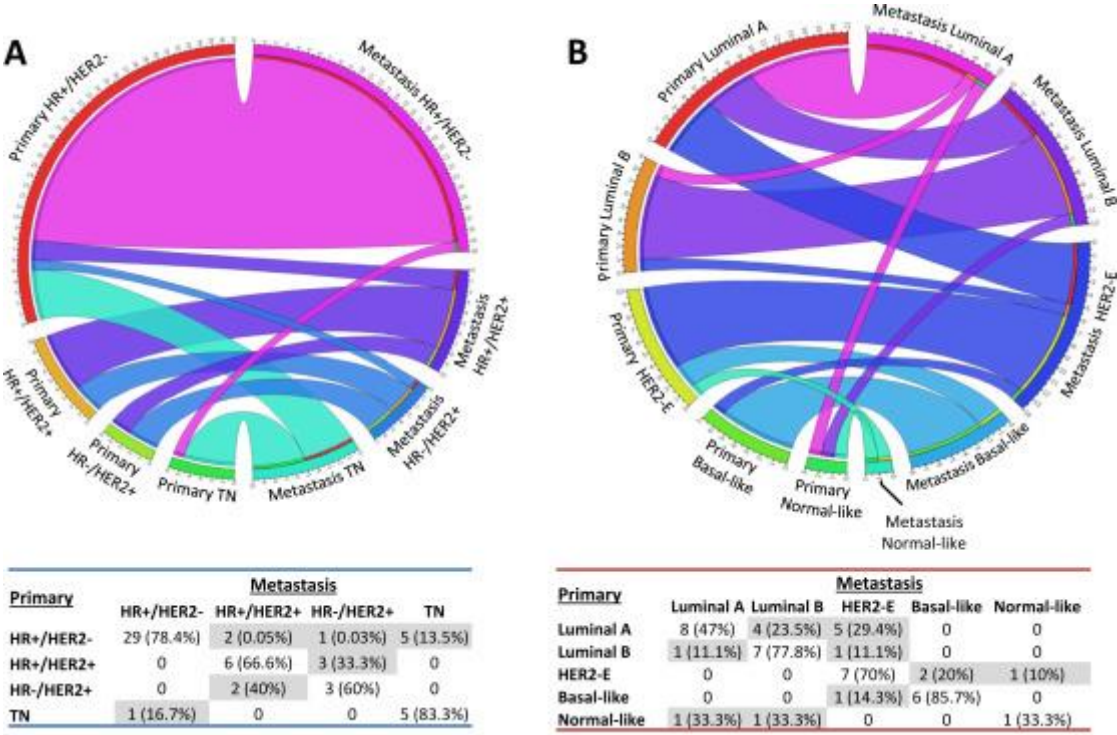


Figure VI. Circos plots displaying the conversion of clinical (A) and intrinsic (B) subtypes in breast cancer metastases. The subtype of primary lesions (left area of the plot) and of the corresponding metastasis (right area of the plot) is represented. Outer segments are labelled according to the different subtypes. Paired specimens are connected by ribbons. TN, triple-negative; HR, hormone receptor (Lluch et al. 2019).

1.4.2 Epithelial to mesenchymal transition and stemness

Breast cancer stem cells (BCSC) represent around 1-5% of tumor cells. These cells were identified thanks to their molecular profile, including CD44 high expression, absence or low expression of CD24 and missing lineage-specific markers expression (Al-Hajj et al. 2003). ALDH1 (aldehyde dehydrogenase 1) is another marker used to identify breast cancer stem cells (Moreb et al. 2012). ALDH1 allows us to distinguish two different sub-populations of BCSC: EMT-BCSC, CD44⁺/CD24^{-/low} and ALDH1⁻ quiescent mesenchymal cells; epithelial proliferative BCSC, CD44⁺/CD24^{-/low} and ALDH1⁺ cells (Zhou et al., 2019). The transition from epithelial to mesenchymal status and vice versa involves several molecules and pathways. EMT mainly involves WNT/PI3K/ β -catenin and TNF pathways that induce and stabilize SNAIL, an inhibitor of E-Cadherin. TNF also affect the expression of other factors as SLUG, TWIST, ZEB-1 and ZEB-2 (Kotiyal and Bhattacharya 2014). In Figure VII, a summary of pathways and factors involved in EMT is reported.

Some authors suggested that HER2 overexpression promotes both EMT and the emergence of cancer stem cells by the activation of metalloproteinases that lead to proteolytic cleavage and shedding of the HER2 receptor. The cleavage caused a downregulation of HER2 extracellular domain and eventually increased trastuzumab resistance (Nami and Wang 2017). On the other hand, clonal evolution of HER2 positive tumors suggest that EMT-BCSC coexist with HER2-positive cells and might be selected and give rise to Triple-negative metastases (see previous paragraph).

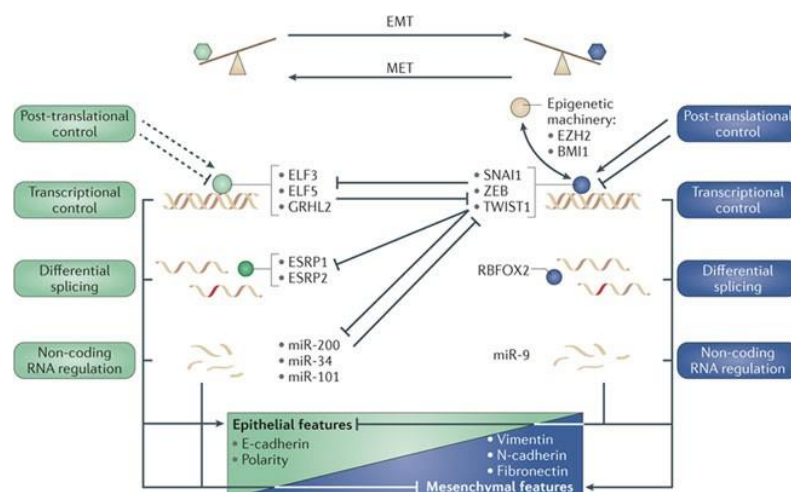


Figure VII. EMT major interconnected regulatory networks (Craene and Berx 2013).

1.4.3 Angiogenesis

The ability to form new blood vessels is one of the ten hallmarks of cancer (Hanahan and Weinberg 2011). The formation of blood vessels in the tumor context can occur by the active recruitment of angioblasts from the bone marrow (vasculogenesis) or by co-opting the existing vasculature (angiogenesis) (Hanahan and Weinberg 2011). In comparison with physiological angiogenesis, the expression of molecules that stimulate or inhibit new vessels formation is not well-coordinated in tumors. This leads to the growth of abnormal vessels, which may lack pericytes and have fenestrations (Langenkamp and Molema 2009). The presence of structural abnormalities and malformations in vessels, leads to chaotic and variable blood flow that impairs oxygen and nutrient supply. Therefore, there are often areas of hypoxia and necrosis within the tumor, which may select more malignant and metastatic cells. Moreover, hypoxic tissues produce HIF- α that stimulates the production of VEGF, and, consequently, the formation of new vessels.

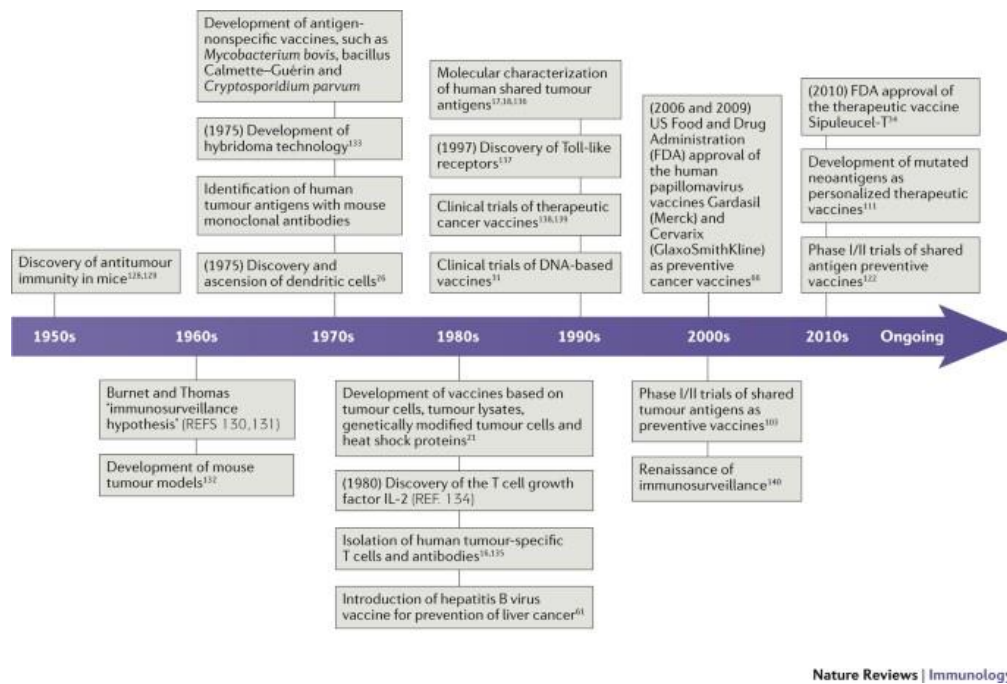
Since VEGF is a key molecular driver of physiological and pathological angiogenesis, its circuit is the main target of anti-angiogenic therapeutic approaches. The two main druggable targets are VEGF itself, inhibited by bevacizumab, or its receptors, inhibited by sunitinib and pazopanib. Sunitinib is an oral small-molecule TKI that targets several receptors, including VEGFRs, PDGFRs, c-Kit, RET, CSF1R and FLT-3. Nowadays, it is approved for the treatment of renal cell cancer (RCC) and gastrointestinal stromal tumors (GIST). Several preclinical and clinical studies have investigated the efficacy of sunitinib in breast cancer. Although sunitinib was effective in preclinical xenograft models (Abrams et al. 2003), some clinical studies reported controversial results. A study reported a benefit as second-line treatment in monotherapy, especially in patients with triple-negative or HER2-positive disease. However, another trial on HER2-negative breast cancer showed a worsening in terms of progression-free survival rate in patients treated with sunitinib alone, in comparison with patients treated with capecitabine. Other studies showed no improvement by the addition of sunitinib to chemotherapy (Koutras et al. 2012). Two clinical trials assessed

the efficacy of sunitinib in combination with trastuzumab in patients with advanced HER2-positive breast cancer, showing a beneficial effect from the combined therapy. In one study, an objective response was observed in 73% of the evaluable patients treated with sunitinib plus docetaxel and trastuzumab (Cardoso et al. 2012). In a following study, which involved a higher number of patients, the objective response rate was only 37%, but it was slightly higher in patients that had not received any other treatment previously (Bachelot et al. 2014).

2. CANCER VACCINES AND IMMUNE CHECKPOINT INHIBITORS

Cancer vaccines constitute the most complete antitumor immunological approach since they are able to enhance both innate and acquired immunity through the stimulation of the cellular compartment and induction of humoral components. In addition, patients acquire an immune memory of the tumor antigen. Cancer vaccines, as all vaccines, work well in a preventive set-up. Unfortunately, numerous phase II and phase III clinical trials have been set up to investigate the effectiveness of cancer vaccines in a therapeutic set-up rather than in a preventive one (Lu et al. 2014; Tan et al. 2015; Donofrio et al. 2018; Cuzzubbo et al. 2020). Only one of these vaccines, sipuleucel-T (Provenge®, Dendreon), was approved by the FDA in 2010 for the therapy of metastatic prostatic adenocarcinoma resistant to chemical castration. Nevertheless, new opportunities to use cancer vaccines in adjuvant regimen or to prevent tumors in high risk patients is becoming feasible (Figure VIII). New hope for the use of vaccines against tumors has emerged thanks to the identifications of tumor neoantigens, through molecular sequencing, and the introduction in the clinical practice of immune checkpoint inhibitors (ICIs). Neoantigens discovery is the basis to

design personalized cancer vaccines that might improve the activity of ICIs or might be improved by ICIs (Lollini et al. 2006; Finn 2018; Palladini et al. 2018a).



Nature Reviews | Immunology

Figure VIII. Timeline of cancer vaccine development (Finn 2018b).

Currently no antitumor vaccine has been approved by the FDA for the prevention or treatment of breast cancer, but several cancer vaccines are being investigated both at the preclinical and clinical level (Page et al. 2014; Harao et al. 2015; Pallerla et al. 2021). The most studied are protein/peptide vaccines and cell vaccines, mainly dendritic cell vaccines. HER2 is the most frequently exploited tumor antigen in the preparation of cancer vaccines in breast cancer (Benavides et al. 2009; Gates et al. 2010; Mittendorf et al. 2012; Sharma et al. 2012). Up to now, anti-HER2 vaccines tested in clinical trials have not improved patient survival rate (Al-Awadhi et al. 2018; Costa and Czerniecki 2020). Possible reasons for these negative reported results include: the negative effect of previous therapies, including chemotherapy and radiation therapy prior to vaccination; the development of immune tolerance to the HER2 antigen; the immune suppressive environment in the metastatic setting. Longer follow-up periods may be needed to determine the clinical benefits in adjuvant trials.

2.1 Antigens for cancer vaccines

Viral proteins are suitable antigens for vaccines that aim to prevent infectious-related cancers. The first approved cancer vaccines were HBV and HPV vaccines able to prevent hepatocellular carcinoma and cervical carcinoma, respectively. The success of anti-HBV vaccine was proved by the results of a Taiwanese study with a twenty-year follow-up, which showed a 70% reduction in the incidence of hepatocellular carcinoma since the beginning of the vaccination program (Chang 2009). Furthermore, three anti-HPV vaccines were afterwards approved: Cervarix (divalent), Gardasil (tetraivalent) and Gardasil-9 (9-valent). Clinical trials have shown a very high preventive antitumor effectiveness for all vaccines, with values that approximate 100% for Gardasil-9 (Joura et al. 2015).

As far as non-infectious related cancers are concerned, antigen classification can be made based on antigen location in the cell (class I, class II, class III) (Lollini et al. 2006; Lollini et al. 2011). Class I antigens are expressed at the level of the plasma membrane of cancer cells; class II antigens are not expressed directly by cancer cells, but are found at the level of the tumour microenvironment, on the plasma membrane of cells in the tumour microenvironment itself or as soluble mediators (Cavallo et al. 2011; Conti et al. 2014); class III antigens are intracellular antigens expressed by cancer cells (Lollini et al. 2010). A specific class of tumor associated antigens (TAA) are oncoantigens (Lollini et al. 2006). Oncoantigens are TAA that play a causal role in the definition of the tumor phenotype, such as HER2, EGFR, IGF1R. Antigens that also contribute to the tumor microenvironment are considered oncoantigens, such as VEGFR, FAP and CTGF. The B and T lymphocytes receptors (BCR and TCR) constitute oncoantigens towards which it is possible to induce an extremely specific immune response. An additional class of oncoantigens consists of adhesion molecules and other surface molecules which, although not directly involved in the process of tumor growth, significantly influence survival, invasion and metastatization processes (Lollini et al. 2006). Lastly, TAA can be divided in antigens with a high tumor specificity and antigens expressed also in normal tissue. A new emergent category of TAA includes

molecules involved in EMT and stemness such as SOX-2, OCT-4, TERT, CD44 and CD133 (Quaglino et al. 2020). One of the most promising antigens able to induce an immune response against BCSC is surely xCT, as proved by the efficacy of different vaccination strategies in distinct preclinical models of breast cancer (Lanzardo et al. 2016; Bolli et al. 2018; Donofrio et al. 2018).

Mutations or rearrangements of genes in tumor cells cause the production of neoantigens, which result from the translation of a previously non-existent amino acid sequence. Neoantigens are completely unknown to the host's immune system, and for this reason T cells that recognize such epitopes are able to bind them with a high affinity (Schumacher and Schreiber 2015). Neoantigens are identified by NGS and are patient-specific targets. Tumors are characterized by different rates of somatic mutations: the contribution of neoantigens to tumour immunogenicity is higher in tumors with a high mutation rate, such as those related to strong environmental carcinogens (*e.g.* lung cancer associated with cigarette smoking and melanoma associated with UV exposure, as well as in 15% of colon carcinomas). Most of these neoantigens are molecules carrying passenger mutations, that are not involved in the carcinogenesis process and in the definition of the tumor phenotype (Schumacher and Schreiber 2015). A minority of neoantigens are encoded by oncogenes and onco-suppressors so they act like driver mutations of the tumorigenesis: some examples of driver mutations capable of generating immunogenic protein products are those concerning RAS, CDK4, β -catenin, p53 and the translocations BCR-ABL, PAX3-FKHR and ETV6-AML1.

2.2 Vaccine types

The interaction between the host's immune system and the antigenic stimulus included in the vaccine can be mediated by several antigenic vehicles (Schlom et al. 2014; Ye et al. 2016). There are three main categories of cancer vaccines: cell vaccines, further subdivided into cancer cell vaccines and dendritic cell vaccines, protein/peptide vaccines and nucleic acid-based vaccines (Figure IX) (Lollini et al.

2015). Cellular vaccines are expensive and not pharmacologically definable, characteristics that make the pharmaceutical production on a large-scale problematic. Dendritic cell vaccines cannot be produced on a large-scale since these vaccines are based on autologous dendritic cells. Molecular-defined synthetic vaccines, such as protein/peptide vaccines and nucleic acid-based vaccines, are more easily adaptable to large volumes of production.

Protein/peptide vaccines are poorly immunogenic, requiring the use of highly immunostimulating adjuvants; in addition, peptide vaccines are effective only in patients with specific HLA haplotypes. Nevertheless, peptides, small-molecule haptens, and self-antigens can elicit high-titer antibody responses when presented on the surface of virus-like particles (VLP) (Caldeira et al. 2020). VLP are nanoparticles that are spontaneously assembled from viral structural proteins and can function as scaffolds for the presentation of epitopes from any source (Crossey et al. 2015; Caldeira et al. 2015; Hu et al. 2017; Lino et al. 2017). VLP are naturally biocompatible and have no viral genome, being, therefore, not contagious. VLP are effectively eliminated or degraded by the human body, limiting the occurrence of side effects. In addition, they present epitopes in dense repetitive arrays, making them effective scaffolds that can elicit antibodies to multiple substances (Caldeira et al. 2020).

Vaccines based on nucleic acids are not adequately internalized by the patient's cells in most cases, resulting in low transgene expression levels, and the ways used to increase the rate of internalization of the transgene in host cells, even if potentially effective, create new problems, such as the poor compliance of the patient in the case of electroporation and the permanence or the neutralization of the virus by pre-formed antibodies in the case of viral vectors (Osada et al. 2009; Aurisicchio and Ciliberto 2012; Lee et al. 2015b). The use of chimeric or xenogenic antigens improves the effectiveness of DNA vaccines (Cavallo et al. 2014; Riccardo et al. 2017).

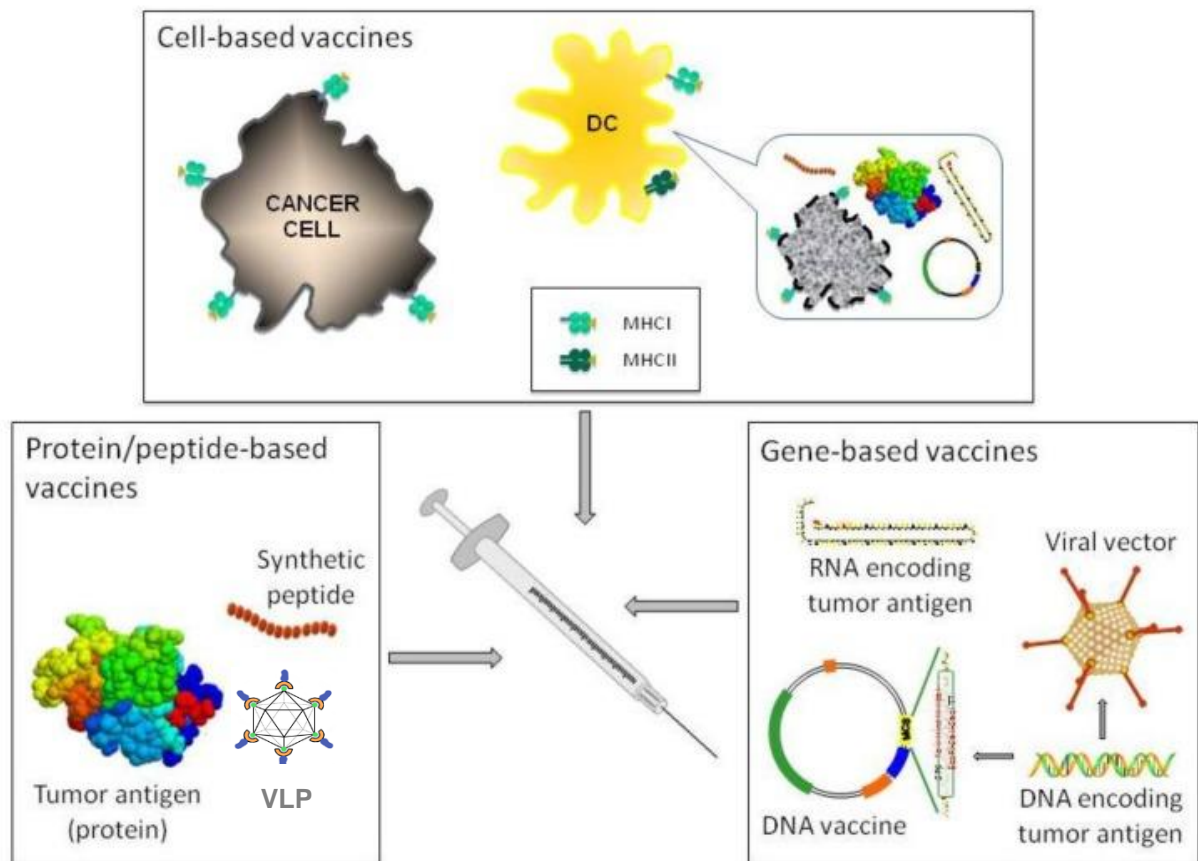


Figure IX. Schematic representation of the different anti-cancer vaccination strategies. Modified from (Lollini et al. 2015).

2.3 Immune checkpoint inhibitors

All the immune responses, including the antitumor ones, are based on the delicate balance between the recognition of non-self and the modulation of duration and intensity of the immune response. Indeed, an uncontrolled immune response is harmful to the organism, as it can damage the affected tissues or give rise to autoimmune responses. For this reason, during the evolutionary process, the immune system has developed a variety of inhibitory mechanisms aimed at controlling the immune response, including the so-called immune checkpoints.

Immune checkpoints represent the main modulators of the immune response and include a fine system of interactions between receptors and ligands that are expressed on the surface of immune cells. Cancer cells can express molecules involved in these immune modulations to evade the antitumor immune response. For this reason,

immune checkpoint inhibitors have been developed, with the aim of promoting the reactivation of the immune system against cancer. CTLA-4, PD-L1 and PD-1 are currently the modulators with the greater clinical relevance. The introduction of ICIs in clinical practise has completely revolutionized the field of oncoimmunology. This new class of immunotherapeutic drugs includes a series of monoclonal antibodies directed against these immune checkpoints (Figure X). The antibody binding interferes with the lymphocytic activity switch off, allowing infiltrated T lymphocytes to rescue their natural effector anti-tumor function (Wei et al. 2018).

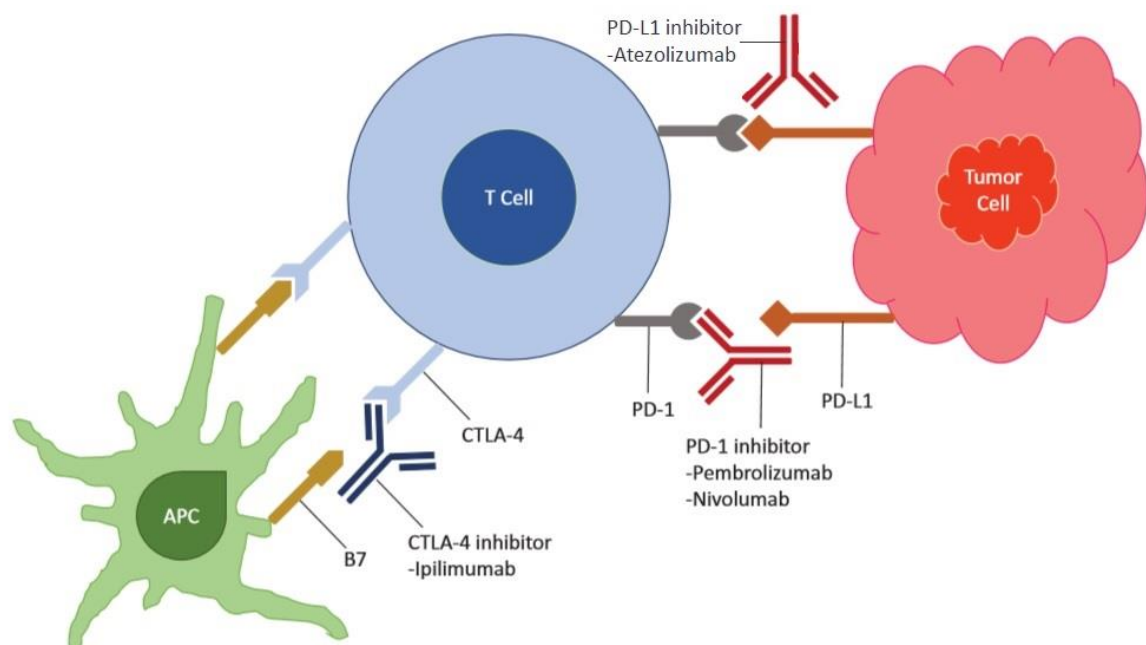


Figure X. Inhibition of immunological checkpoints by ICI - modified by (Ahmed et al. 2019). CTLA-4 inhibitor (ipilimumab) prevents the binding between CTLA-4 and ligand B7 expressed on antigen-presenting cells (APC), blocking the inhibitory signal of T lymphocytes. PD-1 (pembrolizumab and nivolumab) and PD-L1 (atezolizumab) inhibitors prevent PD-1 and PD-L1 binding, blocking the signaling pathway that inhibits T cell activity.

To date, ICI has revolutionized the treatment of patients with advanced cancer and poor prognosis, recording a relevant increase in the overall survival rate, as observed in patients with melanoma, non-small cell lung cancer, prostate cancer, bladder cancer, head and neck cancer, renal cell carcinoma, and hematological tumors (Iwai et al. 2002; Hodi et al. 2010; Motzer et al. 2015; Herbst et al. 2016; Zak et al. 2016; Ferris et al. 2019).

It has been observed that in 10-30% of patients the treatment with antibodies against PD-1, PD-L1 or CTLA-4 leads to a more lasting reduction in tumour size than that observed with traditional therapeutic methods (Champiat et al. 2018), together with an increase in the overall survival rate, especially in the treatment of melanomas and tumors of the head and neck (Ferris et al. 2016; Larkin et al. 2018).

2.3.1 PD-1 and PD-L1

PD-1 (Programmed cell death protein 1), also known as CD279, is an important inhibitory regulator of immune response mainly expressed on the surface of activated T and B lymphocytes, some T regulatory (Treg) cells, NK T cells, monocytes and some dendritic cell subtypes (Riella et al. 2012). The two natural ligands of PD-1 are PD-L1 (also known as B7-H1 or CD274) and PD-L2 (also known as B7-DC or CD273), which are expressed on the surface of APC cells, including dendritic cells, macrophages and monocytes (Hodi et al. 2008; Seidel et al. 2018).

The inhibitory role of PD-1 following binding with its ligands is mediated by phosphatase recruitment, such as SHP2, on the ITSM sequence of the intracellular domain of the receptor. Specifically, SHP2 phosphatase inhibits both the signaling pathways mediated by ZAP70 and PI3K-AKT kinases and the signaling pathway mediated by the RAS protein or mTOR. The result is a decrease of transcriptional factors, such as AP-1 (activator protein-1) and NF- κ B (nuclear factor- κ B) (Sharpe and Pauken 2018), that leads to a reduction of stimulatory cytokines, including IL-2, TNF- α and IFN- γ and an inhibition of the proliferation and effector lymphocytic function (Keir et al. 2008).

PD-1 is one of the main regulators of functional lymphocyte exhaustion, characterised by a loss of the effector function of CD8⁺ T lymphocytes due to the persistent exposure to viral or tumour antigens. It has been shown that PD-1-inhibition by anti-PD-1 monoclonal antibodies reinforced the lymphocytic activity, restoring the effector function (Lee et al. 2015a).

PD-L1 (Programmed cell death-1 ligand-1) is a type I transmembrane glycoprotein, homologous to the B7 ligands (for this reason also known as B7-H1), which physiologically binds the PD-1 receptor. The ligand has an immunoglobulin structure with an extracellular domain, a transmembrane domain and an intracellular tail (Keir et al., 2008; Lin et al., 2008). The ligand is constitutively expressed on cells of myeloid origin, such as dendritic cells or myeloid-derived suppressor cells (MDSC) (Gato-Cañas et al. 2015). However, PD-L1 expression may also be induced in other cell types, primarily cancer cells, as a result of inflammatory cytokines (Ritprajak and Azuma 2015; Liu et al. 2017). An example is IFN- γ , one of the main modulatory cytokines of the immune response, which is produced in the tumour microenvironment by tumor infiltrating T lymphocytes. The binding of IFN- γ with its own receptor activates the JAK/STAT signaling pathway ultimately resulting in the activation of the interferon regulatory factor 1 (IRF1) (Benci et al. 2016), which binds to PD-L1 promoter and stimulates its expression (Ribas et al. 2015; Garcia-Diaz et al. 2017; Fares et al. 2019). This mechanism, which involves several cytokines and transcriptional factors, is a physiologically adaptive process aimed at controlling immune and inflammatory responses, which cancer cells use to their advantage in the immune escape phase. The increased expression of PD-L1 by cancer cells causes the inhibition of the cytotoxic lymphocytic function through the binding between PD-L1 and PD-1, inducing apoptosis, anergy and exhaustion in CD8⁺ T lymphocytes infiltrating the tumor (Dong et al. 2017).

Furthermore, the expression of PD-L1 by cancer cells stimulates survival signals in cancer cell. The intrinsic PD-L1 signal makes the cancer cell resistant to the cytotoxic effect of IFN- γ , by inhibiting STAT3 and interfering with its signaling pathway (Gato-Cañas et al. 2017). In addition, recent studies have shown that PD-L1 can increase tumor survival and proliferation regardless of its binding to PD-1, by interfering with apoptosis, autophagia and mTOR transducer expression. However, these mechanisms have not yet been fully clarified (Azuma et al. 2008; Clark et al. 2016; Escors et al. 2018; Lamberti et al. 2020b).

PD-L2 (Programmed cell death 1 ligand 2) is expressed on activated dendritic cells, macrophages, bone marrow-derived mast cells and peritoneal B1 cells (Zhong et al. 2007). PD-L2 expression can be induced by LPS and BCR in B cells and by GM-CSF and IL-4 on DCs (Latchman et al. 2001). PD-L2 is expressed on solid tumors as well as in hematopoietic malignancies, even though it is expressed to a lesser extent when compared to PD-L1 (Ohigashi et al. 2005; Yang et al. 2019). However, PD-L2 binds to PD-1 with a higher affinity as compared to PD-L1 (Keir et al. 2008). The immunosuppressive role of PD-L2 in cancer and its prognostic value, together with the therapeutic potential of PD-L2 blockade, will require further investigations (Solinas et al. 2020).

Nivolumab is a human IgG4 monoclonal antibody, directed against the human PD-1 receptor (Wang et al. 2014; Robert et al. 2015). In 2014, nivolumab was approved by the FDA for the treatment of advanced metastatic melanoma, refractory to conventional therapies and treatment with ipilimumab (Larkin et al. 2018). About a year later, FDA approval was extended to the second-line treatment in patients with non-small cell lung cancer (NSCLC) (Raju et al. 2018). Considering the promising data observed in a phase II study with advanced metastatic melanoma patients treated with nivolumab and ipilimumab, in 2016 the FDA approved the combined therapy of the two monoclonal antibodies for the treatment of patients with non-resectable melanoma without the BRAF mutation (Hodi et al. 2016). This was the first FDA approval of a combined regimen of two immunotherapeutic drugs in cancer treatment. In the following years, the FDA approved nivolumab associated with ipilimumab, as a second-line therapy, for the treatment of head and neck tumors (Ferris et al. 2019), urothelial carcinoma (Sharma et al. 2017), colorectal carcinoma (Overman et al. 2017), hepatocellular carcinoma (El-Kenawy et al. 2017; El-Khoueiry et al. 2017) and advanced renal carcinoma (Motzer et al. 2018).

Pembrolizumab is a humanized IgG4 monoclonal antibody directed against the human PD-1 receptor (Du Rusquec et al. 2019). Pembrolizumab, similarly to nivolumab, recognizes the PD-1 receptor and prevents the binding between PD-L1 or

PD-L2 ligands to the receptor. The several clinical studies carried out on the use of pembrolizumab, known with the acronym KEYNOTE, have focused on the use of the antibody as first or second line of therapy for the treatment of patients with different types of advanced-stage cancers, including NSCLC, melanoma, bladder cancer, cervical cancer, gastrointestinal tumors, hepatocellular tumors and head and neck tumors (Du Rusquec et al. 2019). Considering the results of clinical trials, in 2014, the FDA approved the use of pembrolizumab in the treatment of advanced melanoma, refractory to other therapies (Cowey et al. 2018). In the following years the approval was also extended to patients with NSCLC refractory to the conventional therapies, and in patients with high expression of PD-L1 (tumor proportion score 50%) as a first-line therapy (Pai-Scherf et al. 2017)

Atezolizumab is a monoclonal IgG1 antibody that selectively binds the PD-L1 ligand, but not PD-L2, preventing its binding with the PD-1 receptor and enhancing the anticancer activity of T lymphocytes (Blair 2018). In 2016, atezolizumab was approved by the FDA as a second-line treatment of urothelial metastatic carcinoma (Rosenberg et al. 2016). In the following years, approval was extended to third-line treatment of metastatic NSCLC (Fehrenbacher et al. 2016; Rittmeyer et al. 2017) and to treat patients with triple-negative breast cancer, positive for PD-L1 (expression 5% on cancer cells or immune cells infiltrating the tumor) (Shah et al. 2018).

Durvalumab is a monoclonal IgG1 antibody directed against the PD-L1 ligand. In 2017, the FDA approved the use of the antibody as a second-line therapy for patients with metastatic or advanced localized urothelial cancer (U.S. FDA. Highlights of prescribing information. Imfinzi™ (durvalumab), 2017) thanks to the positive results of the clinical trial that evidenced a clinical response of 5.1% and a median overall survival of 18.2 months (Powles et al. 2017). In 2018, FDA approval was extended to the use of durvalumab as a maintenance therapy for advanced stage NSCLC patients who had previously undergone traditional chemotherapy. The Phase III PACIFIC clinical study showed a good efficacy in the use of the antibody as consolidation

therapy in patients with advanced localized, not operable NSCLC, compared to the placebo group (Antonia et al. 2018).

2.3.2 Resistance to ICI

Immune checkpoint inhibitors have now entered in clinical practice, becoming the standard therapy for the treatment of multiple forms of cancer. Despite this, it is estimated that the response to PD-1/PD-L1 inhibitor monotherapy varies between 20% and 40% (Borghaei et al. 2015).

A recent analysis of 262 patients with 19 different types of cancer and treated with ICI showed an overall response rate of 29% and a long-term response rate (> 2 years) of 11.8% (Gauci et al. 2019). The response to ICI-based monotherapies is closely related to the type of treated tumor: highly sensitive tumors such as Hodgkin's lymphoma, melanoma at an advanced stage and NSCLC show a rate of response between 20% and 65% (Wolchok et al. 2013; Larkin et al. 2015), compared to particularly resistant tumors such as colorectal cancer with stable microsatellites, which shows a rate of response of less than 10% (Le et al. 2017). Despite this, many patients with "ICI-high sensitive tumors" still do not respond to therapy. In fact, in the treatment of advanced melanoma it is estimated that about 40-60% of patients show no significant therapeutic response during treatment and a substantial proportion of responsive patients experience cancer recurrence within 2 years of treatment (Robert et al. 2015; Larkin et al. 2018). Similarly, it has been observed that only 20-30% of NSCLC patients are responsive to therapy (Topalian et al. 2014). Understanding the mechanisms that influence the response to therapy and identifying patients that may be more susceptible to develop resistance to ICI treatment is essential to choose the most suitable therapy for them.

The mechanisms of resistance to immune checkpoint inhibitors can be determined both by intrinsic factors, which are linked to the tumor cell characteristics, and by factors extrinsic to the tumor cells, related to its microenvironment. Resistance mechanisms include reduced tumour antigenicity or alteration of the mechanisms of

antigen presentation, which are responsible for the low T cell infiltration into the tumour microenvironment, alterations of signaling pathways, that may interfere with the antitumour immune response, or production of immunosuppressive cytokines. In addition, the presence of an immunosuppressive tumor microenvironment and the progressive loss of function of T cells, epigenetic modifications and activation of alternative immune checkpoints may contribute to the resistance to ICI therapies observed in patients (Pitt et al. 2016; Jenkins et al. 2018; Schoenfeld and Hellmann 2020).

2.3.2.1 Hyperprogressive disease

Hyperprogressive disease (HPD) was a condition in which patients showed a rapid disease progression after the initiation of ICI therapy. We have recently summarized some aspects of HPD in the manuscript of Angelicola and colleagues (Angelicola et al. 2021) and here I have briefly reported the main relevant points included in the manuscript.

4-29% of cancer patients develops HPD, being even a more frequent event in patients with NSCLC (from 8 to 21%), advanced gastric cancer (from 10 to 29%), head and neck squamous cell carcinoma (29%) and melanoma (9%) (Saâda-Bouزيد et al. 2017; Champiat et al. 2017; Ferrara et al. 2018). Several groups assessed the phenomenon and proposed different criteria for HPD definition, which resulted in noticeable variations in HPD rates. Kas *et al.* have recently suggested an optimized and homogenized definition of HPD (Kas et al. 2020).

Many studies have identified several factors associated with an increased risk of developing HPD during ICI therapy, among which was older age (≥ 65 years) (Motzer et al. 2015; Brahmer et al. 2015; Borghaei et al. 2015; Champiat et al. 2017). Previous irradiation is also associated with higher incidence of hyperprogression (Saâda-Bouزيد et al. 2017). Hyperprogression was significantly associated with the presence of more than 2 metastatic sites before the treatment (Ferrara et al. 2018). Mouse double minute homolog (MDM2/MDM4) amplification and EGFR alterations were indicated as

genomic markers of the increased risk of hyperprogression (Kato et al. 2017). Furthermore, patients with oncogene-addicted NSCLC, *e.g.* ALK, EGFR and STK11, did not benefit from IC blockade therapy, probably because of the “cold” nature of these tumors (Lamberti et al. 2020a). Hyperprogression was also associated with elevated serum lactate dehydrogenase (LDH) concentration.

No associations between HPD and tumor histology, baseline tumor size and previous lines of therapy have been reported (Champiat et al. 2017; Saâda-Bouزيد et al. 2017; Kato et al. 2017). As far as the association of PD-L1 expression with HPD is concerned, studies have shown discordant results. Nevertheless, a significant inverse correlation between PD-L1 expression in tumor cells and HPD has been detected in NSCLC patients (Lo Russo et al. 2019).

ICs, such as CTLA-4, PD-1 and PD-L1, can be overexpressed on Treg cells. A rapid expansion of forkhead box P3+ (Foxp3+) Treg cells has been observed in the tumors of HPD patients with advanced gastric cancer treated with nivolumab. Moreover, PD-1 blockade augments the proliferation and suppressive activity of human Treg cells *in vitro* (Kamada et al. 2019).

IC blockade therapy can also induce compensatory mechanisms and lead to T-cell exhaustion, local immune suppression and tumor escape. Two independent studies have reported the compensatory upregulation of ICs, including lymphocyte activation gene-3 (LAG-3), T-cell immunoglobulin and mucin domain-3 (TIM-3) and CTLA-4, on CD8+ T cells after PD-1 blockade in immunocompetent murine models of ovarian cancer and lung adenocarcinoma (Koyama et al. 2016; Huang et al. 2017). IC blockade therapy can also upregulate CD38 on tumor cells, leading to immune suppression and resistance to therapy (Chen et al. 2018). In addition, the aberrant expansion of peripheral exhausted CD4+ memory T cells has been reported to occur after the first administration of anti-PD-1/PD-L1 antibodies in patients with HPD, unlike non-HPD patients (Zuazo-Ibarra et al. 2018).

The compensatory immune response triggered by IC blockade can induce the production of immunosuppressive cytokines and other soluble mediators. In

preclinical studies, PD-1/PD-L1 blockade has been observed to increase IL-10 secretion by tumor infiltrating dendritic cells (DCs) and the upregulation of PD-L1 on DCs, leading to tumor immune escape. In addition, tumor-specific CD8⁺ PD-1⁺ T cells, in patients with advanced melanoma under PD-1 blockade therapy, overexpressed the IL-10 receptor (IL-10R). The blockade of IL-10 strengthened the effect of anti-PD-1 antibodies in expanding tumor-specific CD8⁺ T cells, and thus reinforced their antitumor action (Lamichhane et al. 2017).

Angiopoietin-2 (ANGPT2) has been proposed to act as a predictive and prognostic marker in ICI-treated patients with advanced melanoma. High levels of ANGPT2 in serum before treatment were associated with reduced response and/or overall survival and with higher levels of immunosuppressive M2 macrophages in ICI-treated patients (Scholz et al. 2011; Wu et al. 2017).

Aberrant inflammation that is caused by increased T helper 1 (Th1) and Th17-dependent secretion of inflammatory cytokines, such as IFN- γ , IL-6 and IL-17, which are associated with neutrophil recruitment, has been observed in patients with prostate cancer and melanoma that were treated with PD-1/PD-L1 inhibitors (Dulos et al. 2012). Neutrophil depletion and IL-6 blockade have been found to be effective antitumor immune responses in mouse models (Stein et al. 2019). Moreover, the interaction between the Fc domain of ICIs and Fc-receptors (FcR) induces macrophage reprogramming, from the M1 to M2 phenotype, in patients with HPD (Lo Russo et al. 2019).

Tumor-specific non-lytic CD8⁺ T cells induce the overexpression of PD-L1 and IDO1, which are associated with adaptive immune resistance and stemness phenotype in tumor cells (Stein et al. 2019).

MDM2 is an oncoprotein that is involved in the degradation and inhibition of the p53 tumor suppressor protein. The amplification of this gene has frequently been observed in HPD patients. IFN- γ -induced interferon regulatory factor 8 (IRF-8) induces MDM2 overexpression by binding its promoter (Zhou et al. 2009; Kato et al. 2017).

The activation of the PD-1 axis on T cells reduces T-cell proliferation (Yao et al. 2018), while PD-1 inhibition on neoplastic T cells induces growth acceleration. PD-1 expression on tumor cells drives melanoma tumorigenesis via PD-1/PD-L1 interaction (Kleffel et al. 2015). Conversely, preclinical data suggest that PD-1 blockade may increase tumor growth by interfering with the PD-1-dependent upregulation of proapoptotic proteins, *e.g.* BIM, p15INK4 and cyclin-dependent kinase 2 (Du et al. 2018).

PD-1/PD-L1 interaction transmits antiapoptotic signals to cancer cells, leading to resistance to T-cell-mediated cytotoxicity and Fas-mediated apoptosis. The elimination of the intracellular domain of PD-L1 ablated cancer resistance to immune response, leading to tumor regression (Azuma et al. 2008). PD-L1 expression also protects tumor cells from IFN- γ -antitumor action by inhibiting STAT3-caspase 7 signaling (Gato-Cañás et al. 2017). Finally, activating mutations of EGFR drive PD-L1 expression on several tumor types, including NSCLC and breast cancer (Sun et al. 2018). The EGFR-dependent mechanism of PD-L1 regulation involves post-translational modifications. Indeed, the inhibition of EGFR signaling has been seen to destabilize PD-L1 expression in mouse models, leading to enhanced PD-1 blockade therapeutic efficacy.

IFN- γ and CD38 are factors associated with resistance to ICI therapy. We have recently proposed their possible involvement in HPD (Angelicola et al. 2021). We suggested that IFN- γ contributes to HPD onset in predisposed patients via the induction of the inflammasome pathway and consequent MDSC recruitment, the induction of IDO1 activity, which may result in the downregulation of p53 in tumor cells, and the activation of activation-induced cell death (AICD), which leads to T-cell depletion. On the other hand, CD38 upregulation after IC blockade therapy may contribute to the development of hyperprogression through the release of high levels of adenosine into the TME, and the consequent activation of the ADORA2a pathway, which may lead to tumor insensitivity to IFN- γ action, the downregulation of p53 with consequent tumor growth, and strong immunosuppression. CD38 upregulation may also be an adaptive immune response to a hyperactivated immune setting induced by

ICI therapy. In this context, CD38 may promote the apoptosis of effector T cells via the AICD process, leading to a protumorigenic setting. Finally, CD38 may enhance hypoxia signaling pathways in tumor cells or endothelial cells, leading to increased angiogenesis, immunosuppression and tumor proliferation.

Aim of the work

Target therapy has significantly improved the management and the outcome of different types of tumors, including HER2-positive breast cancers. Nevertheless, overall, target therapy has also shown several limitations over the years, as demonstrated by the significant rate of patients who developed resistance to therapy. Tumor heterogeneity is a major hindrance to the success of target therapy.

The aim of this thesis was to find alternative approaches to overcome tumor heterogeneity by modulating antitumor immunity and searching for new druggable targets.

HER2 is a suitable target antigen for cancer vaccines, as proved by the therapeutic use of monoclonal antibodies in HER2-positive breast cancer patients. In the Chapter 1 of the Results, I reported the activity of a cancer vaccine, based on HER2-conjugated virus-like particles (VLPs), in different preclinical models of HER2-positive mammary carcinoma, highlighting the advantages brought by the treatment and the limitations of the distinct preclinical models investigated. Subsequently, I described strategies to enhance antitumor immune responses.

The ability to identify new therapeutic targets is strictly related to the availability of preclinical models able to mirror the dynamic condition of tumor growth, reflecting tumor progression and evolution observed in patients. In the Chapter 2 of the Results, I took advantage of distinct models of breast cancer based on either cell lines, derived from HER2 transgenic mice, and patient-derived xenograft (PDX) models, obtained through the implantation of HER2-positive tumor fragments. I introduced new targets that could be relevant for therapeutic and preventive approaches, both immunological and otherwise, against HER2-positive mammary carcinoma. These results clearly do not claim to clarify the complex condition of tumor heterogeneity, but they lay the groundwork for the development of new therapeutic strategies that consider the tumor as a community of distinct and separate subpopulations.

Results

1. IMMUNOLOGICAL STRATEGIES

The immune system is a physiological weapon against tumor onset. Overall, antitumor immunological strategies consist in leveraging immune system components to counterattack tumors.

Anti-HER2 cancer vaccines might boost anti-HER2 monoclonal antibody activity by inducing both a comprehensive anti-HER2 polyclonal antibody response and immunological memory.

Nevertheless, the immune system response against tumor antigens is not so easily inducible and immune responses are not so long-lasting. Two key points involved in these limitations are the break of immune tolerance against a self-antigen such as HER2 and the immune response switch off by immune checkpoints.

In this chapter the activity of the HER2-VLP vaccine was investigated in different HER-2-positive mammary carcinoma models and compared with an anti-HER2 DNA vaccine (pHuRT). These data, resulted from a collaboration with Prof. Adam Sander (University of Copenhagen, Copenhagen, Denmark) have been included in the manuscript of Palladini and colleagues (Palladini et al. 2018b).

Then, the study was also focused on approaches aimed at both breaking the immune tolerance and to enhancing the immune response, together with their limits. Some of these results have been included in published manuscripts (Nanni et al. 2018; De Giovanni et al. 2019b; De Giovanni et al. 2019a).

1.1 Anti-HER2 cancer vaccines: HER2-VLP and pHuRT

1.1.1 Anti-HER2 cancer vaccines in the prevention of mammary carcinoma

The antigen displayed on HER2-VLP vaccine was the extracellular domain of human HER2 (HER2-ECD). The antigen was produced in S2 insect cells transfected with the

SpyCatcher-HER2-ECD sequence coding the fusion antigen (Figure 1A). Virus-like particles were used as a vehicle of the SpyCatcher-HER2-ECD (Figure 1B).

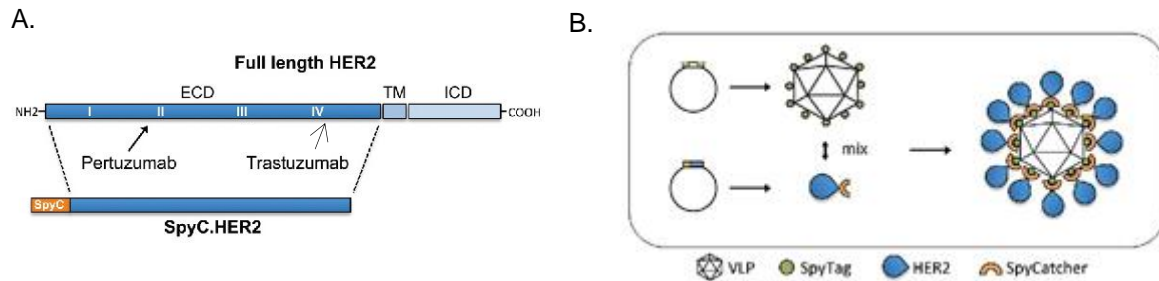


Figure 1. HER2-VLP vaccine production. A. The HER2 extracellular domain (ECD) was genetically fused at the N-terminus to SpyCatcher (SpyC). TM = trans membrane, ICD = intracellular domain. Arrows indicate HER2 subdomains targeted by pertuzumab and trastuzumab mAbs. B. Schematic showing the HER2-VLP vaccine development process. The Spytagged VLP subunit and the SpyCatcher-HER2 antigen are separately expressed and purified, and then mixed. The tag/catcher conjugation insures a directional, high-density ‘virus-like’ display of HER2 on the surface of the VLPs (Palladini et al. 2018b).

HER2-VLP vaccine induced complete protection from mammary tumors in Delta16 mice with only three vaccine administrations. On the other hand, pHuRT DNA vaccine, effective in preventing lower aggressive mammary carcinogenesis of HER2 mice (De Giovanni et al. 2014), failed to elicit an immune stimulation able to delay tumor onset (Figure 2A). In double transgenic HER2/Delta16 F1 mice almost 50% of mice chronically treated with HER2-VLP vaccine were tumor-free at 1-year of age, while pHuRT treated mice were not protected (Figure 2B).

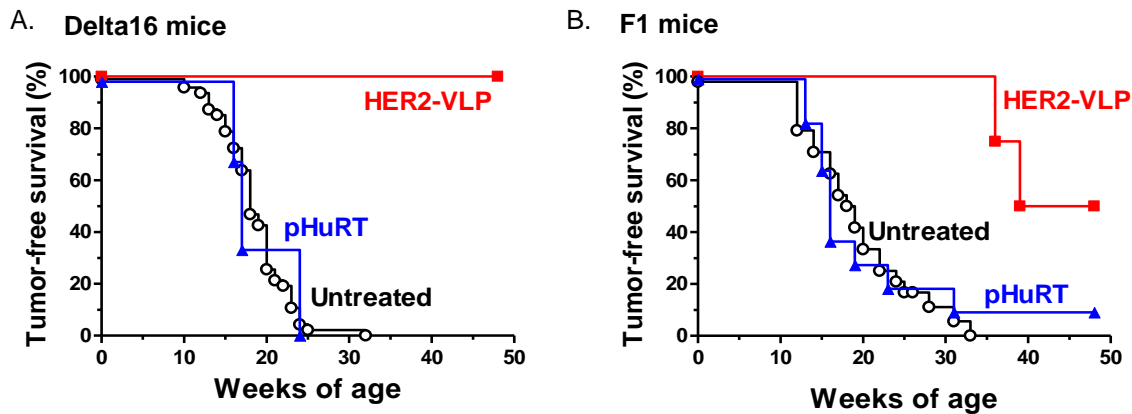


Figure 2. Preventive activity of HER2-VLP vaccination against HER2-driven mammary carcinogenesis. A. Groups of 3 Delta16 mice were treated intramuscular (i.m.) with HER2-VLP vaccine or electroporated pHuRT DNA vaccine. Mantel-Haenszel test: HER2-VLP vs pHuRT, $p < 0.01$; HER2-VLP vs Untreated, $p < 0.001$. B. Groups of 7–11 HER2/Delta16 F1 mice were vaccinated with HER2-VLP or with electroporated pHuRT vaccine. Mantel-Haenszel test: HER2-VLP vs pHuRT or Untreated, $p < 0.001$. Modified by (Palladini et al. 2018b)

1.1.2 Anti-HER2 antibodies induced by cancer vaccines in the preventive set-up

The anti-HER2 antibody production by HER2-VLP vaccine was higher than the one induced by pHuRT vaccine, both in Delta16 mice ($p < 0.05$, at least by Student's t-test) and F1 mice ($p < 0.001$, at least by Student's t test), and this production in Delta16 mice was ten-times higher than in HER2/Delta16 F1 mice (Figure 3). Although both transgenic mice showed a fast tumor growth, Delta16 mice were probably less tolerogenic against the ECD of HER2 full-length isoform, antigen included in HER2-VLP vaccine preparation or produced by pHuRT plasmid. This point might explain why HER2/Delta16 F1 mice were not completely protected. Although we did not test vaccine activity in mice transgenic for only HER2 full-length isoform, due to long tumor latency (De Giovanni et al. 2014; Palladini et al. 2017), we managed induction of antibodies with HER2-VLP vaccine, confirming a level quite similar to that of F1 mice (Figure 3A). We concluded that the most suitable tumor-aggressive model to test anti-HER2 vaccines is the double transgenic F1 mouse, since it combines an aggressive tumor phenotype with immune tolerance against both Delta16 and HER2 full-length isoforms.

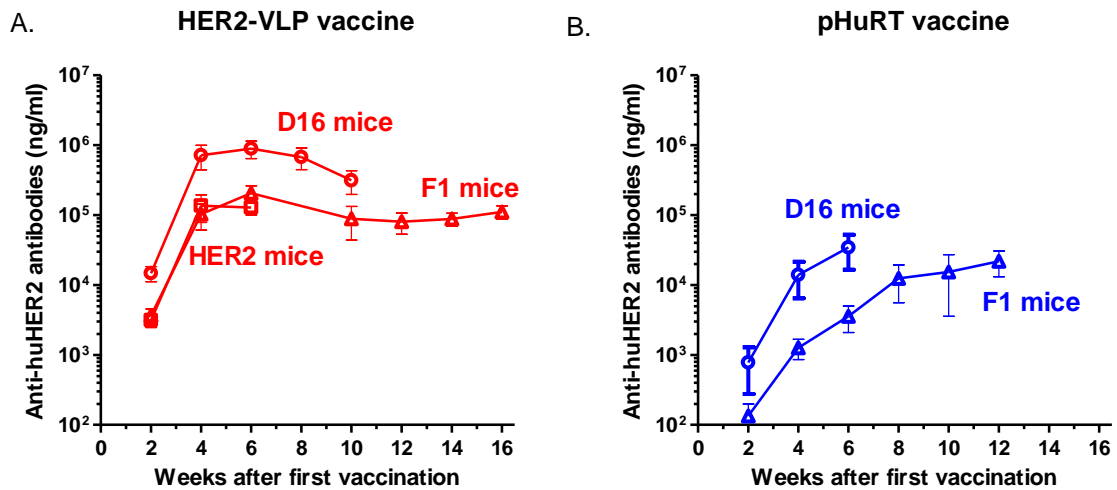


Figure 3. Kinetics of anti-human (hu) HER2 antibodies. Antibodies in mouse sera were tested by ELISA. Each point represents the mean \pm SEM of 3–13 individual sera of different mice. F1 mice were treated according to a chronic protocol. FVBhuHER2 (HER2) and Delta16 (D16) mice were treated according to a short (3 vaccinations) protocol. A. HER2-VLP vaccinated mice. Antibody concentrations elicited by HER2-VLP in Delta16 mice were significantly higher than in F1 and HER2 mice: $p < 0.05$, at least (Student's t-test). B. pHuRT vaccinated mice. Antibody concentrations elicited by pHuRT in Delta16 mice were significantly higher than in F1 mice: $p < 0.05$, at least (Student's t-test).

1.1.3 HER2-VLP vaccine activity in the therapeutic set-up

We evaluated HER2-VLP vaccine activity in a therapeutic set-up, using wild-type mice grafted with HER2-expressing mammary carcinoma cells. For this purpose, we induced tumor growth in immunocompetent FVB mice by injecting MamBo89HER2^{stable} cell line (Figure 4A and B). We established this cell line from a HER2-positive spontaneous mammary tumor arisen in a HER2 transgenic mouse. A second model was based on the engraftment in FVB mice of HER2-positive tumor fragments from primary transgenic mammary carcinomas of HER2 mice (Figure 4C and D). Mice were biweekly immunized with HER2-VLP vaccine until the end of the experiment and the treatment significantly inhibited tumor growth. In both models, HER2-VLP vaccine induced the production of high and comparable levels of anti-HER2 antibodies. Nevertheless, the vaccine was more effective in mice grafted with tumor fragments, in which we observed 4 of 5 mice remaining tumor-free, compared

to mice bearing MamBo89HER2^{stable} tumors, which showed only a delayed tumor growth.

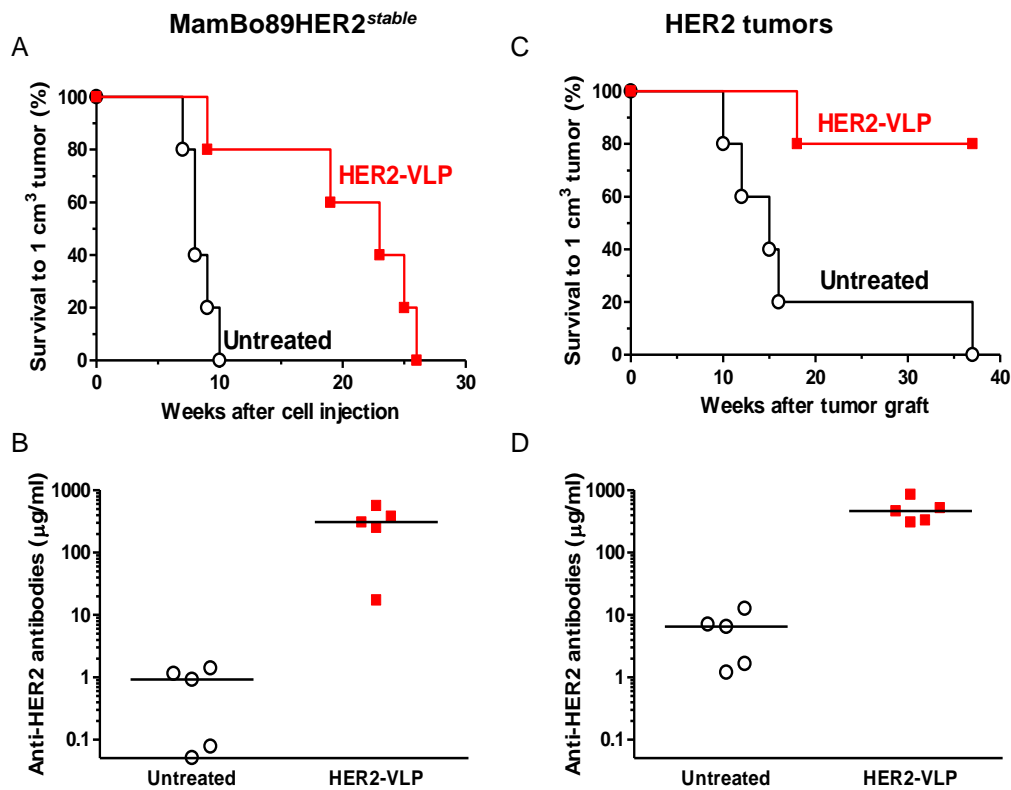


Figure 4. Therapeutic activity of HER2-VLP vaccine against HER2-positive mammary carcinomas. Treatment was administered in mice subcutaneously (s.c.) injected with MamBo89HER2^{stable} cells (A-B) or transplanted with mammary carcinoma fragments (C-D). A and C: Kaplan-Meier analysis of mice with tumors smaller than 1 cm³. Significance of difference by the Mantel-Haenszel test: $p < 0.01$ (A), $p < 0.01$ (C). B and D: anti-HER2 antibodies induced by HER2-VLP vaccination and measured by ELISA. Statistical significance of difference by the non-parametric Mann Whitney Rank Sum Test: $p < 0.01$. (Palladini et al. 2018b)

Previous data indeed reported an intrinsic resistance of MamBo89HER2^{stable} cells *in vitro* to HER2 inhibitors as trastuzumab and TKI, *e.g.* lapatinib (Palladini et al. 2017) and neratinib (unpublished data).

We have evidenced above that all mice vaccinated with HER2-VLP produced a high-titer of anti-HER2 antibodies, as measured by ELISA. The binding of sera to HER2-positive human tumor cells expressing HER2 at different levels was tested through immunofluorescence. We concluded that there was a strong binding to the HER2-positive human tumor cells, but no binding to HER2-negative

rhabdomyosarcoma SJ-RH4 cells, used as negative control (Figure 5A and B). The staining intensity of induced anti-HER2 antibodies was comparable to that obtained using the anti-HER2 monoclonal antibody clone MGR2.

1.1.4 Isotypes, affinity and avidity of anti-HER2 antibodies

To better understand the role of these antibodies in the immune response induced by the vaccine, we analysed the isotypes through flow cytometry, by leveraging the high expression of native HER2 molecules in human SK-OV-3 cells. The IgG isotypic class is the most relevant in tumor surveillance, allowing the activation of the classical complement pathway and ADCC. Among the different classes of mouse IgG (IgG1, IgG2a, IgG2b, IgG3), the subclasses IgG2a and IgG2b show a stronger anti-tumor potential *in vivo*, compared to IgG1 and IgG3 subclasses (Kipps et al. 1985; Nimmerjahn and Ravetch 2005; Hamaguchi et al. 2008). According to the ELISA assay, immunofluorescence showed higher levels of antibodies in Delta16 mice, compared to F1 mice, regardless of the type of immunization with the protein vaccine HER2-VLP or with the pHuRT DNA vaccine (Figure 5C). Analysis of IgG isotypes as percentage of total IgG (Figure 5D) evidenced that HER2-VLP induced a higher proportion of IgG1 subclass antibodies (F1 mice, 40%; Delta16 mice, 22%) than pHuRT vaccine (10% for both models). IgG2a and IgG2b isotype subclasses were less represented than IgG1 in HER2-VLP vaccinated mice: Delta16 mice, IgG2a 7% and IgG2b 4%; F1 mice, IgG2a 1.5% and IgG2b 0.5%. pHuRT vaccine promoted a quite similar level of all three subclasses, both in Delta16 mice (IgG1, 10%; IgG2a, 11%; IgG2b, 4%) and F1 mice (IgG1, 10%; IgG2a, 8%; IgG2b, 4%). We can conclude that pHuRT vaccine induced a more marked antibody-switch towards IgG2a isotype than HER2-VLP vaccine (although the statistical significance was reached only for F1 mice). This polarized switch was also true for IgG2b subclass, but only when comparing HER2-VLP treatment with pHuRT treatment in F1 mice. Since HER2-VLP was the most effective vaccine in both Delta16 and F1 mice, we concluded that this higher efficacy may be

due to the IgG1 subclass. On the other hand, the absolute level of IgG2a was quite similar for both vaccines. Therefore, the stronger activity of HER2-VLP might lie in the combination of a faster induced antibody rise, higher IgG1 level that promoted an immune storm and the presence of IgG2a antibodies which, although less in terms of percentage, reached the same absolute levels observed after pHuRT treatment.

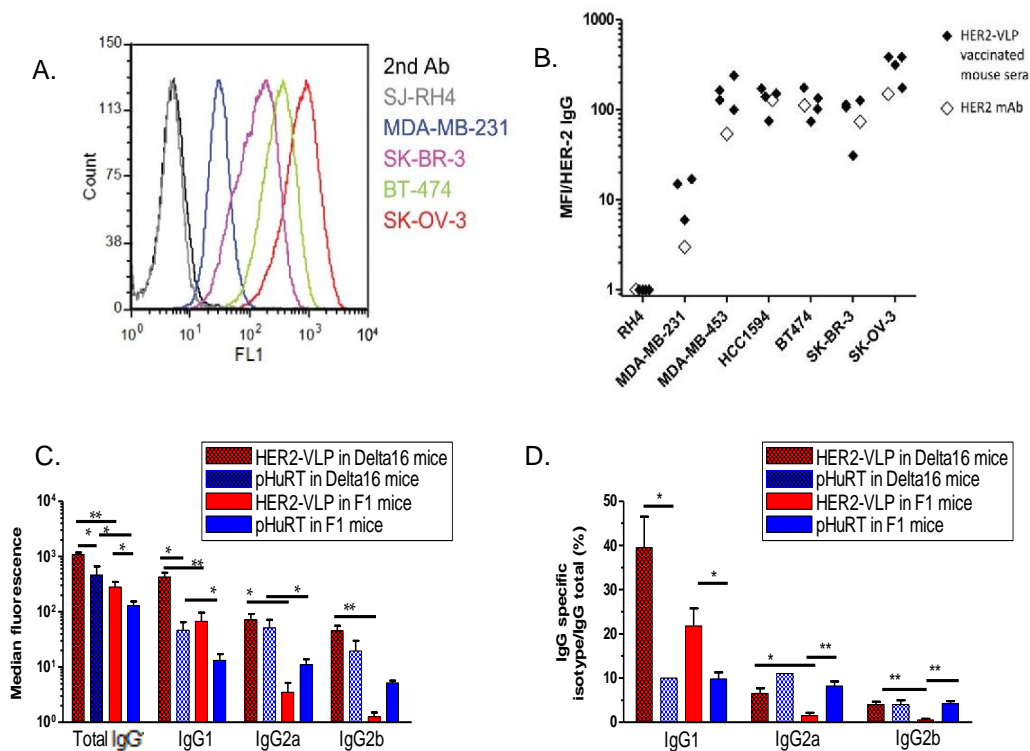


Figure 5. Characterization of HER2-VLP and pHuRT induced antibodies. Flow cytometry profiles of cells expressing known amounts of HER2, from completely negative (SJ-RH4) to highly positive (SK-OV-3) cells, stained with the serum of one representative F1 mouse vaccinated with HER2-VLP. B. Comparison of staining either with sera of 3–4 individual F1 mice vaccinated with HER2-VLP (closed diamonds) or with anti-HER2 mAb MGR2 (open diamonds). Fluorescence intensities measured by flow cytometry were normalized by the concentration of IgG against HER2 measured by ELISA in each serum (Median fluorescence intensity/HER2 IgG). C. IgG subtypes elicited by the indicated vaccinations, determined by flow cytometry of SK-OV-3 cells after indirect immunofluorescence with subtype-specific secondary Abs. Each bar represents the mean and SEM of 2–5 individual sera of different mice obtained two weeks after the third vaccination. D. IgG subtype levels measured by indirect immunofluorescence (C) reported as percentage of total IgG. Statistical significance of difference by Student’s t-test: *p<0.05; **p<0.001. Modified by (Palladini et al. 2018b)

We then performed an ELISA-based avidity assay to measure the avidity of anti-HER2 antibodies induced by HER2-VLP and pHuRT vaccines. pHuRT immunization induced antibodies with a lower activity compared to HER2-VLP-induced ones. The

avidity of anti-HER2 antibodies increased with the number of administrations. In addition, it rose at a faster rate for HER2-VLP treated mice than pHuRT treated mice (Figure 6A). We also tested the affinity of these antibodies to HER2 by Attana A200 Quartz Crystal Microbalance Biosensor. Recombinant HER2-ECD was immobilized on an amine reactive surface and we measured its binding interaction with vaccine-induced anti-HER2 IgG (Figure 6B) or trastuzumab mAb (Figure 6C). The analysis of vaccine induced anti-HER2 IgG binding showed the characteristics of multiple binding factors with different binding kinetics, consistent with a polyclonal IgG population. Approximately 1000 seconds after sample injection, the (Δ Hz) response curve showed a constant dissociation rate, which at this point was in a similar range to that measured for trastuzumab. We concluded that HER2-VLP vaccine can induce anti-HER2 IgG with affinities that are comparable to that of trastuzumab.

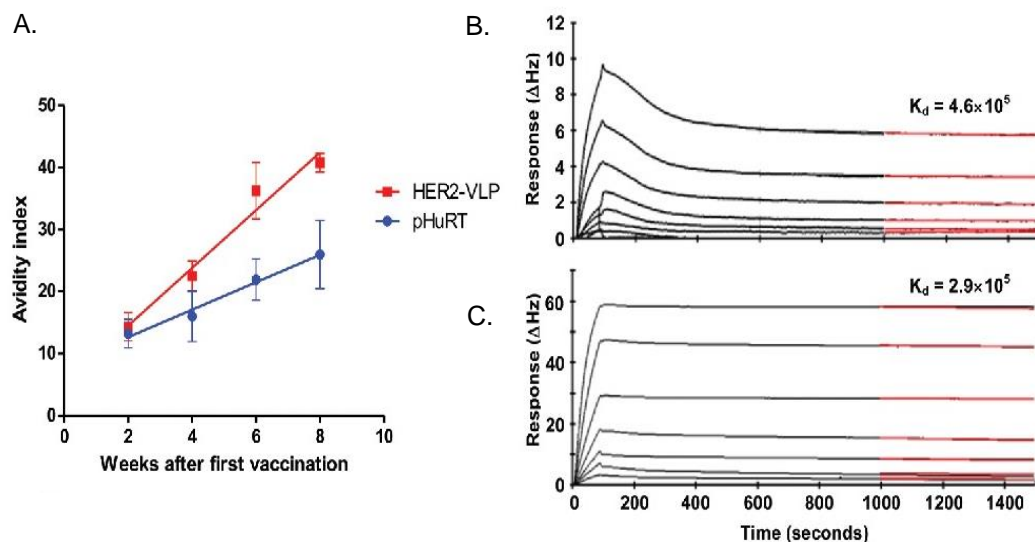


Figure 6. Avidity and affinity of anti-HER2 IgG Abs elicited by vaccination. A. Avidity index, as determined by avidity ELISA, of Abs elicited by the indicated vaccinations. Each point represents the mean \pm SEM of 3–5 sera. The slopes of linear regression lines are significantly different ($p < 0.02$). B and C. The Attana Quartz Crystal Microbalance biosensor was used to measure dissociation rates for the kinetic binding between recombinant HER2-ECD and purified total IgG from HER2-VLP immunized mice (B) or Trastuzumab mAb (C). Different dilutions of anti-HER2 IgG were flushed over a surface of recombinant HER2-ECD immobilized at 50 μ g/ml. Binding is shown as change in frequency over time (Δ Hz). The black curve represents the real-time trace, while the red curve shows the fit of the dissociation rate measured for 500 seconds (1000–1500 seconds after injection). Dissociation rate constants (K_d) were obtained by applying a dissociation rate model using the TraceDrawer software. (Palladini et al. 2018b)

1.1.5 *In vitro* activity of anti-HER2 antibodies

Trastuzumab activity is dual since on the one hand the drug interferes with HER2 homodimerization and, consequently, HER2 homodimer signaling, while on the other hand the monoclonal antibody promotes immune system activation, mainly through NK. Thus, we decided to evaluate growth inhibition by mouse sera of both HER2-positive trastuzumab-sensitive BT-474 breast cancer cell line and trastuzumab-resistant clone BT-474-C5. Cells were cultured in 3D condition, since non-adherence condition better mirrors *in vivo* growth. Both cell lines were cultured in parallel in presence of only culture medium, trastuzumab 10 µg/ml or two different sera of HER2-VLP vaccinated mice. 3D growth of BT-474 cells was equally and strongly inhibited in the presence of trastuzumab or sera of HER2-VLP immunized Delta16 mice. The latter were diluted 1:100 to achieve a concentration like that of trastuzumab (10 µg/ml trastuzumab), *i.e.*, M1 Delta16 serum 11.5 µg/ml and M2 Delta16 serum 9.7 µg/ml. Delta16 serum concentrations were quantified by the ELISA test. Treatment with trastuzumab at the final concentration of 10 µg/ml succeeded in inhibiting three-dimensional anchorage-independent growth of the BT-474 cell line, reaching an inhibition percentage of 95%, compared to cells cultured with culture medium alone (Student's t-test, $p < 0.001$). Cell growth was also inhibited by sera of the two Delta16 vaccinated mice. The percentage of inhibition was directly proportional to the concentration of anti-HER2 antibodies: serum M1, 98.9%; serum M2, 74.4% (Figure 7). Under the same culture conditions, the BT-474-C5 clone was resistant to trastuzumab, showing a number of colonies that was similar to that of untreated cells, while BT-474-C5 cells were found to be sensitive to both sera, with an inhibition percentage of 38% for M1 and 26% for M2. We concluded that humoral anti-HER2 polyclonal response managed to overcome trastuzumab resistance in BT-474-C5 cells.

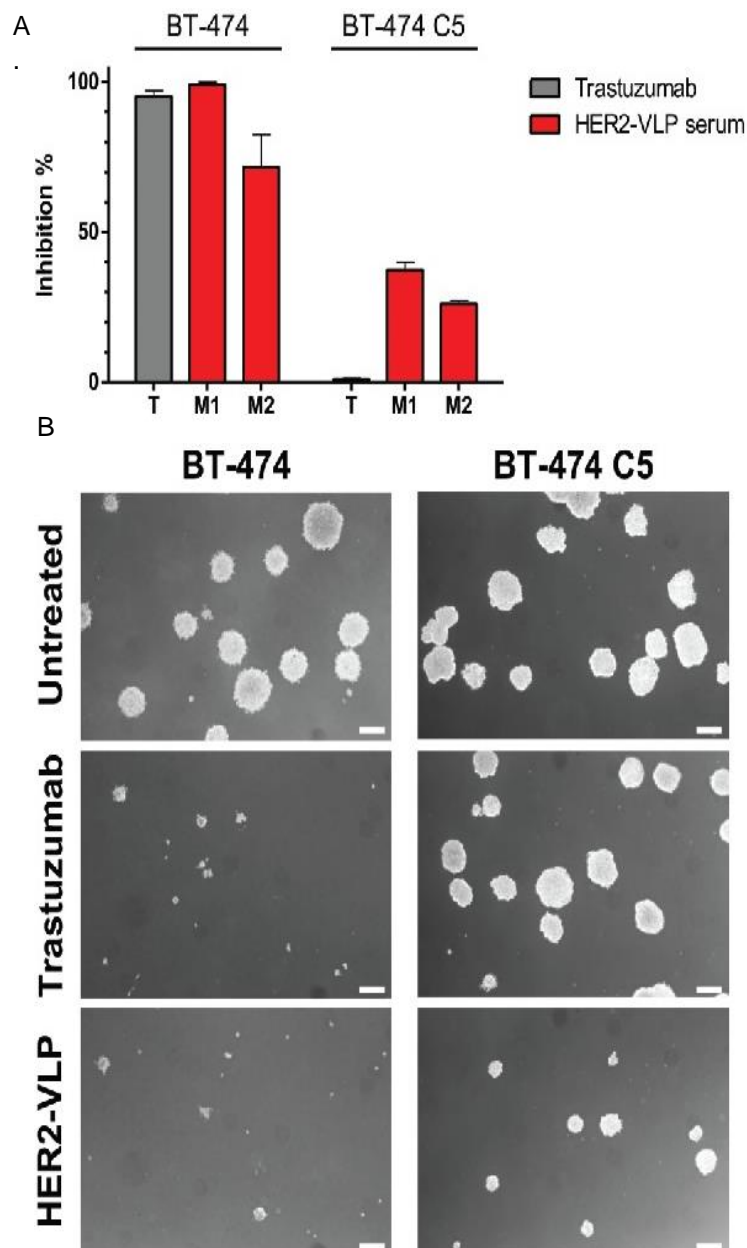


Figure 7. 3D growth inhibition by HER2-VLP induced antibodies. HER2-positive BT-474 cells and the trastuzumab-resistant clone BT-474-C5 were seeded in soft agar containing either trastuzumab (10 $\mu\text{g/ml}$) or sera (diluted 1:100) from two Delta16 mice (labelled as M1 and M2), vaccinated with HER2-VLP. The concentration of anti-HER2 Abs in mouse sera, as determined by ELISA, was comparable to that of trastuzumab (9.7–11.5 $\mu\text{g/ml}$). A. Inhibition of agar colony number counted 18 days after seeding. Each bar represents the mean (and SEM) inhibition of colony number in two independent plates. Inhibition by trastuzumab or anti-HER2 sera was calculated in reference to wells containing medium alone and untreated mouse serum, respectively. B. Dark-field micrographs of colonies in agar. The label 'HER2-VLP' correspond to serum M1 in (A). White bar corresponds to 200 μm . (Palladini et al. 2018b)

1.1.6 Cytokine production

We further quantified HER2-VLP and pHuRT vaccine-induced cytokines (Figure 8). In F1 mice vaccination with HER2-VLP resulted in an increased concentration of IFN-

γ , pleiotropic cytokine secreted mainly by CD4⁺ Th1 cells, CD8⁺ T cells and NK cells, and MIP-1 α (CCL3) and MIP-1 β (CCL4) chemokines, which are involved not only in the control of macrophages and NK migration but also in the crosstalk between lymphocytes and dendritic cells. The DNA chimeric vaccine led to a reduction in serum concentration of IL-12(p40) and TNF-alpha. We concluded that HER2-VLP vaccination induced specific increases in the levels of various cytokines involved in chemotaxis, antigen presentation and type 1 helper T cell response.

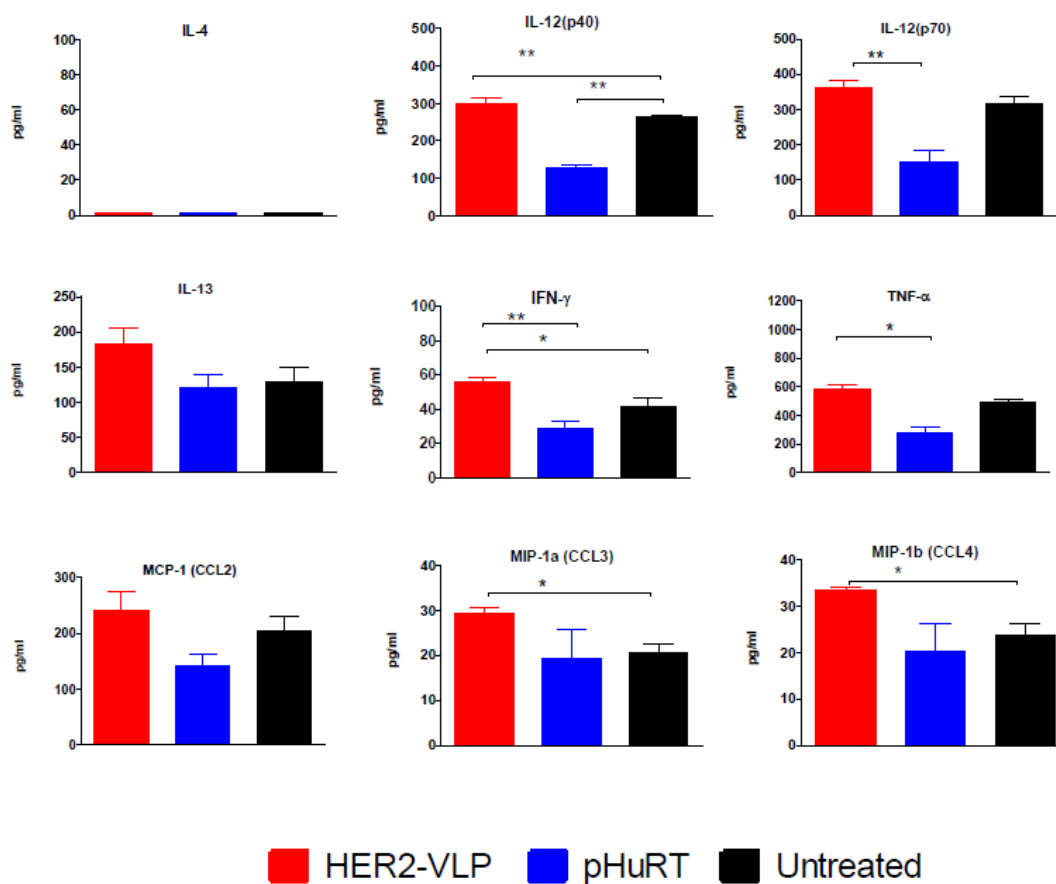


Figure 8. Cytokine pattern in sera of F1 mice treated with HER2-VLP or pHuRT. Analysed sera were collected after 4 vaccinations. N= 2 mice (untreated and pHuRT); n=3 mice HER2-VLP). Significance difference: *p<0.05, by Student's t-test; p<0.01, by Student's t-test. (Palladini et al. 2018b)

The preventive effect of HER2-VLP was more limited in F1 mice than Delta16 mice. In the therapeutic set-up almost all mice implanted with HER2 fragments were tumor-free at the end of the follow-up, while mice bearing MamBo89HER2^{stable} tumors had

only a delay in tumor growth. We concluded that HER2-VLP vaccine might need to be improved or combined with other components to overcome these limits.

1. 2 Triggering the immune response

Several strategies might reinforce the vaccine-induced antitumor immune responses. In this section I have reported four different approaches to modulate the activation of the immune system against tumor (Figure 9). First, we used a DNA vaccine codifying the human insulin-like growth factor 2 (IGF-II or IGF2) antigen with the aim of preventing mouse rhabdomyosarcoma lung metastases (De Giovanni et al. 2019b). A second approach to break the immune tolerance against a target antigen was the use of a “combo” vaccine including two antigens: rat HER2/neu and mouse insulin-like growth factor 1 receptor (IGF1R). This combination resulted effective in the prevention of spontaneous murine rhabdomyosarcoma. Then, we moved to approaches able to modulate immune checkpoint activity. We tested the activity of anti-OX40 combined with a cellular vaccine against rat HER2/neu in a mouse HER2/neu-driven mammary carcinoma model.

We compared two different schedules of administration, which resulted in different effects on mammary tumor prevention, one of which was worse (Nanni et al. 2018).

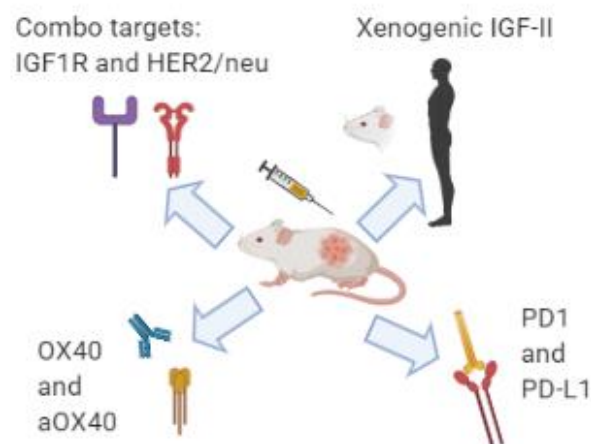


Figure 9. Graphical summary of strategies investigated to modulate immune system to overcome cancer vaccine limitations.

The chance that an immune stimulation can produce a non-beneficial effect, known as hyperprogressive disease (HD) led us to focus on this dark side of immune checkpoint therapy, taking advantage of an *in vivo* and *in vitro* model of murine melanoma.

1.2.1 The break of tolerance against IGF2

IGF circuit is one of the most relevant in rhabdomyosarcoma genesis. BALB/p53Neu male mice, which carry a p53 null allele and a rat HER2/neu heterozygous transgene, develop pelvic rhabdomyosarcomas, at a median age of 14 weeks, along with almost concomitant salivary gland carcinomas (Nanni et al. 2003). IGF circuit plays a key role in rhabdomyosarcomas, but not in salivary carcinomas, in this murine model (Nanni et al. 2003; Ianzano et al. 2014). Tumor dependence on this circuit has been assessed over a murine rhabdomyosarcoma cell line (RMSp53Neu5) derived from a rhabdomyosarcoma tumor from a BALB/p53Neu male mouse. We treated *in vitro* RMSp53Neu5 cells with specific siRNAs or with NVP-AEW541, a small molecule inhibitor of IGF1R (Figure 10). Both treatments inhibited the 3D colony growth of

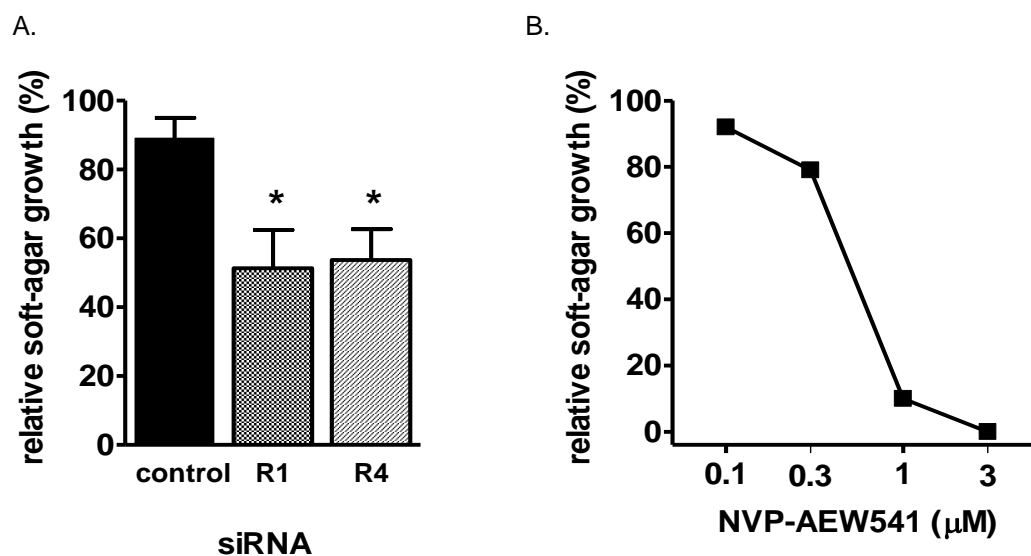


Figure 10. Activity of IGF1R-neutralizing approaches on 3D growth of murine rhabdomyosarcoma RMSp53Neu5 cell line. A. Effect on 3D growth of two different siRNAs against IGF1R (R1 and R4). Control bar refers to cells cultured in the presence of control siRNA not homologous to any mouse mRNA. Percentage of growth relative to oligofectamine only is shown. Significantly difference: * $p < 0.05$ vs control siRNA by Student's t-test. B. Dose-related growth inhibition in the presence of the IGF1R inhibitor NVP-AEW541. Dose "0" corresponds to controls containing vehicle alone. (De Giovanni et al. 2019b)

RMSp53Neu5 cells, thus confirming that IGF1R is the mediator of an IGF autocrine loop on rhabdomyosarcoma cells.

We decided, therefore, to switch off this circuit by targeting IGF2. Thus, we treated BALB/p53Neu male mice with antibodies against IGFs. The treatment was started in mice at 5-6 weeks of age, when they were tumor-free, and they were treated up to 14 weeks of age. Untreated mice developed almost simultaneously (around 15 weeks of age) IGF2-dependent rhabdomyosarcoma and IGF2-independent salivary carcinoma, thus allowing us to evaluate the preventive effect of anti-IGFs antibodies on both tumor types. Passive administration of anti-IGFs antibodies delayed, in a dose-dependent manner, the onset of rhabdomyosarcoma (Figure 11A), while salivary carcinoma latency was unaffected (Figure 11B). The overall survival significantly increased; a result likely due to the delayed rhabdomyosarcoma onset (Figure 11C).

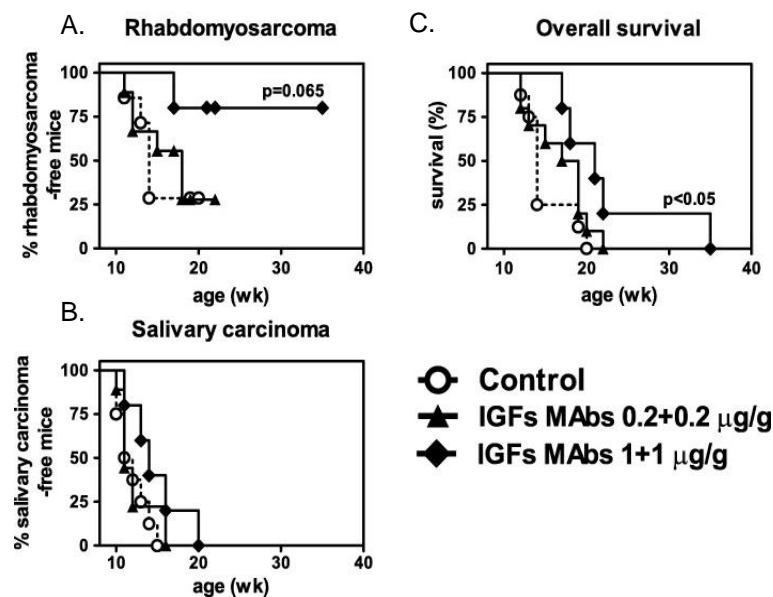


Figure 11. Prevention of spontaneous rhabdomyosarcoma by IGFs-neutralizing monoclonal antibodies. BALB/p53Neu male mice received passive administration of IGFs MAbs consisted of a 1:1 mixture of KM3168 + KM1468 monoclonal antibodies. A. Rhabdomyosarcoma-free survival. B. Salivary carcinoma-free survival. C. Overall survival. n=5-7. Statistical significance by the Mantel-Haenszel test versus untreated controls is reported inside each panel. (De Giovanni et al. 2019b)

We, subsequently, moved to a DNA vaccine against IGF2, making use of two expression plasmids carrying murine or human IGF2 gene isoform. The use of a plasmid codifying for the human IGF2, even though highly homologous to mouse IGF2, had the advantage of fostering the break of immune tolerance against the target. We vaccinated BALB/c mice to test the ability of both vaccines to induce anti-IGF2 antibodies. The DNA vaccine against mouse IGF2 did not elicit antibodies, even when combined with Treg depletion. The pre-treated mice then received intravenous injection of RMSp53Neu5 cells, but the number of lung metastases was the same both in untreated and previously treated mice (data not shown). On the other hand, in mice immunized with human IGF2 vaccine we detected anti-hIGF2 antibodies, which also recognized the murine IGF2 isoform (Figure 12A-C).

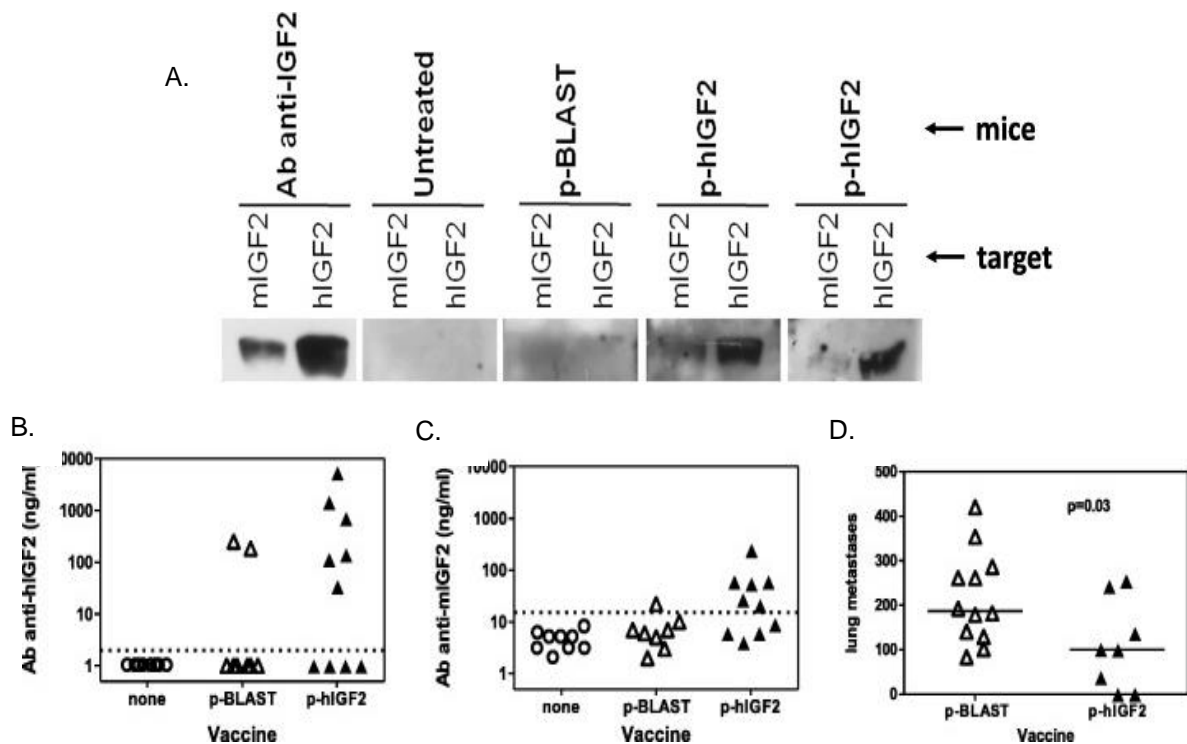


Figure 12. Activity of anti-IGF2 antibodies elicited by anti-human IGF2 DNA vaccine. A. Western blot analysis of sera from BALB/c mice untreated or vaccinated with empty vector (p-BLAST) or p-hIGF2 (two independent mice are shown). For each mouse, sera were used to stain mIGF2 protein (left lane) or hIGF2 protein (right lane). B. ELISA assay for anti-hIGF2 antibodies in sera from BALB/c mice untreated, vaccinated with empty vector or with p-hIGF2. Dashed line: sensitivity threshold as determined by the level of untreated mice. C. ELISA assay for anti-mIGF2 antibodies. D. Prevention of RMSp53Neu5-induced metastasis in mice vaccinated with the empty vector or with the p-hIGF2 plasmid and electroporated. Two similar experiments were pooled. Significance of difference by Wilcoxon test ($p=0.03$). (De Giovanni et al. 2019b)

Two mice vaccinated with control p-BLAST vector displayed an over-threshold reactivity against hIGF2, but they were devoid of any reactivity against mIGF2. Mice vaccinated with p-hIGF2 DNA vaccine or pBLAST received the intravenous (i.v.) injection of RMsP53Neu5 cells. We detected in the former group a significant decrease, in the number of lung metastases (60%) compared to latter one (Figure 12D).

1.2.2 The break of tolerance against IGF1R

To further investigate the role of IGF circuit in rhabdomyosarcoma we carried out immunizations with two expression plasmid vectors carrying human sequence of IGF1R (hIGF1R) or a murine optimized mIGF1R sequence (mIGF1Ropt). hIGF1R DNA vaccine takes advantage of a possible adjuvant effect of the non-self, even though it is a highly homologous molecule (Yang et al. 2014). We did not detect anti-mIGF1R antibodies in mice treated with electroporated mIGF1Ropt or hIGF1R DNA vaccines (Figure 13A, lanes 4 to 7 and Figure 13E, lanes 2 to 3, respectively). DNA vaccine for hIGF1R induced antibodies against the human IGF1R (Figure 13D, lanes 2 to 3). To improve immune stimulation by vaccine we investigated other adjuvant stimuli combined with DNA vaccines, such as combinations with IL12 and allogeneic histocompatibility (H-2D^q)-carrying plasmids (pIL12 and pD^q respectively) (Figure 13A, lanes 8 to 10), with pIL12 alone (Figure 13B, lanes 7 to 8) or Treg depleting pre-treatment (anti-CD25 antibodies) (Figure 13B, lanes 4 to 6), but anti-mIGF1R antibodies were never elicited. DNA vaccination against rat HER2/neu was chosen as a positive control for the vaccinal procedure (De Giovanni et al. 2019a), and, as expected, it induced a strong antibody response against rat HER2/neu (data not shown).

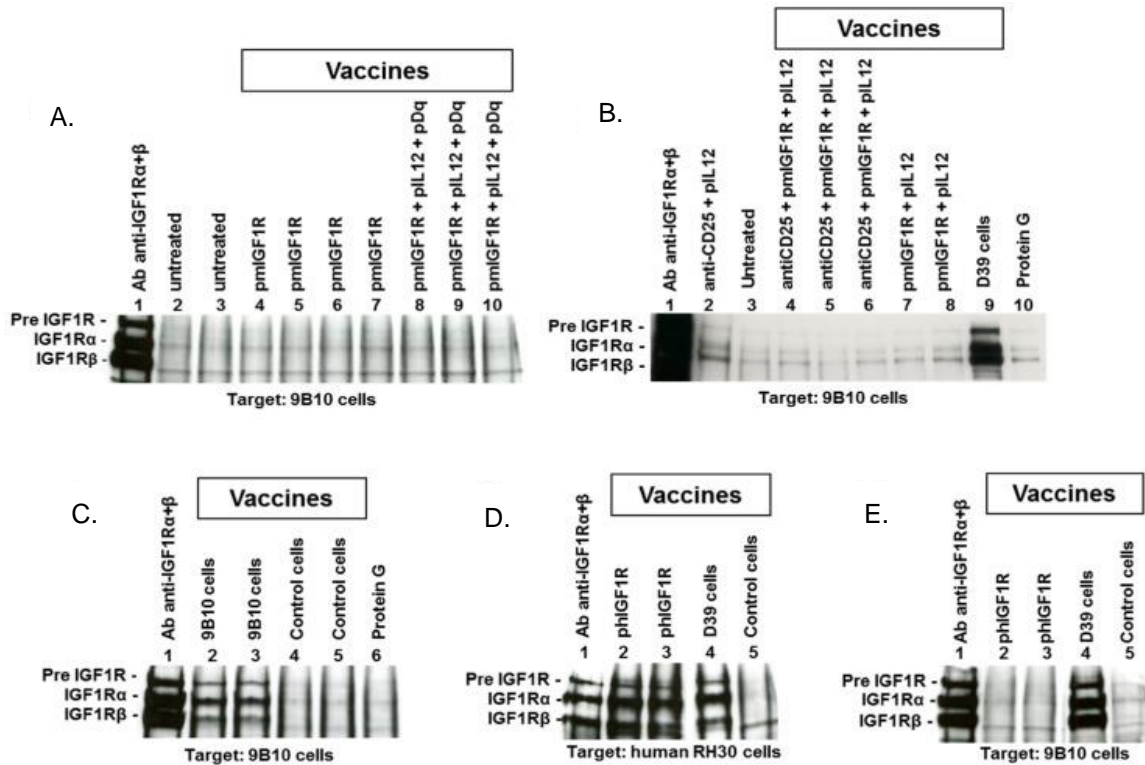


Figure 13. Immunoprecipitation and Western blot analysis of sera to evaluate the induction of antibodies recognizing murine or human IGF1R. In each panel sera used for immunoprecipitation are reported over each lane, while tumor cell lysate (target) is reported under each panel. A. lane 1, positive control; lanes 2 to 3, sera from untreated BALB/c mice; lanes 4 to 7, sera from BALB/c mice after four vaccinations with pmIGF1Ropt plasmid; lanes 8 to 10, sera from BALB/c mice after four vaccinations with a combination of plasmids (pmIGF1Ropt, pIL12 and pDq). B. lane 1, positive control; lane 2, serum from BALB/p53Neu pre-treated with anti-CD25 and vaccinated with pIL12; lane 3, untreated; lanes 4 to 6, sera from BALB/p53Neu mice pretreated with anti-CD25 and vaccinated with pmIGF1Ropt and pIL12 plasmids; lanes 7 to 8, sera from BALB/p53Neu after three vaccinations with pmIGF1Ropt and pIL12 plasmids; lane 9, serum from BALB/p53Neu vaccinated with hIGF1R-expressing D39 cell vaccine (three vaccination cycles); lane 10, protein G alone (negative control). C. lane 1, positive control; lanes 2 to 3, sera from BALB/c mice vaccinated with mIGF1R-expressing 9B10 cells (three cycles); lanes 4 to 5, sera from mice vaccinated with #20 control cells (three cycles); lane 6, protein G alone (negative control). D and E. The same sera were used to immunoprecipitate either hIGF1R (D) or mIGF1R (E) as follows: Lane 1, positive control; lanes 2 to 3, sera from BALB/c mice after four vaccinations with p-hIGF1R plasmid; lane 4, serum from BALB/c mouse after three vaccination cycles with hIGF1R-expressing D39 cells; lane 5, serum from mouse vaccinated with #20 control cells (three cycles). (De Giovanni et al. 2019a)

Subsequently, we developed cellular vaccines to further improve the immune response. We obtained, through transfection, cells expressing mIGF1R or hIGF1R, along with HER2/neu, allogeneic histocompatibility complex and IL12. The mIGF1R-transduced cell vaccine 9B10 gave rise to antibodies recognizing mIGF1R (Figure 13C, lanes 2 to 3). The hIGF1R-transduced cell line D39 elicited antibodies against hIGF1R (Figure 13D, lane 4), which cross-recognize the mIGF1R (Figure 13B, lane 9 and Figure 13E, lane 4). Control cell vaccine (#20 recipient cells, expressing HER2/neu, allogeneic H-2D^a and IL12, not subjected to transfection with IGF1R gene) did not elicit anti-IGF1R antibodies (Figure 13C, lanes 4 to 5, Figure 13D, lane 5, and Figure 13E, lane 5). Both human and mouse IGF1R-engineered cell vaccines promoted the rise of antibodies recognizing murine IGF1R although 9B10 cell vaccine induced a significantly higher level of antibodies compared to D39 cell vaccine. Sera from mice vaccinated with parental #20 cells, as well as sera from non-vaccinated mice, did not show specific binding even at 1:200 dilution (Figure 14A). We investigated the anti-IGF1R isotypes in sera of 9B10 vaccinated mice. We mainly detected IgG1, IgG2a, and IgG3 isotypes while no IgG2b were found (Figure 14B). Besides vaccination with hIGF1R-expressing D39 cells did not induce IgG3 isotype.

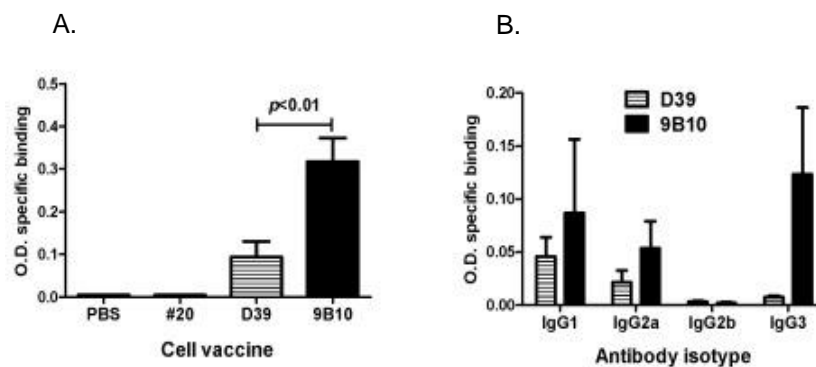


Figure 14. Anti-IGF1R and anti-HER2/neu antibodies elicited by cell vaccines co-targeting HER2/neu and IGF1R. A. Anti-mIGF1R antibodies determined by ELISA. Sera were collected from BALB/p53Neu mice after two vaccination cycles and diluted 1:400. Statistical significance (Student's t-test) of difference between D39 (n = 8) and 9B10 (n = 6) is reported in the figure. B. Analysis of antibody isotypes induced by cell vaccines in (A) (n = 3 mice per group). (De Giovanni et al. 2019a)

Cell vaccines co-targeting HER2/neu and mIGF1R or hIGF1R (9B10 and D39 cell lines, respectively) were administered to BALB/p53Neu mice starting at an early age corresponding to the preneoplastic stage (Figure 15). mIGF1R-expressing cell vaccine induced a delay of rhabdomyosarcoma onset (Figure 15A) but not of salivary carcinoma (Figure 15B). On the other hand, #20 cell vaccine rapidly induced a high level of anti-HER2/neu antibodies able to prevent salivary carcinomas. The preventive ability of D39 cell vaccine was lower than B10 cell vaccine, probably because of the lower levels of induced anti-mIGF1R antibodies.

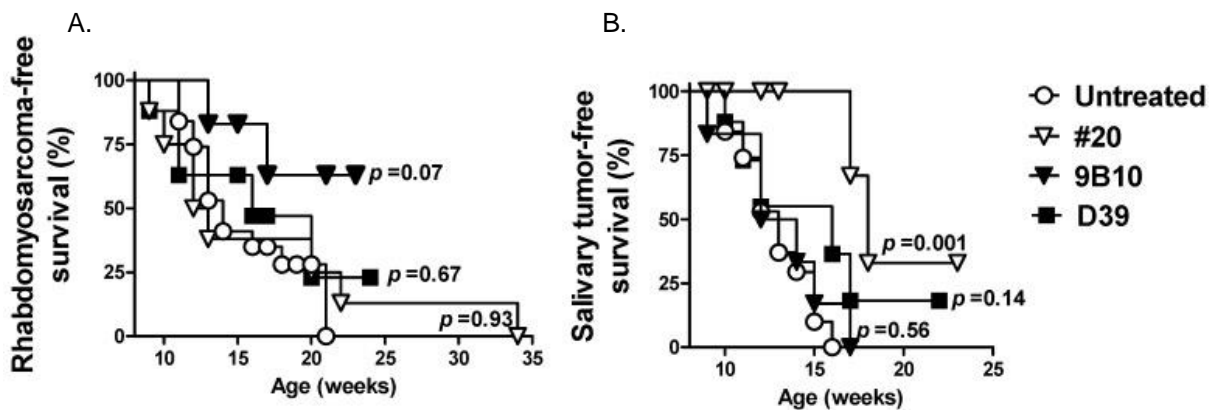


Figure 15. Preventive efficacy of anti-mIGF1R- or -hIGF1R cell vaccines in BALB/p53Neu mice. A. Rhabdomyosarcoma. B. Salivary carcinoma. Tumor-free survival (%) is shown. n=6-20. Statistical significance (Mantel-Haenszel test) vs. untreated is reported in the figure. Statistical significance vs. #20 parental cell vaccine is as follows: for rhabdomyosarcomas, D39 $p = 0.65$, and 9B10 $p = 0.10$; for salivary tumors, D39 $p = 0.12$ and 9B10 $p = 0.006$. (De Giovanni et al. 2019a)

1.2.3 Modulation of the immune checkpoint OX40

Treg inactivation is a good strategy to enhance immune stimulation induced by vaccines, *i.e.* the break of the immune tolerance against the antigen carried by the vaccine. In order to improve vaccine efficacy, we investigated the combined treatment based on an anti-HER2/neu cellular vaccine and Treg inhibition. We tested this schedule in BALBneuT mice transgenic for rat HER2/neu oncogene. These mice show a spontaneous onset of mammary carcinoma, with the first tumor being observed at a median time of 16 weeks of age. Triplex vaccine, based on engineered IL12-producing allogeneic HER2/neu-positive cells, prevent almost completely this aggressive

mammary carcinogenesis when administered according to a life-long schedule. Vaccine-induced immune mechanisms include host production of both anti-neu antibodies and IFN- γ (De Giovanni et al. 2004). We induced Treg inhibition by triggering OX40 with an agonistic antibody (OX86, here referred to as aOX40). OX40 belongs to the TNFR immune checkpoint family and is constitutively expressed on murine Treg and on activated CD4 and CD8 T cells. We chose a suboptimal vaccine schedule to better value either increased or decreased preventive efficacy of the vaccine in the combined treatment with OX40 agonist. Thus, we started immunization at 10 weeks of age for three monthly cycles. Two distinct schedules of aOX40 administration were used: concomitant to cell vaccine (aOX40+vax) or after the completion of 3 cycles of vaccination (aOX40postvax) (Figure 16A). Cell vaccine alone significantly delayed the spontaneous onset of mammary carcinoma, with the first tumor being observed at a median time of 35 weeks (Figure 16B). aOX40 administered concomitant to vaccine (aOX40+vax) partially weakened the preventive vaccine efficacy, causing a significantly earlier tumor onset (at a median time of 28.5 weeks) and higher numbers of tumors per mouse, with respect to the vaccine alone. The aOX40 administration after the end of vaccinations slightly increased ($p < 0.01$ by Mantel-Haenszel test) the vaccine efficacy with a delay of tumor onset at a median age of 39 weeks and fewer tumors per mouse (Figure 16B and C).

Anti-HER2/neu antibodies played a key role in vaccine-induced protection. Triplex vaccine induced a progressive increase of anti-HER2/neu antibodies. After the end of immunizations, we then observed a decrease in the levels of antibodies and, consequently, the onset of mammary tumors. aOX40 administered concomitant with cell vaccine (aOX40+vax) significantly reduced anti-HER2/neu antibody production (Figure 17A). Isotype analysis of HER2/neu vaccine-induced antibodies evidenced a significantly lower level of IgG2a and IgG3, together with total IgG, in sera of OX40+vax-treated mice, compared to mice treated only with Triplex vaccine (Figure

17B and C). The decreased antibody levels correlated well with the decreased immunoprevention by cell vaccine.

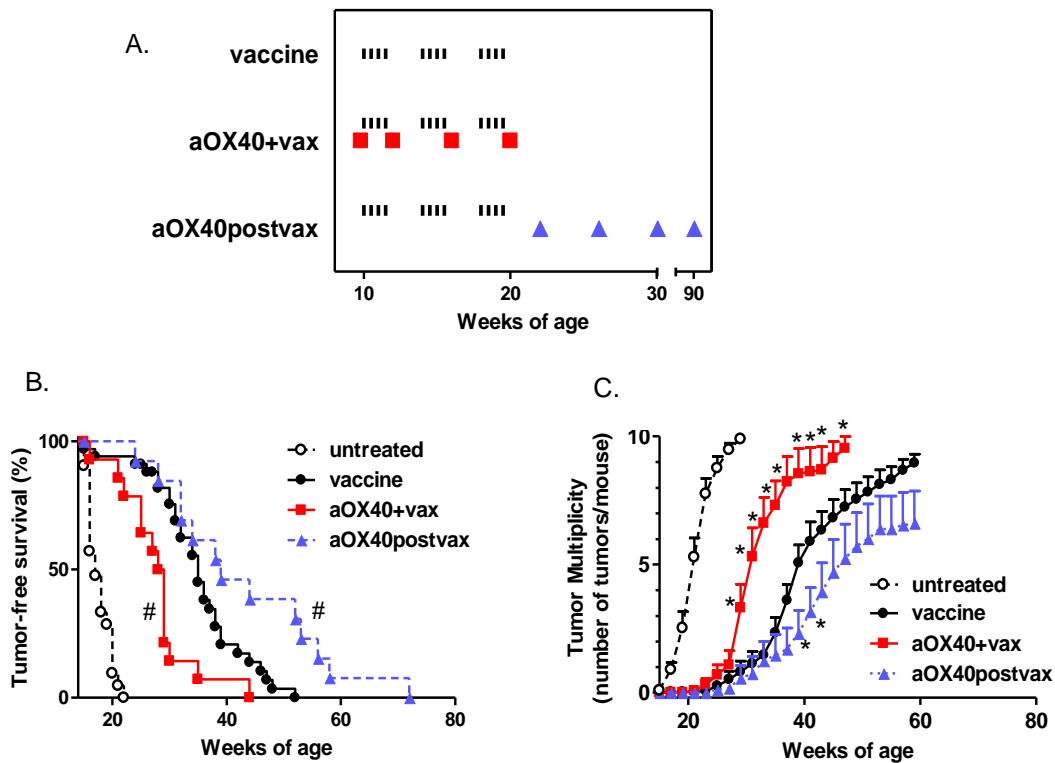


Figure 16. Preventive efficacy of combined treatments with aOX40 and anti-HER2/neu cell vaccine on mammary carcinoma. A. Treatment schedule. Black ticks: intraperitoneal (i.p.) injection of a cell vaccine dose. Red squares: i.p. injection of aOX40 concomitant to vaccine (aOX40+vax). Blue triangles: i.p. injection of aOX40 after completion of vaccine cycles (aOX40postvax). B. Tumor-free survival curves. Groups: untreated, n = 21; vaccine: n = 34; aOX40+vax, n = 13; aOX40postvax, n = 18. #p < 0.01 vs vaccine only group (Mantel-Haenszel test). All treated groups were significantly different from untreated (p < 0.01 at least). C. Tumor multiplicity. Mean ± SEM. *p < 0.05 at least vs vaccine only (Student's t-test). Untreated mice received vehicle (PBS) alone. (Nanni et al. 2018)

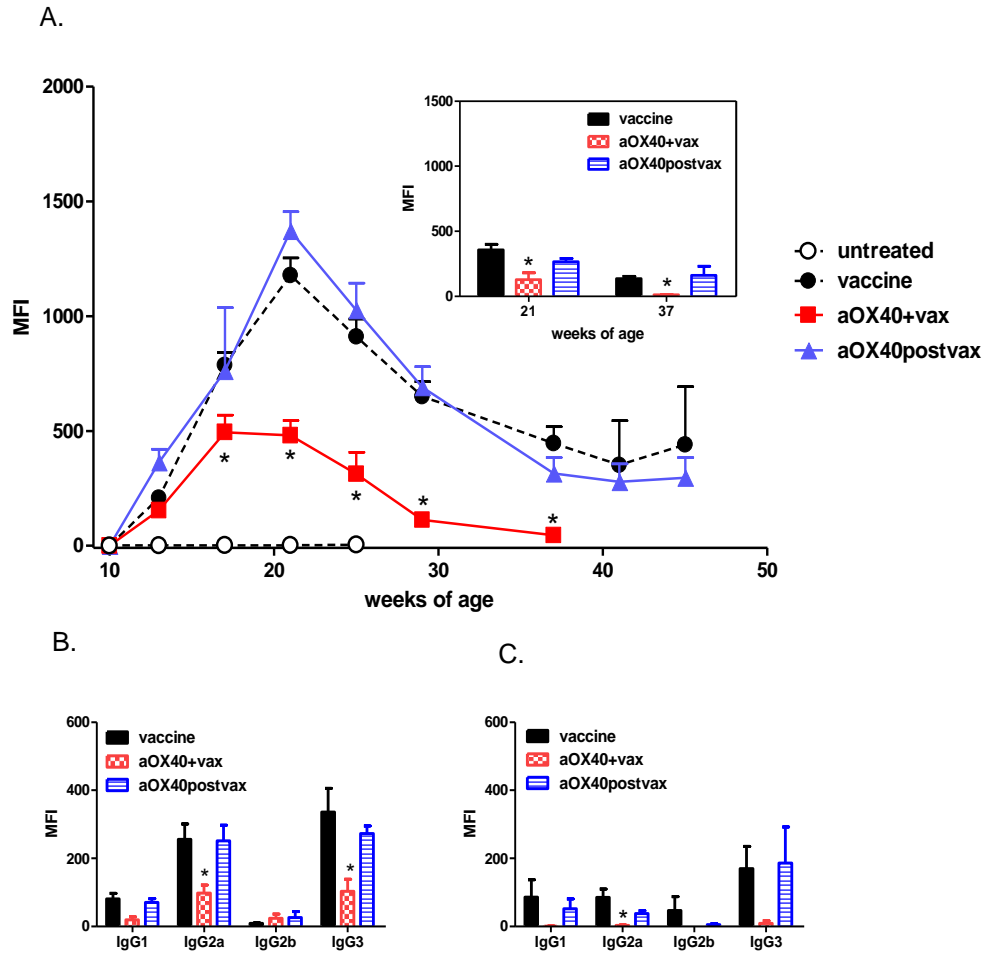


Figure 17. Anti-vaccine antibodies induced by different schedules of aOX40 administration combined to vaccination. A. Kinetics of anti-vaccine antibodies. MFI = Median fluorescence intensity. Mean \pm SEM is shown for each point. * $p < 0.01$ at least vs vaccine only group (Student's t-test). Inset: anti-H-2q antibodies at two time points (21 and 37 weeks of age). * $p < 0.05$ at least vs vaccine only group (Student's t-test). B. Anti-vaccine antibody isotypes at 21 weeks of age. MFI as in (A). Mean \pm SEM is shown for each point. * $p < 0.05$ at least vs vaccine only group (Student's t-test). C. Anti-vaccine antibody isotypes at 37 weeks of age. MFI as in (A). Mean \pm SEM is shown for each point. * $p < 0.05$ at least vs vaccine only group (Student's t-test). (Nanni et al. 2018)

Mice treated with aOX40 after the end of the three vaccine cycles (aOX40postvax) showed kinetics and isotypes of anti-HER2/neu antibodies superimposable to those of vaccine alone (Figure 17A-C). We concluded that the mechanisms associated with the increased protection observed in these mice were not mediated by anti-HER2/neu antibodies.

Since Treg cells were the target of aOX40, we investigated how the treatment affected these cells. At 17 weeks of age, BALBneuT mice showed about 15% of Treg in spleen (Figure 18). The different treatments did not affect Treg number. Nevertheless, the frequency of Treg expressing the activation marker CD103 significantly increased in aOX40+vax treated mice. Thus, we can conclude that in aOX40+vax, aOX40 induced an activation of Treg cells that was responsible for the reduced vaccine efficacy.

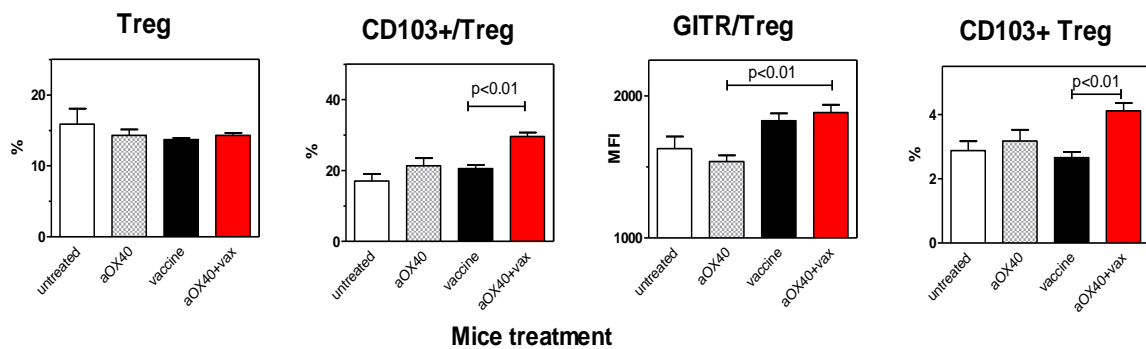


Figure 18. Effect of aOX40+vax combined treatment on Treg number and phenotype. Each bar represents the mean and SEM from mice of the different groups studied (at 17 weeks of age). Panels from left to right show: Treg frequency over total splenocytes, CD103+ cells over Treg, GITR expression level (Mean fluorescence intensity, MFI) over Treg, CD103+ Treg frequency in gated CD4+ splenocytes. For comparison, data from untreated mice and from mice treated with aOX40 alone are shown. Groups: untreated, n = 3; aOX40, n = 10; vaccine, n = 20; aOX40+vax, n = 25. Significance at the Student's t-test is reported. (Nanni et al. 2018)

On the other hand, aOX40postvax schedule did not modify the frequency of Treg and effector memory T cells (Tem), with respect to the vaccine-only group (Figure 19). Splenocytes of aOX40postvax mice, restimulated for 6 days with HER2/neu cells, showed a significantly higher production of GM-CSF and IL10, compared to the splenocytes of mice treated with vaccine only, whereas there was no difference in IFN- γ secretion (Figure 19B).

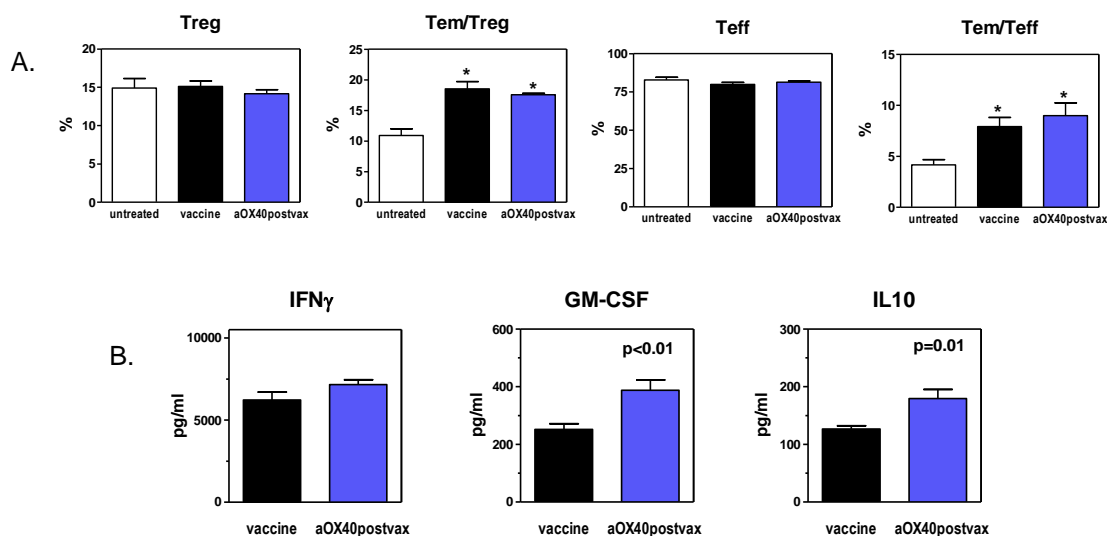


Figure 19. Effects of aOX40postvax treatment. A. Frequency of Treg, effector memory (Tem)/Treg, T effector (Teff) and effector memory/Teff. Each bar represents the mean and SEM from mice of the different groups studied (at 32 weeks of age). Groups: untreated, n = 4; vaccine, n = 8; aOX40postvax, n = 8. * $p \leq 0.01$ vs untreated group (Student's t test). B. Cytokine production by restimulated spleen cells (collected from mice at 32 weeks of age). Each bar represents the mean and SEM from mice of the different groups studied. Groups: vaccine, n = 6; aOX40postvax, n = 6. Significance at the Student's t-test is reported. (Nanni et al. 2018)

This study suggested that the immune checkpoint switch off can induce either clinical benefits or drawbacks. Several factors can influence the balance between immune surveillance and tumor immune escape. Among them, the immune populations infiltrating the tumor microenvironment, the tumor dimension and the cytokine production played a major role. Checkpoint inhibitors can perturbate this equilibrium and the effect might be different according to the timing of administrations.

1.2.4 Modulation of the immune checkpoint PD-L1

The controversial results regarding aOX40 led us to carry out a further investigation into the effects of immune checkpoint inhibition, focusing on the negative effects on tumor growth obtained with these treatments. In clinical practise, immune checkpoint inhibitors are widely used in melanoma and NSCLC therapies. Although ICI improved survival of patients with advanced tumors (Topalian et al. 2014; Ahamadi et al. 2017; Vaddepally et al. 2020), several studies reported a failure of the treatment in a proportion of patients (Borcoman et al. 2019). Therefore, we explored the effect of anti-PD-L1 polyclonal and monoclonal antibodies in a murine melanoma model, consisting of cell lines B16 and B16-F10. These cell lines showed a low immunogenicity, so they are representative of tumors reported to be less responsive to ICI. Afterwards, we evaluated how the anti-PD-L1 treatment modified the *in vivo* tumorigenesis of B16 and/or B16-F10 cell lines injected in C57BL/6 mice. ICI activity on tumor cells was also investigated *in vitro*, in absence of the immune system components.

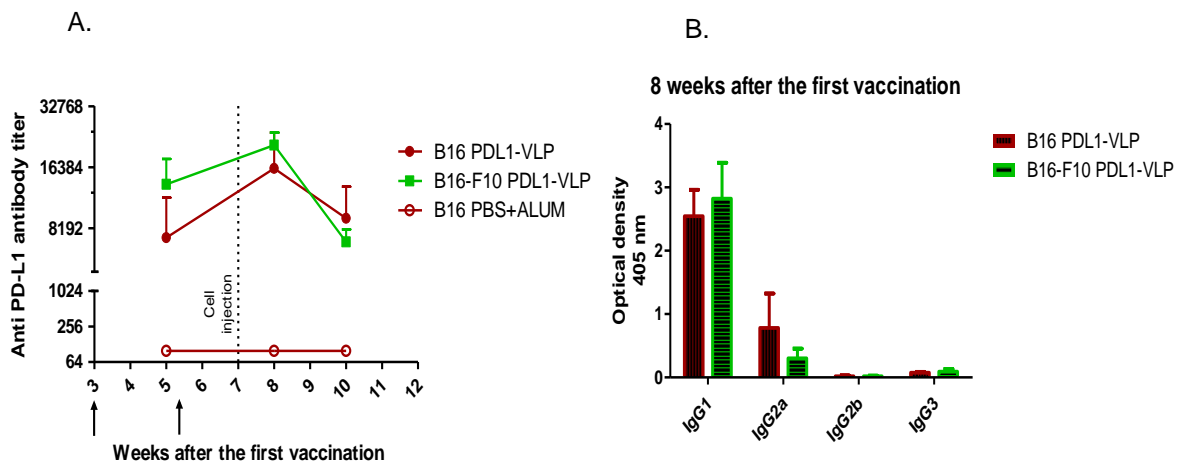


Figure 20. Anti-PD-L1 antibody titer and isotypes. A. Kinetics of anti-PD-L1 antibodies detected in mouse sera by ELISA test. We analysed sera collected after 5, 8 and 10 weeks from the first immunization. Each point represents the mean and SEM from 5 mice of the different studied groups. The black arrows indicate the second and the third vaccination. The dashed vertical line indicates the week at which B16 or B16-F10 cells were inoculated. The endpoint titer, considering as cut off the value obtained by sum of the mean and the standard deviation of the values obtained in blank wells, multiplied by 3, is indicated in y-axis and directly related to the antibody titer. B. Analysis of antibody isotypes induced by PDL1-VLP vaccine+alum. We performed the analysis by ELISA. Each bar represents the mean and SEM from mice of the different groups studied (n = 6). Significance difference between IgG1 and other isotypes for each cell line: $p < 0.05$, at least by Student's t-test.

1.2.4.1 Therapy of B16 and B16-F10 with polyclonal anti-PD-L1 antibodies

We immunized C57BL/6 mice with a PDL1-VLP vaccine, against mouse PD-L1, combined to alum. To induce a high PD-L1 antibody titer we performed two boosts after the first vaccine administration. Since alum consistently enhances total IgG1 production (Jin et al. 2013), IgG1 resulted to be the most representative isotype among anti-PD-L1 IgGs (Figure 20A and B). A control group treated with PBS+ALUM run in parallel. A week after the third vaccination, mice received a s.c. injection of B16 or B16-F10 cells. Polyclonal anti-PD-L1-induced antibodies did not affect the *in vivo* growth of B16-derived tumors (Figure 21A). Spontaneous metastases were found only in one mouse per group although the number of lung nodules was a half in PDL1-VLP treated mouse (12 metastases) than in the control group. The mean spleen weight of PDL1-VLP treated mice was one third less than the PBS+ALUM group. This difference, while not reaching statistical significance (Student's t-test, $p < 0.09$), suggested a tendency that may correlate with the presence of an anti-PD-L1 polyclonal response (Figure 21B). The absence of therapeutic effect on B16 tumors was confirmed also in mice bearing B16-F10 tumors. The tumor growth was indeed not only not delayed, but we also observed a growth acceleration, starting after 13 days after cell injection (Student's t-test, $p < 0.05$) in mice treated with PDL1-VLP, compared to those in the control group (Figure 21C). Spontaneous lung metastases were observed in 2 of 5 mice in the former group (with 2 and 32 lung nodes, respectively) and only 1 of 5 mice in the latter one (with only one metastasis). Similarly to mice bearing B16 tumors, we observed a significant decrease by half of the mean spleen weight in PDL1-VLP treated group, compared to the untreated one (Student's t-test, $p < 0.05$) (Figure 21D).

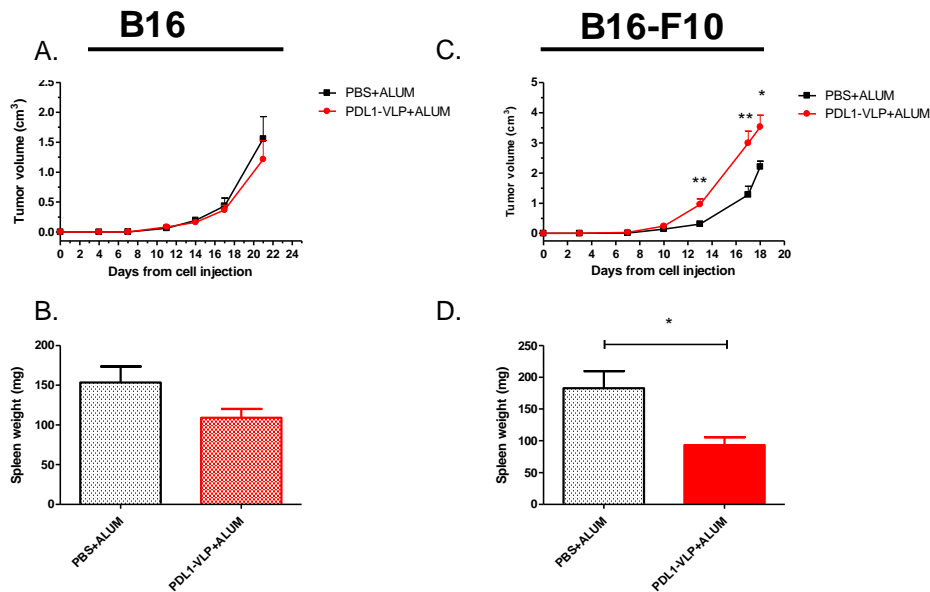


Figure 21. Tumor growth of B16 and B16-F10 in mice pre-treated with PDL1-VLP+ALUM vaccine. A. and B. Tumor growth of 10^5 B16 cells s.c. injected in C57BL/6 mice (A) and spleen weight at the end of the follow-up (B). C. and D. Tumor growth of 0.5×10^6 B16-F10 cells s.c. injected in C57BL/6 mice (C) and spleen weight at the end of the follow-up (D). In (A) and (C) each point represents the mean and SEM from mice of different groups (n=5). In (B) and (D) each bar represents the mean and SEM of mice of different groups. In (C) significance difference: *p<0.05 and **p<0.01 by Student's t-test. In (D) statistical difference by Student's t-test: *p<0.05.

1.2.4.2 Therapy of B16 and B16-F10 with monoclonal anti-PD-L1 antibodies

Since in clinical practise patients are treated with monoclonal antibodies, we proceeded with a second set of experiments in B16-F10-injected mice, making use of two different anti-PD-L1 antibodies. The first was the anti-mouse PD-L1 rat IgG2b antibody clone 10F.9G2 (BioXCell), here referred to as 10F.9G2, while the second one was atezolizumab, *i.e.* a human IgG1 able to bind both human and mouse PD-L1. We used rat IgG2b anti-LTF2 as isotype control to treat a group of mice which run in parallel to 10F.9G2. All antibodies were administered i.p. every 3-4 days with different schedules.

The first schedule with 10F.9G2 (dose: 9 mg/kg) consisted of three injections before the challenge with B16-F10 cells. After the challenge, C57BL/6 mice continued the treatment until the end of the experiment. Overall, 10F.9G2 antibody did not reduce nor accelerate tumor growth, in respect to the isotype control group or the untreated

group. Nevertheless, we highlighted a little increase in tumor growth at 7 and 15 days after cell injection, compared to isotype control (Student's t-test, $p < 0.01$) (Figure 22A). The evaluation of metastases revealed an involvement of lungs, lymph nodes and, rarely, spleen. Almost all mice developed lymph node metastases (3/3 untreated mice, 5/6 isotype control mice, 6/6 10F.9G2-treated mice). In the spleen, metastases were observed in 1/3 mice in the untreated group and 1/6 mice in the group treated with 10F.9G2 antibody. Lung metastases affected 33% of untreated group (a mouse with 1 metastasis) and 50% of isotype (median number of nodes 0.5, range 0-44) and 10F.9G2 groups (median number of nodes 1, range 0-9). No significant differences were observed in terms of lung lesion number. We concluded that 10F.9G2 did not affect metastatization. We evidenced a decreased spleen weight in the isotype control group compared to the 10F.9G2-treated group. No statistically significant differences were found between untreated and isotype groups, nor between untreated and 10F.9G2-treated groups (Figure 22E).

In the second schedule, we increased the antibody dose to 12 mg/Kg and performed 4 treatments before challenge and 4 treatments after challenge. Mice concluded the treatment two weeks before the end of the experiment. Treatment with anti-PD-L1 antibody did not modify tumor growth and we did not evidence any changes between the treated, untreated and isotype groups (Figure 22B). Unlike what was observed in the previous experiment, metastases involved the lymph node in only 1/6 mice in the 10F.9G2-treated group. The incidence of lung metastases was higher in mice treated with anti-PD-L1 antibody (83%), compared with the isotype control (57%) and the untreated group (25%): these differences in incidence were not significant (χ^2 test). We did not observe differences in the metastatic load between isotype group (median 1, range 0-26) and 10F.9G2-treated mice (median 2, range 0-4) while the latter showed a significant difference with untreated mice (median 0, range 0-1) ($p < 0.05$ by Student's t-test). The spleen weight of the three groups did not show any significant difference,

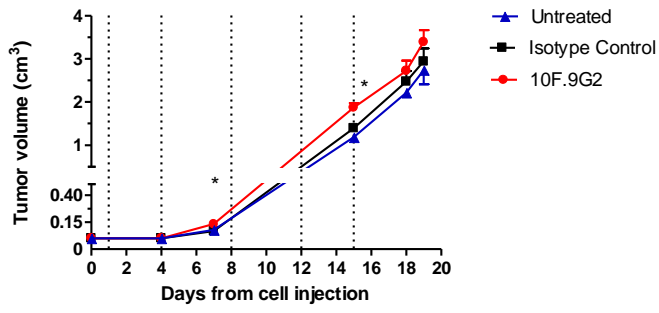
although the treatment with antibodies induced an increase of the weight compared to the untreated group (Figure 22F).

The third schedule was based on anti-PD-L1 treatment with 10F.9G2 only before the challenge with B16-F10 cells. Thus, mice received only four antibody treatments (9 mg/Kg). Despite small significant differences in tumor growth (Figure 22C), these results confirmed the absence of the therapeutic effect of anti-PD-L1 antibody 10F.9G2. We evaluated metastases only in the two antibody-treated groups. Invaded lymph nodes were found in 83% of mice in the isotype control group and all mice of 10F.9G2 group. Despite this, the incidence of lung metastases was higher in the former (29%, a mouse with 1 node and the other one with 2 nodes) compared to the latter (14%, a mouse with 5 nodes). Evaluation of spleen weight did not reveal any significant differences between the three groups (Figure 22G).

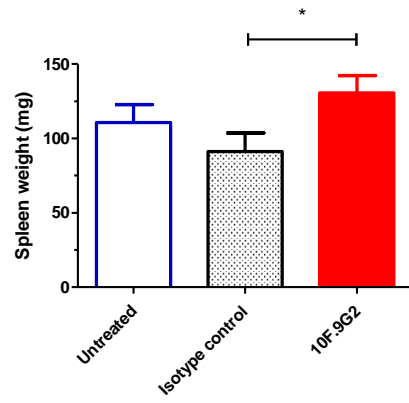
We also tested 10F.9G2 against lung metastases induced by B16-F10 i.v. injection, but we did not find significant differences in the number of lung metastases between these mice and untreated or isotype control-treated mice (data not shown).

Finally, mice injected with B16-F10 were treated with atezolizumab starting from the day after cell injection. They received atezolizumab 10 mg/Kg every 3-4 days until the end of the experiment (Figure 22D). Even, in these conditions, B16-F10 tumor growth was not influenced by atezolizumab treatment. However, 43% of atezolizumab treated mice showed spleen invasion by tumor cells while all spleens of untreated mice were tumor-free. Lung metastases were found in 71% of untreated mice and 23% of atezolizumab-treated mice (difference not significant by χ^2 test for incidence and Student's t-test for number of lung nodules). Overall, the mean spleen weight was higher in the atezolizumab group compared to the untreated one (Figure 22H).

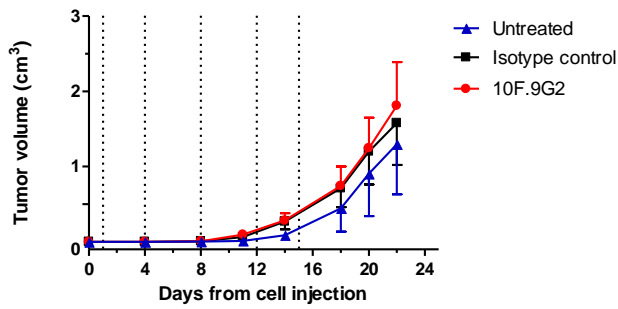
A.



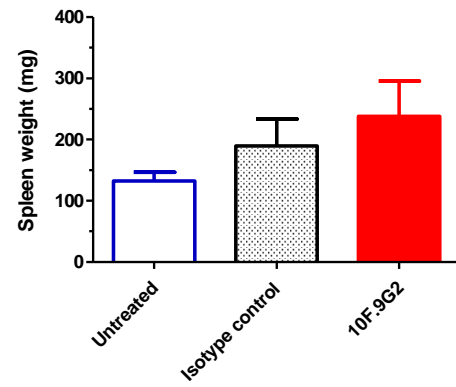
E.



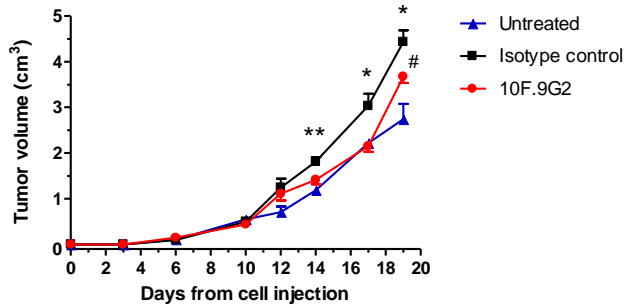
B.



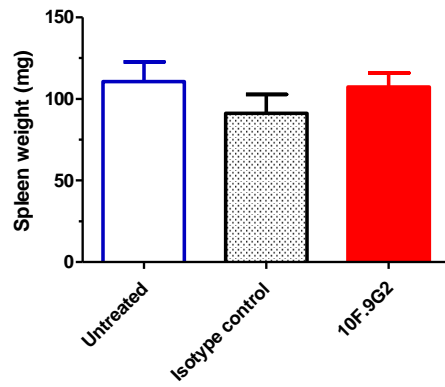
F.



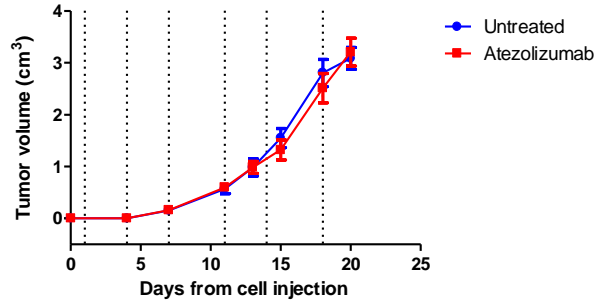
C.



G.



D.



H.

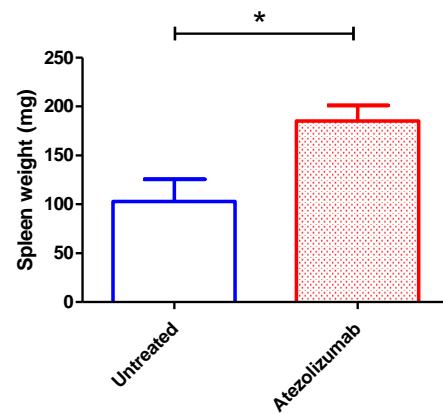


Figure 22. Tumor growth (left panels) of B16-F10 in C57BL/6 mice and spleen weight (right panels). Mice were treated with anti-PD-L1 antibodies 10F.9G2 or atezolizumab. Day 0 is the day of cell injection. Dashed lines indicate antibody treatments after cell injections (C is without dashed lines because mice received antibody-treatment only before cell injection). Dose of injected cells and treatment schedule details are reported below for each experiment. Statistical analysis was done by Student's t-test. A and E. 0.5×10^6 cells s.c.; 9 mg/kg 10F.9G2 or isotype control Abs i.p. administered at days -9, -6, -2, +1, +4, +8, +12, +15. Untreated= 3, Isotype control=6 and 10F.9G2=6. * $p < 0.05$, 10F.9G2 vs isotype control. B and F. 10^5 cells s.c.; 12 mg/kg 10F.9G2 or isotype control Abs i.p. administered at days -12, -9, -6, -2, +1, +4, +8, +12, +15. Untreated= 4, Isotype control=7 and 10F.9G2=7. C and G. 0.5×10^6 cells s.c.; 9 mg/kg 10F.9G2 or isotype control Abs i.p. administered at days -9, -7, -4, -1. Untreated= 2, Isotype control=7 and 10F.9G2=7. * $p < 0.05$ and ** $p < 0.01$, isotype control vs 10F.9G2; # $p < 0.05$, 10F.9G2 vs untreated. D and H. 0.5×10^6 cells s.c.; 10 mg/kg atezolizumab Ab i.p. administered at days +1, +4, +7, +11, +14, +18. Untreated= 7, atezolizumab=7. * $p < 0.05$.

1.2.4.3 Mechanisms underlying resistance to PD-L1 treatment

As previously described, mice that were pre-treated with PDL1-VLP before cell injection showed an acceleration of B16-F10 tumor growth, unlike B16 tumors. Thus, we investigated potential mechanisms related to resistance to immune checkpoint inhibition therapy by Real-Time PCR on tumor samples, collected at the end of the follow-up. We found that *Cd38*, an alternative immune checkpoint (Chen et al. 2018), was highly expressed in tumors induced by B16-F10 cells, unlike tumors induced by B16 cells (Student's t-test, $p < 0.01$) (Figure 23A). In the latter, a significant reduction of *Cd38* expression was also observed in mice pre-treated with the PDL1-VLP vaccine, compared to the control group (Student's t-test, $p < 0.01$). B16-F10 tumors also showed an increased expression of the *Cd4* marker compared to B16 tumors, likely suggesting an increase in Treg lymphocytes (Student's t-test, $p < 0.05$) (Figure 23B). Finally, a significant reduction in the expression of the *Arg1* gene, representative of myeloid populations such as M2 macrophages, was observed in B16 tumors developed in mice treated with PDL1-VLP, compared to the control group (Student's t-test, $p < 0.05$). Interestingly, this decrease was not observed in B16-F10 tumors (Figure 23C).

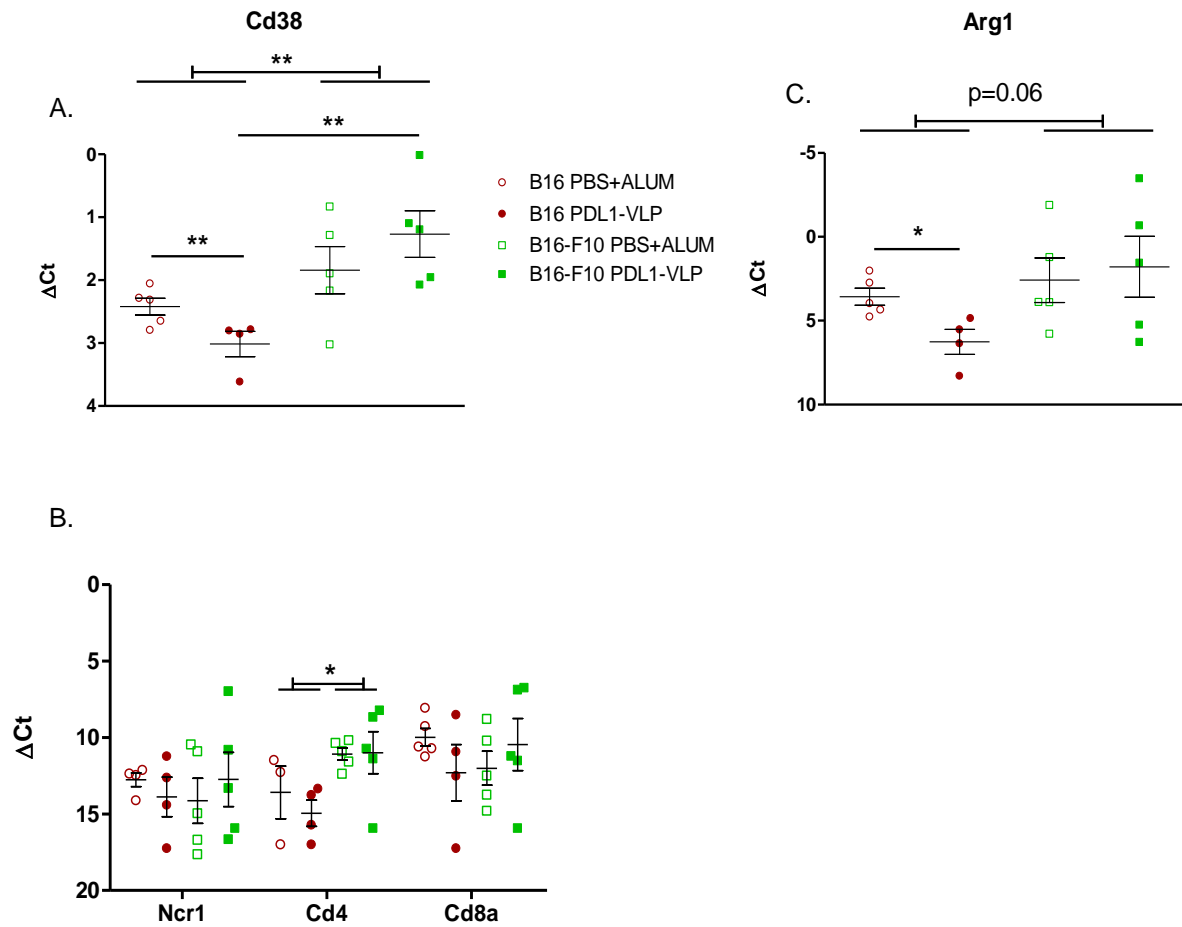


Figure 23. Molecular analysis of B16 and B16-F10 tumors from mice pre-treated or no with PDL1-VLP. Expression levels of reported genes were measured by Real-Time PCR. Statistical analysis was performed by Student's t-test: * $p < 0.05$; ** $p < 0.01$. $\Delta Ct = Ct_{\text{gene of interest}} - Ct_{\text{Tbp}}$. A. Immune checkpoint Cd38 expression. B. Ncr1 (codifying Nkp46 antigen, marker of NK cells), Cd4 (marker of Th and Treg cells) and Cd8a (marker of cytotoxic T lymphocytes). C. Arg1 expression (marker of M2 cell population).

In order to understand the different behaviour of B16 and B16-F10 tumors, we also investigated the response of these cell lines to IFN- γ , a cytokine that plays a crucial role in the PD-1/PD-L1 circuit. The growth of the B16 cell line was strongly inhibited by IFN- γ (more than 80% of inhibition after 72 hours of treatment), unlike B16-F10 cell line, in which the inhibition level did not exceed 30%, even in the presence of high doses of IFN- γ (1000 U/ml) (Figure 24A). Moreover, B16-F10 cells showed greater *Cd38* expression compared to B16. Prolonged treatment with IFN- γ at doses 100 and 1000 U/ml seemed to reduce this expression (Figure 24B). Then, we evaluated the

modulation of H-2 molecules by IFN- γ . H-2 baseline expression was found to be very low in B16 cells (about 30 arbitrary fluorescence units) and even lower in the B16-F10 cell line (about 10 arbitrary fluorescence units). Nevertheless, the presence of IFN- γ induced an increase of H-2 molecules in both cell lines (Figure 24C). PD-L1 protein, whose expression is very low in normal culture condition, was significantly upregulated in the presence of IFN- γ (Figure 24D). We finally evaluated the *in vitro* effect of anti-PD-L1 treatment with 10F.9G2: B16-F10 cells were treated with IFN- γ (100 U/ml) and/or anti-PD-L1 (10 μ g/ml). However, no changes in cell growth were observed (data not shown).

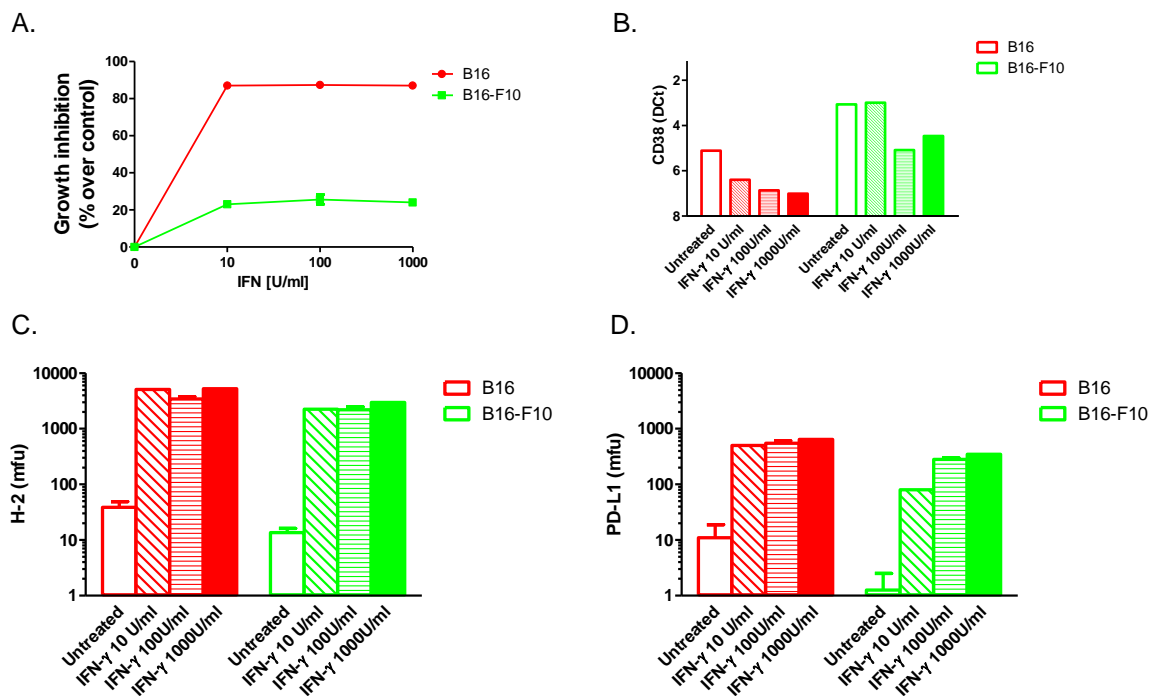


Figure 24. B16 and B16-F10 cultured *in vitro* in the presence of IFN- γ . A. Growth inhibition at 72 hours after treatments. B. Real-Time PCR molecular analysis of Cd38 transcript. C and D. H-2 and PD-L1 expression on membrane by flow cytometry.

These data, together with aOX40 experiments, showed that immune checkpoint inhibitors actually have a dual behaviour. Several factors might influence the potential clinical benefits induced by ICI therapy. Key points that surely require future studies are the influence exerted by the treatment schedule and the role played by IFN- γ and CD38 in the context of ICI therapy.

2. DISCOVERY OF NEW THERAPEUTIC TARGETS

HER2 is a perfect target to counteract HER2-positive mammary carcinoma progression. Several therapeutic approaches against HER2 have been developed, including monoclonal antibodies, small tyrosine-kinase inhibitors, and CAR-T. Nevertheless, all these treatments had limits and a number of patients ended up developing resistance, resulting in tumor progression.

The ability to identify new therapeutic targets is strictly related to the availability of preclinical models able to mirror the clinical condition of patients.

In this Chapter, I described new targets against HER2-positive mammary carcinoma through the study of cell lines derived from HER2 transgenic mice and patient-derived xenograft (PDX) models.

Some data reported in this section were included in two manuscripts (Giusti et al., submitted and (Landuzzi et al. 2021)).

2.1 Dynamic model of HER2 expression

We developed a dynamic model of HER2 expression based on cell lines originally derived from spontaneous mammary carcinomas of HER2 mice. HER2 loss was associated to an increase of stemness and EMT skills. Thus, we investigated alternative therapeutic targets to HER2, which could be eventually used in patients with tumors which are no longer HER2 addicted or that lose HER2 during progression.

2.1.1 Dynamic model of HER2 expression panel

This panel included two HER2 positive master cell lines: MamBo89HER2^{stable} cell line which displayed a high and stable HER2 expression that was maintained upon *in vivo* injection, and MamBo43HER2^{labile} cell line which, despite its comparably high HER2 expression, gave rise to HER2-negative tumors *in vivo*. The third key player of this panel was the MamBo38HER2^{loss} cell line, derived from *in vivo* growth of the MamBo43HER2^{labile} cell line (Figure 25A): when we injected the latter cell line in either

immunocompetent or immunodeficient mice, we always obtained HER2 negative tumors (Figure 25B), from one of these immunocompetent mice we derived the MamBo38HER2^{loss} cell line (Figure 25A). MamBo38HER2^{loss} did not express HER2 either on the cell surface (Figure 25A), nor at the intracellular level (Figure 25C), despite maintaining the same HER2 gene copy number as the parental MamBo43HER2^{labile} cell line (Table 1). Upon orthotopic *in vivo* injection, the MamBo38HER2^{loss} cell line (green curve) displayed higher tumorigenicity compared to the HER2-positive cell lines (Figure 25D). Tumor vessels of MamBo43HER2^{labile} and MamBo38HER2^{loss} cell lines, unlike MamBo89HER2^{stable} cell line, were lacking in pericytes (Figure 25E). Upon intravenous injection in HER2 mice, the MamBo38HER2^{loss} cell line displayed the highest experimental metastatic ability that led to the complete substitution of lungs with metastatic nodules (>200) within 3 weeks. On the contrary, HER2-positive cell lines gave rise to few (MamBo89HER2^{stable} cells, median number of metastasis 2, range 0-4, and incidence 4/5 mice) or no (MamBo43HER2^{labile} cells) lung metastases 18 weeks after cell injection.

MamBo89HER2^{stable} and MamBo43HER2^{labile} appeared *in vitro* as polygonal cells, whereas the MamBo38HER2^{loss} cell line formed a multilayer of spindle-like cells. MamBo38HER2^{loss} cells had a molecular profile resembling EMT (Figure 26).

Table 1.

Number of huHER2 gene copies quantified by Real-Time PCR. $\Delta Ct = C_{thiHER2} - C_{thi/mPTGER2}$. Expression level of $2^{-(\Delta Ct \text{ MDA-MB-231} + \Delta Ct \text{ MCF7})/2}$ was associated to two HER2 copies. TS/A is a murine mammary cancer cell line.

Cell line	ΔCt	huHER2 copy number
Mambo89HER2 ^{stable}	-7.27	51
Mambo43HER2 ^{labile}	-5.83	19
Mambo38HER2 ^{loss}	-5.79	18
TS/A	7.26	0
Non-transgenic normal tissue	4.25	0
HER2-transgenic normal tissue	-5.96	26
HER2-transgenic mammary tumor	-6.60	32
HCC1954	-9.34	215
BT-474	-7.53	61
SKBr3	-5.25	13
MDA-MB-453	-4.14	6

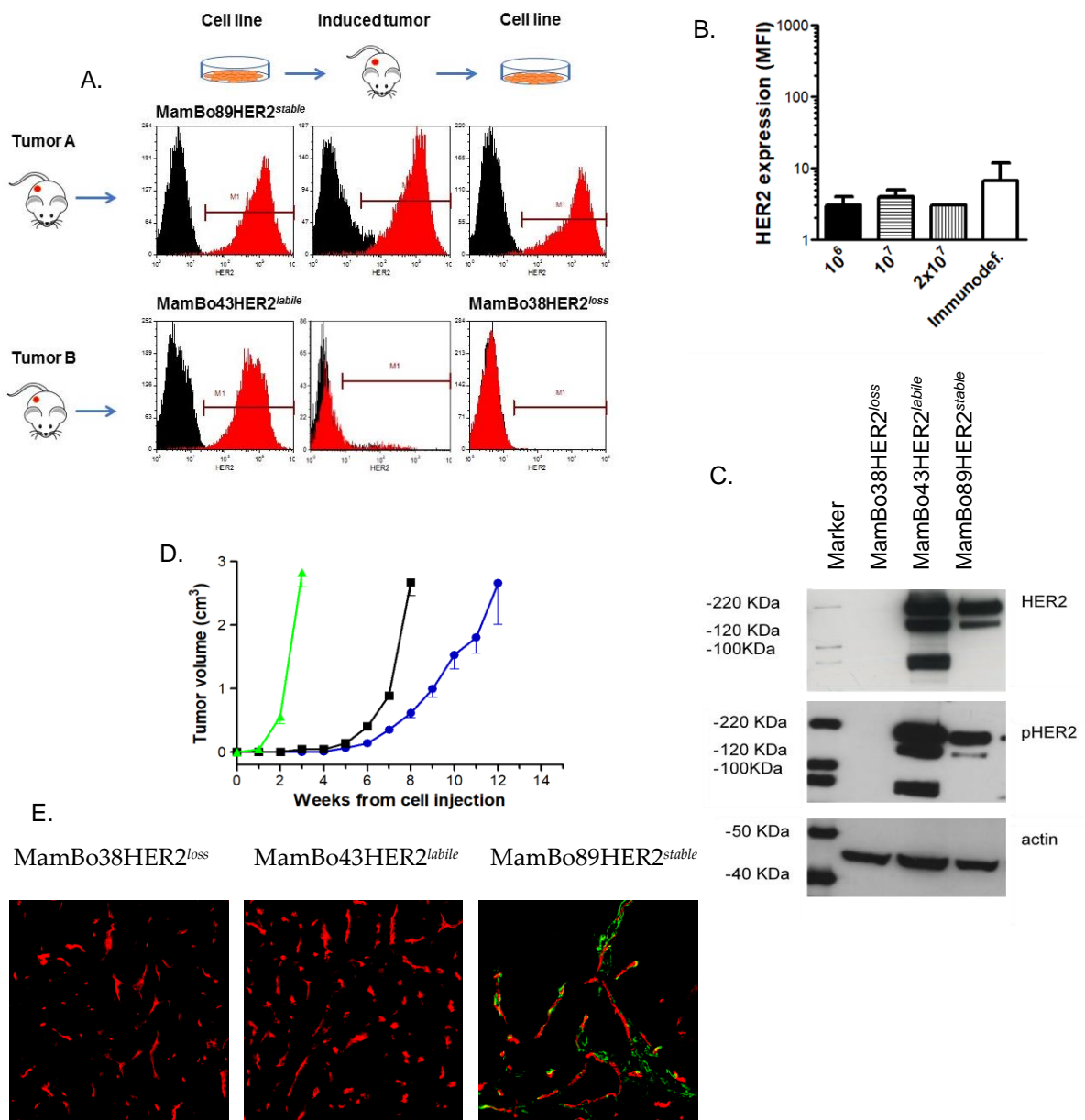


Figure 25. MamBo cell lines and dynamic HER2 expression. A. Panels show representative profiles of HER2 level as measured by cytofluorimetric analysis. Black profile, secondary antibody alone; red profile, anti-HER2 antibody. B. HER2 expression in tumors by MamBo43HER2^{labile} cells injected at different doses in immunocompetent mice (close black bar and bars with pattern) and in immunodeficient mice (open bar) detected by cytofluorimetric analysis. C. Expression of HER2 protein and of its phosphorylated isoform pHER2 in MamBo cell lines (Western blot). D. *In vivo* growth of MamBo cell lines (after injection of 10⁶ cells in m.f.p.) in HER2 female mice. Cell lines: MamBo38HER2^{loss} (green triangle), MamBo43HER2^{labile} (black square) and MamBo89HER2^{stable} (blue circle). Mean and SEM from 3-9 mice per group is shown. MamBo38HER2^{loss} growth was significantly faster, from 2 weeks after cell injection onwards, than MamBo43HER2^{labile} and MamBo89HER2^{stable} cell lines, $p < 0.01$ by Student's t-test. From 7 weeks after cell injection, MamBo43HER2^{labile} cells also grew faster compared to the MamBo89HER2^{stable} cell line, $p < 0.01$ by Student's t-test. E. Representative micrographs of tumor vessels were reported: CD31/CD105, red staining; NG2, green staining.

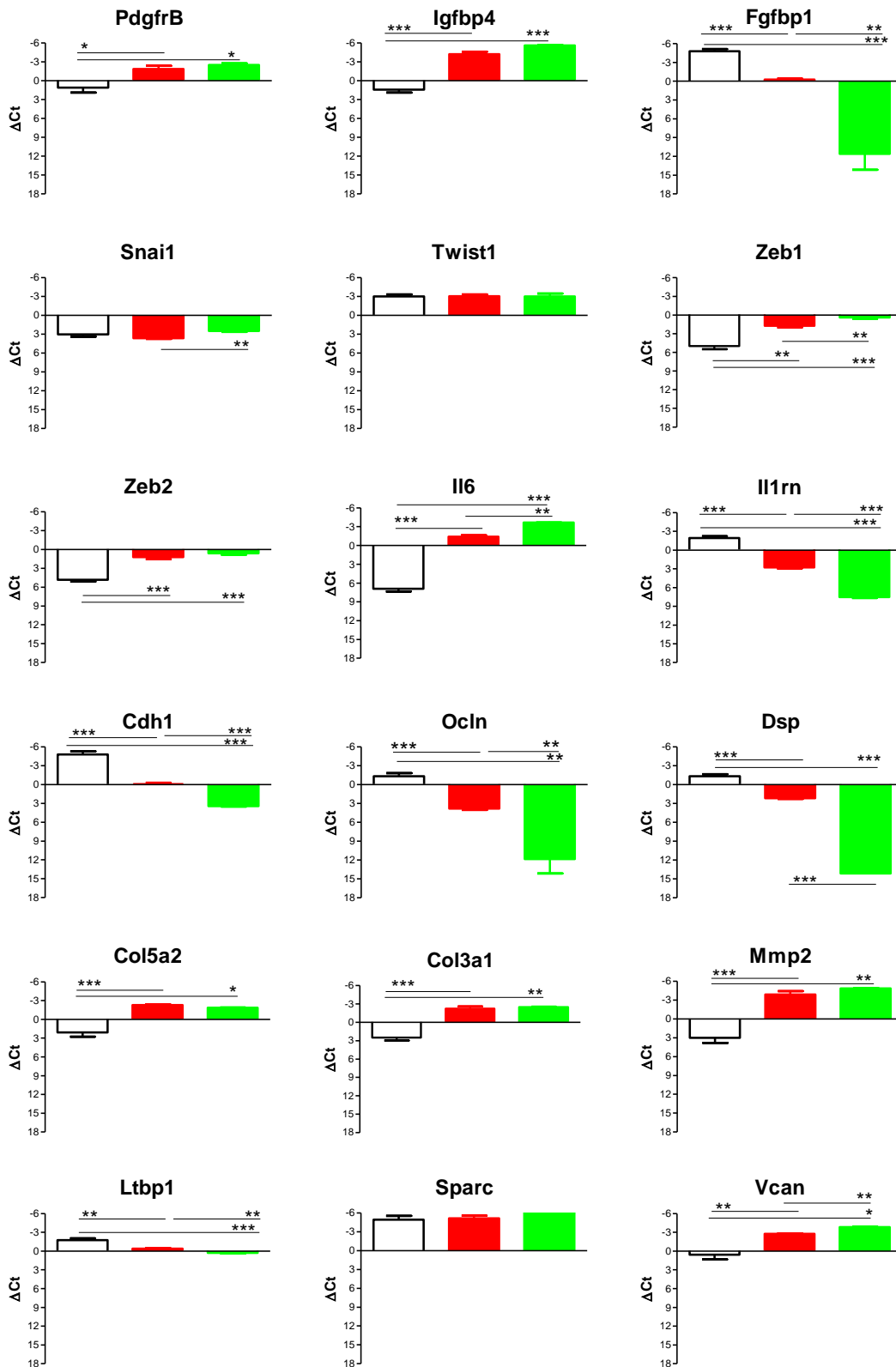


Figure 26. EMT profile by Real-Time PCR of MamBo43HER2^{labile} (empty bar), continuous long-term culture of MamBo43HER2^{labile} treated with trastuzumab (red bar) and MamBo38HER2^{loss} (green bar) cells; n=2-4. Each bar shows mean and SEM. *p<0.05; **p<0.01; ***p<0.001, by Student's t-test.

The MamBo38HER2^{loss} cell line displayed a higher capacity to form mammospheres, compared to MamBo89HER2^{stable} and MamBo43HER2^{labile} cell lines (Figure 27A), together with highly staminal features, with over 95% of cells being CD24^{negative}/CD44^{high}. The MamBo89HER2^{stable} cell line had a staminal profile with 3% of cells being CD24^{low}/CD44^{high} while MamBo43HER2^{labile} presented only a tiny sub-population of cells (1%) displaying staminal characteristics (Figure 27B).

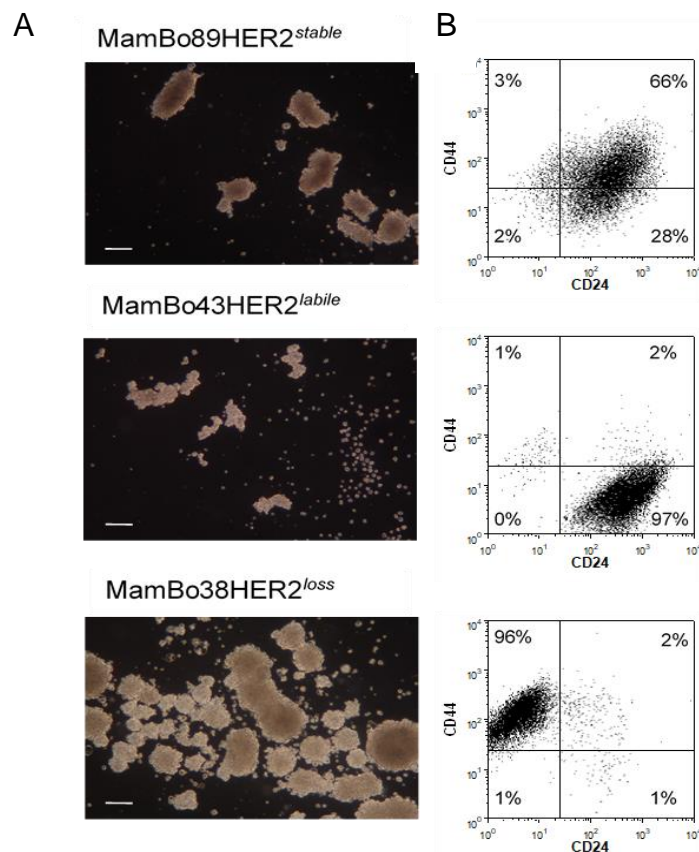


Figure 27. Stemness profile of MamBo cell lines. A. Dark-field micrographs of mammosphere formation assay. White bar corresponds to 200 μ m. Number of mammospheres (n=4): MamBo89HER2^{stable}, 23 \pm 1; MamBo43HER2^{labile}, 17 \pm 1; MamBo38HER2^{loss}, 69 \pm 9; MamBo38HER2^{loss} vs MamBo89HER2^{stable} and MamBo43HER2^{labile} cell lines, p<0.01 by Student's *t*-test. B. Expression of HER2 and stemness markers CD24 and CD44 in cells cultured under 2D-adherent conditions, measured by cytofluorimetric analysis.

The loss of HER2 observed *in vitro* was probably the result of a selection among several populations coexisting within MamBo43HER2^{labile} cells. We isolated AG24F and AG11F clones that were indeed spindle-like clones with a stemness profile similar to

the one of MamBo38HER2^{loss} cells. AD56D5 and AD56C1 were quite similar to MamBo43HER2^{labile} cell line, while AD56iota cells were almost all HER2 negative, with a quite spindle morphology, but, contrary to MamBo38HER^{loss} cells, this clone showed a different stemness profile, which was more similar to the one of MamBo89HER2^{stable} cell line (Figure 28).

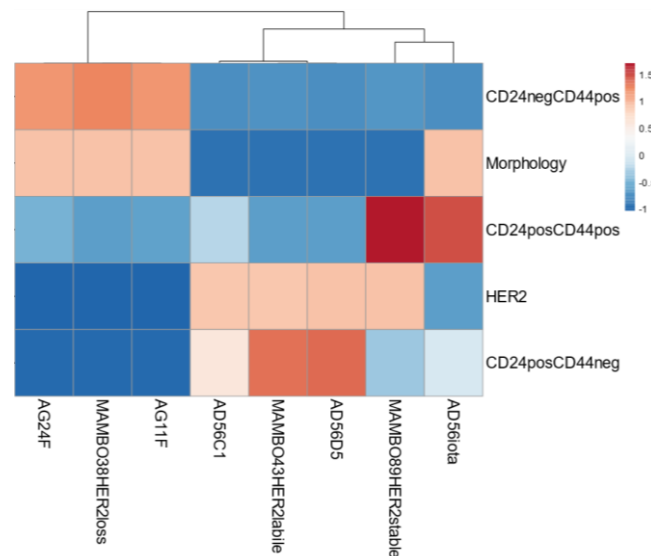


Figure 28. Clustering of clones isolated from MamBo43HER2^{labile} cell line based on HER2 expression (percentage of positive cells), morphology (spindle-like, pink; epithelial, blue) and stemness (percentage of CD24^{neg}/CD44^{pos}, CD24^{pos}/CD44^{pos}, CD24^{pos}/CD44^{neg}).

We studied the dynamic among subpopulations of MamBo43HER2^{labile} cells *in vitro*, evaluating which conditions promoted the emergence of HER2-negative and stemness-high subpopulation (Figure 29). We proved that continuous *in vitro* culture with trastuzumab at 30 µg/ml for 2 months resulted in an almost complete HER2-negative culture (HER2-positive cells were less than 10%) with a spindle-like morphology (although tiny islets of polygonal cells remained interspersed within the multilayer) and 65% of cells showed staminal features (CD24^{negative}/CD44^{high}) (Figure 29B and G).

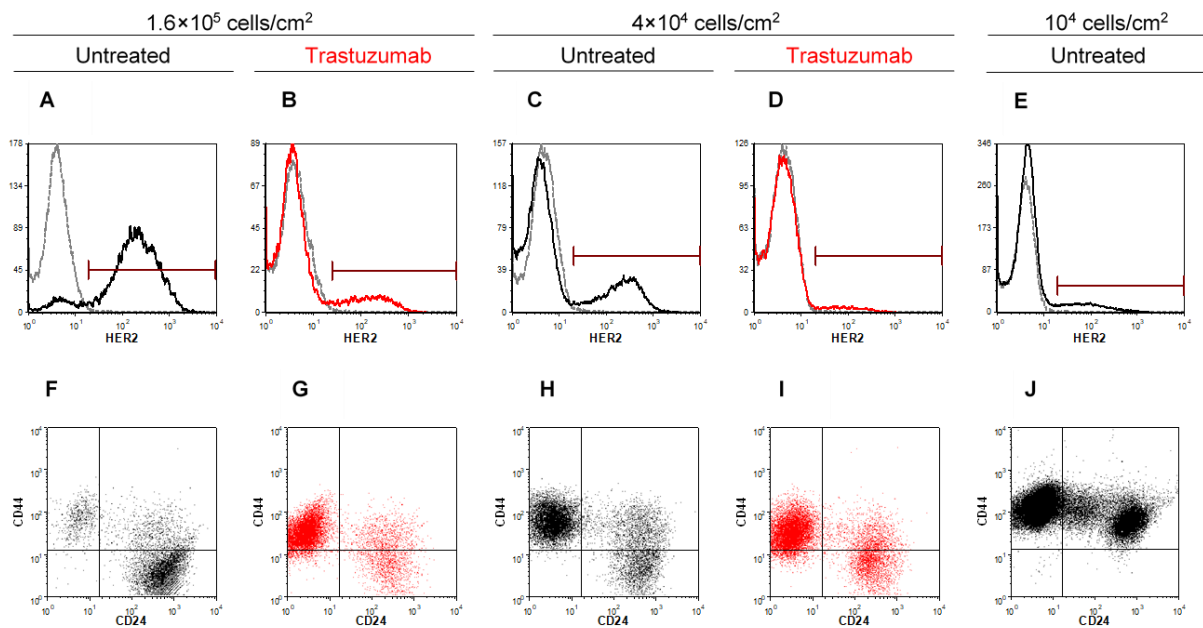


Figure 29. Effect of cell seeding and trastuzumab on phenotypic profile of MamBo43HER2^{labile} cells. Continuous cultures in control medium (A, C, E, F, H, J) or trastuzumab 30 $\mu\text{g}/\text{ml}$ (B, D, G, I). Level of HER2 (A-E) and stemness markers CD24 and CD44 (F-J) were measured by cytofluorimetric analysis. Cell seeding dose: 1.6×10^5 cells/cm², 60 days of culture (A-B, F-G); 4×10^4 cells/cm², 60 days of culture (C-D, H-I); 10^4 cells/cm², 30 days of culture (E, J).

This result was an off-target consequence of any treatment that alters cell density, as proved when we seeded MamBo43HER2^{labile} cells at lower doses than in the previous experiment (4×10^4 cells/cm² versus 1.6×10^5 cells/cm²) and again treated with trastuzumab at 30 $\mu\text{g}/\text{ml}$ for two months (Figure 29C, D, H, I). Trastuzumab-treated cells acquired spindle-like morphology and the HER2-negative population took over (Figure 29D). Moreover, 70% of the cells showed a stemness profile at the end of the long-term culture (Figure 29I), as well as in high density cell seeding (Figure 29B and G). Unexpectedly, even untreated cells spontaneously and gradually acquired spindle-like morphology at lower seeding density, and HER2 expression was detectable in less than 25% of cells after two months (Figure 29C). At the same time, 70% of cells acquired a staminal phenotype (Figure 29H). A further reduction in cell seeding dose (10^4 cells/cm²) prompted the fast-track acquisition of the spindle-like morphology, the loss

of HER2 expression and an enhancement in stemness within only one month, even in the absence of trastuzumab treatment (Figure 29E and J).

The comprehension of the mechanisms underlying the absence of HER2 expression in cells with multiple copies of HER2 was for us unclear, together with the molecular reasons for the dominance of the HER2-negative stemness-high population in critical conditions as *in vivo* injection and *in vitro* low-density cultures. This model did not offer the chance to focus on epigenetic patterns or transcriptional factors binding HER2 promoter since the HER2 transgene consisted of cDNA of human HER2 under the MMTV promoter without HER2 enhancers. Thus, we decided to use this dynamic model as a mirror of human HER2-positive tumors that maintain HER2 or, over the time, give rise to new tumors or metastases with a lower or absent HER2 expression.

2.1.2 Molecular portrait of HER2 dynamic expression

The need to identify predictive factors of HER2-loss and new therapeutic targets encouraged us to analyse in depth molecular changes associated with the dynamic expression of HER2. We performed an RNA-Seq analysis including several samples to reinforce the robustness of results. In the class of HER2-stable cell lines we included MamBo89HER2^{stable}, its clone MamBo89HER2^{stable}AG3 and MamBo89HER2^{stable} cells treated *in vitro* with trastuzumab for 30 days, and then cultured in medium for another month, or 60 days. Trastuzumab-treated cells maintained HER2 expression and the stemness profile of MamBo89HER2^{stable} cell line as well as MamBo89HER2^{stable}AG3 clone too. In the class of HER2-labile cells we had only MamBo43HER2^{labile} cells. Finally, in HER2-negative class we included MamBo38HER2^{loss} cells untreated or treated with trastuzumab for 30 or 60 days, since these cultures maintained the same features of the MamBo38HER2^{loss} one (data not shown). Moreover, we considered here also MamBo43HER2^{labile} cells treated with trastuzumab for 30 or 60 days, both HER2 negative and showing high stemness and spindle-like morphology. All the above

reported similarities were well described by principal component analysis (PCA) (Figure 30).

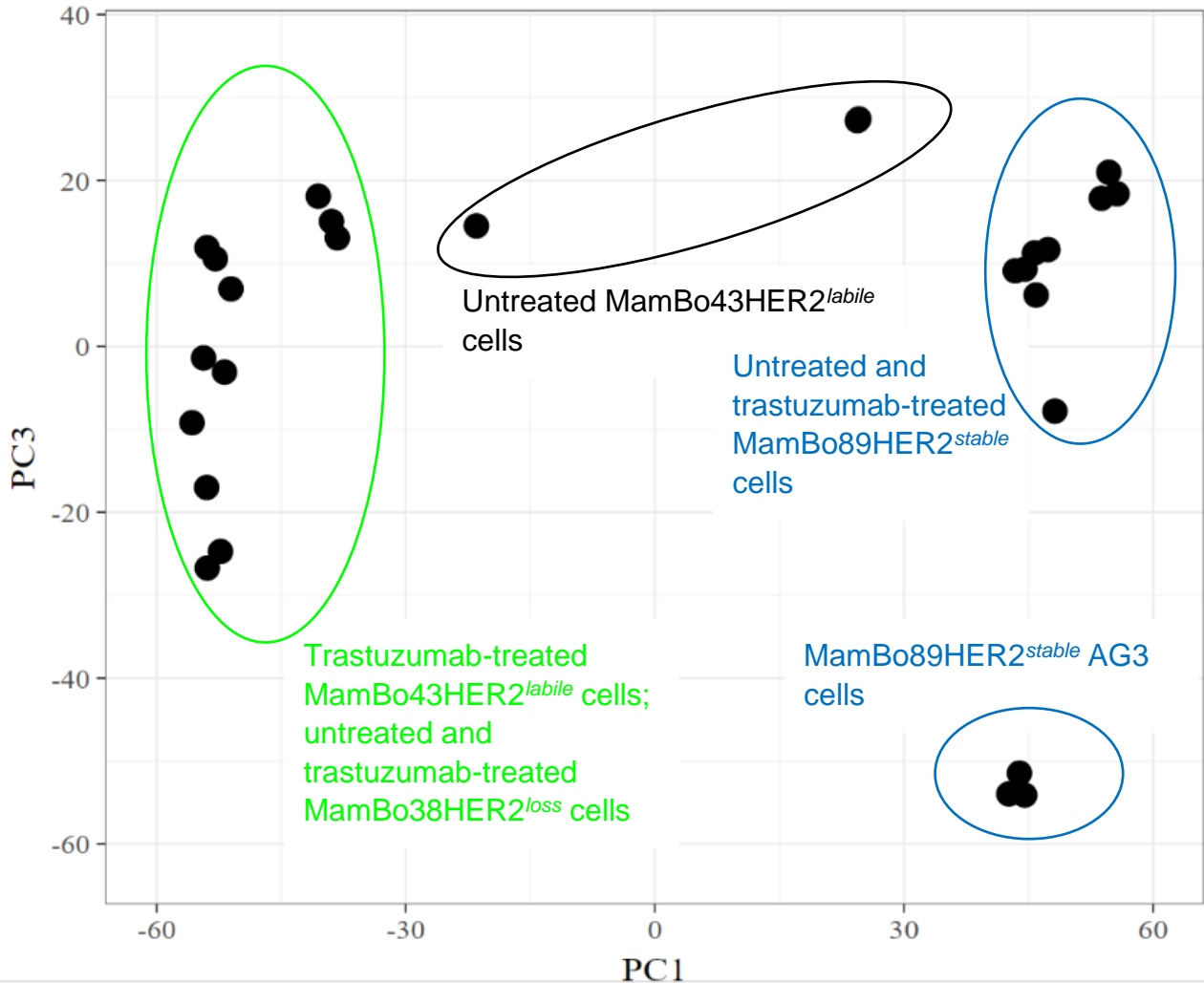


Figure 30. Principal component analysis of samples analysed by RNA-Seq.

We compared the HER2-stable group to the HER2-negative group. This comparison evidenced 138 up-regulated genes and 124 genes down-regulated in HER2-negative one (Figure 31). Hierarchical clustering showed how MamBo43HER2^{labile} cells had a profile in part similar to the one of HER2-negative cells and in part similar to HER2-stable cells.

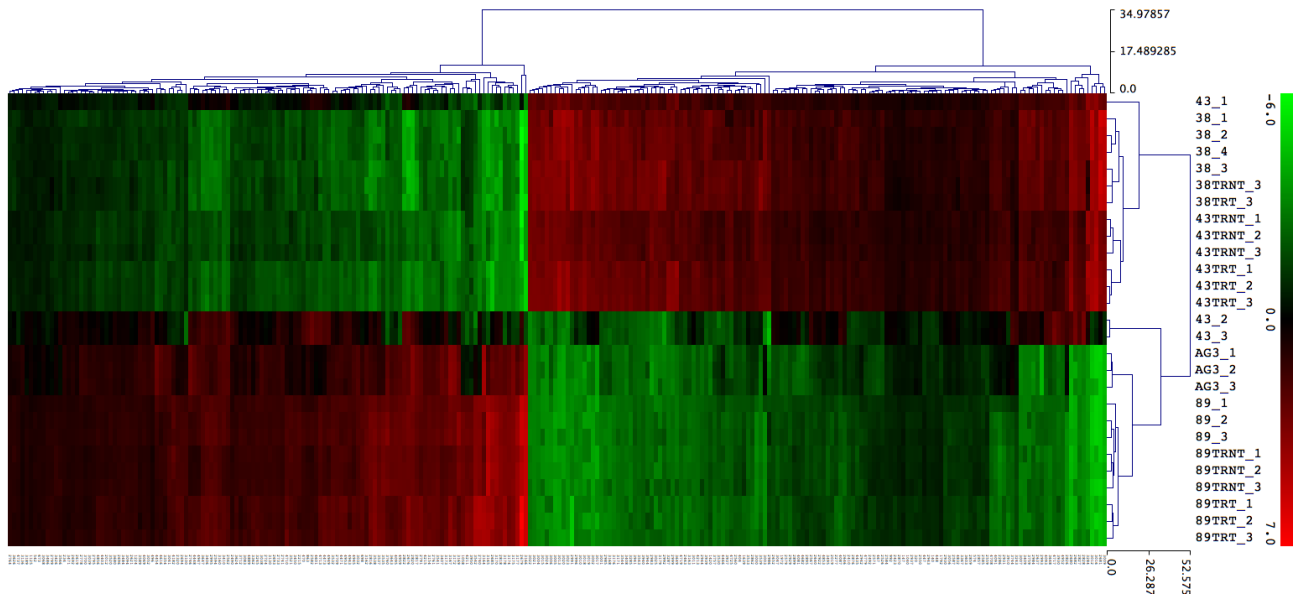


Figure 31. The list of genes differentially expressed between HER2-stable and -negative cell lines were used to manage a hierarchical clustering of RNA-Seq samples (TRNT= 30 days trastuzumab-treatment; TRT= 60 days trastuzumab-treatment; _n=replicate number).

The differentially expressed genes are involved in insulin growth factor binding (*Igfbp 4, 2, 6*) and vinculin binding (*Sorbs3* and *Synn*). *Tgfb1* was overexpressed in HER2-negative cells, while *Tgfb3* in HER2-stable cells. Furthermore, we found several genes involved in EMT signature (*Lrp1, Itgb3, Htra1, Loxl1, Glipr1, Efemp2, Lgals1, Sgcd, Dpysl3, Tgfb1, Prrx1, Gadd45a, Igfbp4, Tpm2, Igfbp2, Pcolce, Emp3, Dcn, Sfrp1, Mmp14, Col3a1, Vcan, Col1a2, Lox* and *Sntb1*). We also identified genes involved in adipogenesis (*Rtn3, Gadd45a, Lpcat3, Chchd10, Pim3, Cd302, Dhcr7, Dnajc15*) and Interferon Alpha Response (*Plscr1, Cnp, Dhx58, Ncoa7, Psmb8*) through Enrichr analysis (MSigDB-Hallmark2020).

According to RNA-Seq, MamBo89HER2^{stable} and MamBo89HER2^{stable}AG3 had a lower expression of *Sorbs3* (Sorbin And SH3 Domain Containing 3) compared to the other cell lines (Figure 32A left panel). These data were confirmed by Real-Time PCR and immunofluorescence on adherent cells (Figure 32A right panel, and B). The downmodulation of *SORBS3*, relative to tumors that are diploid for this gene, was associated with a worse overall survival rate in HER2-positive mammary carcinoma patients (Figure 32E). Since other genes neighbouring with *Sorbs3* (in mouse chromosome) were less expressed in MamBo89HER2^{stable} in respect to

MamBo38HER2^{loss} and MamBo43HER2^{labile} cell lines, such as *Mmp14*, *Lmo7*, *Ghitm*, *Sucla2*, *Sngt1* and *Ipo4*, we speculated that this chromosome region was absent in MamBo89HER2^{stable} and MamBo89HER2^{stable}AG3 cell lines. The absence of *SORBS3* was associated to a higher activation of STAT3 (Ploeger et al. 2016) that we also found in MamBo89HER2^{stable} cell line (Figure 32D) and that could be related to the intrinsic trastuzumab-resistance of these cells observed *in vitro*. Indeed, the higher STAT3 activation, together with the ability of these cells to produce IL6 (Figure 32C), suggest the presence of a HER2-alternative signaling able to sustain tumor growth.

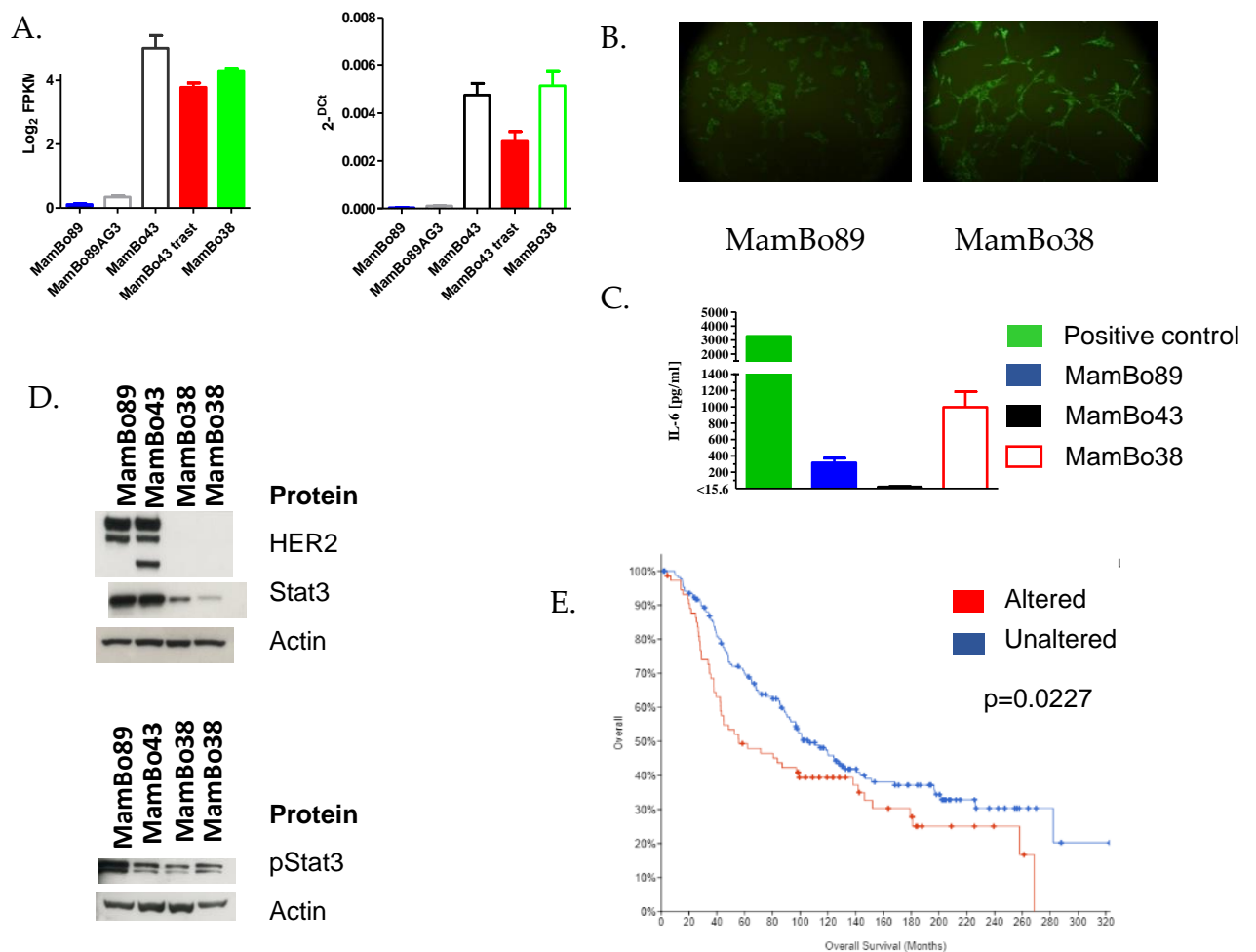


Figure 32. SORBS3 as a possible therapeutic target in mammary carcinoma. A. Expression of *Sorbs3* detected through RNA-Seq (left) and Real-Time PCR (right). B. SORBS3 immunofluorescence on MamBo89HER2^{stable} (left panel) and MamBo38HER2^{loss} (right panel) adherent cells. C. IL6 level measured by ELISA. D. STAT3 and pSTAT3 level in MamBo cell lines detected through Western Blot. E. Correlation between SORBS3 down-modulation and overall survival in HER2-positive mammary carcinomas through C-Bioportal analysis; Logrank Test P-value=0.0227.

The opportunity to restore *SORBS3* expression in order to resensitize MamBo89HER2^{stable} cells to trastuzumab might be considered.

We also looked for predictive genes of HER2 loss. For this purpose, we crossed up-regulated genes in the HER2-labile vs the HER2-stable group and up-regulated genes in the HER2-negative group vs the HER2-stable group. Genes common to both lists might be considered up-regulated through HER2 lability condition (Table 2, UP). Similarly, we performed the same analysis for down regulated genes (Table 2, DOWN). These analyses evidenced 42 up-regulated genes in both HER2-labile and HER2-negative cells compared to HER2-stable cells alongside 47 down-modulated genes. Functional analysis of these genes confirmed the presence of genes involved in EMT process (*Efemp2*, *Mmp14*, *Tgfb1*, *Col1a2*, *Lrp1*, *Prrx1*, *Pcolce*, *Dcn*), apoptosis (*Gstm1*, *Cav1*, *Timp2*, *Igfbp6*, *Dcn*), K-ras signaling (*Mmp11*, *Prrx1*, *Psmb8*), TGF-B signaling (*Tgfb1* and *Rab31*), Cholesterol Homeostasis (*Plscr1* and *Gpx8*) and IFN-gamma response (*Plscr1*, *Tnfaip2*, *Psmb8*).

Table 2. List of genes suggested as predictors of HER2 lability and loss

UP			DOWN		
Abhd4	Gprc5a	Pdhh	Ammecr1	Csn2	Pgf
Aebp1	Gpx8	Plscr1	Arhgef1	Csn3	Pik3r3
Akr1b3	Gstm1	Prrx1	Atxn7l3	Dhcr7	Plvap
Arhgdib	Igfbp6	Psmb8	Bnip1	Dhx58	Sfrp1
Armcx2	Ikbip	Rab31	Bpifb1	Dmd	Shf
Cav1	Lamb1	Rbpms	Bpifb4	Fam53b	Slc9a3r1
Cbx6	Lhfp	Slc25a37	Cd14	Foxo4	Spsb4
Cd302	Lmo7	Slc43a3	Cdk16	Gcnt4	Syng2
Col1a2	Lrp1	Sorbs3	Chil1	Hmgb3	Synm
Cpq	Mmp11	Tgfb1	Chl1	Igfbp2	Tacstd2
Cuedc2	Mmp14	Timp2	Chmp6	Klf13	Tfap2c
Dcn	Mt2	Tnfaip2	Chsy1	Krt15	Tm4sf1
Dnajc15	Npdc1		Cited1	Lgr4	Tsc22d4
Efemp2	Ogn		Cnp	Lpcat2	Tspan1
Gde1	Pcolce		Crispld2	Ly6d	Wfdc3
			Csn1s1	Ocr1	

Finally, the comparison between HER2-positive, including HER2-stable and -labile cell lines, vs HER2-negative cell lines identified 402 up-regulated genes in HER2-negative cell lines, whereas 349 were down-regulated. Differentially expressed genes were significantly associated with processes related to angiogenesis, migration ability, exocytosis, cell-cell adherence and communication and cellular differentiation. The up-regulated genes in HER2-negative cells are involved in extracellular matrix organization (*Fn1* and *Vim*) and angiogenesis (*Vegfa*, *Ptgs2* and *Hif- α*). Furthermore, several genes are known to play a role in promoting both tumor-cell aggressiveness and EMT, and in sustaining the proliferation of mesenchymal cells (*Dcn*, *Cav1*, *Cdkn1a*, *Myc*, *Qsox1* and *Pdgfrb*). On the other hand, down-regulated genes in HER2-negative cells are directly linked to HER2 overexpression and HER2-positive breast cancers (e.g. *Stat*, *Ptpn1*, *Pak1*, *Efnb1*) and polygonal shape (such as *Cecam1*, *Jup*, *Cdh1*, *Notch1* and *Kit*).

2.1.3 p95HER2 and PHLDA1

In MamBo43HER2^{labile} cells, we detected the presence of the p95HER2 fragments. This fragment was absent, or expressed at a lower level, in MamBo89HER2^{stable} cells and obviously absent in MamBo38HER2^{loss} cells (Figure 25C and Figure 33A and B). PHLDA1 (Pleckstrin homology-like domain family A member 1) was found to be associated to p95HER2 611-CTF (Pedersen et al. 2009), although its role in tumorigenesis process was controversial. We found that, as expected, MamBo43HER^{labile} cells expressed high levels of PHLDA1 (Figure 33A) and that the inhibition of its expression reduced cell migration (Figure 33C and 33D). This target will require future investigations both *in vivo* and *in vitro*.

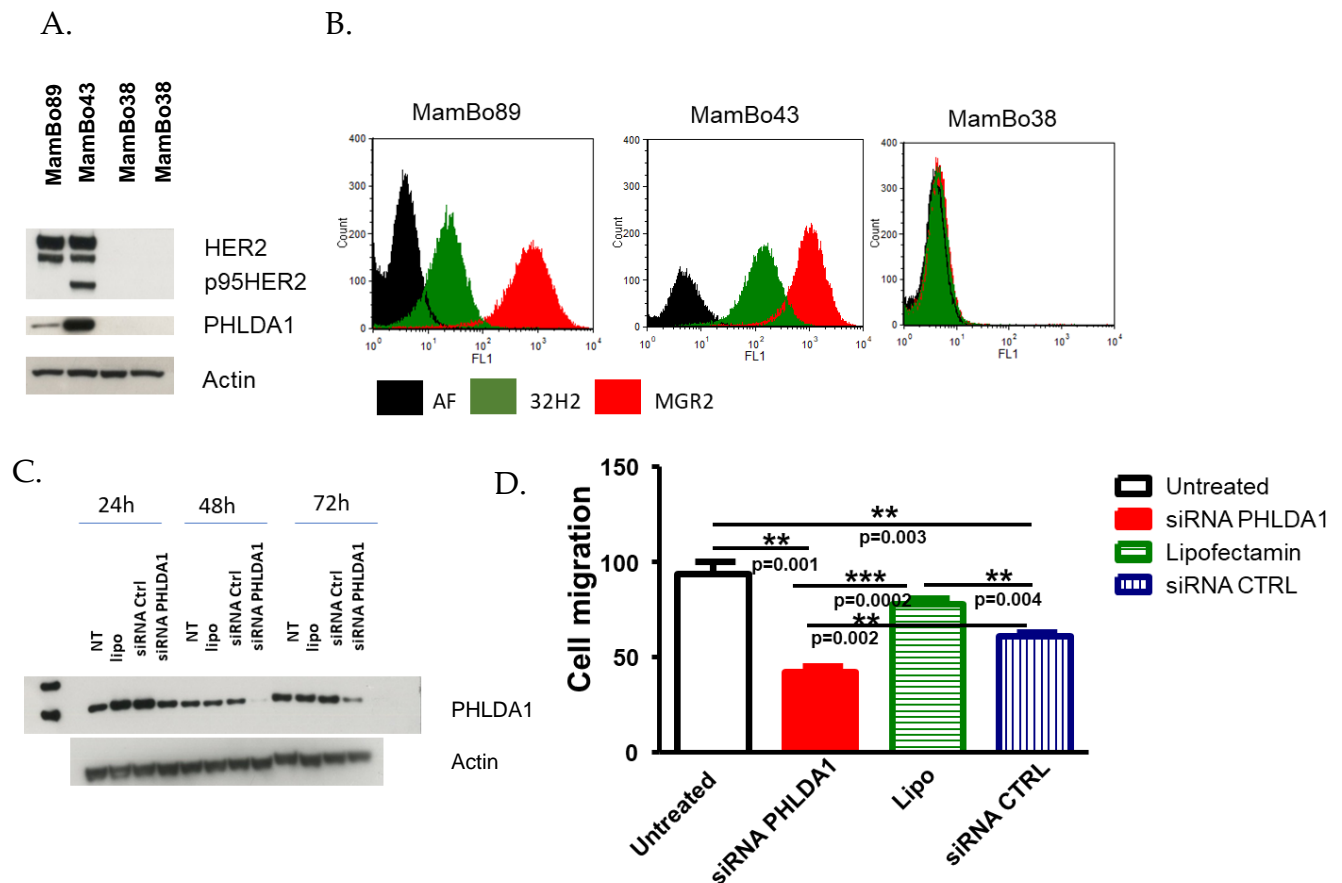


Figure 33. PHLDA1 as possible new therapeutic target in mammary carcinoma. A. Expression of p95HER2 fragments and PHLDA1, detected through Western Blot. B. Expression of HER2-full length (MGR2 antibody) and p95HER2-611CTF (32H2 antibody), detected through flow cytometry. C. Inhibition of PHLDA1 expression in MamBo43HER2^{labile} cells by siRNA treatment. D. Effect of siRNA on cell migration (y axis= number of migrated cells). Lipo, lipofectamine. Significance difference by Student's t-test.

2.1.4 PDGFR-B as a therapeutic target for HER2 loss cells

Molecular analysis revealed that PDGFR-B may be one of the molecules that sustains the growth of HER2-negative cell lines (Figure 34A). Thus, we tested the ability of sunitinib, a pan TKI inhibitor that includes both VEGFR and PDGFR-B among its targets, to inhibit the growth of MamBo38HER2^{loss} cells, both *in vitro* and *in vivo*. We found that sunitinib reduced the growth of both MamBo43HER2^{labile} (Figure 34B) and MamBo38HER2^{loss} cells *in vivo* (Figure 34C). Furthermore, sunitinib reduced IL6 production (Figure 34D) and inhibited its downstream pathway through down-

modulation of pStat3 (Figure 34E). Finally, sunitinib reduced MamBo38HER2^{loss} mammosphere formation by 50%, as well as cell migration ability (Figure 34F and G).

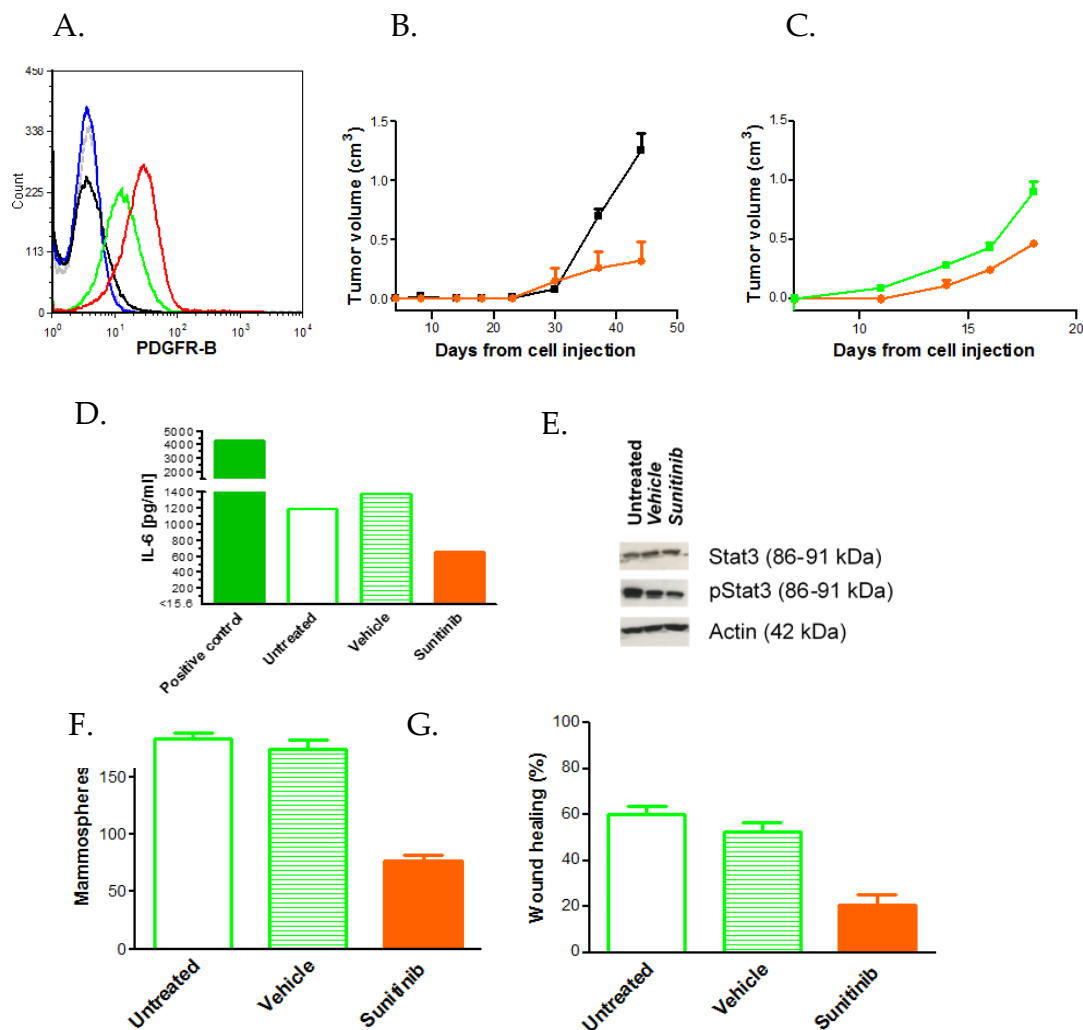


Figure 34. Targeting PDGFR-B *in vivo* and *in vitro*. A. PDGFR-B level measured by cytofluorimetric analysis. Profiles: grey, secondary antibody; blue, MamBo89HER2^{stable} cell line; black, MamBo43HER2^{labile} cell line; green, MamBo38HER2^{loss} cell line; red, trastuzumab-treated MamBo43HER2^{labile} cell line. B. Effect of sunitinib on MamBo43HER2^{labile} tumor growth. Sunitinib significantly reduced tumor growth from the 37th day after cell injection onward, $p < 0.05$, at least, by Student's t-test. C. Effect of sunitinib on MamBo38HER2^{loss} tumor growth. Sunitinib significantly reduced tumor growth from the 14th day after cell injection onward, $p < 0.05$, at least, by Student's t-test. In (B-C) untreated mice (black square, MamBo43HER2^{labile} or green square, MamBo38HER2^{loss}) or 60 mg/Kg sunitinib-treated mice (orange circle). Data shown are the mean and SEM from 3-5 mice per group. D-G. Effect of sunitinib (5 μ M) on MamBo38HER2^{loss} *in vitro*: (D) IL6 production detected by ELISA; (E) Western blotting analysis for STAT3 and pSTAT3 on cells treated with sunitinib; (F) Mammosphere formation assay. Data shown are the mean and SEM, $n = 2-4$ for each group; $p < 0.01$, sunitinib vs untreated or vehicle by Student's t-test; (G) Wound-healing assay. Data shown are the mean and SEM, $n = 6-8$ for each sunitinib-treated group. $p < 0.01$, vs untreated or vehicle by Student's t-test.

2.2 Dynamic model of HER2-positive breast cancer progression

We derived a panel of PDX that were obtained from surgical samples of patients with HER2-positive breast cancers. Among these lines, PDX-BRB4 was negative for HER1, positive for BCL2 and had very high expression of p53.

In order to better characterize the HER2 molecules, we also investigated the expression of both HER2 full-length and its aggressiveness-related isoform Delta 16 through *in situ* hybridization. HER2-full-length expression showed score 4 (in a 0-4 score scale), while HER2-Delta16 isoform expression showed score 2 (Figure 35A-D). Serial *in vivo* passaging of PDX-BRB4 did not cause the loss of HER2-Full-length and HER2-Delta16 expression, nor affected the ratio between the isoforms. PDX-BRB4 at >9 *in vivo* passages showed a slight decrease of both HER2 isoform expression, which however remained as high as the BT-474 HER2-positive breast cancer cell line control (Figure 35E).

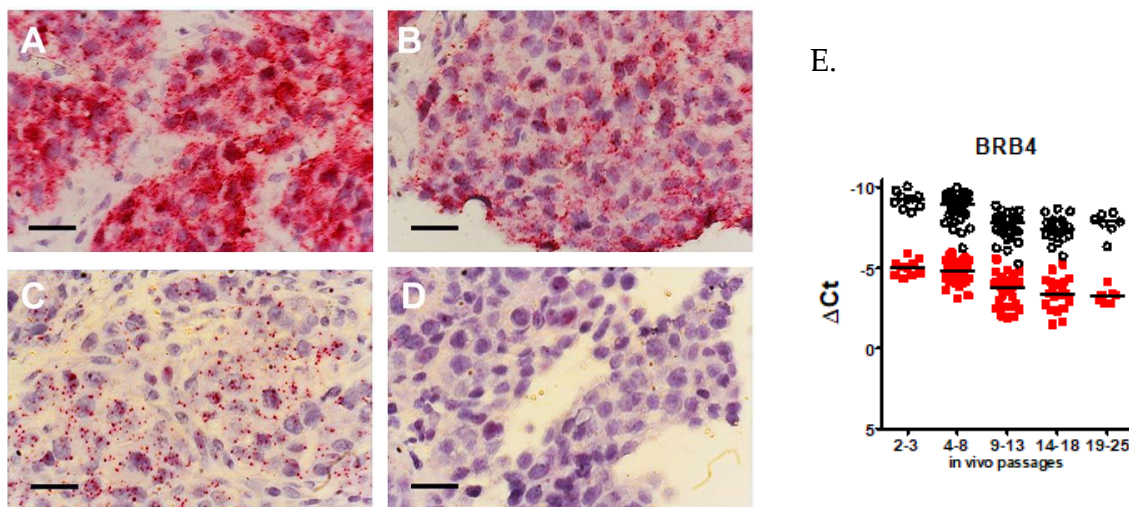


Figure 35. HER2-full length and HER2-Delta16 transcript levels in PDX-BRB4. A-D. In situ hybridization (BaseScope assay on formalin-fixed, paraffin-embedded tissue sections). A. HER2 probe hybridizing all isoforms, score 4 (>6 dots/cell, >10% positive cells have dot clusters); B. HER2 probe hybridizing HER2 full-length isoform, score 4; C. D16 probe hybridizing HER2-D16 splice variant, score 2 (2-3 dots/cell); D. negative control probes. Magnification 40 \times , Scale bar = 33 μ m. E. Expression of HER2 full-length (open black circles) and HER2-D16 (red closed squares) mRNA isoforms in HER2-positive PDX after serial *in vivo* passage. $\Delta Ct = Ct$ of relevant gene – Ct of hTBP reference gene. Individual samples are plotted, with median (horizontal line). RT-PCR analysis was performed in parallel on a high HER2-positive (BT-474) and a HER2-negative (RH4) human tumor cell lines. Mean ΔCt of BT-474 positive controls were: HER2 = -6.97; D16 = -2.75. Mean ΔCt of RH4 negative controls were: HER2 = 4.74; D16 = 9.11. (Landuzzi et al. 2021)

2.2.1 Progression of HER2-positive PDX-BRB4 line

To investigate PDX tumor progression trend, HER2-positive amplified PDX-BRB4 was split after the second passage in six different sublines, which were then re-transplanted separately to analyze random and selective events in long-term evolution (Figure 36A). One out of six sublines (named PDX-BRB4-A1), passaged up to 25 times along approximately 4 years, progressively acquired a significantly increased tumor growth rate (Figure 36B). High-passage A1 subline showed an increased ability to form mammospheres *in vitro*, compared to its low-passage counterpart (Figure 36C), and it showed a CD24^{low}/CD44^{high} phenotype (data not shown), denoting an enriched cancer stem cell phenotype.

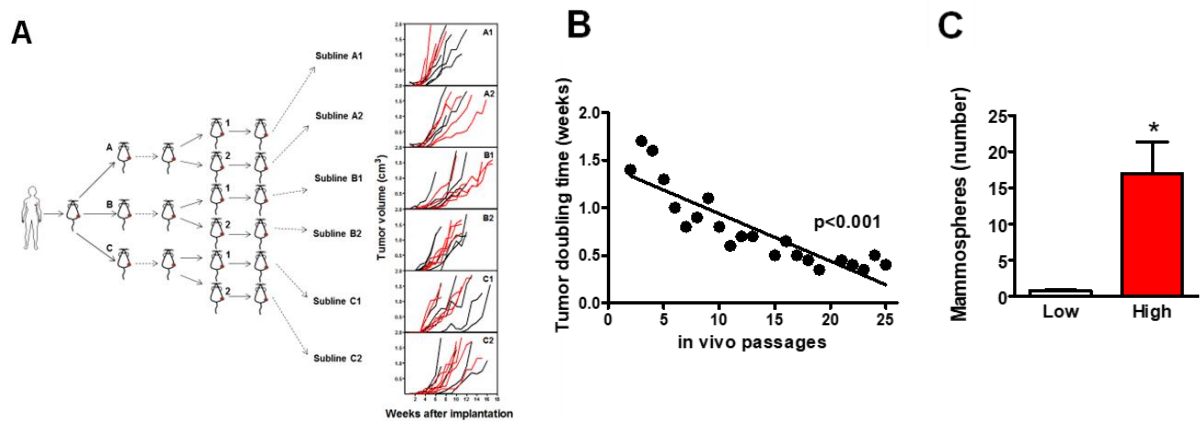


Figure 36. Random progression in sublines of PDX-BRB4. A. Origin of independent sublines of PDX-BRB4 and growth kinetics during *in vivo* passages. Right panels show individual tumor growth curves of sublines at low-passage (passage 4-8, black lines) and high-passage (14-18, red lines). B. Tumor doubling time of the subline PDX-BRB4-A1 during long-term *in vivo* passages (up to approximately 4 year), calculated in the exponential growth phase. Significance at linear regression test is shown in the panel. C. Mammospheres formed *in vitro* by PDX-BRB4-A1 at low- (8) and high-passage (23-26). Mean and SEM from 3-4 independent determinations (6 replicates each) is shown. *, p<0.05. (Landuzzi et al. 2021)

High-passage PDX-BRB4-A1 subline showed a progressively decrease of BCL2 expression, detected by immunohistochemistry, with a shift from a highly positive to an intermediate/negative phenotype, confirmed by RT-PCR analysis (Figure 37).

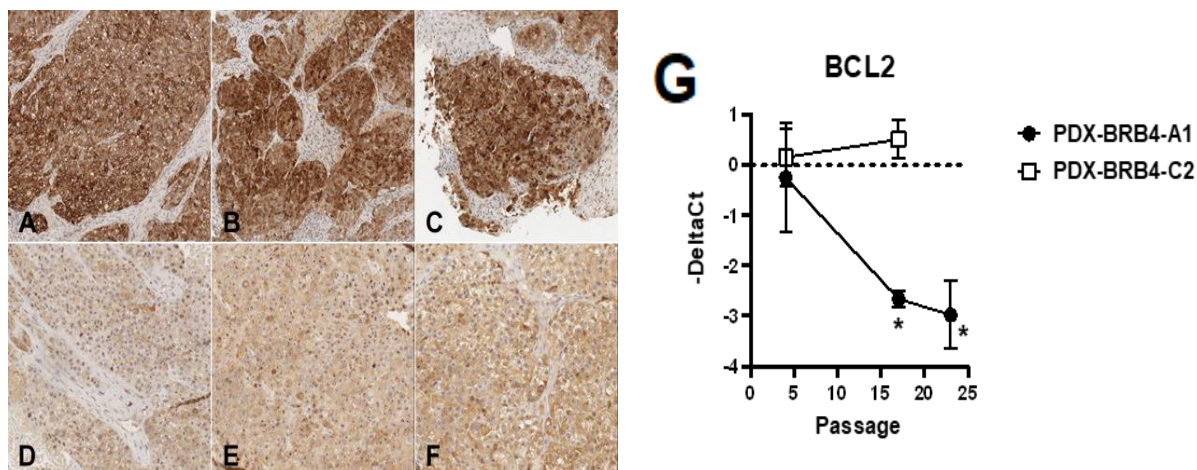


Figure 37. Decrease of BCL2 expression during tumor progression. A-F. Immunohistochemical expression of BCL2 in PDX-BRB4-A1 at low-passage (5-7 passages, panels A-C) and in its progressed high-passage subline (23-26 passages, panels D-F). Sections were stained with antibodies against BCL2 biomarker. G. RT-PCR expression level of BCL2 α in PDX-BRB4 sublines at different *in vivo* passages. Mean and SEM from three independent replicates is shown. Significance: linear regression of BCL2 in PDX-BRB4-A1 subline, $p < 0.01$; * $p < 0.05$ high-passage PDX-BRB4-A1 subline *versus* low-passage PDXBRB4-A1 subline and *versus* PDX-BRB4-C2 subline. (Landuzzi et al. 2021)

Macroscopic and molecular evidence of metastatic spread was absent in low-passage PDX-BRB4-A1 subline. In contrast, metastatic cells were detected sporadically in the lungs from high-passage PDX-bearing mice. To better evidence the different metastatic ability between the low- and the high-passage settings, cells dissociated from *in vivo* passaged PDX-BRB4 sublines were injected i.v. in mice to evaluate hematogenous metastatization. Low-passage A1 did not produce metastatic deposits in the lungs, whereas high-passage progressed A1 subline gave rise to overt lung metastases (Table 3). Moreover, low- and high-passage A1 sublines of PDX-BRB4 also differed in the ability to grow in cultures: low-passage PDX cultures stopped growing and underwent senescence more rapidly than high-passage A1 (Table 3). No difference, on the contrary, was found between low and high passages of non-progressed PDX-BRB4 sublines, which rapidly underwent senescence.

2.2.2 Molecular profile associated to HER2-positive PDX subline progression

RNA-Seq analysis of progressed A1 subline of PDX-BRB4 was conducted. Acquirement of a progressing phenotype by PDX-BRB4-A1 subline from low to high passages (as defined based on the concomitant increase in growth rate, stemness, lung metastatic ability and resistance to *in vitro* cell senescence) was investigated through the comparative analysis of the low- and high-passage transcription profiles, which were compared with the ones of low and high passages of a non-progressing subline (C1).

Table 3. Functional progression of PDX-BRB4-A1 subline (Landuzzi et al. 2021)

PDX-BRB4 Subline	<i>In vivo</i> passages (range)	Tumor doubling time (weeks)	Lung metastases* (mice with metastases/total number of mice)	Time to <i>in vitro</i> senescence (days, mean and SEM)
A1	3-5	1.5 ± 0.1	0/4	52.0 ± 4.4
A1	15-24	0.5 ± 0.03 ^{a,b}	4/4	145.8 ± 16.9 ^{a,b}
C2	3-5	1.4 ± 0.6	nd ^c	50.3 ± 22.8
C2	14-17	0.8 ± 0.1	0/3 ^d	11.7 ± 5.0

*after i.v. injection of dissociated cells

^a $P < 0.05$ at least *vs* A1 3-5 passages (Student's *t* test)

^b $P < 0.05$ at least *vs* C2 14-17 passages (Student's *t* test)

^cnot done

^dnegativity confirmed by molecular assay

Differential expression analysis was performed by comparing progressed A1 subline at passage 17 with respect to those at passage 4. RNA-Seq analysis was carried out on triplicate independent samples per group. A total of 834 differentially expressed genes were detected. Transcription profiles of A1 subline at passage 24 were nearly superimposable to those of A1 at passage 17 and they were not considered in the differential expression analysis so that comparison between the two groups could be kept balanced. Hierarchical clustering (Figure 38A) of the 834 differentially expressed genes was used to identify the subset of genes characterizing the progressed phenotype, by comparing progressed phenotype (passages 17 and 24 of A1 subline) to

non-progressed sublines (passage 4 of A1 subline and passages 4 and 17 of C1 subline). Only genes showing a difference in expression between progressed phenotype and all the other samples were kept: 193 genes up-modulated in progressed phenotype (Figure 38B) and 288 genes down-modulated in progressed phenotype (Figure 38C). The 481 differentially expressed genes (193 up-modulated and 288 down-modulated) detected by hierarchical clustering were loaded in an IPA pathway.

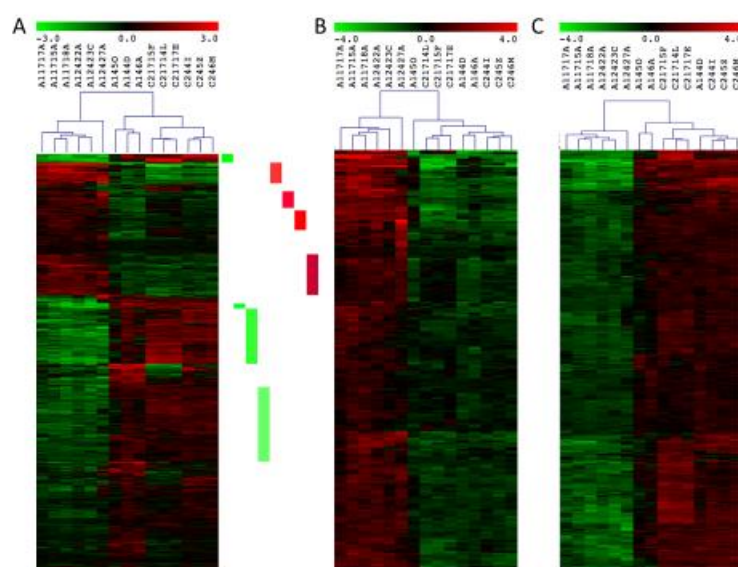


Figure 38. Hierarchical clustering (Euclidean distance, average linkage) of differentially expressed genes in progressed subline (see Legend Table enclosed for codes of independent samples examined along with their progression phenotypes). A. 834 differentially expressed genes detected comparing progressed (passage 17) with non-progressed (passage 4) A1 subline of PDX-BRB4. Red and green lateral bars indicate the gene subsets showing homogeneous progressed phenotype (passages 17 and 24) with respect to non-progressed low-passage 4 (same subline) or 17 (C1 subline). B. 193 differentially expressed genes up modulated in progressed A1 subline (passage 17 and 24, see red bars of panel A). C. 288 DE genes downmodulated in progressed A1 subline (passage 17 and 24, see green bars of panel A). (Landuzzi et al. 2021)

Legend of studied sample:

PDX-BRB4 subline	<i>In vivo</i> passage	Progressed phenotype ^a	Code of independent samples	Time of <i>in vivo</i> passaging (years)
A1	4	No	A144D, A145O, A146A	1.5
A1	17	Yes	A1175A, A1177A, A1178A	3.5
A1	24	Yes	A12422A, A12423C, A12427A	>4.0
C1	4	No	C244I, C245Z, C246M	1.5
C1	17	No	C21714L, C21715F, C21717E	>4.0

The genes were then connected together by using only direct interaction, e.g. an article describing that gene X is affecting gene Y activity, between genes. Within this network we identified that *BCL2*, which is down-modulated in progressed phenotype, is connected to three main hub genes, which are down-regulated too: *CDKN2A*, *STAT5A* and *WT1* (Figure 39). Looking at genes up- and down-modulated in the EMT, we found that progressed A1 subline had increased expression of some genes usually up-modulated in EMT (such as *COL6A3*, *ITGB3*, *SNAI2/SLUG*, *TGFbeta1* and *BMP2*) and decreased expression of some genes usually down-modulated in EMT (such as *CLDN10*, *CLDN3* and *BMP5*), compared to non-progressed cell variants. Nevertheless, the main driver or inducer genes of EMT (such as *TWIST*, *ZEB1*, *ZEB2*, *SNAIL*, *E-CAD*, *VIM*, *PTGS2* and *NOTCH*) did not result to be differentially expressed. Such expression pattern suggests that progressed A1 subline is undergoing a partial EMT, as also shown by the maintained epithelial cell morphology.

These results were in accordance with data obtained in the previous model of HER2 loss. In fact, for both models, stemness and EMT appeared together with tumor progression.

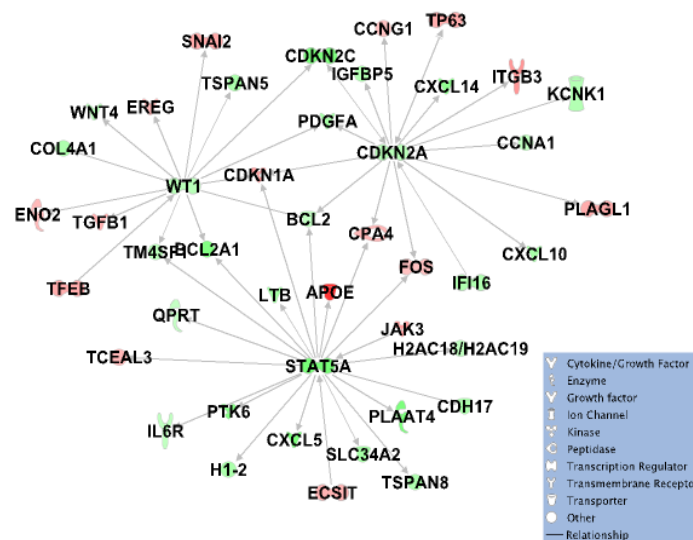


Figure 39. IPA sub-network showing that *BCL2*, which is down-modulated in progressed A1 subline (passage 17 and 24), is connected to three main hub genes, which also are down-regulated (*CDKN2A*, *STAT5A* and *WT1*). (Landuzzi et al. 2021)

Discussion

Target therapy has significantly improved the management of cancer patients with oncogene-addicted tumors. The use of trastuzumab in HER2-positive breast cancer patients or the treatment with TKIs in NSCLC patients bearing EGFR, ALK and ROS1 mutations led to an unprecedented increased survival rate. Nevertheless, a high number of patients develops trastuzumab resistance (Winter et al. 2007; Narayan et al. 2009; Gajria and Chandarlapaty 2011) and virtually all TKI-treated patients develop resistance by on-target or off-target mechanisms (Lamberti et al. 2020a). In the light of this, in 2016 the National Cancer Institute outlined the “Cancer Moonshot Blue Ribbon” panel that was based on ten recommendations to encourage the cancer community to focus on specific issues. The development of approaches to overcome cancer resistance to therapy is one of these great challenges (Jacks et al. 2016).

Resistance to target therapy is a multifactorial phenomenon since several alterations, either genomic-related or non-genetic, are responsible for the loss of drug effectiveness (Konieczkowski et al. 2018). Tumor heterogeneity is a further key factor in resistance to target therapy. This heterogeneity can be spatial, both within a single tumor and among multiple metastases (Gerlinger et al. 2012; Romano et al. 2013; van Allen et al. 2014; Patel et al. 2014; Cooper et al. 2015; Sanborn et al. 2015; Yates et al. 2015) as well as temporal (*e.g.* adaptation as a result of the selective pressure induced by therapy) (Menzies et al. 2014; Bhang et al. 2015; Juric et al. 2015; Kwak et al. 2015). New approaches are needed to account for this complexity and facilitate future biological and therapeutic insight. The results reported in this thesis fit well in this frame. The plethora of previously described HER2-positive mammary carcinoma models allowed us to determine multiple traits of HER2-positive breast cancer. Through these models we identified new potential druggable targets and we developed strategies to modulate anti-tumor immune responses.

“HER2-positive breast cancer” is a label that identifies mammary carcinomas with different levels of amplification and/or expression of HER2 (Cardoso et al. 2019).

Besides other than HER2 itself, its isoforms such as Delta16 and p95HER2, can also be expressed at different levels, adding to the complexity of the HER2 positive breast cancer landscape (Scaltriti et al. 2007; Castagnoli et al. 2014; Palladini et al. 2017; Chervo et al. 2020). The inter-tumor heterogeneity, due to the expression variability of other molecular markers beyond HER2, has an immediate effect on the short- and long-term responses to anti-HER2 therapies (Marchiò et al. 2020). Because of this, in the last two decades several studies have tried to identify molecular signatures associated with HER2-positive breast cancer (Sørli et al. 2001; Curtis et al. 2012; The Cancer Genome Atlas Network 2012; Pereira et al. 2016). At the same time, there have been several collaborations set up to define guidelines for the access to different anti-HER2 treatments approved for clinical use (Wolff et al. 2018; Burstein et al. 2019).

Heterogeneity is also evident inside the tumor. During 1980's, *in vitro* and *in vivo* pioneering studies proved the presence of co-existing subpopulations within a same tumor, characterized by peculiarities and distinct abilities (Nowell 1976; Tsuruo et al. 1983; Fidler 1983; Nanni et al. 1986). The advancement of -omic technologies combined to single cell analysis techniques has improved knowledge of the molecular profile and the evolution process of breast cancer subpopulations (Chung et al. 2017; Walens et al. 2020; Jackson et al. 2020). Clonal selection due to therapeutic pressure or to the “physiological” tumor evolution causes the inter-lesion heterogeneity, which is a condition that requires a change in therapeutic regimen. In HER2-positive breast cancer, pathologists observed inter-lesion heterogeneity in presence of tumor recurrences or metastases that lose HER2 expression. This phenomenon, known as HER2 conversion from positive to negative, has been reported, according to a pooled meta-analysis, in 20% of patients (Schrijver et al. 2018). Little is known about the molecular profile of these primitive tumors and the mechanisms responsible for the conversion. Nonetheless, HER2 conversion urgently requires the identification of new therapeutic approaches, alternative to HER2-target therapy.

1. IMMUNOLOGICAL STRATEGIES

The first goal of this thesis was the development of immunological strategies to overcome mammary carcinoma heterogeneity. In a recent paper, Galon and colleagues provided an elegant overview on the role of the intra-tumor pre-existing immune system subpopulations emphasising how some immune signatures have both a prognostic and predictive value. They also analysed mechanistic immune signatures, defined how immune signatures increased in patients responsive to therapy, and evidenced how there are signatures common to two or more different therapeutic strategies, such as immunotherapy, targeted therapy, chemotherapy or radiotherapy (Bruni et al. 2020). Thus, strategies able to enhance specific anti-tumor immune responses are, first, an alternative to overcome monoclonal antibodies and TKI-resistance and, secondly, an approach to improve the response to other therapeutic strategies. In another report, Wheeler and colleagues profiled 110 patients with an exceptional response to therapy looking for distinct traits. They concluded that these exceptional responders shared common features including an abundant B cell population and an activated NK population (Wheeler et al. 2020).

1.1 Cancer vaccines

The first challenge of a cancer vaccine is overcoming the tolerance against the target antigen. The difficulties associated with breaking these immune-tolerogenic mechanisms have limited the success of vaccine trials (Curigliano et al. 2016; Marmé 2016; Chackerian and Frieze 2016). VLP, which offers the chance of a multivalent display of a self-antigen and is also a highly effective means of overcoming B cell tolerance, resulted to be effective in both preclinical studies and clinical trials (Bachmann et al. 1993; Chackerian et al. 2008; Jennings and Bachmann 2009; Caldeira et al. 2020). HER2-VLP vaccine was obtained thanks to a modular VLP-based antigen display platform (Zakeri et al. 2012; Thrane et al. 2016) able to generate stable VLPs presenting multiple copies of the HER2-ECD. HER2-VLP vaccine activity was proved

on different HER2-driven mammary carcinoma models, both in a preventive and therapeutic set-up. Overall, the vaccine induced a polyclonal anti-HER2 antibody response, which was able to prevent mammary carcinogenesis and inhibit tumor growth. The vaccine efficacy relied on a rapid and strong induction of antibodies, which are key factors for the success of a cancer vaccine (Nanni et al. 2004; Palladini et al. 2010). The tested pHuRT DNA vaccine was less effective than HER2-VLP one. The preventive efficacy of pHuRT vaccine was previously proved on HER2 transgenic mice (De Giovanni et al. 2014). However, these mice showed a slower tumor onset than Delta16 and F1 mice (Palladini et al. 2017) and this could justify the failure of pHuRT vaccine. The delay of a definitely very aggressive mammary carcinogenesis may require the rapid induction of a stronger antibody response with higher avidity than that induced by pHuRT DNA vaccine.

HER2-VLP-induced antibodies inhibited 3D growth of the HER2-positive human breast cancer BT-474 cell line to a similar extent as trastuzumab, and the trastuzumab-resistant clone BT-474-C5. Trastuzumab-resistance of BT-474-C5 cells depends on the increased formation of EGFR/HER2 heterodimers (Ritter et al. 2007) and vaccine-induced polyclonal antibody response can abrogate this heterodimerization. Moreover, preclinical studies have shown that a polyclonal anti-HER2 Ab response, which simultaneously targets multiple epitopes, is capable of mediating multiple cytotoxic mechanisms (Triulzi et al. 2010; Clay et al. 2011). In a translational perspective, an active vaccination approach capable of inducing a polyclonal anti-HER2 Ab response may thus have a multitude of effects against HER2: induction of a more comprehensive signaling blockade and preventing cancer cells in acquiring resistance due to escape mutations.

The use of multiple preclinical models gave us the opportunity to observe the HER2-VLP ability to counterattack tumor growth and also its limits at the same time. Among these limits we found an incomplete break of tolerance in double transgenic HER2/Delta16 F1 mice and an only partial therapeutic effect on MamBo89HER2^{stable}

tumor growth, probably due to a non-complete addiction of these tumor cells to HER2. Consequently, a stronger ability to break HER2 tolerance is surely a future requirement for the scale-up of HER2-VLP vaccine.

1.2 Triggering the immune response

The IGF1R-based system evolved as a tightly tolerized system (Geenen 2012). We therefore worked therefore on this circuit to test some strategies to foster the break of immune tolerance and induce specific immune responses. Rhabdomyosarcoma is an IGF2-dependent tumor, due to the autocrine overexpression of IGF2 (De Giovanni et al. 2009a) and male mice knock-out for p53 and transgenic for rat HER2 (BALB/p53Neu) are used as model of spontaneous rhabdomyosarcoma (Nanni et al. 2003). To induce the production of antibodies neutralizing IGF2 by a DNA vaccine, we included a xenogeneic gene in the vaccine (Quaglino et al. 2010; Denies et al. 2016). While DNA vaccine for murine IGF2 failed in eliciting antibodies, DNA vaccination with the highly homologous human IGF2 elicited antibodies recognizing murine IGF2 that were able to partially protect mice from lung metastases induced by an intravenous challenge with IGF2-overexpressing murine rhabdomyosarcoma cells. The second strategy explored was the co-targeting of the two receptor tyrosine kinases (RTKs) IGF1R and HER2/neu through cellular vaccines. Cell vaccines overexpressing transduced murine IGF1R, along with HER2/neu and adjuvant stimuli (allogenicity and IL12 production) were able to elicit antibodies recognizing murine IGF1R instead. A slight, nearly significant, delay of rhabdomyosarcoma onset was also obtained with cell vaccine co-targeting mIGF1R and HER2/neu, while cell vaccine expressing only HER2/neu and adjuvants gave superimposable onset to the non-vaccinated control group.

Immune checkpoint inhibitors are a promising strategy to tune immune antitumor response. Checkpoint inhibitors have shown the ability to elicit powerful long-lasting immune responses leading to clinical benefit in 20–30% of patients (Aspeshlagh et al.

2016). However, most patients are resistant to therapy, and about 10% of patients undergo a rapid progression under checkpoint inhibitor treatment (Champiat et al. 2017). As combining immunomodulating strategies could increase the proportion of responders (Kaumaya et al. 2020), a powerful cancer vaccine was combined with an agonistic antibody triggering OX40 (aOX40). The preventive activity of this vaccine against mammary carcinoma was weakened by the concomitant administration of aOX40 antibody. On the other hand, treatment with aOX40 after the completion of vaccinations induced a weak but significant increase in vaccine efficacy, in accordance with published results showing that OX40 activation boosted a previous cell vaccination (Curti et al. 2003). Thus, the “Janus” effect of aOX40 was affected by the timing of administration. Both reduction and increase of immune suppression upon OX40 engagement are possible in different model systems (Linch et al. 2016; Aspeslagh et al. 2016; Foote et al. 2017). The only observed variation associated with the increased efficacy was a higher production of GM-CSF and IL10. Increased expression of both these cytokines was reported by OX40 triggering in some studies (Shibahara et al. 2015; Linch et al. 2016). Moreover, IL10, which is generally considered as a suppressor cytokine, also has antitumor activities (Giovarelli et al. 1995; Oft 2014; Wang et al. 2015). Concomitant administration of aOX40 and cancer vaccines reduced antibody production and determined an activated Treg enrichment.

Authors found that reactivation of low antigen-dependent stimulated lymphocytes induced an excessive stimulation of these cells, which caused apoptosis via activation-induced cell death (AICD) (Pai et al. 2019). This consideration may be translated to the study reported in this thesis since if on one hand the concomitant administration of aOX40 with the vaccine found lymphocytes in an early stimulation state, on the other hand aOX40 post-vaccine administration already acted on a polarized immune system trained to produce a specific antigenic response by the vaccine.

The negative interference observed with OX40 triggering concomitant with cancer vaccine suggests that preclinical models should be thoroughly investigated to

establish the optimal timing of administration, the mechanisms of resistance to ICI therapies and tumor growth acceleration (Olson et al. 2018). We thus moved to PD-L1 immune checkpoint, which is a target of several ICIs developed for clinical use. We moved to a different model in order to better study the role of PD-1/PD-L1 with the future aim to apply the lesson learned to breast cancer. Since patients with melanoma or NSCLC have benefitted from anti-PD-1/PD-L1 treatment (Topalian et al. 2014; Ahamadi et al. 2017; Vaddepally et al. 2020) we developed a preclinical model based on murine melanoma B16 and B16-F10 cell lines, widely used in immunological studies and characterized by a different degree of immunogenicity (Overwijk and Restifo 2000; Giavazzi and Decio 2014). B16-F10 cells showed a lower sensitivity to the anti-proliferative action of IFN- γ compared to B16 cells *in vitro*. IFN- γ raised the expression of both H-2 and PD-L1 molecules and, even though the baseline level of these two markers was lower in B16-F10 than in B16, induced levels of H-2 and PD-L1 were similar between these cell lines. *In vivo* tumor growth of B16 and B16-F10 cell lines was not reduced by pre-treatment with PDL1-VLP vaccine. Furthermore, B16-F10 tumors showed an accelerated growth rate that resembled the hyperprogressive disease (HPD) phenomenon in patients treated with ICI. The mechanisms underlying hyperprogression after IC blockade therapy are still unknown. Nevertheless, proposed hypotheses include alterations in T-cell subpopulations, cytokine secretion, inflammation, and tumor-cell alterations (Scholz et al. 2011; Koyama et al. 2016; Huang et al. 2017; Lamichhane et al. 2017; Chen et al. 2018; Zuazo-Ibarra et al. 2018; Kamada et al. 2019). We found that B16-F10 cells had a higher expression of the *Cd38* immune checkpoint compared to B16 cells. IFN- γ induced a decrease of *Cd38* expression in B16 cell already at 10U/ml *in vitro*, while in B16-F10 cell line a higher dose (100 U/ml) was needed to observe a similar effect, and the lowest level of reached *Cd38* expression was almost the same as to the baseline level of B16. *In vivo* pre-treatment with PDL1-VLP decreased the level of *Cd38* expression only in B16 tumors, while we did not observe any effects in B16-F10 tumors. Interestingly, CD38 expression has been correlated with

resistance to ICI therapy. In fact, PD-1/PD-L1 blockade has been reported to upregulate CD38, not only on CD8⁺ cytotoxic T cells, but also on tumor cells (Chen et al. 2018; Feng et al. 2017). CD38 expression can be induced in monocytes, bone-marrow progenitor cells and CLL cells by IFN- γ (Snoeck et al. 1993; Musso et al. 2001; Bürgler et al. 2015). Treatment with the anti-CD38 antibody in animals that were resistant to IC blockade therapy inhibited tumor growth, enhanced effector CD8⁺ and CD4⁺ T-cell responses and reduced both CD4⁺ Treg cells and MDSCs (Chen et al. 2018). CD38 expression in tumors has indeed been recognized as a biomarker of poor response to ICI therapy (Yi et al. 2018). CD38 upregulation after IC blockade therapy may contribute to the development of HPD through the release of high levels of adenosine into the TME, and the consequent activation of the ADORA2a pathway, which may lead to tumor insensitivity to IFN- γ action, the downregulation of p53 with consequent tumor growth, and strong immunosuppression. CD38 upregulation may also be an adaptive immune response to the hyperactivated immune setting induced by ICI therapy. In this context, CD38 may promote the apoptosis of effector T cells via the AICD process, leading to a protumorigenic tumor microenvironment. Moreover, CD38 may enhance hypoxia signaling pathways in tumor cells or endothelial cells, leading to increased angiogenesis, immunosuppression and tumor proliferation (Angelicola et al. 2021). Lastly, B16-F10 tumors showed higher expression levels of *Arg1*, a marker of M2 macrophages, and *Cd4*, compared to B16 tumors. M2 macrophages are typically related to immunosuppressive activity (Arlaukas et al. 2018). The reduction of the macrophage levels in B16 tumors arisen in mice pre-treated with PDL1-VLP is therefore indicative of an immunologically activated microenvironment. Conversely, unchanged levels of M2 macrophages in B16-F10 tumors of pre-treated mice may suggest a role of M2 macrophages in the hyperprogressive phenomenon, as previously proposed (Lo Russo et al. 2019). The treatment with PDL1-VLP vaccine enhanced several immune mechanisms beyond the

production of polyclonal PD-L1 antibodies, including the stimulation of dendritic cells and B lymphocytes (Mohsen et al. 2018; Palladini et al. 2018b).

In order to work with a model closer to clinical condition of patients we then evaluated the effects of the *in vivo* administration of two therapeutic monoclonal anti-PD-L1 antibodies on B16-F10 tumor growth. This second approach gave us the opportunity to exclude the effect of immunological components not-antibody related. The adjustment of the vaccination schedule into the monoclonal antibody schedule required the evaluation of several timings of administration. Treatment with anti-PD-L1 10F.9G2 antibody induced only a modest tumor growth compared to untreated control group, when administered before and after challenge, together with an increase of spleen weight. The administration of 10F.9G2 at a higher dose or only before the challenge did not instead delay nor promote tumor growth. Atezolizumab treatment increased spleen dimension without affecting B16-F10 tumor growth. We can conclude that neither antibody treatments were able to reproduce the hyperprogression phenomenon observed in PDL1-VLP pre-treated mice. Future experiments will include treatment with anti-PD-L1 durvalumab antibody or combination treatment with different monoclonal antibodies. The PDL1-VLP treatment will be further investigated in terms of its effect on the composition of immune microenvironment and cytokine production. It might also be opportune to test *in vitro* the effects of ICI treatment on the expression of CD38 and other markers, including IDO1, ADORA2a, and on inflammasome pathway and AICD components. In addition, this study may be extended to preclinical models of mammary carcinoma and lung adenocarcinoma and enriched with data from primary cultures of tumor specimens.

2. DISCOVERY OF NEW THERAPEUTIC TARGETS

The second goal of this thesis was the identification of alternative targets to HER2. We worked with several models, as for immunological studies previously described, to determine different aspects of HER2-positive breast cancer heterogeneity.

2.1 Dynamic model of HER2 expression

Our models panel included murine mammary carcinoma cell lines bearing huHER2 amplification, since directly or indirectly derived from HER2 transgenic mice, that exhibited a different ability to preserve HER2 expression both *in vitro* and *in vivo*. HER2-negative cell lines, resulted from HER2 loss, showed a spindle-like morphology, an EMT gene expression profile, increased stemness and high aggressivity *in vivo*. The loss of HER2 was influenced by cell density in *in vitro* cultures according to previous results in cell lines that were derived from mammary tumors of HER2/neu transgenic mice, in which density considerably influenced the expression of HER2/neu and/or EMT traits (Jenndahl et al. 2005). Moreover, our model had similarities with the human breast cancer cell line JIMT-1, which showed a progressively loss of HER2 after the 60th culture passage, associated with an enrichment of the CD24^{neg}/CD44^{pos} subpopulation and a higher expression of IL6 and MMP proteins (Oliveras-Ferraros et al. 2010). Nevertheless, long-term culture did not cause a complete loss of HER2, as observed by us, but only a decrease in protein expression.

The main issue for the success of HER2-targeted therapies is to ensure that most tumor cells are addicted to HER2 expression for the maintenance of the malignant phenotype (Escrivá-de-Romaní et al. 2018). Anti-HER2 target therapies normally cause the extinction of HER2-positive cells. These treatments in tumors exhibiting intra-tumor heterogeneity, with HER2-positive and HER2-negative sub-clones, may fail to eradicate tumor, resulting in HER2-negative relapse (Marchiò et al. 2020). In our model, the addition of trastuzumab to low-density MamBo43HER2^{labile} culture accelerated the spontaneous loss of HER2 expression and the emergence of the highly staminal and aggressive population as reported for HER2/neu model (Song et al. 2014; Creedon et al. 2016; Sharieh et al. 2016; Nami and Wang 2017). Contrasting data were reported on the effect of neoadjuvant and adjuvant therapy with trastuzumab on promoting the loss of HER2 expression in metastasis (Song et al. 2014; Timmer et al.

2017; Ignatov et al. 2019; Branco et al. 2019). We can thus conclude that HER2-negative cells characterized by high stemness became the dominant clone inside MamBo43HER2^{labile} cell line in specific conditions. HER2-negative cells growth was probably not addicted to HER2 from the origin. This hypothesis was supported by studies in other models, in which the artificial inactivation of HER2 has been invariably associated with either tumor regression or tumorigenicity loss (Nanni et al. 2000; Moasser 2007; Song et al. 2014; Creedon et al. 2016; Sharieh et al. 2016), in line with the theory of “oncogene addiction” (Weinstein and Joe 2008).

We could continue to ask ourselves why HER2-amplified cells did not express HER2, but probably, from a translational point of view, the more pertinent two questions would be: could this model help to predict the future HER2 conversion, in HER2 positive tumors? Could this model help us to find new targeted therapies for patients with HER2 conversion? In order to answer these last two questions, we focused our attention on HER2-negative cells. The molecular profile of these cells resembles the peculiar traits of claudin-low-expressing tumors, which are defined as tumors with low expression of cell-cell adhesion genes, high expression of EMT genes and stem-cell-like/less differentiated gene expression patterns (Prat et al. 2015). Fougner and colleagues (Fougner et al. 2020) have recently redefined claudin-lowness as a condition that is present in various intrinsic subtypes, rather than in a distinct subtype. This observation led us to hypothesize that HER2-positive primary lesions can progress through acquisition of claudin-lowness. Due to the fact that there is a paucity of repository data including molecular profiles of matched primary tumor and metastasis, and since HER2 conversion is a low frequency phenomenon, we were not able to compare our results with a database of clinical data. Nevertheless, we evaluated the data set “Metastatic Breast Cancer Project” in C-Bioportal which includes RNA-Seq of primary tumors and matched metastases. Two patients (MBC-MBCProject_6vTVHzur and d5CbUNTb) showed a decrease of HER2 levels between primary tumor and metastasis, according to RNA-Seq data. Metastases of these

patients showed an increase of several genes that are up-regulated in MamBo HER2-negative cells, including *DCN*, *VIM*, *VCAN*, *MMP2*, *TGFB1*, *CAV1*, *PDGFRB*, *IGFBP4*, *ZEB1* and *ZEB2*. This is obviously a preliminary result that will require future investigation on a higher number of samples.

The molecular comparison between HER2-positive and HER2-negative cells revealed a higher expression of PDGFR-B in the latter. Molecular data about the two patients reported above showed that HER2 decrease was associated to an increase of this receptor. PDGFR-B sustains breast cancer progression by promoting EMT and stemness phenotype (Jechlinger et al. 2006; Meng et al. 2015). PDGFR-B is also a pericyte marker and its expression on tumor cells with a mesenchymal phenotype suggested these cells have a role in angiogenesis as pericyte-like cells (Shenoy et al. 2016). These data match well with immunofluorescence of MamBo43HER2^{labile} and MamBo38HER2^{loss} tumors that showed vessels without NG2 positive cells (pericytes). MamBo38HER2^{loss} cells may substitute pericyte cells and their function in the vascular architecture of tumors. PDGFR-B is a druggable target by sunitinib, a pan-TKI able to inhibit also VEGFR, which we found to be up-regulated in HER2-negative cells. Sunitinib was effective in halting the growth of MamBo38HER2^{loss} cells and the emergence of HER2-negative tumors from MamBo43HER2^{labile} cells. Sunitinib also reduced IL-6 production by MamBo38HER2^{loss} *in vitro*. IL6 up-regulation has been reported in a model of long-term-trastuzumab-treated BT-474/PTEN^{-/-} cells, which became spindle-like following this treatment; IL6 appeared to trigger an inflammatory loop, which led to the acquisition of a staminal, basal-like phenotype, together with resistance to trastuzumab (Burnett et al. 2015). The efficacy of sunitinib as an anti-EMT target therapy has been proven in claudin-low human breast cancer cell lines (Hollier et al. 2013), and this drug may be able to take advantage of IL6 inhibition. Taken together, these data indicate the putative efficacy of the therapeutic targeting of PDGFR-B by sunitinib in HER2-negative cells. Nevertheless, treatment with sunitinib did not eradicate HER2-negative tumors, thus indicating that the PDGFR-B signaling

pathway clearly sustains the growth of HER2-negative cells, but is probably not the only driver of their malignancy. Interestingly, combined treatment including sunitinib, trastuzumab and chemotherapy in advanced breast cancer has been studied (Bachelot et al. 2014).

Preliminary results suggest two other potential targets, PHLDA1 and SORBS3. MamBo43HER2^{labile} cells expressed both HER2 full-length and p95HER2 and we also found a higher expression of PHLDA1 in these cells. The role of PHLDA1 was controversial, although its expression was found to correlate with p95HER2-611CTF (Pedersen et al. 2009). A recent paper suggested that PHLDA1 may inhibit HER2-HER3 dimerization (Magi et al. 2018). This inhibition may encourage the driver role of HER2 homodimers (including p95HER2 homodimers that are resistant to trastuzumab). Inhibition of PHLDA1 reduced the *in vitro* migration of MamBo43HER2^{labile} cells. Further studies will be required to evaluate how PHLDA1 switch off may influence trastuzumab sensitivity. On the other hand, the incomplete HER2 addiction of MamBo89HER2^{stable} cells may be justified by the absence of SORBS3. The lack of this protein may permit a higher activation of STAT3. Thus, if on one hand MamBo89HER2^{stable} cells produced high level of IL6, which induced STAT3 activation, on the other hand the absence of SORBS3 might keep this circuit constantly activated (Ploeger et al. 2016).

2.2 Dynamic model of HER2-positive breast cancer progression

Finally, we took advantage PDX-BRB4 derived from an HER2-positive breast cancer patient to develop a new model of tumor progression based on serial *in vivo* passages. However, despite several efforts, metastatic growth and tumor progression *per se* or after therapeutic treatments have been rarely obtained and, even by selecting metastatic PDX variants, the results have not been satisfactory at all (Paez-Ribes et al. 2016). In our study the long-term *in vivo* re-transplantation for up to 25 passages of PDX-BRB4 allowed the random emergence of a progressed phenotype. Of 6 different

sublines, only one (PDX-BRB4-A1) showed the shift toward a progressed phenotype, with faster *in vivo* growth, acquirement of metastatic ability after i.v. injection, enriched stem cell phenotype and lower *in vitro* cell senescence. HER2-amplified PDX-BRB4 showed a progressive decrease of BCL2 expression after long-term *in vivo* passage, becoming almost negative for its expression after ≥ 22 passages. High level expression of BCL2 in breast cancer is associated with a better prognosis (Treré et al. 2007; Dawson et al. 2010; Hwang et al. 2018; Ceccarelli et al. 2019). Therefore, the downregulation observed during the *in vivo* passages of our PDX could be linked to the selection of more aggressive variants, revealing a positive prognostic role for the biomarker BCL2, as observed in clinical studies.

BCL2 gene product (mainly its alpha isoform) normally plays an anti-apoptotic role (Cooper et al. 2015; Warren et al. 2019). The paradox of low BCL2 levels associated with a bad prognosis in breast cancer could be related to Beclin-1 inhibition. Beclin-1 induces autophagy leading to the improvement of the survival rate and maintenance of cancer stem cells (Bottini et al. 2000). BCL2 is a negative regulator of Beclin-1 (Artibani et al. 2017) and it can inhibit its pro-tumorigenic effects, inducing cell senescence and growth arrest (Warren et al. 2019). Our data highlighted a complex interaction between BCL2 and CDKN2A, STAT5 and WT1, which are concordantly downregulated in the progressed A1 subline. In our progressed model low levels of BCL2 are not related to therapy resistance, as also reported in clinical studies (Bottini et al. 2000). On the other hand, a high expression of WT1 in breast cancer is clinically associated with increased malignancy, bad prognosis, lower responsivity to therapies and to a mesenchymal phenotype. Breast cancer cell lines with mesenchymal *versus* epithelial phenotypes were reported to show divergent behaviors when subjected to WT1 silencing or hyperexpression (Artibani et al. 2017), suggesting that the EMT could play a role on the way towards bad prognosis and lower responsivity to therapies. In our study, the progressed PDX-BRB4-A1 subline underwent an only partial EMT. A1 progressed subline showed increased malignancy and stemness but maintained

epithelial morphology and did not acquire resistance to therapy with trastuzumab nor neratinib treatment (Landuzzi et al. 2021). A higher stemness and metastatic ability could be linked to early events of EMT, while resistance to therapies could require further steps during the transition process.

3. CONCLUSIONS

The development of anti-tumor target therapies requires preclinical models able to reproduce the clinical condition. Deep sequencing and -omics technologies are teaching us that each tumor subtype has tumor subclusters with specific molecular profiles. In addition, each tumor is characterized by distinct clones that coexist and, over time, may dynamically expand or shrink. Finally, the immunological components of the tumor microenvironment have been shown to evolve over time, both qualitatively and quantitatively. The keyword that best describes all of these aspects is “heterogeneity”.

The results reported in this thesis introduce therapeutic approaches or identify new therapeutic targets towards HER2-positive breast cancer, taking into account the dynamics inherent to the tumor progression.

The VLP vaccine is a starting point to overcome the phenomenon of resistance to therapy. The possibility of using strategies to reinforce vaccine effects, such as the use of xenogeneic antigens, multiple antigens or ICI, is concrete but at the same time the switch-on/switch-off of lymphocytes, by ICI, is a system that still requires a lot of study, since the clinical response can be not only ineffective but even harmful.

Tumor progression of MamBo43HER2^{labile} cell line as well as PDX-BRB4-A1 subline presented EMT traits and increased stemness. Molecules involved in these processes might become new targets for therapeutic approaches. The tumor progression can be also counteracted by turning off alternative survival circuits to HER2 once the addiction to this gene is lost. We evidenced how SORBS3 might play a key role in the

switch off of IL6/STAT3 signaling. Moreover, the functional role of PHLDA1 in mammary carcinoma invasion was also suggested. Lastly, the progression of HER2-positive mammary carcinomas can lead to the loss of expression of HER2 and to a mesenchymal phenotype. Antiangiogenic drugs such as sunitinib can slow the growth of these new claudin-low tumors.

Materials and Methods

1. IMMUNOLOGICAL STRATEGIES

Parts of Materials and Methods reported in this Chapter were included in the manuscripts of Palladini and colleagues (Palladini et al. 2018b), De Giovanni and colleagues (De Giovanni et al. 2019a; De Giovanni et al. 2019b) and, Nanni and colleagues (Nanni et al. 2018).

1.1 Anti-HER2 cancer vaccines

1.1.1 Mice

FVBhuHER2 (HER2) mice, transgenic for the full-length human HER2 isoform (Finkle et al. 2004; De Giovanni et al. 2014) were obtained from Genentech (South San Francisco, CA, USA) and bred in our animal facilities. Delta16 mice, transgenic for the Delta16 alternative splicing isoform of HER2, were kindly gifted by Dr. A. Amici (University of Camerino, Camerino, Italy) and Dr. S. Pupa (Fondazione IRCCS, Istituto Nazionale dei Tumori, Milan, Italy) (Marchini et al. 2011; Castagnoli et al. 2014). Delta16 male mice and HER2 female mice were crossed to obtain a double transgenic human HER2/Delta16 progeny, here referred to as HER2/Delta16 F1 or F1 mice (Palladini et al. 2017). All transgenic mice expressed human HER2 and/or Delta16 in the mammary glands under the transcriptional control of mouse mammary tumor virus long terminal repeats, leading to the development of mammary carcinomas. FVB mice (FVB/NCrl) were purchased from Charles River Laboratories (Calco, Como, Italy).

1.1.2 Cell lines

MamBo89HER2^{stable} cell line was established from a mammary tumor of a HER2 mouse. Tumor was minced and set in culture. Cell line was stabilized and cultured in DMEM (Thermo Fisher Scientific, Milan, Italy) that was supplemented with 20% Fetal Bovine

Serum (FBS, Thermo Fisher Scientific), 30 µg/ml bovine pituitary extract (Corning, Turin, Italy) and 0.5% v/v MITO Serum Extender (Corning).

Human ovarian cancer cell line SK-OV-3 and human breast cancer cell lines MDA-MB-453, BT-474 and SKBR3 were kindly given by Dr. S. Pupa (Fondazione IRCCS, Istituto Nazionale dei Tumori, Milan, Italy). Breast cancer cell lines HCC1954 and MDA-MB-231 were purchased from ATCC (Sesto San Giovanni, Milan, Italy). Breast cancer cell line BT-474-C5 was kindly provided by Prof. Adam Sander (University of Copenhagen, Denmark). Cells were routinely cultured in RPMI medium (Thermo Fisher Scientific) supplemented with 10% FBS.

Both MamBo89HER2^{stable} cell line and, human ovarian and breast cancer cell lines described above were maintained at 37°C in a humidified 5% CO₂ atmosphere.

Human rhabdomyosarcoma cell line SJ-RH4, lacking HER2 expression, was provided by Dr. A. Rosolen (University of Padua, Padua, Italy) and Dr. D.N. Shapiro (St. Jude Children's Hospital, Memphis, TN). Cells were cultured in DMEM with 10% FBS and maintained at 37°C in a humidified 7% CO₂ atmosphere.

1.1.3 HER2-VLP and pHuRT vaccines

The HER2-VLP vaccine was based on virus-like particles (VLPs) displaying SpyTags proteins and linked with HER2 extracellular domain (ECD) through a SpyCatcher. HER2-VLP vaccine was produced by Prof. A. Sander and co-workers (University of Copenhagen, Denmark). The detailed description of the design, expression and purification of vaccine components was included in the manuscript of Palladini and colleagues (Palladini et al. 2018b) and here briefly reported. The *Acinetobacter phage*, AP205 coat protein displayed two SpyTags per VLP subunit (Thrane et al. 2016). The Spytags VLP was expressed in *Escherichia coli* One Shot BL21 Star (DE3) cells (Thermo Fisher Scientific) and purified by density gradient ultracentrifugation. The HER2-ECD was designed with the SpyCatcher sequence at the N-terminus and a hexa-histidine purification tag at the C-terminus (Zakeri et al. 2012) and was codon-optimized for

expression in *Drosophila melanogaster* S2 insect cells. The sequence was then subcloned into the pExpres2-2i vector (Expres2ion Biotechnologies, Horsholm, Denmark).

SpyCatcher-HER2 antigen was coupled to the VLP and the level of coupling was determined by densitometric analysis of SDS-PAGE gels. Alhydrogel (2%) (Brenntag, Denmark), here referred to as Alum, was added to the vaccine formulation 1 hour prior to immunizations. For each mouse, 6 µg of VLP-displayed SpyCatcher-HER2 were injected into the tibial muscles.

pHuRT vaccine is a DNA vaccine based on a chimeric human/rat HER2 plasmid, derived from pVAX1 (Thermo Fisher Scientific), that encodes a chimeric protein in which the first 390 extracellular N-terminal residues are from HER2 (1–390 residues) and the remaining extracellular and transmembrane residues from rat HER2/neu (Quaglino et al. 2010). Large-scale production and purification of the plasmids were performed with EndoFree Plasmid Giga kits according to manufacturer's instruction (Qiagen, Valencia, CA, USA).

The pHuRT DNA vaccine consisted of 50 µg plasmid diluted to a final volume of 40 µl per mouse in final concentrations of 0.9% NaCl and 6 mg/ml polyglutamate. The DNA vaccine was injected into the tibial muscles (20 µl in each muscle) then the muscle tissues were immediately subjected to electroporation consisting of two square wave, 25-ms, 375 V/cm pulses generated with a T830 electroporator (BTX, San Diego, CA, USA) (De Giovanni et al. 2014).

1.1.4 HER2-VLP and pHuRT immunization

In the preventive set-up, HER2-VLP and pHuRT vaccines were administered every second week. Delta16 mice received three vaccine administrations starting from 8 weeks of age. HER2/Delta16 F1 mice were treated starting from 5-8 weeks of age, for the entire lifetime of the mouse. Control groups consisted of untreated mice.

The ability of HER2-VLP vaccine to inhibit tumor growth was also evaluated through two different therapeutic set-ups. In the first, MamBo89HER2^{stable} cells (5 ×

10⁶ cells) were subcutaneously (s.c.) injected in 10-20-week-old FVB female mice. Starting 5 weeks after cell injection, mice were immunized every second week with the HER2-VLP vaccine for the entire lifetime of the mouse. Control group consisted of untreated mice. In the second therapeutic experiment, five primary mammary carcinomas of three HER2 transgenic mice were minced and pooled together and implanted in the fourth left mammary fat pad of FVB female mice, approximately 20-weeks-old. Starting 2 weeks after fragment implantation, mice were vaccinated every second week with HER2-VLP vaccine for the entire lifetime of the mouse. Control group consisted of untreated mice.

Mice were monitored weekly by palpation and tumor dimensions were measured with calipers. Masses with a mean diameter exceeding 3 mm were considered tumors. Tumor volume was calculated as $(\pi/6)(\sqrt{ab})^3$ where a = maximal tumour diameter and b = maximal tumour diameter perpendicular to a . Mice were euthanized when tumor burden was equivalent to 10% of body mass. Tumor multiplicity is the number of mammary tumors per mouse at each time point and is expressed as mean \pm SEM for each experimental group. For all experiments, serum samples were collected periodically, one day before every vaccination.

1.1.5 Growth inhibition by HER2-VLP-induced antibodies

The ability of HER2-VLP induced antibodies to inhibit 3D-growth was evaluated on BT-474 (trastuzumab-sensitive) and BT-474 C5 (trastuzumab-resistant) cells. Cells were seeded at 500 cells/well in 24-well plates in RPMI + 10% FBS + 0.33% agar (Sea-Plaque Agarose, Lonza, Basel, Switzerland) containing mouse sera diluted 1:100 or trastuzumab (10 μ g/ml, kindly provided by Genentech). Colonies (diameter > 90 μ m) were counted 18–30 days after seeding under an inverted microscope in dark-field.

1.2 The break of tolerance against IGF1R and IGF-2

1.2.1 Mice

BALB/c p53^{+/-} female mice (BALB/cJ-Trp53^{tm1Tyj}, purchased from The Jackson Laboratory (Bar Harbor, MI, USA) were crossed with BALBneuT male mice, transgenic for a mutant rat HER2/neu, and bred in our facilities as previously described (Nanni et al. 2003). Male BALB/p53Neu mice develop salivary gland carcinomas and pelvic rhabdomyosarcoma in urethral tissue proximal to bladder at about 13 to 15 weeks of age (Nanni et al. 2003).

BALB/c (BALB/cAnNCrl) mice were purchased from Charles River Laboratories.

1.2.2 Cell lines

RMSp53Neu5, derived from a rhabdomyosarcoma of BALB/p53Neu male mouse (Ianzano et al. 2014). Cell culture was grown in DMEM supplemented with 20% FBS.

Human rhabdomyosarcoma cell line SJ-RH30, as well as SJ-RH4, lacks HER2 expression and was provided by Dr. A. Rosolen (University of Padua, Italy) and Dr. D.N. Shapiro (St. Jude Children's Hospital, Memphis, TN). Cells were cultured in DMEM with 10% FBS.

TS/A, derived from a mammary carcinoma arisen in a BALB/c female retired breeder mouse (Nanni et al. 1983b). Cells were routinely grown in DMEM with 10% FBS.

Neu/H-2^q/IL12 clone #20 cells (here indicated as #20), derived from a mammary carcinoma arisen in a FVB female mouse transgenic for rat HER2/neu, and engineered for production of murine IL12 (De Giovanni et al. 2004; De Giovanni et al. 2019b). Cells were cultured in DMEM supplemented with 20% FBS and 125 µg/ml hygromycin (Thermo Fisher Scientific).

N10-F2.1 cell line, derived from a mammary carcinoma expressing rat HER2/neu arisen in a HER2/neu transgenic mouse of a BALB/c background. Cells were routinely grown in DMEM with 20% FBS.

Rhabdomyosarcomas and mammary carcinoma cell lines were maintained at 37°C in a humidified 7% CO₂ and 5% CO₂ atmosphere, respectively.

1.2.3 Anti-IGF1R and anti-IGF2 vaccines

The plasmid pCVNIGF1R, coding for human IGF1R cDNA under the control of the SV40 promoter, was kindly given by Dr. Baserga (Thomas Jefferson University, Philadelphia, USA). Murine IGF1R plasmid pmIGF1R-opt was derived from pcDNA3.1 plasmid by insertion of a codon-optimized cDNA sequence coding for normal murine IGF1R (Genscript Corporation, Piscataway, NJ, USA) under Cytomegalovirus promoter. #20 cell line was transfected with pCVNIGF1R, pmIGF1Ropt or pcDNA3.1, as described by De Giovanni and colleagues (De Giovanni et al. 2019a). Cells were cloned and two clones were selected for high expression of human IGF1R (clone D39) or murine IGF1R (clone 9B10).

Plasmidic pBLAST49-derived expression vectors for murine IGF2 (p-mIGF2) and human IGF2 (p-hIGF2), as well as the empty vector pBLAST49-mcs, were purchased from InvivoGen (San Diego, CA, USA).

Production and purification of the plasmids were performed with EndoFree Plasmid Giga kits.

1.2.4 Anti-IGF1R and anti-IGF2 *in vivo* treatments

1.2.4.1 Anti-IGF1R and IGF-2 DNA vaccines

Mice received the injection of DNA vaccine into the tibial muscles (20 µl in each muscle) according to the protocol previously described for pHuRT vaccine (Materials and Methods 1.1.3).

pCVNIGF1R or pmIGF1R-opt were administered at 6, 8, 13, and 15 weeks of age. In order to induce Treg depletion, DNA vaccine pmIGF1R-opt was also coupled with the administration of the anti-CD25 (PC61) rat monoclonal antibody at the dose of 500 µg/mouse (kind gift from Dr. S. Ferrini, Istituto Nazionale per la Ricerca sul Cancro, Genoa, Italy) five and four days before the first vaccination. pmIGF1R-opt was also combined with other plasmids, such as pIL12-IRES1neo (able to confer expression of murine IL12, here referred to as pIL12) or pD^q (able to transfer H-2D^q expression) (De Giovanni et al. 2009b).

DNA vaccine with human or mouse pIGF-2 plasmids, or empty vector, was administered in BALB/c mice. Vaccination was repeated after 2, 6 and 8 weeks, for a total of 4 vaccinations. Mice were challenged with 3×10^5 murine rhabdomyosarcoma cells, administered by intravenous (i.v.) injection. In some experiments, the first two vaccinations were preceded by Treg depletion at day - 1.

1.2.4.2 Anti-IGF1R cell vaccines

Cell vaccines consisted of IL12-producing HER2-expressing H-2^q murine mammary carcinoma cells stably transfected with murine or human IGF1R (clones 9B10 and D39, respectively). Vaccine cells were proliferation-blocked by treatment with mitomycin C (40 µg/mL Sigma-Aldrich, Milan, Italy) and administered i.p. in 0.4 mL of phosphate-buffered saline (PBS) (Thermo Fisher Scientific). Control mice received PBS alone. A vaccination cycle consisted of 4 vaccinations over 2 weeks, followed by 2 weeks of rest (De Giovanni et al. 2004). Vaccination cycles were life-long repeated.

1.2.4.3 Anti-IGF2 antibodies

Monoclonal antibodies neutralizing IGFs (kindly provided by Kyowa Hakko Kirin Co, Tokyo, Japan) were KM1468 (rat IgG2b, neutralizes human IGF1 and IGF2 and murine IGF2 but not murine IGF1 and human insulin) and KM3168 (rat IgG2a, neutralizes human and murine IGF1, but not human and murine IGF2 and insulin). BALB/p53Neu

male mice at a pre-neoplastic stage (5–6 weeks of age) were randomized based on the weeks of age to three experimental groups: control and two doses of a mixture of IGFs mAbs KM1468 and KM3168 (0.2 and 1 µg/g for each antibody). Mice received two administrations per week in the site of onset of rhabdomyosarcoma for a total of 18 injections. Control group received only vehicle PBS.

For all previously described experiments (1.2.4.1-1.2.4.3) mice were monitored weekly by palpation and, when required, tumor dimensions were measured and mice were subjected to an accurate necropsy as previously reported (Material and Methods 1.1.4). Lungs were perfused with black India ink to outline metastases and fixed in Fekete's solution. Metastases were counted under a dissection microscope. Serum samples were collected periodically.

1.2.5 3D-growth inhibition of IGF circuit

For IGF1R inhibition, cells were seeded at 1000 or 2000 cell/cm² in 6-well plates in culture medium supplemented with 0.33% agar (Sea-Plaque Agarose), over an underlayer of 0.5% agar medium. The IGF1R kinase inhibitor NVP-AEW541 (kindly provided by Novartis Pharma, Basel, Switzerland) was added to medium at doses ranging from 0.1 to 3 µM. Controls contained vehicle alone (DMSO).

For IGF1R silencing two siRNA, siRNA-R1 and siRNA-R4 (Qiagen), directed against two different regions of IGF1R transcript, were used. Control siRNA was run in parallel. Cells were cultured for 48 h in the presence of siRNA at 40 nM concentration using Oligofectamine (Thermo Fischer Scientific) as transfection agent (0.8%). Then, cells were harvested and reseeded in medium containing 0.33% agar without siRNA over a 0.5% agar underlayer medium.

Colony growth was determined by counting at low magnification (25×), 14-22 days after seeding.

1.3 Modulation of the immune checkpoint OX-40

1.3.1 Mice

BALBneuT female mice (H-2^d haplotype), transgenic for a mutant rat HER2/neu oncogene driven by the mouse mammary tumor virus promoter, were bred and genetically screened as reported (Nanni et al. 2001). Female mice develop multiple mammary carcinomas.

1.3.2 Cell lines

TT12.E2 cell line derived from a mammary carcinoma expressing rat HER2/neu arisen in a HER2/neu transgenic mouse of a FVB background. Cells were routinely grown in DMEM with 20% FBS and maintained at 37°C in a humidified 5% CO₂ atmosphere.

1.3.3 Triplex vaccine combined to aOX40 treatment

Triplex vaccine consisted of murine mammary carcinoma cells (haplotype H-2^a) expressing high levels of HER2/neu and releasing transduced IL12 (De Giovanni et al. 2004). Each vaccine dose consisted of 2×10^6 proliferation-blocked (by mitomycin C) cells, administered i.p. to BALBneuT female mice.

Control mice, run in parallel to Triplex-treated mice, received PBS alone. Mice were vaccinated at 10, 11, 14, 15, 18, 19 weeks of age (two doses per week, 12 vaccinations in total). The rat IgG1 monoclonal antibody OX86 (European Collection of Cell Cultures, Salisbury, UK), which binds OX40 with agonist activity (here referred to as aOX40) was administered i.p., according to the following schedules: aOX40+vax, treatment with aOX40 the day before the first vaccination (at 10 weeks of age) and in weeks 12, 16, 20; aOX40postvax, treatment with aOX40 every 4 weeks starting at 22 weeks of age.

Mice were monitored weekly by palpation. Tumor dimensions were measured and tumor volume calculated as reported above. Mice were subjected to an accurate necropsy. Lungs were perfused with black India ink to outline metastases and fixed in Fekete's solution. Metastases were counted under a dissection microscope. Sera were collected after each vaccination cycle.

1.4 Modulation of the immune checkpoint PD-L1

1.4.1 Mice

C57BL/6 (C57BL/6NCrl) mice were purchased from Charles River Laboratories.

1.4.2 Cell lines

The B16-a murine melanoma cell line, in this thesis referred to as B16, was kindly provided by Prof. A. Mantovani (IRCCS, Humanitas Clinical and Research Center, Rozzano, Milan, Italy) (Nanni et al. 1983a). This cell line was derived from a spontaneous melanoma developed in a C57BL/6 mouse. The B16-F10 cell line was kindly provided by Prof. Adam Sander (University of Copenhagen, Denmark). This cell line was obtained as a subpopulation of the B16 parental line, by subsequent *in vivo* selection processes (Fidler 1973). Adherent cell cultures were grown in DMEM with 10% FBS and maintained at 37°C in a humidified 5% CO₂.

1.4.3 Anti-PD-L1 treatments

PDL1-VLP vaccine was produced by Prof. A. Sander and co-workers. The vaccine was based on VLPs displaying mouse PD-L1 extracellular domain. C57BL/6 8-weeks male mice received i.m. administration of PDL1-VLP vaccine. Mice were treated with PDL1-VLP+ Alhydrogel (2%) (Alum) or only with the adjuvant diluted in PBS. Treatment was performed every three weeks. After 7 weeks from the first administration, mice

were subcutaneously challenged with 10^5 B16 cells or 0.5×10^6 B16-F10 cell lines. Sera were collected two weeks after each vaccination.

C57BL/6 male mice of 8-9 weeks of age, challenged with B16-F10 cells, were treated with anti-PDL1 monoclonal antibodies 10F.9G2 (B7-H1, clone 10F.9G2, BioXCell, Lebanon, NH, USA), that binds mouse PD-L1, or atezolizumab (Tecentriq, Genentech) that binds human and mouse PD-L1. Mice treated with the isotype control antibody, rat anti-keyhole limpet hemocyanin IgG2b (clone LTF-2, BioXCell) and untreated mice run in parallel to 10F.9G2 treated mice. Antibodies were i.p. administered.

Schedules of treatment (day 0 is the day of B16-F10 cell injection):

- a. 0.5×10^6 cells s.c.; 9mg/kg 10F.9G2 or isotype control Abs. Days of treatment: -9, -6, -2, +1, +4, +8, +12, +15.
- b. 10^5 cells s.c.; 12mg/kg 10F.9G2 or isotype control Abs. Days of treatment: -12, -9, -6, -2, +1, +4, +8, +12, +15.
- c. 0.5×10^6 cells s.c.; 9mg/kg 10F.9G2 or isotype control Abs. Days of treatment: -9, -7, -4, -1.
- d. 0.5×10^6 cells s.c.; 10mg/kg atezolizumab Ab. Days of treatment: +1, +4, +7, +11, +14, +18

Mice were monitored weekly by palpation and tumor dimensions were measured with calipers. Masses with a mean diameter exceeding 3 mm were considered tumors. Tumor volume was calculated as $(\pi/12)(\sqrt{ab})^3$ where a = maximal tumour diameter and b = maximal tumour diameter perpendicular to a . Mice were euthanized when tumor burden was equivalent to 10% of body mass. Mice were subjected to an accurate necropsy. Lungs were fixed in Fekete's solution and metastases were counted under a dissection microscope.

1.4.4 IFN- γ sensitivity

B16 and B16-F10 cell lines were seeded at 0.25×10^6 cells/25cm². After 24 hours from seeding, murine IFN- γ (kindly gift of Dr. G.R. Adolf, Ernst-Boehringer Institute,

Vienna, Austria) was added to medium to the final concentrations of 10, 100 and 1000 U/ml. After 72 hours from the treatment, cells were harvested and counted. Then, the expression level of PD-L1, PD-1 and H-2 molecules was evaluated by flow cytometry.

1.4.5 Real-Time PCR

RNA was extracted, quantified and reverse transcribed as previously reported (Palladini et al. 2017). cDNA was amplified using Sso Advanced SyBR Green Supermix (Bio-Rad Laboratories, CA, USA) reagents. Reactions were performed in a Thermal Cycler CFX96 (Bio-Rad). Analyses were performed using Bio-Rad CFX Manager 3.1 Software, and relative quantification was calculated as $\Delta Ct = Ct_{\text{gene}} - Ct_{\text{housekeeping}}$. We used the following Bio-Rad assays: Cd4 (qMmuCID0022320); Arg1 (qMmuCID0022400) and Cd38 (qMmuCID0006259); Mouse Tbp (qMmuCID0040542) was used as housekeeping.

1.5 Quantification and characterization of anti-vaccine antibodies

Anti-vaccines antibodies and isotype subclasses were measured by enzyme-linked immunosorbent assay (ELISA), flow cytometry or Western Blotting.

Flow cytometry was performed using the Partec CyFlow® space cytofluorimeter (Sysmex Europe GmbH, Norderstedt, Germany) and analysis was performed with FCS EXPRESS 4 (De Novo Software, Glendale, CA, USA).

1.5.1 Anti-HER2 antibodies induced by HER2-VLP or pHuRT

Anti-HER2 antibodies were detected by specific ELISA assay (De Giovanni et al. 2014). Sera were diluted 1:400-1:102400. A standard curve with anti-HER2 murine mAb clone 4D5 (Genentech) was run in parallel (0.04 to 30 ng/ml).

Anti-HER2 avidity and affinity assays were performed by Prof. A. Sander as previously described (Thrane et al. 2016). To evaluate the affinity of anti-HER2 antibodies the kinetic analysis of the dissociation rates for the binding between

purified total IgG from HER2-VLP immunized mice or trastuzumab mAb to recombinant HER2 ECD was performed on a quartz crystal microbalance biosensor (Attana A200, Attana AB). Protein G columns (Pierce, USA) were used for purification of total IgG from anti-HER2 mouse serum samples. Further details about avidity and affinity assays were reported in the manuscript of Palladini and colleagues (Palladini et al. 2018b).

Anti-HER2 total antibodies and subclasses were also measured by flow cytometry. Sera were diluted 1:65 to detect total anti-HER2 IgG. F(ab')₂ fragments of goat anti-mouse IgG (H+L) labelled with Alexa Fluor 488 (20 µg/ml, Life Technologies) were used as secondary Ab (here after referred to as anti-mouse IgG AF488 antibody). To detect specific anti-HER2 antibody isotypes in 1:20 diluted sera, FITC-conjugated rat anti-mouse IgG1, IgG2a, IgG2b, IgG3 (BD Pharmingen, BD, Milan, Italy) were used. The intensity of fluorescence of each serum sample was normalized to the expression of HER2 by the SK-OV-3 target cells determined using mouse anti-human HER2 primary antibody, clone MGR-2 (Enzo Life Science, Farmingdale, NY, USA).

1.5.2 Anti-IGF1R antibody detection

Production of anti-IGF1R antibodies was detected by immunoprecipitation, followed by Western Blot. Cells expressing murine IGF1R (cell line 9B10) or human IGF1R (SJ-RH30) were lysed and protein concentration was determined as previously described (Crocì et al. 2007). For IGF1R immunoprecipitation, Dynabeads Protein G was used (Thermo Fisher Scientific), according to the manufacturer's instructions. Rabbit polyclonal IGF1R β antibody (C-20) and IGF1R α antibody (N-20), (Santa Cruz Biotechnology, Santa Cruz, CA, USA) added to cellular proteins were used as positive control. Samples, separated on an 8% polyacrylamide gel and then transferred to polyvinylidene difluoride membranes (Bio-Rad Laboratories), were incubated overnight at 4 °C with anti-IGF1R rabbit polyclonal antibody (C-20) 0.5 µg/ml plus rabbit polyclonal antibody IGF1R α (N-20) 0.5 µg/ml.

ELISA assay for anti-mIGF1R antibodies was performed in MicroWell Maxisorp plates (Nunc, Thermo Fisher Scientific) after overnight coating with recombinant murine IGF1R (R&D Systems, Minneapolis, MN, USA) at 40 ng/well in carbonate buffer (Sigma-Aldrich). Sera were diluted 1:200 to 1:400 in assay buffer (4% bovine serum albumin in phosphate-buffered saline) and ELISA was performed following the protocol reported previously (De Giovanni et al. 2014). The semiquantitative evaluation was done, expressing results as O.D. specific binding, calculated as “O.D. of mIGF1R-coated wells—O.D. of buffer-coated wells”. Isotype subclass analysis was carried out in ELISA assays with secondary biotin-labelled anti-mouse IgG1 (clone LO-MG1-2), IgG2a (clone LO-MG2a-2), IgG2b (clone LO-MG2b-2), and IgG3 (clone LO-MG3-7), all purchased from AbD Serotec, Bio-Rad Laboratories. Samples were then incubated with alkaline phosphatase-conjugated Streptavidin (AbD Serotec), developed with p-nitrophenyl phosphate (Sigma-Aldrich) and specific binding calculated as above.

1.5.3 Anti-IGF2 antibody detection

Production of anti-IGF2 antibodies was analysed by Western Blotting. One μg of recombinant mouse or human IGF2 (R&D System, Minneapolis, USA) was run on a 20% polyacrylamide gel. Membranes were incubated with serum of vaccinated or untreated mice, diluted 1:100 in blocking buffer. Monoclonal rat anti-IGF2 antibody (clone #122404, R&D Systems), that shows cross-reactivity with recombinant human/mouse IGF2, was used as positive control at the concentration of 1.7 $\mu\text{g}/\text{ml}$.

A specific ELISA to evaluate the levels of anti-IGF2 antibodies was also performed coating the recombinant mouse or human IGF2 at 2 $\mu\text{g}/\text{ml}$ in 100 μl by overnight incubation. After blocking in Plasma Sample diluent 2x (ImmunoChemistry Technologies) + PBS 0.05% Tween20 and washing incubations, sera of vaccinated or untreated mice were added at 1:100 dilution in blocking buffer. Serum samples obtained after the fourth vaccination were used. Reaction was revealed and measured

as previously described (Materials and Methods 1.5.1). Mouse monoclonal anti-human IGF2 antibody, clone 75.015.11 (R&D Systems), which shows 100% cross-reactivity with murine IGF2, was used to set up a standard curve run in parallel (0.05 to 200 ng/ml).

1.5.4. Anti-HER2/neu antibody detection

Anti-HER2/neu antibody level was studied by indirect immunofluorescence on rat HER2/neu-expressing N10F2.1 or TT12.E2 cells. Cells were incubated with sera at a 1:65. Cytofluorimetric analysis was performed as reported above. Rat HER2/neu expression of N10F2.1 or TT12.E2 target cells was evaluated in parallel tests with anti-c-ErbB2/Neu mouse monoclonal antibody (clone 7.16.4; 5 µg/ml, Oncogene Research Products, Boston, MA, USA). The intensity of fluorescence of each serum sample was normalized to the expression of rat HER2/neu by the target cells. IgG subclasses were also detected by flow cytometry as reported above (Materials and Methods, 1.5.1).

1.5.5 Anti-PDL1 antibodies

Antibodies were detected by ELISA. Sera of PDL1-VLP+Alum-treated mice were diluted 1:900 - 1:656100. Sera of control group mice (PBS+Alum) were diluted 1:100-1:300. In brief, 100 ng/well of recombinant PD-L1 was coated on Nunc MaxiSorp plates overnight at 4°C. Following, after blocking with 0.5% milk (non-fat dry milk, Bio-Rad Laboratories) in PBS for 1 hour and four washes with PBS, sera (50 µl/well) were incubated for 1 hour and then, after 4 washes, goat anti-mouse IgG-HRP (Calbiochem) was added. ELISA was developed as previously described. Anti-PDL1 antibody levels were calculated as the endpoint titer considering as cut off the value obtained by sum of the mean and the standard deviation of the values obtained in blank wells, multiplied by 3.

Anti-PDL1 antibodies isotypes were quantified by ELISA as previously described (Materials and Methods 1.5.2). Sera were diluted 1:300 in milk 0.5%.

1.6 Cytokine production

Levels of cytokines in sera were measured using the Bio-Plex Mouse Cytokine bead assay (Bio-Rad Laboratories), following the manufacturer's instructions.

ELISA assays for serum murine cytokines IFN- γ and IL10 were purchased from Affymetrix eBiosciences (Thermo Fisher Scientific) and R&D Systems, respectively.

1.7 *In vitro* restimulation assay and cytokine release

Mixed lymphocyte-tumor cell cultures (MLTC) were performed with spleen mononuclear cells cocultured at a 50:1 ratio with proliferation-blocked Neu/H-2^q cells for 6 days in RPMI 1640 supplemented with 10% FBS and with 20 units/ml of recombinant IL-2. Supernatants from MLTC were assayed for IFN- γ , GM-CSF and IL10 by ELISA (R&D Systems Inc.).

1.8 Detection of lymphocyte subpopulations

Cell suspensions were obtained from individual lymphoid organs (spleen, bone marrow, lymph nodes) as previously described (Burocchi et al. 2011). PE-Cy7 anti-CD4 (RM4-5), APC anti-Foxp3 (FJK-16s), PE anti-CD103 (2E7) and FITC anti-GITR were purchased from eBioscience. Surface staining was performed on cells obtained from each organ by incubating antibodies at 5 μ g/ml on ice for 30 min in PBS containing 2% FBS. For these analyses, flow cytometry data were acquired on a FACSCalibur (Becton Dickinson) and analysed with FlowJo software (Becton Dickinson). Data from different organs of each mouse, if statistically not different, were pooled in the final elaboration.

2. DISCOVERY OF NEW TARGETS

Materials and Methods reported in this Chapter were included in the manuscripts of Giusti and colleagues (submitted) and Landuzzi and colleagues (Landuzzi et al. 2021).

2.1 Mice

HER2 mice, transgenic for the full-length human HER2 isoform (Finkle et al. 2004; De Giovanni et al. 2014) were obtained from Genentech and bred in our animal facilities. FVB mice (FVB/NCrl) mice were purchased from Charles River Laboratories.

NOD-SCID-II2rg^{-/-} (NSG) female mice (breeders received from Jackson Laboratories) or BALB/cRag2^{-/-}II2rg^{-/-} (BRG) female mice (breeders received from Drs T. Nomura and M. Ito, Central Institute for Experimental Animals, CIEA, Kawasaki, Japan) were kept under sterile conditions and were used as immunodeficient models, lacking B, T and NK immune components.

2.2 Cells

MamBo89HER2^{stable} and MamBo43HER2^{labile} cell lines were established from mammary tumors of HER2 mice. MamBo89HER2^{stable} AG3 clone was obtained by cloning in 3D (soft-agar) conditions. MamBo43HER2^{labile} clones were derived by low density seeding in adherence (AD clones) or 3D (AG clones) conditions. MamBo cell lines and clones were stabilized and cultured in DMEM supplemented with 20% FBS, 30 µg/ml bovine pituitary extract and 0.5% v/v MITO Serum Extender. MamBo cell lines were maintained at 37°C in a humidified 5% CO₂ atmosphere.

Primary cell cultures from PDX-BRB4 (PDX established in the Laboratory of Immunology and Biology of Metastases, University of Bologna; see Materials and Methods 2.3.2) were set up from mechanically dissociated tumors in primary cell culture flasks in HuMEC complete medium (Thermo Fisher Scientific) + 20% FBS. Cells were maintained at 37°C in a 7% CO₂ atmosphere, with frequent medium renewal.

TS/A cell line and human breast cancer cell lines used as positive and negative controls of HER2 copy number testing were previously described (Materials and Methods 1.1.2).

2.3 *In vivo* studies

2.3.1 MamBo cell lines *in vivo* growth and inhibition by sunitinib

To evaluate the tumorigenicity of the MamBo cell lines, HER2 female mice received the injection of 10^6 cells into the mammary fat pad (m.f.p.). Experimental metastatic potential was assessed via the injection of 10^5 cells into a caudal vein. In order to evaluate the dose-dependent tumor growth of MamBo43HER2^{labile} cells in immunocompetent mice, different doses of cells (10^6 , 10^7 and 2×10^7) were s.c. injected into HER2 female mice. MamBo43HER2^{labile} cells (10^5 cells) were also s.c. injected into Rag2^{-/-};Il2Rg^{-/-} immunodeficient female mice to inspect the contribution of adaptive immunity to HER2 loss.

HER2 female mice received s.c. injection of 10^6 MamBo43HER2^{labile} cells. Mice were treated daily with sunitinib 60 mg/kg per os by gavage, starting from 3 days after cell injection. FVB female mice that harboured tumors that were induced by the s.c. injection of MamBo38HER2^{loss} cells (2.5×10^4 cells) were daily treated with sunitinib starting from 1 day after cell injection. Animals in the vehicle group received Methylcellulose 0.5%+Tween80 0.4%.

Mice were monitored weekly by palpation and tumor dimensions were measured with calipers. Masses with a mean diameter exceeding 3 mm were considered tumors. Tumor volume was calculated as $(\pi/12)(\sqrt{ab})^3$ where a = maximal tumour diameter and b = maximal tumour diameter perpendicular to a . Mice were euthanized when tumor burden was equivalent to 10% of body mass. For studies of metastatization, mice were euthanized at any initial sign of metastatic growth or after 18 weeks. Mice were subjected to an accurate necropsy; lungs were perfused with black India ink to outline metastases and fixed in Fekete's solution. Metastases were counted under a dissection microscope.

2.3.2 PDX establishment, propagation and metastatization

BRB4 tumor fragment, from a breast cancer patient, was implanted in the fourth left mammary fat pad. When tumor reached a volume of 1.5-1.9 cm³, animal was euthanized and, after an accurate necropsy, tumor was resected and divided into representative samples for propagation by serial *in vivo* passage or other analysis.

PDX-BRB4 tumor fragments were dissociated by incubation in 0.05% Trypsin - 0.002% EDTA at 37°C for 5 minutes and passed through a 70 µm cell strainer (Becton Dickinson) to obtain single-cell suspension. Cells were *i.v.* injected in a tail vein of BRG mice at doses ranging from 0.5 to 2×10⁶ cells in 0.4 ml PBS.

Mice were monitored weekly by palpation and tumor dimensions were measured with calipers. Masses with a mean diameter exceeding 3 mm were considered tumors. Tumor volume was calculated as $(\pi/6)(\sqrt{ab})^3$ where a = maximal tumour diameter and b = maximal tumour diameter perpendicular to a . Mice were euthanized when tumor burden was equivalent to 10% of body mass. For studies of metastatization, mice were euthanized at any initial sign of metastatic growth or after 40-70 weeks. Lungs, brain, ovaries and femoral bone marrow were collected for molecular detection of metastatic dissemination or, in case of overt lung colonization, metastases were counted at a dissection microscope.

2.4 *In vitro* assay

2.4.1 3D-growth inhibition by sunitinib

Sunitinib sensitivity in MamBo38HER2^{loss} cells (0.5×10³ cells/cm²) was evaluated under 3D non-adherent conditions according to the protocol previously described (1.1.5). Colonies were counted after 14 days.

2.4.2 Cell migration

The migratory ability of MamBo38HER2^{loss} cells in the presence of sunitinib was evaluated in a wound-healing test. Cells were seeded in 24-well plates in complete medium and allowed to grow until confluence. The cell monolayer was scratched with a 200 μ l pipette tip, the medium was changed with or without sunitinib, 5 μ M, and wound width was measured 0 and 24 hours after scratching. Migratory ability was calculated as $\text{width (24h)}/\text{width(t0)}*100$.

The migratory ability of MamBo43HER2^{labile} cells previously treated with siRNA (Dharmacon) to silence PHLDA1 (L048462-01) and GAPDH (D-001830-20-05) or with control siRNA (D-001810-10-05), was evaluated by a migration assay performed in Transwell chambers (Costar) with 8 μ m pore size. Serum-free DMEM was put in the lower compartment of the Transwell chamber; 0.4x10⁶ cells were seeded in serum-free DMEM in the upper compartment of the Transwell chambers and incubated for 18 hours. Cells which migrated through the filter to reach the lower chamber were counted at the inverted microscope.

2.4.3 Mammosphere formation assay

The ability of MamBo cell lines to form mammospheres *in vitro* was assessed using the MammoCult Human Medium Kit (Stem Cell Technologies), according to the manufacturer's protocol. Briefly, 4000 cells were seeded in 4 ml complete MammoCult medium without serum in 6 well UltraLow Adherence plates. Mammospheres that were bigger than 60 μ m were counted on day 7. The same protocol was employed to evaluate the ability of MamBo38HER2^{loss} cells to form mammospheres in presence of sunitinib 5 μ M.

To study mammosphere production, PDX-BRB4 tumor cells were seeded as previously described. After 6-8 days of culture, mammospheres were collected and then dissociated by incubation in Trypsin-EDTA to obtain single cell suspensions for direct immunofluorescence.

2.4.4 Induction of HER2 loss *in vitro*

MamBo43HER2^{labile} cells were cultured for 2 months in the presence of 30 µg/ml trastuzumab. Cells were counted weekly and seeded at a concentration of either 1.6x10⁵ cells/cm² (high density) or 4x10⁴ cells/cm² (low density). In parallel, cells were harvested for molecular analysis, cytofluorimetric analysis of HER2 and stemness marker expression. A third culture, without trastuzumab, was performed by seeding MamBo43HER2^{labile} cells at a lower density (10⁴ cells/cm²).

MamBo89HER2^{stable} and MamBo38HER2^{loss} cell lines were treated with trastuzumab for 30 and 60 days. The treatment did not modify the initial shape, HER2 expression level and stemness profile of correspondent untreated cells. These data were not reported in this thesis, but samples were analysed by RNA-Sequencing

2.4.5 IL-6 quantification

To quantify IL-6 production by MamBo cell lines, supernatants were collected from cells that were seeded 8x10⁴ cells/cm² in medium that contained either sunitinib 5 µM (LC Laboratories, MA, USA) or DMSO 0.05% (here referred as vehicle) or no drug. mIL6 production was analysed using Mouse IL-6 Quantikine ELISA Kit (R&D Systems), according to the manufacturer's protocol. The concentration of each sample was calculated by interpolating values on a standard curve. A stable IL6 producer mouse mammary cancer cell line (TS/A-IL6) was used as positive control of IL6 production (Fattori et al. 1995).

2.5 Tumor and cell phenotyping

2.5.1 Flow Cytometry

Harvested cells and tumor samples, which had previously been dissociated to yield single-cell suspensions, were analysed by immunofluorescence and cytofluorimetric

analysis. The antibodies used for indirect immunofluorescence included: rat anti-mouse CD16-CD32 antibody Fc block (clone 2.4G2; diluted 1:100 dilution; BD, Pharmingen, CA, USA); mouse anti-human HER2 (MGR2, diluted 1:100, Enzo Life Science and also kindly provided by Dr. Elda Tagliabue (IRCCS, Istituto Nazionale dei Tumori, Milan, Italy); mouse anti-p95HER2-611CTF (32H11, diluted 1:350) (Parra-Palau et al. 2014) kindly provided by Dr. Joaquin Arribas (Vall d'Hebron Institute of Oncology, Barcelona, Spain); rat anti-mouse CD140b (PDGFR-B) (APB5, diluted 1:100; Bio-Legend, CA, USA). Anti-mouse IgG AF488 (diluted 1:100; Thermo Fisher Scientific) and anti-rat IgG FITC (diluted 1:40; KPL) were used as secondary antibodies. Direct immunofluorescence made use of: anti-human HER2 PE (clone Neu 24.7, diluted 1:20, Becton Dickinson); anti-mouse CD24 AF488 (clone M1/69; diluted 1:10; Biolegend); anti-mouse-CD44 PE (clone IM7; diluted 1:10, Biolegend); anti-mouse Sca1 PE (clone E13-161.7, 1:100 dilution; Biolegend); and anti-mouse CD29 PE (clone HM β 1-1; diluted 1:10; Biolegend).

PDX analysis was performed using anti-hu-CD24AF488 (clone ML5, BioLegend) and anti-hu-CD44PE (clone IM7, BioLegend).

Data were acquired using CyFlow Space and analyzed using FCSEXPRESS.

Rabbit anti-mouse Sorbs3 polyclonal antibody (clone AP55384SU-N acris) was used to perform immunofluorescence on adherent MamBo cell lines.

The cell senescence process was detected using the Senescence Cells Histochemical Staining Kit (Sigma-Aldrich). Cells were fixed and processed according to the protocol reported by the kit.

2.5.2 Molecular analysis

2.5.2.1 RNA-Sequencing

RNA-sequencing was performed by Prof. Raffaele Calogero (University of Turin, Turin, Italy). Total RNA was extracted from cell pellets using Trizol Reagent (Thermo

Fisher Scientific), according to the manufacturer's instructions. RNA-seq libraries were generated using TruSeq RNA Sample Prep Kit v2 (Illumina), according to the manufacturer's recommendations. High-throughput sequencing was carried out on a NextSeq 500 (Illumina) using 75 nucleotides, in single-end mode. For PDX-BRB4 samples Xenome software (Conway et al. 2012) was used to remove mouse reads. Reads were analyzed on a SeqBox (Beccuti et al. 2018). The generation of Demultiplexing (bcl2fastq Illumina tool version 2.17.1.14-2) counts using STAR (version 2.5) /RSEM (version 1.3.0), and differential gene expression analysis using DESeq2 (version 1.14.1, adjusted P-value < 0.1 and |log₂ fold change| ≥1) were all performed within the SeqBox framework.

For MamBo cell lines distinct analyses were performed on differentially expressed genes. The first analysis considered differentially expressed genes between HER2-stable and HER2-negative cell lines. To identify predictive genes of HER2 loss, up-regulated genes in the HER2-labile *vs* the HER2-stable group and up-regulated genes in the HER2-negative group *vs* the HER2-stable group were crossed. Common genes to both lists might be considered up-regulated through HER2 lability condition. The same analysis was done for down regulated genes. Finally, the comparison between HER2-positive, including HER2-stable and -labile cell lines, and HER2-negative cell lines was also performed. Functional enrichment analysis was performed using the EnrichR web tool (<https://maayanlab.cloud/Enrichr/>).

For PDX-BRB4, hierarchical clustering was done using Morpheus at Broad (<https://software.broadinstitute.org/morpheus/>). Ingenuity Pathway Analysis (IPA) (Qiagen) was used for functional characterization of differentially expressed genes.

2.5.2.2 Real-Time PCR

RNA was extracted, quantified and reverse transcribed as previously reported (Palladini et al. 2017). cDNA was amplified using Sso Advanced SyBR Green Supermix reagents. Reactions were performed in a Thermal Cycler CFX96. Analyses were

performed using Bio-Rad CFX Manager 3.1 Software, and relative quantification was calculated as $\Delta Ct = Ct_{\text{gene}} - Ct_{\text{housekeeping}}$. We used the following Bio-Rad assays: Cdh1 (qMmuCID0006332); Col3a1 (qMmuCID0006332); Col5a2 (qMmuCID0011413); Dsp (qMmuCID0019458); Fgfbp1 (qMmuCID0007813); Igfbp4 (qMmuCID0006155); Il1rn (qMmuCID0009153); Mmp2 (qMmuCID00021124); Ocln (qMmuCID0005446); Pdgrfb (qMmuCID0025167); Sparc (qMmuCID0023536); Vcan (qMmuCID0005235); Snai1 (qMmuCID0024342); Zeb1 (qMmuCID0009095); Zeb2 (qMmuCED0046769); Twist1 (qMmuCED0004065); Ltbp1 (qMmuCED0045004); Sorbs3 (qMmuCID0022725). Custom HER2 primers (Mitra et al. 2009) and human Bcl-2 primers (Dir, CTTTGAGTTCGGTGGGGTCA, Rev: GGGCCGTACAGTTCCACAAA; kindly provided by Prof. Lorenzo Montanaro, Bologna, Italy) were also used. Mouse Tbp (Bieche et al. 2014)] or Bio-Rad assay qMmuCID0040542) and human TBP (Bieche et al. 2014) were used as housekeeping.

2.5.2.3 HER2 copy number

DNA was extracted using a PureLink Genomic DNA Mini kit (Thermo Fisher Scientific), according to the manufacturer's protocol. HER2 copy number was detected by Real-Time PCR using a HER2 primer qHsaCEP0052301 assay (Bio-Rad Laboratories) and was normalized over human/mouse Ptger2 (Alcoser et al. 2011). Amplification was performed using Sso Advanced Universal Probes Supermix (Bio-Rad Laboratories). The copy number of the human and murine cell lines was inferred by considering that MCF7 and MDA-MB231 harbour 2 copies of HER2 in the genome.

2.5.2.4 Molecular metastasis detection

As previously reported (Nanni et al. 2012), genomic DNA was extracted from cellular pellets of lungs, brain, femoral bone marrow and ovaries. A sequence of the α -satellite region of the human chromosome 17 was amplified by Real Time-PCR. DNA extracted from mouse tissues showed no amplification up to 40 cycles. To quantify human cells,

a standard curve was constructed by adding scalar amounts of MDA-MB-453 human cells to a constant number of mouse cells. Ct values obtained from the experimental samples were interpolated in the standard curve run in each PCR (Bio-Rad CFX Manager). The final number of disseminated tumor cells per organ was obtained considering the fraction analyzed for each organ.

2.5.2.5 *In situ* HER2 detection

In situ detection of HER2 isoform RNA expression was performed using the Basescope assay on formalin-fixed, paraffin-embedded (FFPE) tumor tissues in accordance with guidelines provided by the supplier (Advanced Cell Diagnostics-ACD, Newark, CA, USA). Briefly, 5 µm tissue sections were deparaffinized with xylene and 100% ethanol. Then slides were pretreated with Hydrogen Peroxide, Target Retrieval solution and Protease III (Pretreatment Reagents Kit, ACD). Slides were then hybridized in HybEZ Hybridization System with probes detecting HER2 TOT (able to detect both HER2 full-length and HER2-D16) (BaseScope Hs-ERBB2-E1E18), HER2 full-length (BaseScope Hs-ERBB2-E15E16) and HER2-D16 (BaseScope Hs-ERBB2-E15E17). A positive control probe of RNA quality (Hs-PPIB-1zz) and a negative control probe for aspecific signal (DapB-1zz) were also used. After hybridizations, slides were subjected to signal amplification using Basescope Detection Reagent Kit-RED. After counterstaining with Gill's hematoxylin, tissue sections were examined under a standard bright field microscope at 40× magnification. Expression score was based on the estimated number of dots per cell, according to scoring guidelines provided by ACD (scores 0-4, with 4 corresponding to >6 dots/cell).

2.5.3 Western Blotting

Protein extraction and Western blotting were performed as reported previously (De Giovanni et al. 2019a). The following primary antibodies were used: anti-HER2 (clone 3B5, diluted 1:1000, Calbiochem, Merck), anti-pNeu (Tyr 1248) (diluted 1:1000, Santa Cruz Biotechnology), anti-Stat3 (clone 124H6, diluted 1:1000, Cell Signaling, Danvers,

MA), anti-pStat3 (clone D3A7, diluted 1:2000, Cell Signaling), anti-PHLDA1 (clone RN-6E2, diluted 1:250, Santa Cruz). Membranes were either incubated with polyclonal HRP conjugated anti-rat IgG antibody (diluted 1:3000, Bio-Rad Laboratories), or anti-mouse IgG antibody (diluted 1:1000, Santa Cruz Biotechnology). Protein presence was detected by chemiluminescent reaction before film exposure.

2.5.4 Immunohistochemistry and immunofluorescence

BCL2 quantification by immunohistochemistry was performed by Prof. M.P. Foschini and co-workers (Bellaria Hospital, Bologna, Italy). Human tumors or xenografts were fixed in 10% neutral buffered formalin solution (Sigma-Aldrich) and processed to obtain paraffin blocks. Immunostaining was performed on FFPE sections in an automated Benchmark Ultra Autostainer (Ventana Medical Systems, Inc., Tucson, Arizona, USA). The immunologic reaction was visualized using the Ventana UltraView DAB Detection kit, according to the manufacturer's instructions. BCL2 (clone SP66, Ventana) was used as primary antibody. BCL2 expression was semi-quantitatively evaluated by examining all the neoplastic population at 100x and classified as follows: Negative < 10%; Intermediate >10%<30%; Positive >30% of immunostained neoplastic cells. Appropriate positive and negative controls were included in each run.

Immunofluorescence analysis of vessels in tumors from MamBo89HER2^{stable}, MamBo43HER2^{labile} and MamBo38HER2^{loss} cells was performed by Prof. Manuela Iezzi (University G. D'Annunzio, Pescara, Italy) as previously described (Palladini et al. 2017). Primary antibodies used for the staining were: rat monoclonal anti-CD31 (BD Pharmingen), rat monoclonal anti-CD105 (BD Pharmingen) and rabbit polyclonal anti-NG2 (EMD Millipore). Image acquisition was performed using Zeiss LSM 510 META confocal microscope.

3. ETHICAL STATEMENTS

Experiments were approved by the institutional review board of the University of Bologna, authorized by the Italian Ministry of Health and done according to Italian and European laws and guidelines (71674-x/6, 12511-x/10, 4783-X/10, 782/2015-PR, 714/21017-PR, 688/2015-PR and 32/2020-PR).

Human studies were approved and authorized by the local Ethics Committee (Bologna CE-BI, number of study: 14100/CE 2014; prot. N.: 964/CE). All human samples and their metadata including relevant clinical data were de-identified before being shared between laboratories involved in this study.

4. STATISTICAL ANALYSIS

Differences in tumor-free survival curves were analysed by the Mantel–Haenszel test.

Other data were compared by Student's t test or nonparametric Wilcoxon test.

Statistical analyses were performed through Prism 5 software (GraphPad software, La Jolla, CA, USA). Linear regression analysis was used to assess the correlation between tumor doubling time and *in vivo* passages, and the correlation between the number of *in vivo* passages and the expression of BCL2.

References

Abrams, TJ; Lee, LB; Murray, LJ; Pryer, NK; Cherrington, JM (2003): SU11248 inhibits KIT and platelet-derived growth factor receptor beta in preclinical models of human small cell lung cancer. *Molecular cancer therapeutics* 2 (5), pp. 471–478.

Adams, CW; Allison, DE; Flagella, K; Presta, L; Clarke, J; Dybdal, N et al. (2006): Humanization of a recombinant monoclonal antibody to produce a therapeutic HER dimerization inhibitor, pertuzumab. *Cancer immunology, immunotherapy : CII* 55 (6), pp. 717–727. DOI: 10.1007/s00262-005-0058-x.

Ahamadi, M; Freshwater, T; Prohn, M; Li, CH; Alwis, DP de; Greef, R de et al. (2017): Model-Based Characterization of the Pharmacokinetics of Pembrolizumab: A Humanized Anti-PD-1 Monoclonal Antibody in Advanced Solid Tumors. *CPT: pharmacometrics & systems pharmacology* 6 (1), pp. 49–57. DOI: 10.1002/psp4.12139.

Alajati, A; Sausgruber, N; Aceto, N; Duss, S; Sarret, S; Voshol, H et al. (2013): Mammary tumor formation and metastasis evoked by a HER2 splice variant. *Cancer research* 73 (17), pp. 5320–5327. DOI: 10.1158/0008-5472.CAN-12-3186.

Al-Awadhi, A; Lee Murray, J; Ibrahim, NK (2018): Developing anti-HER2 vaccines: Breast cancer experience. *Int J Cancer* 143 (9), pp. 2126–2132. DOI: 10.1002/ijc.31551.

Alcoser, SY; Kimmel, DJ; Borgel, SD; Carter, JP; Dougherty, KM; Hollingshead, MG (2011): Real-time PCR-based assay to quantify the relative amount of human and mouse tissue present in tumor xenografts. *BMC biotechnology* 11, p. 124. DOI: 10.1186/1472-6750-11-124.

Al-Hajj, M; Wicha, MS; Benito-Hernandez, A; Morrison, SJ; Clarke, MF (2003): Prospective identification of tumorigenic breast cancer cells. *Proceedings of the National Academy of Sciences of the United States of America* 100 (7), pp. 3983–3988. DOI: 10.1073/pnas.0530291100.

Andrechek, ER; Hardy, WR; Siegel, PM; Rudnicki, MA; Cardiff, RD; Muller, WJ (2000): Amplification of the neu/erbB-2 oncogene in a mouse model of mammary tumorigenesis. *Proceedings of the National Academy of Sciences of the United States of America* 97 (7), pp. 3444–3449. DOI: 10.1073/pnas.050408497.

Angelicola, S; Ruzzi, F; Landuzzi, L; Scalambra, L; Gelsomino, F; Ardizzoni, A et al. (2021): IFN- γ and CD38 in Hyperprogressive Cancer Development. *Cancers* 13 (2). DOI: 10.3390/cancers13020309.

Anido, J; Scaltriti, M; Bech Serra, JJ; Santiago Josef, B; Todo, FR; Baselga, J; Arribas, J (2006): Biosynthesis of tumorigenic HER2 C-terminal fragments by alternative

initiation of translation. *The EMBO journal* 25 (13), pp. 3234–3244. DOI: 10.1038/sj.emboj.7601191.

Antonia, SJ; Villegas, A; Daniel, D; Vicente, D; Murakami, S; Hui, R et al. (2018): Overall Survival with Durvalumab after Chemoradiotherapy in Stage III NSCLC. *The New England journal of medicine* 379 (24), pp. 2342–2350. DOI: 10.1056/NEJMoa1809697.

Arias-Romero, LE; Villamar-Cruz, O; Pacheco, A; Kosoff, R; Huang, M; Muthuswamy, SK; Chernoff, J (2010): A Rac-Pak signaling pathway is essential for ErbB2-mediated transformation of human breast epithelial cancer cells. *Oncogene* 29 (43), pp. 5839–5849. DOI: 10.1038/onc.2010.318.

Arlaukas, SP; Garren, SB; Garris, CS; Kohler, RH; Oh, J; Pittet, MJ; Weissleder, R (2018): Arg1 expression defines immunosuppressive subsets of tumor-associated macrophages. *Theranostics* 8 (21), pp. 5842–5854. DOI: 10.7150/thno.26888.

Arribas, J; Baselga, J; Pedersen, K; Parra-Palau, JL (2011): p95HER2 and breast cancer. *Cancer research* 71 (5), pp. 1515–1519. DOI: 10.1158/0008-5472.CAN-10-3795.

Arribas, J; Parra-Palau, JL; Pedersen, K (2010): HER2 fragmentation and breast cancer stratification. *Clinical cancer research : an official journal of the American Association for Cancer Research* 16 (16), pp. 4071–4073. DOI: 10.1158/1078-0432.CCR-10-1501.

Arteaga, CL; Engelman, JA (2014): ERBB receptors: from oncogene discovery to basic science to mechanism-based cancer therapeutics. *Cancer cell* 25 (3), pp. 282–303. DOI: 10.1016/j.ccr.2014.02.025.

Artibani, M; Sims, AH; Slight, J; Aitken, S; Thornburn, A; Muir, M et al. (2017): WT1 expression in breast cancer disrupts the epithelial/mesenchymal balance of tumour cells and correlates with the metabolic response to docetaxel. *Scientific reports* 7, p. 45255. DOI: 10.1038/srep45255.

Aspeshlagh, S; Postel-Vinay, S; Rusakiewicz, S; Soria, J-C; Zitvogel, L; Marabelle, A (2016): Rationale for anti-OX40 cancer immunotherapy. *European journal of cancer (Oxford, England : 1990)* 52, pp. 50–66. DOI: 10.1016/j.ejca.2015.08.021.

Aurisicchio, L; Ciliberto, G (2012): Genetic cancer vaccines: current status and perspectives. *Expert opinion on biological therapy* 12 (8), pp. 1043–1058. DOI: 10.1517/14712598.2012.689279.

Azuma, T; Yao, S; Zhu, G; Flies, AS; Flies, SJ; Chen, L (2008): B7-H1 is a ubiquitous antiapoptotic receptor on cancer cells. *Blood* 111 (7), pp. 3635–3643. DOI: 10.1182/blood-2007-11-123141.

Bachelot, T; Garcia-Saenz, JA; Verma, S; Gutierrez, M; Pivot, X; Kozloff, MF et al. (2014): Sunitinib in combination with trastuzumab for the treatment of advanced

breast cancer: activity and safety results from a phase II study. *BMC cancer* 14, p. 166. DOI: 10.1186/1471-2407-14-166.

Bachman, KE; Argani, P; Samuels, Y; Silliman, N; Ptak, J; Szabo, S et al. (2004): The PIK3CA gene is mutated with high frequency in human breast cancers. *Cancer biology & therapy* 3 (8), pp. 772–775. DOI: 10.4161/cbt.3.8.994.

Bachmann, MF; Rohrer, UH; Kündig, TM; Bürki, K; Hengartner, H; Zinkernagel, RM (1993): The influence of antigen organization on B cell responsiveness. *Science (New York, N.Y.)* 262 (5138), pp. 1448–1451. DOI: 10.1126/science.8248784.

Bargmann, CI; Hung, MC; Weinberg, RA (1986): The neu oncogene encodes an epidermal growth factor receptor-related protein. *Nature* 319 (6050), pp. 226–230. DOI: 10.1038/319226a0.

Barnes, CJ; Kumar, R (2004): Biology of the epidermal growth factor receptor family. *Cancer treatment and research* 119, pp. 1–13. DOI: 10.1007/1-4020-7847-1_1.

Baselga, J (2001): Clinical trials of Herceptin(trastuzumab). *European journal of cancer (Oxford, England : 1990)* 37 Suppl 1, S18-24.

Baselga, J; Bradbury, I; Eidtmann, H; Di Cosimo, S; Azambuja, E de; Aura, C et al. (2012): Lapatinib with trastuzumab for HER2-positive early breast cancer (NeoALTTO): a randomised, open-label, multicentre, phase 3 trial. *The Lancet* 379 (9816), pp. 633–640. DOI: 10.1016/S0140-6736(11)61847-3.

Beccuti, M; Cordero, F; Arigoni, M; Panero, R; Amparore, EG; Donatelli, S; Calogero, RA (2018): SeqBox: RNAseq/ChIPseq reproducible analysis on a consumer game computer. *Bioinformatics (Oxford, England)* 34 (5), pp. 871–872. DOI: 10.1093/bioinformatics/btx674.

Benavides, LC; Gates, JD; Carmichael, MG; Patil, R; Patel, R; Holmes, JP et al. (2009): The impact of HER2/neu expression level on response to the E75 vaccine: from U.S. Military Cancer Institute Clinical Trials Group Study I-01 and I-02. *Clin Cancer Res* 15 (8), pp. 2895–2904. DOI: 10.1158/1078-0432.CCR-08-1126.

Benci, JL; Xu, B; Qiu, Y; Wu, TJ; Dada, H; Twyman-Saint Victor, C et al. (2016): Tumor Interferon Signaling Regulates a Multigenic Resistance Program to Immune Checkpoint Blockade. *Cell* 167 (6), 1540-1554.e12. DOI: 10.1016/j.cell.2016.11.022.

Benz, CC; Scott, GK; Sarup, JC; Johnson, RM; Tripathy, D; Coronado, E et al. (1992): Estrogen-dependent, tamoxifen-resistant tumorigenic growth of MCF-7 cells transfected with HER2/neu. *Breast cancer research and treatment* 24 (2), pp. 85–95. DOI: 10.1007/BF01961241.

- Bhang, H-eC; Ruddy, DA; Krishnamurthy Radhakrishna, V; Caushi, JX; Zhao, R; Hims, MM et al. (2015): Studying clonal dynamics in response to cancer therapy using high-complexity barcoding. *Nature medicine* 21 (5), pp. 440–448. DOI: 10.1038/nm.3841.
- Bianchini, G; Gianni, L (2014): The immune system and response to HER2-targeted treatment in breast cancer. *The Lancet Oncology* 15 (2), e58-e68. DOI: 10.1016/S1470-2045(13)70477-7.
- Bieche, I; Vacher, S; Vallerand, D; Richon, S; Hatem, R; Plater, L de et al. (2014): Vasculature analysis of patient derived tumor xenografts using species-specific PCR assays: evidence of tumor endothelial cells and atypical VEGFA-VEGFR1/2 signalings. *BMC cancer* 14, p. 178. DOI: 10.1186/1471-2407-14-178.
- Blair, HA (2018): Atezolizumab: A Review in Previously Treated Advanced Non-Small Cell Lung Cancer. *Targeted oncology* 13 (3), pp. 399–407.
- Bloom, HJ; Richardson, WW (1957): Histological grading and prognosis in breast cancer; a study of 1409 cases of which 359 have been followed for 15 years. *British journal of cancer* 11 (3), pp. 359–377. DOI: 10.1038/bjc.1957.43.
- Bolli, E; O'Rourke, JP; Conti, L; Lanzardo, S; Rolih, V; Christen, JM et al. (2018): A Virus-Like-Particle immunotherapy targeting Epitope-Specific anti-xCT expressed on cancer stem cell inhibits the progression of metastatic cancer in vivo. *Oncoimmunology* 7 (3), e1408746. DOI: 10.1080/2162402X.2017.1408746.
- Bon, G; Pizzuti, L; Laquintana, V; Loria, R; Porru, M; Marchiò, C et al. (2020): Loss of HER2 and decreased T-DM1 efficacy in HER2 positive advanced breast cancer treated with dual HER2 blockade: the SePHER Study. *Journal of experimental & clinical cancer research : CR* 39 (1), p. 279. DOI: 10.1186/s13046-020-01797-3.
- Borcoman, E; Kanjanapan, Y; Champiat, S; Kato, S; Servois, V; Kurzrock, R et al. (2019): Novel patterns of response under immunotherapy. *Annals of oncology : official journal of the European Society for Medical Oncology* 30 (3), pp. 385–396. DOI: 10.1093/annonc/mdz003.
- Borghaei, H; Paz-Ares, L; Horn, L; Spigel, DR; Steins, M; Ready, NE et al. (2015): Nivolumab versus Docetaxel in Advanced Nonsquamous Non-Small-Cell Lung Cancer. *N Engl J Med* 373 (17), pp. 1627–1639. DOI: 10.1056/NEJMoa1507643.
- Bose, R; Kavuri, SM; Searleman, AC; Shen, W; Shen, D; Koboldt, DC et al. (2013): Activating HER2 mutations in HER2 gene amplification negative breast cancer. *Cancer discovery* 3 (2), pp. 224–237. DOI: 10.1158/2159-8290.CD-12-0349.
- Bottini, A; Berruti, A; Bersiga, A; Brizzi, MP; Brunelli, A; Gorzegno, G et al. (2000): p53 but not bcl-2 immunostaining is predictive of poor clinical complete response to

primary chemotherapy in breast cancer patients. *Clinical cancer research : an official journal of the American Association for Cancer Research* 6 (7), pp. 2751–2758.

Bouchard, L; Lamarre, L; Tremblay, PJ; Jolicoeur, P (1989): Stochastic appearance of mammary tumors in transgenic mice carrying the MMTV/c-neu oncogene. *Cell* 57 (6), pp. 931–936. DOI: 10.1016/0092-8674(89)90331-0.

Brahmer, J; Reckamp, KL; Baas, P; Crinò, L; Eberhardt, WE; Poddubskaya, E et al. (2015): Nivolumab versus Docetaxel in Advanced Squamous-Cell Non-Small-Cell Lung Cancer. *The New England journal of medicine* 373 (2), pp. 123–135. DOI: 10.1056/NEJMoa1504627.

Branco, FP; Machado, D; Silva, FF; André, S; Catarino, A; Madureira, R et al. (2019): Loss of HER2 and disease prognosis after neoadjuvant treatment of HER2+ breast cancer. *American journal of translational research* 11 (9), pp. 6110–6116.

Bruni, D; Angell, HK; Galon, J (2020): The immune contexture and Immunoscore in cancer prognosis and therapeutic efficacy. *Nature reviews. Cancer* 20 (11), pp. 662–680. DOI: 10.1038/s41568-020-0285-7.

Burgess, AW; Cho, H-S; Eigenbrot, C; Ferguson, KM; Garrett, TPJ; Leahy, DJ et al. (2003): An Open-and-Shut Case? Recent Insights into the Activation of EGF/ErbB Receptors. *Molecular Cell* 12 (3), pp. 541–552. DOI: 10.1016/s1097-2765(03)00350-2.

Bürgler, S; Gimeno, A; Parente-Ribes, A; Wang, D; Os, A; Devereux, S et al. (2015): Chronic lymphocytic leukemia cells express CD38 in response to Th1 cell-derived IFN- γ by a T-bet-dependent mechanism. *Journal of immunology (Baltimore, Md. : 1950)* 194 (2), pp. 827–835. DOI: 10.4049/jimmunol.1401350.

Burnett, JP; Korkaya, H; Ouzounova, MD; Jiang, H; Conley, SJ; Newman, BW et al. (2015): Trastuzumab resistance induces EMT to transform HER2(+) PTEN(-) to a triple negative breast cancer that requires unique treatment options. *Scientific reports* 5, p. 15821. DOI: 10.1038/srep15821.

Burocchi, A; Pittoni, P; Gorzanelli, A; Colombo, MP; Piconese, S (2011): Intratumor OX40 stimulation inhibits IRF1 expression and IL-10 production by Treg cells while enhancing CD40L expression by effector memory T cells. *Eur. J. Immunol.* 41 (12), pp. 3615–3626. DOI: 10.1002/eji.201141700.

Burstein, HJ; Curigliano, G; Loibl, S; Dubsy, P; Gnant, M; Poortmans, P et al. (2019): Estimating the benefits of therapy for early-stage breast cancer: the St. Gallen International Consensus Guidelines for the primary therapy of early breast cancer 2019. *Annals of oncology : official journal of the European Society for Medical Oncology* 30 (10), pp. 1541–1557. DOI: 10.1093/annonc/mdz235.

- Caldeira, J; Bustos, J; Peabody, J; Chackerian, B; Peabody, DS (2015): Epitope-Specific Anti-hCG Vaccines on a Virus Like Particle Platform. *PloS one* 10 (10), e0141407. DOI: 10.1371/journal.pone.0141407.
- Caldeira, JC; Perrine, M; Pericle, F; Cavallo, F (2020): Virus-Like Particles as an Immunogenic Platform for Cancer Vaccines. *Viruses* 12 (5). DOI: 10.3390/v12050488.
- Campbell, IG; Russell, SE; Choong, DY; Montgomery, KG; Ciavarella, ML; Hooi, CS et al. (2004): Mutation of the PIK3CA gene in ovarian and breast cancer. *Cancer research* 64 (21), pp. 7678–7681. DOI: 10.1158/0008-5472.CAN-04-2933.
- Cardoso, F; Canon, J-L; Amadori, D; Aldrighetti, D; Machiels, J-P; Bouko, Y et al. (2012): An exploratory study of sunitinib in combination with docetaxel and trastuzumab as first-line therapy for HER2-positive metastatic breast cancer. *Breast (Edinburgh, Scotland)* 21 (6), pp. 716–723. DOI: 10.1016/j.breast.2012.09.002.
- Cardoso, F; Kyriakides, S; Ohno, S; Penault-Llorca, F; Poortmans, P; Rubio, IT et al. (2019): Early breast cancer: ESMO Clinical Practice Guidelines for diagnosis, treatment and follow-up†. *Annals of oncology : official journal of the European Society for Medical Oncology* 30 (8), pp. 1194–1220. DOI: 10.1093/annonc/mdz173.
- Carlsson, J; Nordgren, H; Sjöström, J; Wester, K; Villman, K; Bengtsson, NO et al. (2004): HER2 expression in breast cancer primary tumours and corresponding metastases. Original data and literature review. *British journal of cancer* 90 (12), pp. 2344–2348. DOI: 10.1038/sj.bjc.6601881.
- Castagnoli, L; Ghedini, GC; Koschorke, A; Triulzi, T; Dugo, M; Gasparini, P et al. (2017): Pathobiological implications of the d16HER2 splice variant for stemness and aggressiveness of HER2-positive breast cancer. *Oncogene* 36 (12), pp. 1721–1732. DOI: 10.1038/onc.2016.338.
- Castagnoli, L; Iezzi, M; Ghedini, GC; Ciravolo, V; Marzano, G; Lamolinara, A et al. (2014): Activated d16HER2 homodimers and SRC kinase mediate optimal efficacy for trastuzumab. *Cancer research* 74 (21), pp. 6248–6259. DOI: 10.1158/0008-5472.CAN-14-0983.
- Castiglioni, F; Tagliabue, E; Campiglio, M; Pupa, SM; Balsari, A; Ménard, S (2006): Role of exon-16-deleted HER2 in breast carcinomas. *Endocrine-related cancer* 13 (1), pp. 221–232. DOI: 10.1677/erc.1.01047.
- Cavallo, F; Aurisicchio, L; Mancini, R; Ciliberto, G (2014): Xenogene vaccination in the therapy of cancer. *Expert opinion on biological therapy* 14 (10), pp. 1427–1442. DOI: 10.1517/14712598.2014.927433.

Cavallo, F; Giovanni, C de; Nanni, P; Forni, G; Lollini, P-L (2011): 2011: the immune hallmarks of cancer. *Cancer immunology, immunotherapy* : CII 60 (3), pp. 319–326. DOI: 10.1007/s00262-010-0968-0.

Ceccarelli, C; Leo, A de; Chieco, P; Zamagni, C; Zamagni, A; Rubino, D et al. (2019): A simple immunohistochemical bio-profile incorporating Bcl2 curbs those cases of invasive breast carcinoma for which an Oncotype Dx characterization is needed. *PloS one* 14 (6), e0217937. DOI: 10.1371/journal.pone.0217937.

Cejalvo, JM; Martínez de Dueñas, E; Galván, P; García-Recio, S; Burgués Gasión, O; Paré, L et al. (2017): Intrinsic Subtypes and Gene Expression Profiles in Primary and Metastatic Breast Cancer. *Cancer research* 77 (9), pp. 2213–2221. DOI: 10.1158/0008-5472.CAN-16-2717.

Chackerian, B; Durfee, MR; Schiller, JT (2008): Virus-like display of a neo-self antigen reverses B cell anergy in a B cell receptor transgenic mouse model. *Journal of immunology (Baltimore, Md. : 1950)* 180 (9), pp. 5816–5825. DOI: 10.4049/jimmunol.180.9.5816.

Chackerian, B; Fietze, KM (2016): Moving towards a new class of vaccines for non-infectious chronic diseases. *Expert review of vaccines* 15 (5), pp. 561–563. DOI: 10.1586/14760584.2016.1159136.

Champiat, S; Dercle, L; Ammari, S; Massard, C; Hollebecque, A; Postel-Vinay, S et al. (2017): Hyperprogressive Disease Is a New Pattern of Progression in Cancer Patients Treated by Anti-PD-1/PD-L1. *Clinical cancer research : an official journal of the American Association for Cancer Research* 23 (8), pp. 1920–1928. DOI: 10.1158/1078-0432.CCR-16-1741.

Champiat, S; Ferrara, R; Massard, C; Besse, B; Marabelle, A; Soria, J-C; Féré, C (2018): Hyperprogressive disease: recognizing a novel pattern to improve patient management. *Nature reviews / Clinical oncology. Clinical oncology*.

Chang, M-H (2009): Cancer prevention by vaccination against hepatitis B. *Recent results in cancer research. Fortschritte der Krebsforschung. Progres dans les recherches sur le cancer* 181, pp. 85–94. DOI: 10.1007/978-3-540-69297-3_10.

Chazin, VR; Kaleko, M; Miller, AD; Slamon, DJ (1992): Transformation mediated by the human HER-2 gene independent of the epidermal growth factor receptor. *Oncogene* 7 (9), pp. 1859–1866.

Chen, L; Diao, L; Yang, Y; Yi, X; Rodriguez, BL; Li, Y et al. (2018): CD38-Mediated Immunosuppression as a Mechanism of Tumor Cell Escape from PD-1/PD-L1 Blockade. *Cancer discovery* 8 (9), pp. 1156–1175. DOI: 10.1158/2159-8290.CD-17-1033.

Chervo, MF; Cordo Russo, RI; Petrillo, E; Izzo, F; Martino, M de; Bellora, N et al. (2020): Canonical ErbB-2 isoform and ErbB-2 variant c located in the nucleus drive triple negative breast cancer growth. *Oncogene* 39 (39), pp. 6245–6262. DOI: 10.1038/s41388-020-01430-9.

Chmielecki, J; Ross, JS; Wang, K; Frampton, GM; Palmer, GA; Ali, SM et al. (2015): Oncogenic alterations in ERBB2/HER2 represent potential therapeutic targets across tumors from diverse anatomic sites of origin. *The oncologist* 20 (1), pp. 7–12. DOI: 10.1634/theoncologist.2014-0234.

Cho, H-S; Mason, K; Ramyar, KX; Stanley, AM; Gabelli, SB; Denney, DW; Leahy, DJ (2003): Structure of the extracellular region of HER2 alone and in complex with the Herceptin Fab. *Nature* 421 (6924), pp. 756–760. DOI: 10.1038/nature01392.

Christianson, TA; Doherty, JK; Lin, YJ; Ramsey, EE; Holmes, R; Keenan, EJ; Clinton, GM (1998): NH₂-terminally truncated HER-2/neu protein: relationship with shedding of the extracellular domain and with prognostic factors in breast cancer. *Cancer research* 58 (22), pp. 5123–5129.

Chung, W; Eum, HH; Lee, H-O; Lee, K-M; Lee, H-B; Kim, K-T et al. (2017): Single-cell RNA-seq enables comprehensive tumour and immune cell profiling in primary breast cancer. *Nature communications* 8, p. 15081. DOI: 10.1038/ncomms15081.

Citri, A; Yarden, Y (2006): EGF-ERBB signalling: towards the systems level. *Nature reviews. Molecular cell biology* 7 (7), pp. 505–516. DOI: 10.1038/nrm1962.

Clark, CA; Gupta, HB; Sareddy, G; Pandeswara, S; Lao, S; Yuan, B et al. (2016): Tumor-Intrinsic PD-L1 Signals Regulate Cell Growth, Pathogenesis, and Autophagy in Ovarian Cancer and Melanoma. *Cancer research* 76 (23), pp. 6964–6974. DOI: 10.1158/0008-5472.CAN-16-0258.

Clay, TM; Osada, T; Hartman, ZC; Hobeika, A; Devi, G; Morse, MA; Lyerly, HK (2011): Polyclonal immune responses to antigens associated with cancer signaling pathways and new strategies to enhance cancer vaccines. *Immunologic research* 49 (1-3), pp. 235–247. DOI: 10.1007/s12026-010-8186-6.

Clynes, RA; Towers, TL; Presta, LG; Ravetch, JV (2000): Inhibitory Fc receptors modulate in vivo cytotoxicity against tumor targets. *Nature medicine* 6 (4), pp. 443–446. DOI: 10.1038/74704.

Cobleigh, MA; Vogel, CL; Tripathy, D; Robert, NJ; Scholl, S; Fehrenbacher, L et al. (1999): Multinational study of the efficacy and safety of humanized anti-HER2 monoclonal antibody in women who have HER2-overexpressing metastatic breast cancer that has progressed after chemotherapy for metastatic disease. *Journal of clinical*

oncology : official journal of the American Society of Clinical Oncology 17 (9), pp. 2639–2648. DOI: 10.1200/JCO.1999.17.9.2639.

Codony-Servat, J; Albanell, J; Lopez-Talavera, JC; Arribas, J; Baselga, J (1999): Cleavage of the HER2 ectodomain is a pervanadate-activable process that is inhibited by the tissue inhibitor of metalloproteases-1 in breast cancer cells. *Cancer research* 59 (6), pp. 1196–1201.

Conti, L; Ruiu, R; Barutello, G; Macagno, M; Bandini, S; Cavallo, F; Lanzardo, S (2014): Microenvironment, oncoantigens, and antitumor vaccination: lessons learned from BALB-neuT mice. *BioMed research international* 2014, p. 534969. DOI: 10.1155/2014/534969.

Conway, T; Wazny, J; Bromage, A; Tymms, M; Sooraj, D; Williams, ED; Beresford-Smith, B (2012): Xenome--a tool for classifying reads from xenograft samples. *Bioinformatics (Oxford, England)* 28 (12), i172-8. DOI: 10.1093/bioinformatics/bts236.

Cooley, S; Burns, LJ; Repka, T; Miller, JS (1999): Natural killer cell cytotoxicity of breast cancer targets is enhanced by two distinct mechanisms of antibody-dependent cellular cytotoxicity against LFA-3 and HER2/neu. *Experimental hematology* 27 (10), pp. 1533–1541. DOI: 10.1016/s0301-472x(99)00089-2.

Cooper, CS; Eeles, R; Wedge, DC; van Loo, P; Gundem, G; Alexandrov, LB et al. (2015): Analysis of the genetic phylogeny of multifocal prostate cancer identifies multiple independent clonal expansions in neoplastic and morphologically normal prostate tissue. *Nature genetics* 47 (4), pp. 367–372. DOI: 10.1038/ng.3221.

Costa, RL; Czerniecki, BJ (2020): Clinical development of immunotherapies for HER2+ breast cancer: a review of HER2-directed monoclonal antibodies and beyond. *NPJ breast cancer* 6, p. 10. DOI: 10.1038/s41523-020-0153-3.

Cowey, CL; Liu, FX; Black-Shinn, J; Stevinson, K; Boyd, M; Frytak, JR; Ebbinghaus, SW (2018): Pembrolizumab Utilization and Outcomes for Advanced Melanoma in US Community Oncology Practices. *Journal of immunotherapy (Hagerstown, Md. : 1997)* 41 (2), pp. 86–95. DOI: 10.1097/CJI.0000000000000204.

Creedon, H; Gómez-Cuadrado, L; Tarnauskaitė, Ž; Balla, J; Canel, M; MacLeod, KG et al. (2016): Identification of novel pathways linking epithelial-to-mesenchymal transition with resistance to HER2-targeted therapy. *Oncotarget* 7 (10), pp. 11539–11552. DOI: 10.18632/oncotarget.7317.

Croci, S; Landuzzi, L; Nicoletti, G; Palladini, A; Antognoli, A; Giovanni, C de et al. (2007): Expression of connective tissue growth factor (CTGF/CCN2) in a mouse model

of rhabdomyosarcomagenesis. *Pathology oncology research : POR* 13 (4), pp. 336–339. DOI: 10.1007/BF02940313.

Crossey, E; Amar, MJ; Sampson, M; Peabody, J; Schiller, JT; Chackerian, B; Remaley, AT (2015): A cholesterol-lowering VLP vaccine that targets PCSK9. *Vaccine* 33 (43), pp. 5747–5755. DOI: 10.1016/j.vaccine.2015.09.044.

Curigliano, G; Romieu, G; Campone, M; Dorval, T; Duck, L; Canon, J-L et al. (2016): A phase I/II trial of the safety and clinical activity of a HER2-protein based immunotherapeutic for treating women with HER2-positive metastatic breast cancer. *Breast cancer research and treatment* 156 (2), pp. 301–310. DOI: 10.1007/s10549-016-3750-y.

Curti, A; Parenza, M; Colombo, MP (2003): Autologous and MHC class I-negative allogeneic tumor cells secreting IL-12 together cure disseminated A20 lymphoma. *Blood* 101 (2), pp. 568–575. DOI: 10.1182/blood-2002-03-0991.

Curtis, C; Shah, SP; Chin, S-F; Turashvili, G; Rueda, OM; Dunning, MJ et al. (2012): The genomic and transcriptomic architecture of 2,000 breast tumours reveals novel subgroups. *Nature* 486 (7403), pp. 346–352. DOI: 10.1038/nature10983.

Cuzzubbo, S; Mangsbo, S; Nagarajan, D; Habra, K; Pockley, AG; McArdle, SE (2020): Cancer Vaccines: Adjuvant Potency, Importance of Age, Lifestyle, and Treatments. *Frontiers in immunology* 11, p. 615240. DOI: 10.3389/fimmu.2020.615240.

Dawood, S; Broglio, K; Buzdar, AU; Hortobagyi, GN; Giordano, SH (2010): Prognosis of women with metastatic breast cancer by HER2 status and trastuzumab treatment: an institutional-based review. *Journal of clinical oncology : official journal of the American Society of Clinical Oncology* 28 (1), pp. 92–98. DOI: 10.1200/JCO.2008.19.9844.

Dawson, S-J; Makretsov, N; Blows, FM; Driver, KE; Provenzano, E; Le Quesne, J et al. (2010): BCL2 in breast cancer: a favourable prognostic marker across molecular subtypes and independent of adjuvant therapy received. *British journal of cancer* 103 (5), pp. 668–675. DOI: 10.1038/sj.bjc.6605736.

De Giovanni, C; Landuzzi, L; Nicoletti, G; Lollini, P-L; Nanni, P (2009a): Molecular and cellular biology of rhabdomyosarcoma. *Future oncology (London, England)* 5 (9), pp. 1449–1475. DOI: 10.2217/fon.09.97.

De Giovanni, C; Landuzzi, L; Palladini, A; Ianzano, ML; Nicoletti, G; Ruzzi, F et al. (2019a): Cancer Vaccines Co-Targeting HER2/Neu and IGF1R. *Cancers* 11 (4). DOI: 10.3390/cancers11040517.

De Giovanni, C; Nanni, P; Landuzzi, L; Ianzano, ML; Nicoletti, G; Croci, S et al. (2019b): Immune targeting of autocrine IGF2 hampers rhabdomyosarcoma growth and metastasis. *BMC cancer* 19 (1), p. 126. DOI: 10.1186/s12885-019-5339-4.

De Giovanni, C; Nicoletti, G; Landuzzi, L; Astolfi, A; Croci, S; Comes, A et al. (2004): Immunoprevention of HER-2/neu transgenic mammary carcinoma through an interleukin 12-engineered allogeneic cell vaccine. *Cancer research* 64 (11), pp. 4001–4009. DOI: 10.1158/0008-5472.CAN-03-2984.

De Giovanni, C; Nicoletti, G; Palladini, A; Croci, S; Landuzzi, L; Antognoli, A et al. (2009b): A multi-DNA preventive vaccine for p53/Neu-driven cancer syndrome. *Human gene therapy* 20 (5), pp. 453–464. DOI: 10.1089/hum.2008.172.

De Giovanni, C; Nicoletti, G; Quaglino, E; Landuzzi, L; Palladini, A; Ianzano, ML et al. (2014): Vaccines against human HER2 prevent mammary carcinoma in mice transgenic for human HER2. *Breast cancer research : BCR* 16 (1), R10. DOI: 10.1186/bcr3602.

Denies, S; Cicchelerio, L; Polis, I; Sanders, NN (2016): Immunogenicity and safety of xenogeneic vascular endothelial growth factor receptor-2 DNA vaccination in mice and dogs. *Oncotarget* 7 (10), pp. 10905–10916. DOI: 10.18632/oncotarget.7265.

Di Fiore, PP; Pierce, JH; Kraus, MH; Segatto, O; King, CR; Aaronson, SA (1987): erbB-2 is a potent oncogene when overexpressed in NIH/3T3 cells. *Science (New York, N.Y.)* 237 (4811), pp. 178–182. DOI: 10.1126/science.2885917.

Dias, K; Dvorkin-Gheva, A; Hallett, RM; Wu, Y; Hassell, J; Pond, GR et al. (2017): Claudin-Low Breast Cancer; Clinical & Pathological Characteristics. *PloS one* 12 (1), e0168669. DOI: 10.1371/journal.pone.0168669.

Dieci, MV; Barbieri, E; Piacentini, F; Ficarra, G; Bettelli, S; Dominici, M et al. (2013): Discordance in receptor status between primary and recurrent breast cancer has a prognostic impact: a single-institution analysis. *Annals of oncology : official journal of the European Society for Medical Oncology* 24 (1), pp. 101–108. DOI: 10.1093/annonc/mds248.

Dong, Z-Y; Zhong, W-Z; Zhang, X-C; Su, J; Xie, Z; Liu, S-Y et al. (2017): Potential Predictive Value of TP53 and KRAS Mutation Status for Response to PD-1 Blockade Immunotherapy in Lung Adenocarcinoma. *Clinical cancer research : an official journal of the American Association for Cancer Research* 23 (12), pp. 3012–3024. DOI: 10.1158/1078-0432.CCR-16-2554.

Donofrio, G; Tebaldi, G; Lanzardo, S; Ruiu, R; Bolli, E; Ballatore, A et al. (2018): Bovine herpesvirus 4-based vector delivering the full length xCT DNA efficiently protects mice from mammary cancer metastases by targeting cancer stem cells. *Oncoimmunology* 7 (12), e1494108. DOI: 10.1080/2162402X.2018.1494108.

Du, S; McCall, N; Park, K; Guan, Q; Fontina, P; Ertel, A et al. (2018): Blockade of Tumor-Expressed PD-1 promotes lung cancer growth. *Oncoimmunology* 7 (4), e1408747. DOI: 10.1080/2162402X.2017.1408747.

Du Rusquec, P; Calbiac, O de; Robert, M; Campone, M; Frenel, JS (2019): Clinical utility of pembrolizumab in the management of advanced solid tumors: an evidence-based review on the emerging new data. *Cancer management and research* 11, pp. 4297–4312. DOI: 10.2147/CMAR.S151023.

Dulos, J; Carven, GJ; van Boxtel, SJ; Evers, S; Driessen-Engels, LJ; Hobo, W et al. (2012): PD-1 blockade augments Th1 and Th17 and suppresses Th2 responses in peripheral blood from patients with prostate and advanced melanoma cancer. *Journal of immunotherapy (Hagerstown, Md. : 1997)* 35 (2), pp. 169–178. DOI: 10.1097/CJI.0b013e318247a4e7.

El-Kenawy, AE-M; Constantin, C; Hassan, SM; Mostafa, AM; Neves, AF; Araújo, TG de; Neagu, M (2017): Cutaneous Melanoma: Etiology and Therapy. *Nanomedicine in Melanoma: Current Trends and Future Perspectives*. Edited by William H. Ward, Jeffrey M. Farma. Brisbane (AU).

El-Khoueiry, AB; Sangro, B; Yau, T; Crocenzi, TS; Kudo, M; Hsu, C et al. (2017): Nivolumab in patients with advanced hepatocellular carcinoma (CheckMate 040): an open-label, non-comparative, phase 1/2 dose escalation and expansion trial. *Lancet*.

Ellis, MJ; Perou, CM (2013): The genomic landscape of breast cancer as a therapeutic roadmap. *Cancer discovery* 3 (1), pp. 27–34. DOI: 10.1158/2159-8290.CD-12-0462.

Ellis, MJ; Tao, Y; Luo, J; A'Hern, R; Evans, DB; Bhatnagar, AS et al. (2008): Outcome prediction for estrogen receptor-positive breast cancer based on postneoadjuvant endocrine therapy tumor characteristics. *Journal of the National Cancer Institute* 100 (19), pp. 1380–1388. DOI: 10.1093/jnci/djn309.

Elston, CW; Ellis, IO (2002): Pathological prognostic factors in breast cancer. I. The value of histological grade in breast cancer: experience from a large study with long-term follow-up. C. W. Elston & I. O. Ellis. *Histopathology* 1991; 19; 403-410. *Histopathology* 41 (3A), 151-2, discussion 152-3.

Emde, A; Köstler, WJ; Yarden, Y (2012): Therapeutic strategies and mechanisms of tumorigenesis of HER2-overexpressing breast cancer. *Critical reviews in oncology/hematology* 84 Suppl 1, e49-57. DOI: 10.1016/j.critrevonc.2010.09.002.

Eroles, P; Bosch, A; Pérez-Fidalgo, JA; Lluch, A (2012): Molecular biology in breast cancer: intrinsic subtypes and signaling pathways. *Cancer treatment reviews* 38 (6), pp. 698–707. DOI: 10.1016/j.ctrv.2011.11.005.

Escors, D; Gato-Cañas, M; Zuazo, M; Arasanz, H; García-Granda, MJ; Vera, R; Kochan, G (2018): The intracellular signalosome of PD-L1 in cancer cells. *Signal transduction and targeted therapy* 3, p. 26. DOI: 10.1038/s41392-018-0022-9.

Escrivá-de-Romaní, S; Arumí, M; Bellet, M; Saura, C (2018): HER2-positive breast cancer: Current and new therapeutic strategies. *Breast (Edinburgh, Scotland)* 39, pp. 80–88. DOI: 10.1016/j.breast.2018.03.006.

Fan, X; Brezski, RJ; Fa, M; Deng, H; Oberholtzer, A; Gonzalez, A et al. (2012): A single proteolytic cleavage within the lower hinge of trastuzumab reduces immune effector function and in vivo efficacy. *Breast cancer research : BCR* 14 (4), R116. DOI: 10.1186/bcr3240.

Fares, CM; van Allen, EM; Drake, CG; Allison, JP; Hu-Lieskovan, S (2019): Mechanisms of Resistance to Immune Checkpoint Blockade: Why Does Checkpoint Inhibitor Immunotherapy Not Work for All Patients? *American Society of Clinical Oncology educational book. American Society of Clinical Oncology. Annual Meeting* 39, pp. 147–164. DOI: 10.1200/EDBK_240837.

Fattori, E; Sellitto, C; Cappelletti, M; Lazzaro, D; Bellavia, D; Screpanti, I et al. (1995): Functional analysis of IL-6 and IL-6DBP/C/EBP beta by gene targeting. *Annals of the New York Academy of Sciences* 762, pp. 262–273. DOI: 10.1111/j.1749-6632.1995.tb32331.x.

Fehrenbacher, L; Spira, A; Ballinger, M; Kowanetz, M; Vansteenkiste, J; Mazieres, J et al. (2016): Atezolizumab versus docetaxel for patients with previously treated non-small-cell lung cancer (POPLAR): a multicentre, open-label, phase 2 randomised controlled trial. *Lancet*.

Feng, X; Zhang, L; Acharya, C; An, G; Wen, K; Qiu, L et al. (2017): Targeting CD38 Suppresses Induction and Function of T Regulatory Cells to Mitigate Immunosuppression in Multiple Myeloma. *Clinical cancer research : an official journal of the American Association for Cancer Research* 23 (15), pp. 4290–4300. DOI: 10.1158/1078-0432.CCR-16-3192.

Ferrara, R; Mezquita, L; Texier, M; Lahmar, J; Audigier-Valette, C; Tessonier, L et al. (2018): Hyperprogressive Disease in Patients With Advanced Non-Small Cell Lung Cancer Treated With PD-1/PD-L1 Inhibitors or With Single-Agent Chemotherapy. *JAMA oncology* 4 (11), pp. 1543–1552. DOI: 10.1001/jamaoncol.2018.3676.

Ferretti, G; Fabi, A; Felici, A; Papaldo, P (2010): Improved prognosis by trastuzumab of women with HER2-positive breast cancer compared with those with HER2-negative disease. *Journal of clinical oncology : official journal of the American Society of Clinical Oncology* 28 (20), e337; author reply e338-9. DOI: 10.1200/JCO.2010.28.2525.

Ferris, RL; Blumenschein, G; Fayette, J; Guigay, J; Colevas, AD; Licitra, L et al. (2016): Nivolumab for Recurrent Squamous-Cell Carcinoma of the Head and Neck. *N Engl J Med* 375 (19), pp. 1856–1867. DOI: 10.1056/NEJMoa1602252.

Ferris, RL; Licitra, L; Fayette, J; Even, C; Blumenschein, G; Harrington, KJ et al. (2019): Nivolumab in Patients with Recurrent or Metastatic Squamous Cell Carcinoma of the Head and Neck: Efficacy and Safety in CheckMate 141 by Prior Cetuximab Use. *Clinical cancer research : an official journal of the American Association for Cancer Research* 25 (17), pp. 5221–5230. DOI: 10.1158/1078-0432.CCR-18-3944.

Fidler, IJ (1973): Selection of successive tumour lines for metastasis. *Nature: New biology* 242 (118), pp. 148–149. DOI: 10.1038/newbio242148a0.

Fidler, IJ (1983): The Ernst W. Bertner Memorial Award lecture: the evolution of biological heterogeneity in metastatic neoplasms. *Symposium on Fundamental Cancer Research* 36, pp. 5–26.

Fink, MY; Chipuk, JE (2013): Survival of HER2-Positive Breast Cancer Cells: Receptor Signaling to Apoptotic Control Centers. *Genes & cancer* 4 (5-6), pp. 187–195. DOI: 10.1177/1947601913488598.

Finkle, D; Quan, ZR; Asghari, V; Kloss, J; Ghaboosi, N; Mai, E et al. (2004): HER2-targeted therapy reduces incidence and progression of midlife mammary tumors in female murine mammary tumor virus huHER2-transgenic mice. *Clinical cancer research : an official journal of the American Association for Cancer Research* 10 (7), pp. 2499–2511. DOI: 10.1158/1078-0432.ccr-03-0448.

Finn, OJ (2018): A Believer's Overview of Cancer Immunosurveillance and Immunotherapy. *Journal of immunology (Baltimore, Md. : 1950)* 200 (2), pp. 385–391. DOI: 10.4049/jimmunol.1701302.

Foote, JB; Kok, M; Leatherman, JM; Armstrong, TD; Marcinkowski, BC; Ojalvo, LS et al. (2017): A STING Agonist Given with OX40 Receptor and PD-L1 Modulators Primes Immunity and Reduces Tumor Growth in Tolerized Mice. *Cancer immunology research* 5 (6), pp. 468–479. DOI: 10.1158/2326-6066.CIR-16-0284.

Fougner, C; Bergholtz, H; Norum, JH; Sørli, T (2020): Re-definition of claudin-low as a breast cancer phenotype. *Nature communications* 11 (1), p. 1787. DOI: 10.1038/s41467-020-15574-5.

Freudenberg, JA; Wang, Q; Katsumata, M; Drebin, J; Nagatomo, I; Greene, MI (2009): The role of HER2 in early breast cancer metastasis and the origins of resistance to HER2-targeted therapies. *Experimental and molecular pathology* 87 (1), pp. 1–11. DOI: 10.1016/j.yexmp.2009.05.001.

Gajria, D; Chandarlapaty, S (2011): HER2-amplified breast cancer: mechanisms of trastuzumab resistance and novel targeted therapies. *Expert review of anticancer therapy* 11 (2), pp. 263–275. DOI: 10.1586/era.10.226.

Gall, VA; Philips, AV; Qiao, N; Clise-Dwyer, K; Perakis, AA; Zhang, M et al. (2017): Trastuzumab Increases HER2 Uptake and Cross-Presentation by Dendritic Cells. *Cancer research* 77 (19), pp. 5374–5383. DOI: 10.1158/0008-5472.CAN-16-2774.

Garcia-Diaz, A; Shin, DS; Moreno, BH; Saco, J; Escuin-Ordinas, H; Rodriguez, GA et al. (2017): Interferon Receptor Signaling Pathways Regulating PD-L1 and PD-L2 Expression. *Cell reports* 19 (6), pp. 1189–1201. DOI: 10.1016/j.celrep.2017.04.031.

Garrett, JT; Arteaga, CL (2011): Resistance to HER2-directed antibodies and tyrosine kinase inhibitors: mechanisms and clinical implications. *Cancer biology & therapy* 11 (9), pp. 793–800. DOI: 10.4161/cbt.11.9.15045.

Garrett, TPJ; McKern, NM; Lou, M; Elleman, TC; Adams, TE; Lovrecz, GO et al. (2002): Crystal Structure of a Truncated Epidermal Growth Factor Receptor Extracellular Domain Bound to Transforming Growth Factor α . *Cell* 110 (6), pp. 763–773. DOI: 10.1016/S0092-8674(02)00940-6.

Garrett, TPJ; McKern, NM; Lou, M; Elleman, TC; Adams, TE; Lovrecz, GO et al. (2003): The Crystal Structure of a Truncated ErbB2 Ectodomain Reveals an Active Conformation, Poised to Interact with Other ErbB Receptors. *Molecular Cell* 11 (2), pp. 495–505. DOI: 10.1016/s1097-2765(03)00048-0.

Gates, JD; Clifton, GT; Benavides, LC; Sears, AK; Carmichael, MG; Hueman, MT et al. (2010): Circulating regulatory T cells (CD4+CD25+FOXP3+) decrease in breast cancer patients after vaccination with a modified MHC class II HER2/neu (AE37) peptide. *Vaccine* 28 (47), pp. 7476–7482. DOI: 10.1016/j.vaccine.2010.09.029.

Gato-Cañas, M; Martinez de Morentin, X; Blanco-Luquin, I; Fernandez-Irigoyen, J; Zudaire, I; Liechtenstein, T et al. (2015): A core of kinase-regulated interactomes defines the neoplastic MDSC lineage. *Oncotarget* 6 (29), pp. 27160–27175. DOI: 10.18632/oncotarget.4746.

Gato-Cañas, M; Zuazo, M; Arasanz, H; Ibañez-Vea, M; Lorenzo, L; Fernandez-Hinojal, G et al. (2017): PDL1 Signals through Conserved Sequence Motifs to Overcome Interferon-Mediated Cytotoxicity. *Cell reports* 20 (8), pp. 1818–1829. DOI: 10.1016/j.celrep.2017.07.075.

Gauci, M-L; Lanoy, E; Champiat, S; Caramella, C; Ammari, S; Aspeslagh, S et al. (2019): Long-Term Survival in Patients Responding to Anti-PD-1/PD-L1 Therapy and Disease Outcome upon Treatment Discontinuation. *Clinical cancer research : an official journal of*

the American Association for Cancer Research 25 (3), pp. 946–956. DOI: 10.1158/1078-0432.CCR-18-0793.

Geenen, V (2012): The appearance of the thymus and the integrated evolution of adaptive immune and neuroendocrine systems. *Acta clinica Belgica* 67 (3), pp. 209–213. DOI: 10.2143/ACB.67.3.2062657.

Gennari, R; Menard, S; Fagnoni, F; Ponchio, L; Scelsi, M; Tagliabue, E et al. (2004): Pilot study of the mechanism of action of preoperative trastuzumab in patients with primary operable breast tumors overexpressing HER2. *Clinical cancer research : an official journal of the American Association for Cancer Research* 10 (17), pp. 5650–5655. DOI: 10.1158/1078-0432.CCR-04-0225.

Gerlinger, M; Rowan, AJ; Horswell, S; Math, M; Larkin, J; Endesfelder, D et al. (2012): Intratumor heterogeneity and branched evolution revealed by multiregion sequencing. *The New England journal of medicine* 366 (10), pp. 883–892. DOI: 10.1056/NEJMoa1113205.

Ghosh, R; Narasanna, A; Wang, SE; Liu, S; Chakrabarty, A; Balko, JM et al. (2011): Trastuzumab has preferential activity against breast cancers driven by HER2 homodimers. *Cancer research* 71 (5), pp. 1871–1882. DOI: 10.1158/0008-5472.CAN-10-1872.

Gianni, L; Dafni, U; Gelber, RD; Azambuja, E; Muehlbauer, S; Goldhirsch, A et al. (2011): Treatment with trastuzumab for 1 year after adjuvant chemotherapy in patients with HER2-positive early breast cancer: a 4-year follow-up of a randomised controlled trial. *The Lancet Oncology* 12 (3), pp. 236–244. DOI: 10.1016/S1470-2045(11)70033-X.

Giavazzi, R; Decio, A (2014): Syngeneic murine metastasis models: B16 melanoma. *Methods in molecular biology (Clifton, N.J.)* 1070, pp. 131–140. DOI: 10.1007/978-1-4614-8244-4_10;

Giovarelli, M; Musiani, P; Modesti, A; Dellabona, P; Casorati, G; Allione, A et al. (1995): Local release of IL-10 by transfected mouse mammary adenocarcinoma cells does not suppress but enhances antitumor reaction and elicits a strong cytotoxic lymphocyte and antibody-dependent immune memory. *Journal of immunology (Baltimore, Md. : 1950)* 155 (6), pp. 3112–3123.

Goldhirsch, A; Wood, WC; Coates, AS; Gelber, RD; Thürlimann, B; Senn, H-J (2011): Strategies for subtypes--dealing with the diversity of breast cancer: highlights of the St. Gallen International Expert Consensus on the Primary Therapy of Early Breast Cancer 2011. *Annals of oncology : official journal of the European Society for Medical Oncology* 22 (8), pp. 1736–1747. DOI: 10.1093/annonc/mdr304.

Gonzalez-Angulo, AM; Stemke-Hale, K; Palla, SL; Carey, M; Agarwal, R; Meric-Berstam, F et al. (2009): Androgen receptor levels and association with PIK3CA mutations and prognosis in breast cancer. *Clinical cancer research : an official journal of the American Association for Cancer Research* 15 (7), pp. 2472–2478. DOI: 10.1158/1078-0432.CCR-08-1763.

Graus-Porta, D; Beerli, RR; Daly, JM; Hynes, NE (1997): ErbB-2, the preferred heterodimerization partner of all ErbB receptors, is a mediator of lateral signaling. *The EMBO journal* 16 (7), pp. 1647–1655. DOI: 10.1093/emboj/16.7.1647.

Guarneri, V; Frassoldati, A; Bottini, A; Cagossi, K; Bisagni, G; Sarti, S et al. (2012): Preoperative chemotherapy plus trastuzumab, lapatinib, or both in human epidermal growth factor receptor 2-positive operable breast cancer: results of the randomized phase II CHER-LOB study. *Journal of clinical oncology : official journal of the American Society of Clinical Oncology* 30 (16), pp. 1989–1995. DOI: 10.1200/JCO.2011.39.0823.

Guy, CT; Cardiff, RD; Muller, WJ (1992): Induction of mammary tumors by expression of polyomavirus middle T oncogene: a transgenic mouse model for metastatic disease. *Molecular and cellular biology* 12 (3), pp. 954–961. DOI: 10.1128/mcb.12.3.954.

Hamaguchi, Y; Hasegawa, M; Fujimoto, M; Matsushita, T; Komura, K; Kaji, K et al. (2008): The clinical relevance of serum antinuclear antibodies in Japanese patients with systemic sclerosis. *The British journal of dermatology* 158 (3), pp. 487–495. DOI: 10.1111/j.1365-2133.2007.08392.x.

Hanahan, D; Weinberg, RA (2011): Hallmarks of cancer: the next generation. *Cell* 144 (5), pp. 646–674. DOI: 10.1016/j.cell.2011.02.013.

Harao, M; Mittendorf, EA; Radvanyi, LG (2015): Peptide-based vaccination and induction of CD8+ T-cell responses against tumor antigens in breast cancer. *BioDrugs : clinical immunotherapeutics, biopharmaceuticals and gene therapy* 29 (1), pp. 15–30. DOI: 10.1007/s40259-014-0114-1.

Harris, LN; You, F; Schnitt, SJ; Witkiewicz, A; Lu, X; Sgroi, D et al. (2007): Predictors of resistance to preoperative trastuzumab and vinorelbine for HER2-positive early breast cancer. *Clinical cancer research : an official journal of the American Association for Cancer Research* 13 (4), pp. 1198–1207. DOI: 10.1158/1078-0432.CCR-06-1304.

Hennigs, A; Riedel, F; Gondos, A; Sinn, P; Schirmacher, P; Marmé, F et al. (2016): Prognosis of breast cancer molecular subtypes in routine clinical care: A large prospective cohort study. *BMC cancer* 16 (1), p. 734. DOI: 10.1186/s12885-016-2766-3.

Herbst, RS; Baas, P; Kim, D-W; Felip, E; Pérez-Gracia, JL; Han, J-Y et al. (2016): Pembrolizumab versus docetaxel for previously treated, PD-L1-positive, advanced non-small-cell lung cancer (KEYNOTE-010): a randomised controlled trial. *Lancet*.

Hodi, FS; Butler, M; Oble, DA; Seiden, MV; Haluska, FG; Kruse, A et al. (2008): Immunologic and clinical effects of antibody blockade of cytotoxic T lymphocyte-associated antigen 4 in previously vaccinated cancer patients. *Proceedings of the National Academy of Sciences of the United States of America* 105 (8), pp. 3005–3010. DOI: 10.1073/pnas.0712237105.

Hodi, FS; Chesney, J; Pavlick, AC; Robert, C; Grossmann, KF; McDermott, DF et al. (2016): Combined nivolumab and ipilimumab versus ipilimumab alone in patients with advanced melanoma: 2-year overall survival outcomes in a multicentre, randomised, controlled, phase 2 trial. *Lancet oncology* 17 (11), pp. 1558–1568. DOI: 10.1016/S1470-2045(16)30366-7.

Hodi, FS; O'Day, SJ; McDermott, DF; Weber, RW; Sosman, JA; Haanen, JB et al. (2010): Improved survival with ipilimumab in patients with metastatic melanoma. *The New England journal of medicine* 363 (8), pp. 711–723. DOI: 10.1056/NEJMoa1003466.

Hollier, BG; Tinnirello, AA; Werden, SJ; Evans, KW; Taube, JH; Sarkar, TR et al. (2013): FOXC2 expression links epithelial-mesenchymal transition and stem cell properties in breast cancer. *Cancer research* 73 (6), pp. 1981–1992. DOI: 10.1158/0008-5472.CAN-12-2962.

Hu, X; Deng, Y; Chen, X; Zhou, Y; Zhang, H; Wu, H et al. (2017): Immune Response of A Novel ATR-AP205-001 Conjugate Anti-hypertensive Vaccine. *Scientific reports* 7 (1), p. 12580. DOI: 10.1038/s41598-017-12996-y.

Hu, Z; Fan, C; Oh, DS; Marron, JS; He, X; Qaqish, BF et al. (2006): The molecular portraits of breast tumors are conserved across microarray platforms. *BMC genomics* 7, p. 96. DOI: 10.1186/1471-2164-7-96.

Huang, R-Y; Francois, A; McGray, AR; Miliotto, A; Odunsi, K (2017): Compensatory upregulation of PD-1, LAG-3, and CTLA-4 limits the efficacy of single-agent checkpoint blockade in metastatic ovarian cancer. *Oncoimmunology* 6 (1), e1249561. DOI: 10.1080/2162402X.2016.1249561.

Hudziak, RM; Schlessinger, J; Ullrich, A (1987): Increased expression of the putative growth factor receptor p185HER2 causes transformation and tumorigenesis of NIH 3T3 cells. *Proceedings of the National Academy of Sciences of the United States of America* 84 (20), pp. 7159–7163. DOI: 10.1073/pnas.84.20.7159.

- Hwang, K-T; Kim, K; Chang, JH; Oh, S; Kim, YA; Lee, JY et al. (2018): BCL2 Regulation according to Molecular Subtype of Breast Cancer by Analysis of The Cancer Genome Atlas Database. *Cancer research and treatment : official journal of Korean Cancer Association* 50 (3), pp. 658–669. DOI: 10.4143/crt.2017.134.
- Ianzano, ML; Croci, S; Nicoletti, G; Palladini, A; Landuzzi, L; Grosso, V et al. (2014): Tumor suppressor genes promote rhabdomyosarcoma progression in p53 heterozygous, HER-2/neu transgenic mice. *Oncotarget* 5 (1), pp. 108–119. DOI: 10.18632/oncotarget.1171.
- Ibrahim, EM; Kazkaz, GA; Al-Mansour, MM; Al-Foheidi, ME (2015): The predictive and prognostic role of phosphatase phosphoinositol-3 (PI3) kinase (PIK3CA) mutation in HER2-positive breast cancer receiving HER2-targeted therapy: a meta-analysis. *Breast cancer research and treatment* 152 (3), pp. 463–476. DOI: 10.1007/s10549-015-3480-6.
- Ignatov, T; Gorbunow, F; Eggemann, H; Ortmann, O; Ignatov, A (2019): Loss of HER2 after HER2-targeted treatment. *Breast cancer research and treatment* 175 (2), pp. 401–408. DOI: 10.1007/s10549-019-05173-4.
- Iqbal, N; Iqbal, N (2014): Human Epidermal Growth Factor Receptor 2 (HER2) in Cancers: Overexpression and Therapeutic Implications. *Molecular biology international* 2014, p. 852748. DOI: 10.1155/2014/852748.
- Iwai, Y; Ishida, M; Tanaka, Y; Okazaki, T; Honjo, T; Minato, N (2002): Involvement of PD-L1 on tumor cells in the escape from host immune system and tumor immunotherapy by PD-L1 blockade. *Proceedings of the National Academy of Sciences of the United States of America* 99 (19), pp. 12293–12297. DOI: 10.1073/pnas.192461099.
- Jacks, T; Jaffee, E; Singer, D (2016): Cancer Moonshot Blue Ribbon Panel Report 2016. National Cancer Advisory Board, 2016.
- Jackson, C; Browell, D; Gautrey, H; Tyson-Capper, A (2013): Clinical Significance of HER-2 Splice Variants in Breast Cancer Progression and Drug Resistance. *International journal of cell biology* 2013, p. 973584. DOI: 10.1155/2013/973584.
- Jackson, HW; Fischer, JR; Zanutelli, VR; Ali, HR; Mechera, R; Soysal, SD et al. (2020): The single-cell pathology landscape of breast cancer. *Nature* 578 (7796), pp. 615–620. DOI: 10.1038/s41586-019-1876-x.
- Jechlinger, M; Sommer, A; Moriggl, R; Seither, P; Kraut, N; Capodiecci, P et al. (2006): Autocrine PDGFR signaling promotes mammary cancer metastasis. *The Journal of clinical investigation* 116 (6), pp. 1561–1570. DOI: 10.1172/JCI24652.

Jenkins, RW; Barbie, DA; Flaherty, KT (2018): Mechanisms of resistance to immune checkpoint inhibitors. *Br J Cancer* 118 (1), pp. 9–16. DOI: 10.1038/bjc.2017.434.

Jenndahl, LE; Isakson, P; Baeckström, D (2005): c-erbB2-induced epithelial-mesenchymal transition in mammary epithelial cells is suppressed by cell-cell contact and initiated prior to E-cadherin downregulation. *International journal of oncology* 27 (2), pp. 439–448.

Jennings, GT; Bachmann, MF (2009): Immunodrugs: therapeutic VLP-based vaccines for chronic diseases. *Annual review of pharmacology and toxicology* 49, pp. 303–326. DOI: 10.1146/annurev-pharmtox-061008-103129.

Jin, B-R; Kim, S-J; Lee, J-M; Kang, S-H; Han, H-J; Jang, Y-S et al. (2013): Alum Directly Modulates Murine B Lymphocytes to Produce IgG1 Isotype. *Immune network* 13 (1), pp. 10–15. DOI: 10.4110/in.2013.13.1.10.

Joura, EA; Giuliano, AR; Iversen, O-E; Bouchard, C; Mao, C; Mehlsen, J et al. (2015): A 9-valent HPV vaccine against infection and intraepithelial neoplasia in women. *The New England journal of medicine* 372 (8), pp. 711–723. DOI: 10.1056/NEJMoa1405044.

Junttila, TT; Akita, RW; Parsons, K; Fields, C; Lewis Phillips, GD; Friedman, LS et al. (2009): Ligand-independent HER2/HER3/PI3K complex is disrupted by trastuzumab and is effectively inhibited by the PI3K inhibitor GDC-0941. *Cancer cell* 15 (5), pp. 429–440. DOI: 10.1016/j.ccr.2009.03.020.

Juric, D; Castel, P; Griffith, M; Griffith, OL; Won, HH; Ellis, H et al. (2015): Convergent loss of PTEN leads to clinical resistance to a PI(3)K α inhibitor. *Nature* 518 (7538), pp. 240–244. DOI: 10.1038/nature13948.

Kamada, T; Togashi, Y; Tay, C; Ha, D; Sasaki, A; Nakamura, Y et al. (2019): PD-1+ regulatory T cells amplified by PD-1 blockade promote hyperprogression of cancer. *Proceedings of the National Academy of Sciences of the United States of America* 116 (20), pp. 9999–10008. DOI: 10.1073/pnas.1822001116;

Kancha, RK; Bubnoff, N von; Bartosch, N; Peschel, C; Engh, RA; Duyster, J (2011): Differential sensitivity of ERBB2 kinase domain mutations towards lapatinib. *PloS one* 6 (10), e26760. DOI: 10.1371/journal.pone.0026760.

Kas, B; Talbot, H; Ferrara, R; Richard, C; Lamarque, J-P; Pitre-Champagnat, S et al. (2020): Clarification of Definitions of Hyperprogressive Disease During Immunotherapy for Non-Small Cell Lung Cancer. *JAMA oncology* 6 (7), pp. 1039–1046. DOI: 10.1001/jamaoncol.2020.1634.

Kast, RE (2017): Postoperative capecitabine in breast cancer neoadjuvant failures. *Transl. Cancer Res* 6 (S9), S1446-S1447. DOI: 10.21037/tcr.2017.10.52.

Kato, S; Goodman, A; Walavalkar, V; Barkauskas, DA; Sharabi, A; Kurzrock, R (2017): Hyperprogressors after Immunotherapy: Analysis of Genomic Alterations Associated with Accelerated Growth Rate. *Clinical cancer research : an official journal of the American Association for Cancer Research* 23 (15), pp. 4242–4250. DOI: 10.1158/1078-0432.CCR-16-3133.

Kaumaya, PT; Guo, L; Overholser, J; Penichet, ML; Bekaii-Saab, T (2020): Immunogenicity and antitumor efficacy of a novel human PD-1 B-cell vaccine (PD1-Vaxx) and combination immunotherapy with dual trastuzumab/pertuzumab-like HER-2 B-cell epitope vaccines (B-Vaxx) in a syngeneic mouse model. *Oncoimmunology* 9 (1), p. 1818437. DOI: 10.1080/2162402X.2020.1818437.

Keir, ME; Butte, MJ; Freeman, GJ; Sharpe, AH (2008): PD-1 and its ligands in tolerance and immunity. *Annual review of immunology* 26, pp. 677–704. DOI: 10.1146/annurev.immunol.26.021607.090331.

Kipps, TJ; Parham, P; Punt, J; Herzenberg, LA (1985): Importance of immunoglobulin isotype in human antibody-dependent, cell-mediated cytotoxicity directed by murine monoclonal antibodies. *The Journal of experimental medicine* 161 (1), pp. 1–17. DOI: 10.1084/jem.161.1.1.

Kleffel, S; Posch, C; Barthel, SR; Mueller, H; Schlapbach, C; Guenova, E et al. (2015): Melanoma Cell-Intrinsic PD-1 Receptor Functions Promote Tumor Growth. *Cell* 162 (6), pp. 1242–1256. DOI: 10.1016/j.cell.2015.08.052.

Konecny, GE; Pegram, MD; Venkatesan, N; Finn, R; Yang, G; Rahmeh, M et al. (2006): Activity of the dual kinase inhibitor lapatinib (GW572016) against HER-2-overexpressing and trastuzumab-treated breast cancer cells. *Cancer research* 66 (3), pp. 1630–1639. DOI: 10.1158/0008-5472.CAN-05-1182.

Konieczkowski, DJ; Johannessen, CM; Garraway, LA (2018): A Convergence-Based Framework for Cancer Drug Resistance. *Cancer cell* 33 (5), pp. 801–815. DOI: 10.1016/j.ccell.2018.03.025.

Kotiyal, S; Bhattacharya, S (2014): Breast cancer stem cells, EMT and therapeutic targets. *Biochemical and biophysical research communications* 453 (1), pp. 112–116. DOI: 10.1016/j.bbrc.2014.09.069.

Koutras, AK; Starakis, I; Lymperatou, D; Kalofonos, HP (2012): Angiogenesis as a therapeutic target in breast cancer. *Mini reviews in medicinal chemistry* 12 (12), pp. 1230–1238. DOI: 10.2174/138955712802761988.

Koyama, S; Akbay, EA; Li, YY; Herter-Sprie, GS; Buczkowski, KA; Richards, WG et al. (2016): Adaptive resistance to therapeutic PD-1 blockade is associated with

upregulation of alternative immune checkpoints. *Nature communications* 7, p. 10501. DOI: 10.1038/ncomms10501.

Kwak, EL; Ahronian, LG; Siravegna, G; Mussolin, B; Borger, DR; Godfrey, JT et al. (2015): Molecular Heterogeneity and Receptor Coamplification Drive Resistance to Targeted Therapy in MET-Amplified Esophagogastric Cancer. *Cancer discovery* 5 (12), pp. 1271–1281. DOI: 10.1158/2159-8290.CD-15-0748.

Kwong, KY; Hung, MC (1998): A novel splice variant of HER2 with increased transformation activity. *Molecular carcinogenesis* 23 (2), pp. 62–68. DOI: 10.1002/(sici)1098-2744(199810)23:2<62::aid-mc2>3.0.co;2-o.

Labidi, S; Mejri, N; Lagha, A; Daoud, N; El Benna, H; Afrit, M; Boussen, H (2016): Targeted Therapies in HER2-Overexpressing Metastatic Breast Cancer. *Breast care (Basel, Switzerland)* 11 (6), pp. 418–422. DOI: 10.1159/000452194.

Lakhani; Ellis, JO; Schnitt, Stuart J; Tan, Puay Hoon; Van de Vijve, Marc J (2012): WHO/IARC Classification of Tumours of the Breast. *International Agency for Research on Cancer Publications*.

Lamberti, G; Andrini, E; Sisi, M; Rizzo, A; Parisi, C; Di Federico, A et al. (2020a): Beyond EGFR, ALK and ROS1: Current evidence and future perspectives on newly targetable oncogenic drivers in lung adenocarcinoma. *Critical reviews in oncology/hematology* 156, p. 103119. DOI: 10.1016/j.critrevonc.2020.103119.

Lamberti, G; Sisi, M; Andrini, E; Palladini, A; Giunchi, F; Lollini, P-L et al. (2020b): The Mechanisms of PD-L1 Regulation in Non-Small-Cell Lung Cancer (NSCLC): Which Are the Involved Players? *Cancers* 12 (11), p. 3129. DOI: 10.3390/cancers12113129.

Lamichhane, P; Karyampudi, L; Shreeder, B; Krempski, J; Bahr, D; Daum, J et al. (2017): IL10 Release upon PD-1 Blockade Sustains Immunosuppression in Ovarian Cancer. *Cancer research* 77 (23), pp. 6667–6678. DOI: 10.1158/0008-5472.CAN-17-0740.

Landuzzi, L; Palladini, A; Ceccarelli, C; Asioli, S; Nicoletti, G; Giusti, V et al. (2021): Early stability and late random tumor progression of a HER2-positive primary breast cancer patient-derived xenograft. *Sci Rep* 11 (1), p. 1563. DOI: 10.1038/s41598-021-81085-y.

Langenkamp, E; Molema, G (2009): Microvascular endothelial cell heterogeneity: general concepts and pharmacological consequences for anti-angiogenic therapy of cancer. *Cell and tissue research* 335 (1), pp. 205–222. DOI: 10.1007/s00441-008-0642-4.

Lanzardo, S; Conti, L; Rooke, R; Ruiu, R; Accart, N; Bolli, E et al. (2016): Immunotargeting of Antigen xCT Attenuates Stem-like Cell Behavior and Metastatic

Progression in Breast Cancer. *Cancer research* 76 (1), pp. 62–72. DOI: 10.1158/0008-5472.CAN-15-1208.

Larkin, J; Chiarion-Sileni, V; Gonzalez, R; Grob, JJ; Cowey, CL; Lao, CD et al. (2015): Combined Nivolumab and Ipilimumab or monotherapy in untreated melanoma. *The New England journal of medicine*.

Larkin, J; Minor, D; D'Angelo, S; Neyns, B; Smylie, M; Miller, WH et al. (2018): Overall Survival in Patients With Advanced Melanoma Who Received Nivolumab Versus Investigator's Choice Chemotherapy in CheckMate 037: A Randomized, Controlled, Open-Label Phase III Trial. *JCO* 36 (4), pp. 383–390. DOI: 10.1200/JCO.2016.71.8023.

Latchman, Y; Wood, CR; Chernova, T; Chaudhary, D; Borde, M; Chernova, I et al. (2001): PD-L2 is a second ligand for PD-1 and inhibits T cell activation. *Nat Immunol* 2 (3), pp. 261–268. DOI: 10.1038/85330.

Latta, EK; Tjan, S; Parkes, RK; O'Malley, FP (2002): The role of HER2/neu overexpression/amplification in the progression of ductal carcinoma in situ to invasive carcinoma of the breast. *Modern pathology : an official journal of the United States and Canadian Academy of Pathology, Inc* 15 (12), pp. 1318–1325. DOI: 10.1097/01.MP.0000038462.62634.B1.

Le, DT; Durham, JN; Smith, KN; Wang, H; Bartlett, BR; Aulakh, LK et al. (2017): Mismatch repair deficiency predicts response of solid tumors to PD-1 blockade. *Science (New York, N.Y.)* 357 (6349), pp. 409–413. DOI: 10.1126/science.aan6733.

Lee, J; Ahn, E; Kissick, HT; Ahmed, R (2015a): Reinvigorating Exhausted T Cells by Blockade of the PD-1 Pathway. *Forum on immunopathological diseases and therapeutics* 6 (1-2), pp. 7–17. DOI: 10.1615/ForumImmunDisTher.2015014188.

Lee, JC; Vivanco, I; Beroukhi, R; Huang, JH; Feng, WL; DeBiasi, RM et al. (2006): Epidermal growth factor receptor activation in glioblastoma through novel missense mutations in the extracellular domain. *PLoS medicine* 3 (12), e485. DOI: 10.1371/journal.pmed.0030485.

Lee, S-H; Danishmalik, SN; Sin, J-I (2015b): DNA vaccines, electroporation and their applications in cancer treatment. *Human vaccines & immunotherapeutics* 11 (8), pp. 1889–1900. DOI: 10.1080/21645515.2015.1035502.

Lewis Phillips, GD; Li, G; Dugger, DL; Crocker, LM; Parsons, KL; Mai, E et al. (2008): Targeting HER2-positive breast cancer with trastuzumab-DM1, an antibody-cytotoxic drug conjugate. *Cancer research* 68 (22), pp. 9280–9290. DOI: 10.1158/0008-5472.CAN-08-1776.

- Linch, SN; Kasiewicz, MJ; McNamara, MJ; Hilgart-Martiszus, IF; Farhad, M; Redmond, WL (2016): Combination OX40 agonism/CTLA-4 blockade with HER2 vaccination reverses T-cell anergy and promotes survival in tumor-bearing mice. *Proceedings of the National Academy of Sciences of the United States of America* 113 (3), E319–27. DOI: 10.1073/pnas.1510518113.
- Lino, CA; Caldeira, JC; Peabody, DS (2017): Display of single-chain variable fragments on bacteriophage MS2 virus-like particles. *Journal of nanobiotechnology* 15 (1), p. 13. DOI: 10.1186/s12951-016-0240-7.
- Liu, E; Thor, A; He, M; Barcos, M; Ljung, BM; Benz, C (1992): The HER2 (c-erbB-2) oncogene is frequently amplified in in situ carcinomas of the breast. *Oncogene* 7 (5), pp. 1027–1032.
- Liu, Y; Cheng, Y; Xu, Y; Wang, Z; Du, X; Li, C et al. (2017): Increased expression of programmed cell death protein 1 on NK cells inhibits NK-cell-mediated anti-tumor function and indicates poor prognosis in digestive cancers. *Oncogene* 36 (44), pp. 6143–6153. DOI: 10.1038/onc.2017.209.
- Lluch, A; González-Angulo, AM; Casadevall, D; Eterovic, AK; Martínez de Dueñas, E; Zheng, X et al. (2019): Dynamic clonal remodelling in breast cancer metastases is associated with subtype conversion. *European journal of cancer (Oxford, England : 1990)* 120, pp. 54–64. DOI: 10.1016/j.ejca.2019.07.003.
- Lo Russo, G; Moro, M; Sommariva, M; Cancila, V; Boeri, M; Centonze, G et al. (2019): Antibody-Fc/FcR Interaction on Macrophages as a Mechanism for Hyperprogressive Disease in Non-small Cell Lung Cancer Subsequent to PD-1/PD-L1 Blockade. *Clinical cancer research : an official journal of the American Association for Cancer Research* 25 (3), pp. 989–999. DOI: 10.1158/1078-0432.CCR-18-1390.
- Loi, S; Azambuja, E de; Pugliano, L; Sotiriou, C; Piccart, MJ (2011): HER2-overexpressing breast cancer: time for the cure with less chemotherapy? *Current opinion in oncology* 23 (6), pp. 547–558. DOI: 10.1097/CCO.0b013e32834bd4c9.
- Loi, S; Sirtaine, N; Piette, F; Salgado, R; Viale, G; van Eeno, F et al. (2013): Prognostic and predictive value of tumor-infiltrating lymphocytes in a phase III randomized adjuvant breast cancer trial in node-positive breast cancer comparing the addition of docetaxel to doxorubicin with doxorubicin-based chemotherapy: BIG 02-98. *Journal of clinical oncology : official journal of the American Society of Clinical Oncology* 31 (7), pp. 860–867. DOI: 10.1200/JCO.2011.41.0902.
- Lollini, P-L; Cavallo, F; Nanni, P; Forni, G (2006): Vaccines for tumour prevention. *Nature reviews. Cancer* 6 (3), pp. 204–216. DOI: 10.1038/nrc1815.

- Lollini, P-L; Cavallo, F; Nanni, P; Quaglino, E (2015): The Promise of Preventive Cancer Vaccines. *Vaccines* 3 (2), pp. 467–489. DOI: 10.3390/vaccines3020467.
- Lollini, P-L; Nicoletti, G; Landuzzi, L; Cavallo, F; Forni, G; Giovanni, C de; Nanni, P (2011): Vaccines and other immunological approaches for cancer immunoprevention. *Current drug targets* 12 (13), pp. 1957–1973. DOI: 10.2174/138945011798184146.
- Lollini, P-L; Nicoletti, G; Landuzzi, L; Giovanni, C de; Nanni, P (2010): Immunoprevention and immunotherapy of mammary carcinoma. *The breast journal* 16 Suppl 1, S39-41. DOI: 10.1111/j.1524-4741.2010.01002.x.
- Lu, L; Yan, H; Shyam-Sundar, V; Janowitz, T (2014): Cross-sectional and longitudinal analysis of cancer vaccination trials registered on the US Clinical Trials Database demonstrates paucity of immunological trial endpoints and decline in registration since 2008. *Drug design, development and therapy* 8, pp. 1539–1553. DOI: 10.2147/DDDT.S65963.
- Magi, S; Iwamoto, K; Yumoto, N; Hiroshima, M; Nagashima, T; Ohki, R et al. (2018): Transcriptionally inducible Pleckstrin homology-like domain, family A, member 1, attenuates ErbB receptor activity by inhibiting receptor oligomerization. *The Journal of biological chemistry* 293 (6), pp. 2206–2218. DOI: 10.1074/jbc.M117.778399.
- Marchini, C; Gabrielli, F; Iezzi, M; Zenobi, S; Montani, M; Pietrella, L et al. (2011): The human splice variant Δ 16HER2 induces rapid tumor onset in a reporter transgenic mouse. *PloS one* 6 (4), e18727. DOI: 10.1371/journal.pone.0018727.
- Marchiò, C; Annaratone, L; Marques, A; Casorzo, L; Berrino, E; Sapino, A (2020): Evolving concepts in HER2 evaluation in breast cancer: Heterogeneity, HER2-low carcinomas and beyond. *Seminars in cancer biology*. DOI: 10.1016/j.semcancer.2020.02.016.
- Marmé, F (2016): Immunotherapy in Breast Cancer. *Oncology research and treatment* 39 (6), pp. 335–345. DOI: 10.1159/000446340.
- Meng, F; Speyer, CL; Zhang, B; Zhao, Y; Chen, W; Gorski, DH et al. (2015): PDGFR α and β play critical roles in mediating Foxq1-driven breast cancer stemness and chemoresistance. *Cancer research* 75 (3), pp. 584–593. DOI: 10.1158/0008-5472.CAN-13-3029.
- Menzies, AM; Haydu, LE; Carlino, MS; Azer, MW; Carr, PJ; Kefford, RF; Long, GV (2014): Inter- and intra-patient heterogeneity of response and progression to targeted therapy in metastatic melanoma. *PloS one* 9 (1), e85004. DOI: 10.1371/journal.pone.0085004.

Mimura, K; Kono, K; Hanawa, M; Mitsui, F; Sugai, H; Miyagawa, N et al. (2005): Frequencies of HER-2/neu expression and gene amplification in patients with oesophageal squamous cell carcinoma. *British journal of cancer* 92 (7), pp. 1253–1260. DOI: 10.1038/sj.bjc.6602499.

Minckwitz, G von; Procter, M; Azambuja, E de; Zardavas, D; Benyunes, M; Viale, G et al. (2017): Adjuvant Pertuzumab and Trastuzumab in Early HER2-Positive Breast Cancer. *The New England journal of medicine* 377 (2), pp. 122–131. DOI: 10.1056/NEJMoa1703643.

Mitra, D; Brumlik, MJ; Okamgba, SU; Zhu, Y; Duplessis, TT; Parvani, JG et al. (2009): An oncogenic isoform of HER2 associated with locally disseminated breast cancer and trastuzumab resistance. *Molecular cancer therapeutics* 8 (8), pp. 2152–2162. DOI: 10.1158/1535-7163.MCT-09-0295.

Mittendorf, EA; Clifton, GT; Holmes, JP; Clive, KS; Patil, R; Benavides, LC et al. (2012): Clinical trial results of the HER-2/neu (E75) vaccine to prevent breast cancer recurrence in high-risk patients: from US Military Cancer Institute Clinical Trials Group Study I-01 and I-02. *Cancer* 118 (10), pp. 2594–2602. DOI: 10.1002/cncr.26574.

Moasser, MM (2007): The oncogene HER2: its signaling and transforming functions and its role in human cancer pathogenesis. *Oncogene* 26 (45), pp. 6469–6487. DOI: 10.1038/sj.onc.1210477.

Mohsen, MO; Gomes, AC; Vogel, M; Bachmann, MF (2018): Interaction of Viral Capsid-Derived Virus-Like Particles (VLPs) with the Innate Immune System. *Vaccines* 6 (3). DOI: 10.3390/vaccines6030037.

Molina, MA; Sáez, R; Ramsey, EE; Garcia-Barchino, M-J; Rojo, F; Evans, AJ et al. (2002): NH(2)-terminal truncated HER-2 protein but not full-length receptor is associated with nodal metastasis in human breast cancer. *Clinical cancer research : an official journal of the American Association for Cancer Research* 8 (2), pp. 347–353.

Moreb, JS; Ucar, D; Han, S; Amory, JK; Goldstein, AS; Ostmark, B; Chang, L-J (2012): The enzymatic activity of human aldehyde dehydrogenases 1A2 and 2 (ALDH1A2 and ALDH2) is detected by Aldefluor, inhibited by diethylaminobenzaldehyde and has significant effects on cell proliferation and drug resistance. *Chemico-biological interactions* 195 (1), pp. 52–60. DOI: 10.1016/j.cbi.2011.10.007.

Morganella, S; Alexandrov, LB; Glodzik, D; Zou, X; Davies, H; Staaf, J et al. (2016): The topography of mutational processes in breast cancer genomes. *Nature communications* 7, p. 11383. DOI: 10.1038/ncomms11383.

Morrison, C; Zanagnolo, V; Ramirez, N; Cohn, DE; Kelbick, N; Copeland, L et al. (2006): HER-2 is an independent prognostic factor in endometrial cancer: association with outcome in a large cohort of surgically staged patients. *Journal of clinical oncology : official journal of the American Society of Clinical Oncology* 24 (15), pp. 2376–2385. DOI: 10.1200/JCO.2005.03.4827.

Mortenson, ED; Park, S; Jiang, Z; Wang, S; Fu, Y-X (2013): Effective anti-neu-initiated antitumor responses require the complex role of CD4+ T cells. *Clinical cancer research : an official journal of the American Association for Cancer Research* 19 (6), pp. 1476–1486. DOI: 10.1158/1078-0432.CCR-12-2522.

Motzer, RJ; Escudier, B; McDermott, DF; George, S; Hammers, HJ; Srinivas, S et al. (2015): Nivolumab versus Everolimus in Advanced Renal-Cell Carcinoma. *N Engl J Med* 373 (19), pp. 1803–1813. DOI: 10.1056/NEJMoa1510665.

Motzer, RJ; Tannir, NM; McDermott, DF; Arén Frontera, O; Melichar, B; Choueiri, TK et al. (2018): Nivolumab plus Ipilimumab versus Sunitinib in Advanced Renal-Cell Carcinoma. *The New England journal of medicine* 378 (14), pp. 1277–1290. DOI: 10.1056/NEJMoa1712126.

Muller, WJ; Sinn, E; Pattengale, PK; Wallace, R; Leder, P (1988): Single-step induction of mammary adenocarcinoma in transgenic mice bearing the activated c-neu oncogene. *Cell* 54 (1), pp. 105–115. DOI: 10.1016/0092-8674(88)90184-5.

Musso, T; Deaglio, S; Franco, L; Calosso, L; Badolato, R; Garbarino, G et al. (2001): CD38 expression and functional activities are up-regulated by IFN-gamma on human monocytes and monocytic cell lines. *Journal of leukocyte biology* 69 (4), pp. 605–612.

Nahta, R; Yuan, LX; Zhang, B; Kobayashi, R; Esteva, FJ (2005): Insulin-like growth factor-I receptor/human epidermal growth factor receptor 2 heterodimerization contributes to trastuzumab resistance of breast cancer cells. *Cancer Res* 65 (23), pp. 11118–11128. DOI: 10.1158/0008-5472.CAN-04-3841.

Nami, B; Wang, Z (2017): HER2 in Breast Cancer Stemness: A Negative Feedback Loop towards Trastuzumab Resistance. *Cancers* 9 (5). DOI: 10.3390/cancers9050040.

Nanni, P; Colombo, MP; Giovanni, C de; Lollini, PL; Nicoletti, G; Parmiani, G; Prodi, G (1983a): Impaired H-2 expression in B16 melanoma variants. *Journal of immunogenetics* 10 (5), pp. 361–370. DOI: 10.1111/j.1744-313x.1983.tb00348.x.

Nanni, P; De Giovanni, C; Burocchi, A; Nicoletti, G; Landuzzi, L; Palladini, A et al. (2018): OX40 triggering concomitant to IL12-engineered cell vaccine hampers the immunoprevention of HER2/neu-driven mammary carcinogenesis. *Oncoimmunology* 7 (8), e1465164. DOI: 10.1080/2162402X.2018.1465164.

Nanni, P; De Giovanni, C; Lollini, PL; Nicoletti, G; Prodi, G (1986): Clones with different metastatic capacity and variant selection during metastasis: a problematic relationship. *Journal of the National Cancer Institute* 76 (1), pp. 87–93.

Nanni, P; Giovanni, C de; Lollini, PL; Nicoletti, G; Prodi, G (1983b): TS/A: a new metastasizing cell line from a BALB/c spontaneous mammary adenocarcinoma. *Clinical & experimental metastasis* 1 (4), pp. 373–380. DOI: 10.1007/BF00121199.

Nanni, P; Landuzzi, L; Nicoletti, G; De Giovanni, C; Rossi, I; Croci, S et al. (2004): Immunoprevention of mammary carcinoma in HER-2/neu transgenic mice is IFN-gamma and B cell dependent. *Journal of immunology (Baltimore, Md. : 1950)* 173 (4), pp. 2288–2296. DOI: 10.4049/jimmunol.173.4.2288.

Nanni, P; Nicoletti, G; De Giovanni, C; Croci, S; Astolfi, A; Landuzzi, L et al. (2003): Development of rhabdomyosarcoma in HER-2/neu transgenic p53 mutant mice. *Cancer research* 63 (11), pp. 2728–2732.

Nanni, P; Nicoletti, G; Giovanni, C de; Landuzzi, L; Di Carlo, E; Cavallo, F et al. (2001): Combined allogeneic tumor cell vaccination and systemic interleukin 12 prevents mammary carcinogenesis in HER-2/neu transgenic mice. *Journal of Experimental Medicine* 194 (9), pp. 1195–1205. DOI: 10.1084/jem.194.9.1195.

Nanni, P; Nicoletti, G; Palladini, A; Croci, S; Murgo, A; Ianzano, ML et al. (2012): Multiorgan metastasis of human HER-2+ breast cancer in Rag2-/-;Il2rg-/- mice and treatment with PI3K inhibitor. *PloS one* 7 (6), e39626. DOI: 10.1371/journal.pone.0039626.

Nanni, P; Pupa, SM; Nicoletti, G; De Giovanni, C; Landuzzi, L; Rossi, I et al. (2000): p185(neu) protein is required for tumor and anchorage-independent growth, not for cell proliferation of transgenic mammary carcinoma. *Int J Cancer* 87 (2), pp. 186–194.

Narayan, M; Wilken, JA; Harris, LN; Baron, AT; Kimbler, KD; Maihle, NJ (2009): Trastuzumab-induced HER reprogramming in "resistant" breast carcinoma cells. *Cancer research* 69 (6), pp. 2191–2194. DOI: 10.1158/0008-5472.CAN-08-1056.

Natrajan, R; Lambros, MB; Rodríguez-Pinilla, SM; Moreno-Bueno, G; Tan, DS; Marchió, C et al. (2009). *Clinical cancer research : an official journal of the American Association for Cancer Research* 15 (8), pp. 2711–2722. DOI: 10.1158/1078-0432.CCR-08-1878.

Niederst, MJ; Engelman, JA (2013): Bypass mechanisms of resistance to receptor tyrosine kinase inhibition in lung cancer. *Science signaling* 6 (294), re6. DOI: 10.1126/scisignal.2004652.

- Nimmerjahn, F; Ravetch, JV (2005): Divergent immunoglobulin g subclass activity through selective Fc receptor binding. *Science (New York, N.Y.)* 310 (5753), pp. 1510–1512. DOI: 10.1126/science.1118948.
- Nowell, PC (1976): The clonal evolution of tumor cell populations. *Science (New York, N.Y.)* 194 (4260), pp. 23–28. DOI: 10.1126/science.959840.
- Oft, M (2014): IL-10: master switch from tumor-promoting inflammation to antitumor immunity. *Cancer immunology research* 2 (3), pp. 194–199. DOI: 10.1158/2326-6066.CIR-13-0214.
- Ogiso, H; Ishitani, R; Nureki, O; Fukai, S; Yamanaka, M; Kim, J-H et al. (2002): Crystal Structure of the Complex of Human Epidermal Growth Factor and Receptor Extracellular Domains. *Cell* 110 (6), pp. 775–787. DOI: 10.1016/s0092-8674(02)00963-7.
- Ohigashi, Y; Sho, M; Yamada, Y; Tsurui, Y; Hamada, K; Ikeda, N et al. (2005): Clinical significance of programmed death-1 ligand-1 and programmed death-1 ligand-2 expression in human esophageal cancer. *Clin Cancer Res* 11 (8), pp. 2947–2953. DOI: 10.1158/1078-0432.CCR-04-1469.
- Oliveras-Ferraros, C; Vazquez-Martin, A; Martin-Castillo, B; Cufí, S; Del Barco, S; Lopez-Bonet, E et al. (2010): Dynamic emergence of the mesenchymal CD44(pos)CD24(neg/low) phenotype in HER2-gene amplified breast cancer cells with de novo resistance to trastuzumab (Herceptin). *Biochemical and biophysical research communications* 397 (1), pp. 27–33. DOI: 10.1016/j.bbrc.2010.05.041.
- Olson, B; Li, Y; Lin, Y; Liu, ET; Patnaik, A (2018): Mouse Models for Cancer Immunotherapy Research. *Cancer discovery* 8 (11), pp. 1358–1365. DOI: 10.1158/2159-8290.CD-18-0044.
- Osada, T; Yang, XY; Hartman, ZC; Glass, O; Hodges, BL; Niedzwiecki, D et al. (2009): Optimization of vaccine responses with an E1, E2b and E3-deleted Ad5 vector circumvents pre-existing anti-vector immunity. *Cancer gene therapy* 16 (9), pp. 673–682. DOI: 10.1038/cgt.2009.17.
- Overman, MJ; McDermott, R; Leach, JL; Lonardi, S; Lenz, H-J; Morse, MA et al. (2017): Nivolumab in patients with metastatic DNA mismatch repair-deficient or microsatellite instability-high colorectal cancer (CheckMate 142): an open-label, multicentre, phase 2 study. *Lancet oncology*.
- Overwijk, WW; Restifo, NP (2000): Autoimmunity and the immunotherapy of cancer: targeting the "self" to destroy the "other". *Critical reviews in immunology* 20 (6), pp. 433–450.

Paez-Ribes, M; Man, S; Xu, P; Kerbel, RS (2016): Development of Patient Derived Xenograft Models of Overt Spontaneous Breast Cancer Metastasis: A Cautionary Note. *PLoS one* 11 (6), e0158034. DOI: 10.1371/journal.pone.0158034.

Page, DB; Naidoo, J; McArthur, HL (2014): Emerging immunotherapy strategies in breast cancer. *Immunotherapy* 6 (2), pp. 195–209. DOI: 10.2217/imt.13.166.

Pai, C-CS; Huang, JT; Lu, X; Simons, DM; Park, C; Chang, A et al. (2019): Clonal Deletion of Tumor-Specific T Cells by Interferon- γ Confers Therapeutic Resistance to Combination Immune Checkpoint Blockade. *Immunity* 50 (2), 477-492.e8. DOI: 10.1016/j.immuni.2019.01.006.

Pai-Scherf, L; Blumenthal, GM; Li, H; Subramaniam, S; Mishra-Kalyani, PS; He, K et al. (2017): FDA Approval Summary: Pembrolizumab for Treatment of Metastatic Non-Small Cell Lung Cancer: First-Line Therapy and Beyond. *Oncologist*.

Palladini, A; Landuzzi, L; Lollini, P-L; Nanni, P (2018a): Cancer immunoprevention: from mice to early clinical trials. *BMC immunology* 19 (1), p. 16. DOI: 10.1186/s12865-018-0253-0.

Palladini, A; Nicoletti, G; Lamolinara, A; Dall'Ora, M; Balboni, T; Ianzano, ML et al. (2017): HER2 isoforms co-expression differently tunes mammary tumor phenotypes affecting onset, vasculature and therapeutic response. *Oncotarget* 8 (33), pp. 54444–54458. DOI: 10.18632/oncotarget.17088.

Palladini, A; Nicoletti, G; Pappalardo, F; Murgio, A; Grosso, V; Stivani, V et al. (2010): In silico modeling and in vivo efficacy of cancer-preventive vaccinations. *Cancer research* 70 (20), pp. 7755–7763. DOI: 10.1158/0008-5472.CAN-10-0701.

Palladini, A; Thrane, S; Janitzek, CM; Pihl, J; Clemmensen, SB; Jongh, WA de et al. (2018b): Virus-like particle display of HER2 induces potent anti-cancer responses. *Oncoimmunology* 7 (3), e1408749. DOI: 10.1080/2162402X.2017.1408749.

Pallerla, S; Abdul, AU; Comeau, J; Jois, S (2021): Cancer Vaccines, Treatment of the Future: With Emphasis on HER2-Positive Breast Cancer. *IJMS* 22 (2). DOI: 10.3390/ijms22020779.

Park, IH; Kwon, Y; Ro, JY; Lee, KS; Ro, J (2010): Concordant HER2 status between metastatic breast cancer cells in CSF and primary breast cancer tissue. *Breast cancer research and treatment* 123 (1), pp. 125–128. DOI: 10.1007/s10549-009-0627-3.

Park, K; Han, S; Kim, HJ; Kim, J; Shin, E (2006): HER2 status in pure ductal carcinoma in situ and in the intraductal and invasive components of invasive ductal carcinoma determined by fluorescence in situ hybridization and immunohistochemistry. *Histopathology* 48 (6), pp. 702–707. DOI: 10.1111/j.1365-2559.2006.02403.x.

- Parra-Palau, JL; Morancho, B; Peg, V; Escorihuela, M; Scaltriti, M; Vicario, R et al. (2014): Effect of p95HER2/611CTF on the response to trastuzumab and chemotherapy. *Journal of the National Cancer Institute* 106 (11). DOI: 10.1093/jnci/dju291.
- Patel, AP; Tirosh, I; Trombetta, JJ; Shalek, AK; Gillespie, SM; Wakimoto, H et al. (2014): Single-cell RNA-seq highlights intratumoral heterogeneity in primary glioblastoma. *Science (New York, N.Y.)* 344 (6190), pp. 1396–1401. DOI: 10.1126/science.1254257.
- Pedersen, K; Angelini, P-D; Laos, S; Bach-Faig, A; Cunningham, MP; Ferrer-Ramón, C et al. (2009): A naturally occurring HER2 carboxy-terminal fragment promotes mammary tumor growth and metastasis. *Molecular and cellular biology* 29 (12), pp. 3319–3331. DOI: 10.1128/MCB.01803-08.
- Pereira, B; Chin, S-F; Rueda, OM; Vollan, H-KM; Provenzano, E; Bardwell, HA et al. (2016): The somatic mutation profiles of 2,433 breast cancers refines their genomic and transcriptomic landscapes. *Nature communications* 7, p. 11479. DOI: 10.1038/ncomms11479.
- Perou, CM; Sørlie, T; Eisen, MB; van de Rijn, M; Jeffrey, SS; Rees, CA et al. (2000): Molecular portraits of human breast tumours. *Nature* 406 (6797), pp. 747–752. DOI: 10.1038/35021093.
- Petrelli, F; Barni, S (2011): Should adjuvant trastuzumab be offered in very early-stage (pT1a/bN0M0) HER2-neu-positive breast cancer? A current debate. *Medical oncology (Northwood, London, England)* 28 (2), pp. 401–408. DOI: 10.1007/s12032-010-9460-0.
- Piccart-Gebhart, M; Holmes, E; Baselga, J; Azambuja, E de; Dueck, AC; Viale, G et al. (2016): Adjuvant Lapatinib and Trastuzumab for Early Human Epidermal Growth Factor Receptor 2-Positive Breast Cancer: Results From the Randomized Phase III Adjuvant Lapatinib and/or Trastuzumab Treatment Optimization Trial. *Journal of clinical oncology : official journal of the American Society of Clinical Oncology* 34 (10), pp. 1034–1042. DOI: 10.1200/JCO.2015.62.1797.
- Pinkas-Kramarski, R; Soussan, L; Waterman, H; Levkowitz, G; Alroy, I; Klapper, L et al. (1996): Diversification of Neu differentiation factor and epidermal growth factor signaling by combinatorial receptor interactions. *The EMBO journal* 15 (10), pp. 2452–2467.
- Pitt, JM; Vétizou, M; Daillère, R; Roberti, MP; Yamazaki, T; Routy, B et al. (2016): Resistance Mechanisms to Immune-Checkpoint Blockade in Cancer: Tumor-Intrinsic and -Extrinsic Factors. *Immunity* 44 (6), pp. 1255–1269. DOI: 10.1016/j.immuni.2016.06.001.

Ploeger, C; Waldburger, N; Fraas, A; Goepfert, B; Pusch, S; Breuhahn, K et al. (2016): Chromosome 8p tumor suppressor genes SH2D4A and SORBS3 cooperate to inhibit interleukin-6 signaling in hepatocellular carcinoma. *Hepatology (Baltimore, Md.)* 64 (3), pp. 828–842. DOI: 10.1002/hep.28684.

Powles, T; O'Donnell, PH; Massard, C; Arkenau, H-T; Friedlander, TW; Hoimes, CJ et al. (2017): Efficacy and Safety of Durvalumab in Locally Advanced or Metastatic Urothelial Carcinoma: Updated Results From a Phase 1/2 Open-label Study. *JAMA oncology* 3 (9), e172411. DOI: 10.1001/jamaoncol.2017.2411.

Prat, A; Parker, JS; Karginova, O; Fan, C; Livasy, C; Herschkowitz, JI et al. (2010): Phenotypic and molecular characterization of the claudin-low intrinsic subtype of breast cancer. *Breast cancer research : BCR* 12 (5), R68. DOI: 10.1186/bcr2635.

Prat, A; Perou, CM (2011): Deconstructing the molecular portraits of breast cancer. *Molecular oncology* 5 (1), pp. 5–23. DOI: 10.1016/j.molonc.2010.11.003.

Prat, A; Pineda, E; Adamo, B; Galván, P; Fernández, A; Gaba, L et al. (2015): Clinical implications of the intrinsic molecular subtypes of breast cancer. *Breast (Edinburgh, Scotland)* 24 Suppl 2, S26-35. DOI: 10.1016/j.breast.2015.07.008.

Quaglino, E; Conti, L; Cavallo, F (2020): Breast cancer stem cell antigens as targets for immunotherapy. *Seminars in immunology* 47, p. 101386. DOI: 10.1016/j.smim.2020.101386.

Quaglino, E; Mastini, C; Amici, A; Marchini, C; Iezzi, M; Lanzardo, S et al. (2010): A better immune reaction to ErbB-2 tumors is elicited in mice by DNA vaccines encoding rat/human chimeric proteins. *Cancer research* 70 (7), pp. 2604–2612. DOI: 10.1158/0008-5472.CAN-09-2548.

Raju, S; Joseph, R; Sehgal, S (2018): Review of checkpoint immunotherapy for the management of non-small cell lung cancer. *ImmunoTargets and therapy* 7, pp. 63–75. DOI: 10.2147/ITT.S125070.

Rakha, EA; El-Sayed, ME; Lee, AH; Elston, CW; Grainge, MJ; Hodi, Z et al. (2008): Prognostic significance of Nottingham histologic grade in invasive breast carcinoma. *Journal of clinical oncology : official journal of the American Society of Clinical Oncology* 26 (19), pp. 3153–3158. DOI: 10.1200/JCO.2007.15.5986.

Reis-Filho, JS; Lakhani, SR (2008): Breast cancer special types: why bother? *The Journal of pathology* 216 (4), pp. 394–398. DOI: 10.1002/path.2419.

Rexer, BN; Arteaga, CL (2012): Intrinsic and acquired resistance to HER2-targeted therapies in HER2 gene-amplified breast cancer: mechanisms and clinical implications. *Critical reviews in oncogenesis* 17 (1), pp. 1–16. DOI: 10.1615/critrevoncog.v17.i1.20.

Ribas, A; Butler, M; Lutzky, J; Lawrence, DP; Robert, C; Miller, W et al. (2015): Phase I study combining anti-PD-L1 (MEDI4736) with BRAF (dabrafenib) and/or MEK (trametinib) inhibitors in advanced melanoma. *JCO* 33 (15_suppl), p. 3003. DOI: 10.1200/jco.2015.33.15_suppl.3003.

Riccardo, F; Bolli, E; Macagno, M; Arigoni, M; Cavallo, F; Quaglino, E (2017): Chimeric DNA Vaccines: An Effective Way to Overcome Immune Tolerance. *Current topics in microbiology and immunology* 405, pp. 99–122. DOI: 10.1007/82.2014.426.

Riella, LV; Paterson, AM; Sharpe, AH; Chandraker, A (2012): Role of the PD-1 pathway in the immune response. *American journal of transplantation : official journal of the American Society of Transplantation and the American Society of Transplant Surgeons* 12 (10), pp. 2575–2587. DOI: 10.1111/j.1600-6143.2012.04224.x.

Ritprajak, P; Azuma, M (2015): Intrinsic and extrinsic control of expression of the immunoregulatory molecule PD-L1 in epithelial cells and squamous cell carcinoma. *Oral oncology* 51 (3), pp. 221–228. DOI: 10.1016/j.oraloncology.2014.11.014.

Ritter, CA; Perez-Torres, M; Rinehart, C; Guix, M; Dugger, T; Engelman, JA; Arteaga, CL (2007): Human breast cancer cells selected for resistance to trastuzumab in vivo overexpress epidermal growth factor receptor and ErbB ligands and remain dependent on the ErbB receptor network. *Clinical cancer research : an official journal of the American Association for Cancer Research* 13 (16), pp. 4909–4919. DOI: 10.1158/1078-0432.CCR-07-0701.

Rittmeyer, A; Barlesi, F; Waterkamp, D; Park, K; Ciardiello, F; Pawel, J von et al. (2017): Atezolizumab versus docetaxel in patients with previously treated non-small-cell lung cancer (OAK): a phase 3, open-label, multicentre randomised controlled trial. *Lancet*.

Robert, C; Long, GV; Brady, B; Dutriaux, C; Maio, M; Mortier, L et al. (2015): Nivolumab in previously untreated melanoma without BRAF mutation. *The New England journal of medicine* 372 (4), pp. 320–330. DOI: 10.1056/NEJMoa1412082.

Romano, E; Pradervand, S; Paillusson, A; Weber, J; Harshman, K; Muehlethaler, K et al. (2013): Identification of multiple mechanisms of resistance to vemurafenib in a patient with BRAFV600E-mutated cutaneous melanoma successfully rechallenged after progression. *Clinical cancer research : an official journal of the American Association for Cancer Research* 19 (20), pp. 5749–5757. DOI: 10.1158/1078-0432.CCR-13-0661.

Rosenberg, JE; Hoffman-Censits, J; Powles, T; van der Heijden, MS; Balar, AV; Necchi, A et al. (2016): Atezolizumab in patients with locally advanced and metastatic urothelial carcinoma who have progressed following treatment with platinum-based chemotherapy: a single-arm, multicentre, phase 2 trial. *Lancet*.

Ross, JS; Wang, K; Gay, LM; Al-Rohil, RN; Nazeer, T; Sheehan, CE et al. (2014): A high frequency of activating extracellular domain ERBB2 (HER2) mutation in micropapillary urothelial carcinoma. *Clinical cancer research : an official journal of the American Association for Cancer Research* 20 (1), pp. 68–75. DOI: 10.1158/1078-0432.CCR-13-1992.

Russnes, HG; Navin, N; Hicks, J; Borresen-Dale, A-L (2011): Insight into the heterogeneity of breast cancer through next-generation sequencing. *The Journal of clinical investigation* 121 (10), pp. 3810–3818. DOI: 10.1172/JCI57088.

Saâda-Bouzid, E; Defaucheux, C; Karabajakian, A; Coloma, VP; Servois, V; Paoletti, X et al. (2017): Hyperprogression during anti-PD-1/PD-L1 therapy in patients with recurrent and/or metastatic head and neck squamous cell carcinoma. *Annals of oncology : official journal of the European Society for Medical Oncology* 28 (7), pp. 1605–1611. DOI: 10.1093/annonc/mdx178.

Sáez, A; Andreu, FJ; Seguí, MA; Baré, ML; Fernández, S; Dinarés, C; Rey, M (2006): HER-2 gene amplification by chromogenic in situ hybridisation (CISH) compared with fluorescence in situ hybridisation (FISH) in breast cancer-A study of two hundred cases. *Breast (Edinburgh, Scotland)* 15 (4), pp. 519–527. DOI: 10.1016/j.breast.2005.09.008.

Sanborn, JZ; Chung, J; Purdom, E; Wang, NJ; Kakavand, H; Wilmott, JS et al. (2015): Phylogenetic analyses of melanoma reveal complex patterns of metastatic dissemination. *Proceedings of the National Academy of Sciences of the United States of America* 112 (35), pp. 10995–11000. DOI: 10.1073/pnas.1508074112.

Scaltriti, M; Chandarlapaty, S; Prudkin, L; Aura, C; Jimenez, J; Angelini, PD et al. (2010): Clinical benefit of lapatinib-based therapy in patients with human epidermal growth factor receptor 2-positive breast tumors coexpressing the truncated p95HER2 receptor. *Clinical cancer research : an official journal of the American Association for Cancer Research* 16 (9), pp. 2688–2695. DOI: 10.1158/1078-0432.CCR-09-3407.

Scaltriti, M; Nuciforo, P; Bradbury, I; Sperinde, J; Agbor-Tarh, D; Campbell, C et al. (2015): High HER2 expression correlates with response to the combination of lapatinib and trastuzumab. *Clinical cancer research : an official journal of the American Association for Cancer Research* 21 (3), pp. 569–576. DOI: 10.1158/1078-0432.CCR-14-1824.

Scaltriti, M; Rojo, F; Ocaña, A; Anido, J; Guzman, M; Cortes, J et al. (2007): Expression of p95HER2, a truncated form of the HER2 receptor, and response to anti-HER2 therapies in breast cancer. *Journal of the National Cancer Institute* 99 (8), pp. 628–638. DOI: 10.1093/jnci/djk134.

Schechter, AL; Stern, DF; Vaidyanathan, L; Decker, SJ; Drebin, JA; Greene, MI; Weinberg, RA (1984): The neu oncogene: an erb-B-related gene encoding a 185,000-Mr tumour antigen. *Nature* 312 (5994), pp. 513–516. DOI: 10.1038/312513a0.

Schlom, J; Hodge, JW; Palena, C; Tsang, K-Y; Jochems, C; Greiner, JW et al. (2014): Therapeutic cancer vaccines. *Advances in cancer research* 121, pp. 67–124. DOI: 10.1016/B978-0-12-800249-0.00002-0.

Schneeweiss, A; Chia, S; Hickish, T; Harvey, V; Eniu, A; Hegg, R et al. (2013): Pertuzumab plus trastuzumab in combination with standard neoadjuvant anthracycline-containing and anthracycline-free chemotherapy regimens in patients with HER2-positive early breast cancer: a randomized phase II cardiac safety study (TRYPHAENA). *Annals of oncology : official journal of the European Society for Medical Oncology* 24 (9), pp. 2278–2284. DOI: 10.1093/annonc/mdt182.

Schoenfeld, AJ; Hellmann, MD (2020): Acquired Resistance to Immune Checkpoint Inhibitors. *Cancer cell* 37 (4), pp. 443–455. DOI: 10.1016/j.ccell.2020.03.017.

Scholz, A; Lang, V; Henschler, R; Czabanka, M; Vajkoczy, P; Chavakis, E et al. (2011): Angiopoietin-2 promotes myeloid cell infiltration in a β_2 -integrin-dependent manner. *Blood* 118 (18), pp. 5050–5059. DOI: 10.1182/blood-2011-03-343293.

Schrijver, WA; Suijkerbuijk, KP; van Gils, CH; van der Wall, E; Moelans, CB; van Diest, PJ (2018): Receptor Conversion in Distant Breast Cancer Metastases: A Systematic Review and Meta-analysis. *Journal of the National Cancer Institute* 110 (6), pp. 568–580. DOI: 10.1093/jnci/djx273.

Schumacher, TN; Schreiber, RD (2015): Neoantigens in cancer immunotherapy. *Science (New York, N.Y.)* 348 (6230), pp. 69–74. DOI: 10.1126/science.aaa4971.

Segatto, O; King, CR; Pierce, JH; Di Fiore, PP; Aaronson, SA (1988): Different structural alterations upregulate in vitro tyrosine kinase activity and transforming potency of the erbB-2 gene. *Molecular and cellular biology* 8 (12), pp. 5570–5574. DOI: 10.1128/mcb.8.12.5570.

Seidel, JA; Otsuka, A; Kabashima, K (2018): Anti-PD-1 and Anti-CTLA-4 Therapies in Cancer: Mechanisms of Action, Efficacy, and Limitations. *Front. Oncol.* 8, p. 86. DOI: 10.3389/fonc.2018.00086.

Senkus, E; Kyriakides, S; Ohno, S; Penault-Llorca, F; Poortmans, P; Rutgers, E et al. (2015): Primary breast cancer: ESMO Clinical Practice Guidelines for diagnosis, treatment and follow-up. *Annals of oncology : official journal of the European Society for Medical Oncology* 26 Suppl 5, v8-30. DOI: 10.1093/annonc/mdv298.

Shah, NJ; Kelly, WJ; Liu, SV; Choquette, K; Spira, A (2018): Product review on the Anti-PD-L1 antibody atezolizumab. *Human vaccines & immunotherapeutics* 14 (2), pp. 269–276. DOI: 10.1080/21645515.2017.1403694.

Sharieh, EA; Awidi, AS; Ahram, M; Zihlif, MA (2016): Alteration of gene expression in MDA-MB-453 breast cancer cell line in response to continuous exposure to Trastuzumab. *Gene* 575 (2 Pt 2), pp. 415–420. DOI: 10.1016/j.gene.2015.09.019.

Sharma, A; Koldovsky, U; Xu, S; Mick, R; Roses, R; Fitzpatrick, E et al. (2012): HER-2 pulsed dendritic cell vaccine can eliminate HER-2 expression and impact ductal carcinoma in situ. *Cancer* 118 (17), pp. 4354–4362. DOI: 10.1002/cncr.26734.

Sharma, P; Retz, M; Siefker-Radtke, A; Baron, A; Necchi, A; Bedke, J et al. (2017): Nivolumab in metastatic urothelial carcinoma after platinum therapy (CheckMate 275): a multicentre, single-arm, phase 2 trial. *Lancet oncology*.

Sharpe, AH; Pauken, KE (2018): The diverse functions of the PD1 inhibitory pathway. *Nat Rev Immunol* 18 (3), pp. 153–167. DOI: 10.1038/nri.2017.108.

Shattuck, DL; Miller, JK; Carraway, KL; Sweeney, C (2008): Met receptor contributes to trastuzumab resistance of Her2-overexpressing breast cancer cells. *Cancer Res* 68 (5), pp. 1471–1477. DOI: 10.1158/0008-5472.CAN-07-5962.

Shenoy, AK; Jin, Y; Luo, H; Tang, M; Pampo, C; Shao, R et al. (2016): Epithelial-to-mesenchymal transition confers pericyte properties on cancer cells. *The Journal of clinical investigation* 126 (11), pp. 4174–4186. DOI: 10.1172/JCI86623.

Shibahara, I; Saito, R; Zhang, R; Chonan, M; Shoji, T; Kanamori, M et al. (2015): OX40 ligand expressed in glioblastoma modulates adaptive immunity depending on the microenvironment: a clue for successful immunotherapy. *Molecular cancer* 14, p. 41. DOI: 10.1186/s12943-015-0307-3.

Siegel, PM; Muller, WJ (1996): Mutations affecting conserved cysteine residues within the extracellular domain of Neu promote receptor dimerization and activation. *Proceedings of the National Academy of Sciences of the United States of America* 93 (17), pp. 8878–8883. DOI: 10.1073/pnas.93.17.8878.

Siegel, PM; Ryan, ED; Cardiff, RD; Muller, WJ (1999): Elevated expression of activated forms of Neu/ErbB-2 and ErbB-3 are involved in the induction of mammary tumors in transgenic mice: implications for human breast cancer. *The EMBO journal* 18 (8), pp. 2149–2164. DOI: 10.1093/emboj/18.8.2149.

Simpson, PT; Reis-Filho, JS; Lambros, MB; Jones, C; Steele, D; Mackay, A et al. (2008): Molecular profiling pleomorphic lobular carcinomas of the breast: evidence for a

common molecular genetic pathway with classic lobular carcinomas. *The Journal of pathology* 215 (3), pp. 231–244. DOI: 10.1002/path.2358.

Singh, JC; Jhaveri, K; Esteva, FJ (2014): HER2-positive advanced breast cancer: optimizing patient outcomes and opportunities for drug development. *British journal of cancer* 111 (10), pp. 1888–1898. DOI: 10.1038/bjc.2014.388.

Slamon, D (2001): Rationale for trastuzumab (Herceptin) in adjuvant breast cancer trials. *Seminars in Oncology* 28, pp. 13–19. DOI: 10.1016/s0093-7754(01)90188-5.

Slamon, DJ; Clark, GM; Wong, SG; Levin, WJ; Ullrich, A; McGuire, WL (1987): Human breast cancer: correlation of relapse and survival with amplification of the HER-2/neu oncogene. *Science (New York, N.Y.)* 235 (4785), pp. 177–182. DOI: 10.1126/science.3798106.

Slamon, DJ; Godolphin, W; Jones, LA; Holt, JA; Wong, SG; Keith, DE et al. (1989): Studies of the HER-2/neu proto-oncogene in human breast and ovarian cancer. *Science (New York, N.Y.)* 244 (4905), pp. 707–712. DOI: 10.1126/science.2470152.

Sliwkowski, MX; Lofgren, JA; Lewis, GD; Hotaling, TE; Fendly, BM; Fox, JA (1999): Nonclinical studies addressing the mechanism of action of trastuzumab (Herceptin). *Seminars in Oncology* 26 (4 Suppl 12), pp. 60–70.

Snoeck, HW; Lardon, F; Lenjou, M; Nys, G; van Bockstaele, DR; Peetermans, ME (1993): Differential regulation of the expression of CD38 and human leukocyte antigen-DR on CD34+ hematopoietic progenitor cells by interleukin-4 and interferon-gamma. *Experimental hematology* 21 (11), pp. 1480–1486.

Solinas, C; Aiello, M; Rozali, E; Lambertini, M; Willard-Gallo, K; Migliori, E (2020): Programmed cell death-ligand 2: A neglected but important target in the immune response to cancer? *Translational oncology* 13 (10), p. 100811. DOI: 10.1016/j.tranon.2020.100811.

Song, H; Kim, TO; Ma, SY; Park, J-H; Choi, J-H; Kim, J-H et al. (2014): Intratumoral heterogeneity impacts the response to anti-neu antibody therapy. *BMC cancer* 14, p. 647. DOI: 10.1186/1471-2407-14-647.

Sonnenblick, A; Fumagalli, D; Sotiriou, C; Piccart, M (2014): Is the differentiation into molecular subtypes of breast cancer important for staging, local and systemic therapy, and follow up? *Cancer treatment reviews* 40 (9), pp. 1089–1095. DOI: 10.1016/j.ctrv.2014.07.005.

Sorlie, T; Tibshirani, R; Parker, J; Hastie, T; Marron, JS; Nobel, A et al. (2003): Repeated observation of breast tumor subtypes in independent gene expression data sets.

Proceedings of the National Academy of Sciences of the United States of America 100 (14), pp. 8418–8423. DOI: 10.1073/pnas.0932692100.

Sørli, T; Perou, CM; Tibshirani, R; Aas, T; Geisler, S; Johnsen, H et al. (2001): Gene expression patterns of breast carcinomas distinguish tumor subclasses with clinical implications. *Proceedings of the National Academy of Sciences of the United States of America* 98 (19), pp. 10869–10874. DOI: 10.1073/pnas.191367098.

Sperinde, J; Jin, X; Banerjee, J; Penuel, E; Saha, A; Diedrich, G et al. (2010): Quantitation of p95HER2 in paraffin sections by using a p95-specific antibody and correlation with outcome in a cohort of trastuzumab-treated breast cancer patients. *Clinical cancer research : an official journal of the American Association for Cancer Research* 16 (16), pp. 4226–4235. DOI: 10.1158/1078-0432.CCR-10-0410.

Stagg, J; Loi, S; Divisekera, U; Ngiow, SF; Duret, H; Yagita, H et al. (2011): Anti-ErbB-2 mAb therapy requires type I and II interferons and synergizes with anti-PD-1 or anti-CD137 mAb therapy. *Proceedings of the National Academy of Sciences of the United States of America* 108 (17), pp. 7142–7147. DOI: 10.1073/pnas.1016569108.

Stein, RG; Ebert, S; Schlahsa, L; Scholz, CJ; Braun, M; Hauck, P et al. (2019): Cognate Nonlytic Interactions between CD8+ T Cells and Breast Cancer Cells Induce Cancer Stem Cell-like Properties. *Cancer research* 79 (7), pp. 1507–1519. DOI: 10.1158/0008-5472.CAN-18-0387.

Stephens, P; Hunter, C; Bignell, G; Edkins, S; Davies, H; Teague, J et al. (2004): Lung cancer: intragenic ERBB2 kinase mutations in tumours. *Nature* 431 (7008), pp. 525–526. DOI: 10.1038/431525b.

Stephens, PJ; Tarpey, PS; Davies, H; van Loo, P; Greenman, C; Wedge, DC et al. (2012): The landscape of cancer genes and mutational processes in breast cancer. *Nature* 486 (7403), pp. 400–404. DOI: 10.1038/nature11017.

Stockmeyer, B; Beyer, T; Neuhuber, W; Repp, R; Kalden, JR; Valerius, T; Herrmann, M (2003): Polymorphonuclear granulocytes induce antibody-dependent apoptosis in human breast cancer cells. *Journal of immunology (Baltimore, Md. : 1950)* 171 (10), pp. 5124–5129. DOI: 10.4049/jimmunol.171.10.5124.

Sun, C; Mezzadra, R; Schumacher, TN (2018): Regulation and Function of the PD-L1 Checkpoint. *Immunity* 48 (3), pp. 434–452. DOI: 10.1016/j.immuni.2018.03.014.

Swain, SM; Baselga, J; Kim, S-B; Ro, J; Semiglazov, V; Campone, M et al. (2015): Pertuzumab, trastuzumab, and docetaxel in HER2-positive metastatic breast cancer. *The New England journal of medicine* 372 (8), pp. 724–734. DOI: 10.1056/NEJMoa1413513.

Swain, SM; Ewer, MS; Cortés, J; Amadori, D; Miles, D; Knott, A et al. (2013a): Cardiac tolerability of pertuzumab plus trastuzumab plus docetaxel in patients with HER2-positive metastatic breast cancer in CLEOPATRA: a randomized, double-blind, placebo-controlled phase III study. *The oncologist* 18 (3), pp. 257–264. DOI: 10.1634/theoncologist.2012-0448.

Swain, SM; Kim, S-B; Cortés, J; Ro, J; Semiglazov, V; Campone, M et al. (2013b): Pertuzumab, trastuzumab, and docetaxel for HER2-positive metastatic breast cancer (CLEOPATRA study): overall survival results from a randomised, double-blind, placebo-controlled, phase 3 study. *The Lancet Oncology* 14 (6), pp. 461–471. DOI: 10.1016/S1470-2045(13)70130-X.

Tan, AC; Goubier, A; Kohrt, HE (2015): A quantitative analysis of therapeutic cancer vaccines in phase 2 or phase 3 trial. *Journal for immunotherapy of cancer* 3, p. 48. DOI: 10.1186/s40425-015-0093-x.

The Cancer Genome Atlas Network (2012): Comprehensive molecular portraits of human breast tumours. *Nature* 490 (7418), pp. 61–70. DOI: 10.1038/nature11412.

Thrane, S; Janitzek, CM; Matondo, S; Resende, M; Gustavsson, T; Jongh, WA de et al. (2016): Bacterial superglue enables easy development of efficient virus-like particle based vaccines. *Journal of nanobiotechnology* 14, p. 30. DOI: 10.1186/s12951-016-0181-1.

Timmer, M; Werner, J-M; Röhn, G; Ortmann, M; Blau, T; Cramer, C et al. (2017): Discordance and Conversion Rates of Progesterone-, Estrogen-, and HER2/neu-Receptor Status in Primary Breast Cancer and Brain Metastasis Mainly Triggered by Hormone Therapy. *Anticancer research* 37 (9), pp. 4859–4865. DOI: 10.21873/anticanres.11894.

Topalian, SL; Sznol, M; McDermott, DF; Kluger, HM; Carvajal, RD; Sharfman, WH et al. (2014): Survival, durable tumor remission, and long-term safety in patients with advanced melanoma receiving nivolumab. *Journal of clinical oncology : official journal of the American Society of Clinical Oncology* 32 (10), pp. 1020–1030. DOI: 10.1200/JCO.2013.53.0105.

Treré, D; Montanaro, L; Ceccarelli, C; Barbieri, S; Cavrini, G; Santini, D et al. (2007): Prognostic relevance of a novel semiquantitative classification of Bcl2 immunohistochemical expression in human infiltrating ductal carcinomas of the breast. *Annals of oncology : official journal of the European Society for Medical Oncology* 18 (6), pp. 1004–1014. DOI: 10.1093/annonc/mdm074.

Triulzi, C; Vertuani, S; Curcio, C; Antognoli, A; Seibt, J; Akusjärvi, G et al. (2010): Antibody-dependent natural killer cell-mediated cytotoxicity engendered by a kinase-

inactive human HER2 adenovirus-based vaccination mediates resistance to breast tumors. *Cancer research* 70 (19), pp. 7431–7441. DOI: 10.1158/0008-5472.CAN-10-0493.

Tsuruo, T; Yamori, T; Naganuma, K; Tsukagoshi, S; Sakurai, Y (1983): Characterization of metastatic clones derived from a metastatic variant of mouse colon adenocarcinoma 26. *Cancer research* 43 (11), pp. 5437–5442.

Tzahar, E; Waterman, H; Chen, X; Levkowitz, G; Karunakaran, D; Lavi, S et al. (1996): A hierarchical network of interreceptor interactions determines signal transduction by Neu differentiation factor/neuregulin and epidermal growth factor. *Molecular and cellular biology* 16 (10), pp. 5276–5287. DOI: 10.1128/mcb.16.10.5276.

Vaddepally, RK; Kharel, P; Pandey, R; Garje, R; Chandra, AB (2020): Review of Indications of FDA-Approved Immune Checkpoint Inhibitors per NCCN Guidelines with the Level of Evidence. *Cancers* 12 (3). DOI: 10.3390/cancers12030738.

van Allen, EM; Wagle, N; Sucker, A; Treacy, DJ; Johannessen, CM; Goetz, EM et al. (2014): The genetic landscape of clinical resistance to RAF inhibition in metastatic melanoma. *Cancer discovery* 4 (1), pp. 94–109. DOI: 10.1158/2159-8290.CD-13-0617.

Vargo-Gogola, T; Rosen, JM (2007): Modelling breast cancer: one size does not fit all. *Nature reviews. Cancer* 7 (9), pp. 659–672. DOI: 10.1038/nrc2193.

Verma, S; Miles, D; Gianni, L; Krop, IE; Welslau, M; Baselga, J et al. (2012): Trastuzumab emtansine for HER2-positive advanced breast cancer. *The New England journal of medicine* 367 (19), pp. 1783–1791. DOI: 10.1056/NEJMoa1209124.

Viale, G (2012): The current state of breast cancer classification. *Annals of oncology : official journal of the European Society for Medical Oncology* 23 Suppl 10, x207-10. DOI: 10.1093/annonc/mds326.

Viale, G; Rotmensz, N; Maisonneuve, P; Orvieto, E; Maiorano, E; Galimberti, V et al. (2009): Lack of prognostic significance of "classic" lobular breast carcinoma: a matched, single institution series. *Breast cancer research and treatment* 117 (1), pp. 211–214. DOI: 10.1007/s10549-008-0112-4.

Vogel, CL; Cobleigh, MA; Tripathy, D; Gutheil, JC; Harris, LN; Fehrenbacher, L et al. (2002): Efficacy and safety of trastuzumab as a single agent in first-line treatment of HER2-overexpressing metastatic breast cancer. *Journal of clinical oncology : official journal of the American Society of Clinical Oncology* 20 (3), pp. 719–726. DOI: 10.1200/JCO.2002.20.3.719.

Walens, A; Lin, J; Damrauer, JS; McKinney, B; Lupo, R; Newcomb, R et al. (2020): Adaptation and selection shape clonal evolution of tumors during residual disease and recurrence. *Nature communications* 11 (1), p. 5017. DOI: 10.1038/s41467-020-18730-z.

- Wang, C; Thudium, KB; Han, M; Wang, X-T; Huang, H; Feingersh, D et al. (2014): In vitro characterization of the anti-PD-1 antibody nivolumab, BMS-936558, and in vivo toxicology in non-human primates. *Cancer immunology research* 2 (9), pp. 846–856. DOI: 10.1158/2326-6066.CIR-14-0040.
- Wang, L; Liu, J-Q; Talebian, F; Liu, Z; Yu, L; Bai, X-F (2015): IL-10 enhances CTL-mediated tumor rejection by inhibiting highly suppressive CD4+ T cells and promoting CTL persistence in a murine model of plasmacytoma. *Oncoimmunology* 4 (7), e1014232. DOI: 10.1080/2162402X.2015.1014232.
- Wang, SE; Narasanna, A; Perez-Torres, M; Xiang, B; Wu, FY; Yang, S et al. (2006): HER2 kinase domain mutation results in constitutive phosphorylation and activation of HER2 and EGFR and resistance to EGFR tyrosine kinase inhibitors. *Cancer cell* 10 (1), pp. 25–38. DOI: 10.1016/j.ccr.2006.05.023.
- Wang, SE; Xiang, B; Guix, M; Olivares, MG; Parker, J; Chung, CH et al. (2008): Transforming growth factor beta engages TACE and ErbB3 to activate phosphatidylinositol-3 kinase/Akt in ErbB2-overexpressing breast cancer and desensitizes cells to trastuzumab. *Mol. Cell. Biol.* 28 (18), pp. 5605–5620. DOI: 10.1128/MCB.00787-08.
- Warren, CF; Wong-Brown, MW; Bowden, NA (2019): BCL-2 family isoforms in apoptosis and cancer. *Cell death & disease* 10 (3), p. 177. DOI: 10.1038/s41419-019-1407-6.
- Wei, SC; Duffy, CR; Allison, JP (2018): Fundamental Mechanisms of Immune Checkpoint Blockade Therapy. *Cancer discovery* 8 (9), pp. 1069–1086. DOI: 10.1158/2159-8290.CD-18-0367.
- Weigelt, B; Geyer, FC; Reis-Filho, JS (2010): Histological types of breast cancer: how special are they? *Molecular oncology* 4 (3), pp. 192–208. DOI: 10.1016/j.molonc.2010.04.004.
- Weigelt, B; Reis-Filho, JS (2009): Histological and molecular types of breast cancer: is there a unifying taxonomy? *Nature reviews. Clinical oncology* 6 (12), pp. 718–730. DOI: 10.1038/nrclinonc.2009.166.
- Weiner, DB; Kokai, Y; Wada, T; Cohen, JA; Williams, WV; Greene, MI (1989): Linkage of tyrosine kinase activity with transforming ability of the p185neu oncoprotein. *Oncogene* 4 (10), pp. 1175–1183.
- Weinstein, IB; Joe, A (2008): Oncogene addiction. *Cancer research* 68 (9), 3077-80; discussion 3080. DOI: 10.1158/0008-5472.CAN-07-3293.

Wheeler, DA; Takebe, N; Hinoue, T; Hoadley, KA; Cardenas, MF; Hamilton, AM et al. (2020): Molecular Features of Cancers Exhibiting Exceptional Responses to Treatment. *Cancer cell*. DOI: 10.1016/j.ccell.2020.10.015.

Winter, JL; Stackhouse, BL; Russell, GB; Kute, TE (2007): Measurement of PTEN expression using tissue microarrays to determine a race-specific prognostic marker in breast cancer. *Archives of pathology & laboratory medicine* 131 (5), pp. 767–772. DOI: 10.1043/1543-2165(2007)131[767:MOPEUT]2.0.CO;2.

Wolchok, JD; Kluger, H; Callahan, MK; Postow, MA; Rizvi, NA; Lesokhin, AM et al. (2013): Nivolumab plus ipilimumab in advanced melanoma. *The New England journal of medicine* 369 (2), pp. 122–133. DOI: 10.1056/NEJMoa1302369.

Wolff, AC; Hammond, ME; Allison, KH; Harvey, BE; Mangu, PB; Bartlett, JM et al. (2018): Human Epidermal Growth Factor Receptor 2 Testing in Breast Cancer: American Society of Clinical Oncology/College of American Pathologists Clinical Practice Guideline Focused Update. *Journal of clinical oncology : official journal of the American Society of Clinical Oncology* 36 (20), pp. 2105–2122. DOI: 10.1200/JCO.2018.77.8738.

Wood, ER; Truesdale, AT; McDonald, OB; Yuan, D; Hassell, A; Dickerson, SH et al. (2004): A unique structure for epidermal growth factor receptor bound to GW572016 (Lapatinib): relationships among protein conformation, inhibitor off-rate, and receptor activity in tumor cells. *Cancer research* 64 (18), pp. 6652–6659. DOI: 10.1158/0008-5472.CAN-04-1168.

Wu, X; Giobbie-Hurder, A; Liao, X; Connelly, C; Connolly, EM; Li, J et al. (2017): Angiopoietin-2 as a Biomarker and Target for Immune Checkpoint Therapy. *Cancer immunology research* 5 (1), pp. 17–28. DOI: 10.1158/2326-6066.CIR-16-0206.

Yang, B; Jeang, J; Yang, A; Wu, TC; Hung, C-F (2014): DNA vaccine for cancer immunotherapy. *Human vaccines & immunotherapeutics* 10 (11), pp. 3153–3164. DOI: 10.4161/21645515.2014.980686.

Yang, H; Zhou, X; Sun, L; Mao, Y (2019): Correlation Between PD-L2 Expression and Clinical Outcome in Solid Cancer Patients: A Meta-Analysis. *Front. Oncol.* 9, p. 47. DOI: 10.3389/fonc.2019.00047.

Yano, T; Doi, T; Ohtsu, A; Boku, N; Hashizume, K; Nakanishi, M; Ochiai, A (2006): Comparison of HER2 gene amplification assessed by fluorescence in situ hybridization and HER2 protein expression assessed by immunohistochemistry in gastric cancer. *Oncology reports* 15 (1), pp. 65–71.

- Yao, H; Wang, H; Li, C; Fang, J-Y; Xu, J (2018): Cancer Cell-Intrinsic PD-1 and Implications in Combinatorial Immunotherapy. *Frontiers in immunology* 9, p. 1774. DOI: 10.3389/fimmu.2018.01774.
- Yarden, Y; Pines, G (2012): The ERBB network: at last, cancer therapy meets systems biology. *Nature reviews. Cancer* 12 (8), pp. 553–563. DOI: 10.1038/nrc3309.
- Yarden, Y; Sliwkowski, MX (2001): Untangling the ErbB signalling network. *Nature reviews. Molecular cell biology* 2 (2), pp. 127–137. DOI: 10.1038/35052073.
- Yates, LR; Gerstung, M; Knappskog, S; Desmedt, C; Gudem, G; van Loo, P et al. (2015): Subclonal diversification of primary breast cancer revealed by multiregion sequencing. *Nature medicine* 21 (7), pp. 751–759. DOI: 10.1038/nm.3886.
- Ye, Z; Li, Z; Jin, H; Qian, Q (2016): Therapeutic Cancer Vaccines. *Advances in experimental medicine and biology* 909, pp. 139–167. DOI: 10.1007/978-94-017-7555-7_3.
- Yersal, O; Barutca, S (2014): Biological subtypes of breast cancer: Prognostic and therapeutic implications. *World journal of clinical oncology* 5 (3), pp. 412–424. DOI: 10.5306/wjco.v5.i3.412.
- Yi, M; Jiao, D; Xu, H; Liu, Q; Zhao, W; Han, X; Wu, K (2018): Biomarkers for predicting efficacy of PD-1/PD-L1 inhibitors. *Molecular cancer* 17 (1), p. 129. DOI: 10.1186/s12943-018-0864-3.
- Zak, KM; Grudnik, P; Guzik, K; Zieba, BJ; Musielak, B; Dömling, A et al. (2016): Structural basis for small molecule targeting of the programmed death ligand 1 (PD-L1). *Oncotarget* 7 (21), pp. 30323–30335. DOI: 10.18632/oncotarget.8730.
- Zakeri, B; Fierer, JO; Celik, E; Chittock, EC; Schwarz-Linek, U; Moy, VT; Howarth, M (2012): Peptide tag forming a rapid covalent bond to a protein, through engineering a bacterial adhesin. *Proceedings of the National Academy of Sciences of the United States of America* 109 (12), E690-7. DOI: 10.1073/pnas.1115485109.
- Zhong, X; Tumang, JR; Gao, W; Bai, C; Rothstein, TL (2007): PD-L2 expression extends beyond dendritic cells/macrophages to B1 cells enriched for V(H)11/V(H)12 and phosphatidylcholine binding. *Eur. J. Immunol.* 37 (9), pp. 2405–2410. DOI: 10.1002/eji.200737461.
- Zhou, JX; Lee, CH; Qi, CF; Wang, H; Naghashfar, Z; Abbasi, S; Morse, HC (2009): IFN regulatory factor 8 regulates MDM2 in germinal center B cells. *Journal of immunology (Baltimore, Md. : 1950)* 183 (5), pp. 3188–3194. DOI: 10.4049/jimmunol.0803693.
- Zuazo-Ibarra, M; Arasanz, H; Fernández-Hinojal, G; María, G-C; Hernández-Marín, B; Martínez-Aguillo, M et al. (2018): Highly differentiated CD4 T cells Unequivocally

Identify Primary Resistance and Risk of Hyperprogression to PD-L1/PD-1 Immune Checkpoint Blockade in Lung Cancer. DOI: 10.1101/320176.